UNIVERSITY OF SOUTHAMPTON

Christopher David Fallows CEng, MSc, FIEE, RCNC

Thesis for the degree of Doctor of Philosophy

CHARACTERISATION OF THE PROPULSION SYSTEMS OF AUTONOMOUS UNDERWATER VEHICLES

Faculty of Engineering Science

Ship Science

September 2004

UNIVERSITY OF SOUTHAMPTON

ABSTRACT

FACULTY OF ENGINEERING SCIENCE

SHIP SCIENCE

Doctor of Philosophy

CHARACTERISATION OF THE PROPULSION SYSTEMS OF AUTONOMOUS UNDERWATER VEHICLES

By Christopher David Fallows

The process of engineering involves devising machines capable of performing new functions, developing them and standardising them. Machines to perform higher order or multiple functions are created by integrating sets of standard components into systems. As the number of components integrated increases the systems become more complex, both internally and in terms of their interaction with the rest of the world. During development, simplifying assumptions are necessarily made in order to predict the performance of the overall system. Trials in an idealised environment are performed. Once the system is considered to have demonstrated the minimum performance requirement it is put into production. However, although the system now meets the minimum performance requirement in the environment in which it was tested, if it is at all complex it is most unlikely that it will have been tested under all of the conditions it will experience during its in-service life; it will not have been fully characterised in terms of defining its performance under all conditions; and its overall performance is unlikely to have been globally optimised.

This Thesis describes a means of improving the performance of in-service complex systems by more fully characterising them. The method addresses the full complexity of the system. This necessarily involves the measurement of its response to a large number of parameters. Taguchi experimental methods are used to make this feasible. Complementary sets of measurements under controlled conditions on a physical model in the laboratory and measurements on the full-scale system in service are devised.

The method is developed in the context of the propulsion system of a specific Autonomous Underwater vehicle (AUV), AUTOSUB. The generic properties of AUV systems and their propulsion requirements are described, together with that of the subject vehicle. A Systems Engineering approach is taken to describe the system and determine its response to its principal characteristics. The issue of complexity is discussed and the case made for the propulsion system of a multi-function AUV being considered as a complex system. The requirement for laboratory experiments and full-scale trials is derived and their design developed. A description of the conduct of these and the results of the experiments and trials are provided, together with the method for analysing the results. Finally conclusions are drawn, both in generic terms and in terms of the vehicle under discussion.

CONTENTS

List of Figures

List of Tables

ACKNOWLEDGEMENTS

My thanks go to my supervisors Prof Grant Hearn and Steve McPhail for their guidance and encouragement. I am also indebted to all those in the AUTOSUB team of the Southampton Oceanography Centre for their help and patience, especially Gwyn Griffiths and Pete Stevenson. Finally no acknowledgement would be complete without mentioning my partners in crime, Alan Murphy and Maaten Furlong, without whose physical aid, sense of humour and (more-or-less) helpful comments I would not be in the state I am.

Manufacture of the AUTOSUB model was possible as a result of funds received by SOC from SubSea 7.

Nomenclature

A	Aspect ratio
	Wave amplitude
A_T	Cross sectional area of tank
A_m	Cross sectional area of model
a	Acceleration
aa	Aft ADCP
aaa	Aft ADCP with open annulus
abp	Aft blanking plate
a_e	Lift/curve slope
B	Beam
C_B	Block Coefficient
C_d	Drag coefficient
C_L	Lift coefficient
D	Diameter
d	Number of diameters
	Water depth
E	Energy
E_x	Effect of factor x
F_b	Drag due to blockage effects
F_d	Frictional drag
F_e	Estimated force
F_f	Form drag
F_i	Inertial force
F_m	Measured force
F_n	Froude number
F_{nh}	Froude depth number
F_p	Pole drag
F_t	Total drag
F_w	Wave resistance
$\overline{F}$	Mean of all force measurements
$\overline{F}_{fl}$	Mean of frd ADCP force measurements at level l
$\overline{F}_{al}$	Mean of aft ADCP force measurements at level l
$\overline{F}_{\alpha l}$	Mean of force measurements at angle-of-attack α and level l
$\overline{F}_{\delta l}$	Mean of force measurements at hydroplane angle δ and level l
f	Number of factors
	Frequency
fa	Forward ADCP
faa	Forward ADCP with open annulus
fbp	Forward blanking plate

g	Acceleration due to gravity
H_a	Hydroplane angle
h	Tank depth
J	A factor for standard wing section series
l	Number of levels in experiment Length
m_a	Added mass
m_d	Displacement mass
m_e	Mass of entrained water
m_{pl}	Payload mass
m_t	Total mass
n	Number of independent measurements or experiments
n_{min}	Minimum number of experiments
n_f	Number of factors in an experiment
n_l	Number of levels of a factor
P_{pl}	Payload power demand
P_s	Hotel load power demand
P_t	Total power demand
R	Range of vehicle
R_e	Reynolds Number
R_t	Total resistance
R_v	Viscous resistance
S	Variance
s	Surface area of vehicle Speed step number
T	Temperature
t	Mission time
t_r	Sampling time
t_s	Time at speed step s
t_t	Time for transients to die
u	Forward speed
u_d	Downward velocity
u_e	Easterly velocity
u_n	Northerly velocity
V	Volume of model
v_h	Volume of hotel load

v_{pl}	Payload volume
v_t	Total volume of vessel
x	Displacement in the forward direction
y	Displacement in the lateral direction
z	Displacement in the vertical direction
α	Angle-of-attack
α_{los}	Angle of zero lift
δ	Hydroplane angle
ε	Angle of twist
η	Total propulsion efficiency
η_m	Motor efficiency
η_p	Propeller efficiency
λ	Wavelength
ν	Kinematic viscosity
ρ_e	Energy mass density
ρ_p	Propulsion power density
ρ_{pl}	Payload density
ρ_{sw}	Seawater density
σ	Standard deviation
θ	Angular displacement about the axis of the vehicle

List of Abbreviations

ADC	Analogue to Digital Converter
ADCP	Acoustic Doppler Current Profiler
ANOVA	Analysis of variance
AoA	Angle-of-attack
AUI	AUTOSUB Under Ice configuration
AUV	Autonomous Underwater Vehicle
CTD	Conductivity, Temperature and Depth
DERA	Defence Evaluation and Research Agency
DFT	Discrete Fourier Transform
EM	Electromagnetic
Frd	Forward
GPS	Global Positioning System
IIR	Infinite Impulse Response
INS	Inertial Navigation System
ITTC	International Towing Tank Conference
MVA	Multivariate Linear Analysis
MOSFET	Metal Oxide Semiconductor Field Effect Transistor
NC	Numerically Controlled
NERC	Natural Environment Research Council
PWM	Pulse Width Modulation
QA	Quality Assurance
SI	Southampton Institute
ROV	Remotely Operated Vehicle
S/N	Signal to noise ratio
SOC	Southampton Oceanography Centre
rf	Radio frequency

PREFACE

This thesis addresses the subject of how to characterise the performance of complex systems in their real environment, taking into account the full complexity of both the system and its environment.

1.1.1 Concept of systems

Early machines were usually single purpose and stand-alone. Limited functionality was achieved through a single, comparatively simple, assembly of components. By contrast, many needs today are met by systems of components, each of which may have a defined stand-alone function, but which together achieve the higher functionality sought. Development of such systems requires many of the specialist systems engineering techniques, such as formal requirement definition and overt control of interfaces between the components.

1.1.2 System complexity

As with the phenomenon of life, that of the development of man-made systems appears to lead inexorably towards greater complexity with time. In a way analogous to the pressures of evolution, economic pressures, competition and the growth of knowledge result in systems of ever-greater complexity. For example, at the beginning of the last century this thesis would have been typed on a simple mechanical typewriter, comprising a set of levers that cause cast letter dies to impact on an ink ribbon held against a sheet of paper. A hand powered mechanism for moving the paper enabled control of the relative spacing of the letter imprints. In today's word-processor, the input keyboard bears superficial similarity to that of the typewriter, but the rest of the mechanism, mouse, PC, display and full colour dot matrix printer, bears no relationship, either in design, in part count, or in the number of parameters needed to describe it or its performance. By any measure, its complexity is orders of magnitude greater. Furthermore, although the basic purpose of the two machines is identical, the functionality of the more modern machine is considerably greater. We can characterise the latter type of machine as being more complex. Formal definitions of complexity are considered later, but for now it is sufficient to consider it as a property of a system such that: many parameters are required to describe the system; where the output of the system may be a function of the

interaction between sets of these parameters; and where these interactions may be non-linear. As in the example above, new, more complex systems may be developed to produce better ways of achieving an existing capability. More interestingly, they may be used to enable new functions.

1.1.3 Environment complexity

All machines operate in an environment. Often this is well controlled and benign, as is normally the case for the word-processor. However, the more interesting systems are required to work in harsh, dynamic environments, such as deep space, or the depths of the ocean. Here, determining the performance of the system becomes a greater challenge, both because of the difficulty of simulating the environment, and because of the complexity of possible interactions between the system and its environment.

1.1.4 Determination of performance

The design process for complex systems is a matter of establishing which parameters are most important to the required system performance and finding the best compromise between them. Of necessity, the full complexity of the system cannot be addressed during design. For any reasonably complex system it will invariably prove impractical to take account of all possible system and environmental parameter interactions. Simplifying assumptions are inevitably made when calculating the effects of alternatives, or when measuring them under laboratory conditions. Cost and timescale pressures will lead to one of a large number of sub-optimal solutions being chosen. System performance may meet the specified performance when it enters service, but it is likely to be sub-optimal in terms of what the system could achieve.

Before entering service, systems are subject to a series of acceptance tests to establish their performance. However, these are usually carried out for contractual purposes and are designed to establish whether performance meets specification. The full capability of the system may, therefore, still be unknown in so far as all corners of its envelope need not have been explored. In particular, it is often the case that some performance parameters, although critical, are very difficult to measure and so remain untested. As an example, for a missile system, the ability to engage the specified range of targets in all weathers from flat calm (with its multi-path problems) to full storm conditions (with its clutter and attenuation problems) is likely to be impossible to simulate and so not be

directly measured, even though it is possibly one of the key performance parameters of the system. So for many cases actual performance under operational conditions will not be known.

Additionally, even in those areas where performance on delivery is fully characterised, performance will change with time during service due both to modification and to deterioration. So confidence in performance and performance optimisation will deteriorate with time.

For all of these reasons, a means of readily determining key performance parameters under actual operating conditions is needed, both on entering service and, thereafter, throughout life. Where the parameters are readily measurable, this is comparatively simple to achieve. For these cases, most systems are reasonably comprehensively instrumented, both for direct system output purposes and for in-service maintenance. Many systems have continual monitoring of these parameters together with logging of the data. However, where key parameters cannot readily be measured in-service (e.g. the sub-clutter visibility of a radar system, where independent determination of the clutter present is difficult, or, as in the subject of this thesis, the drag force of a vehicle, where no drag transducer exists), a means needs to be developed of doing so.

1.1.5 Performance estimation

Usually system performance models are devised during development as an aid to decision making as to how most economically to meet the requirement. For the reasons given above, modelling of the system outputs is necessarily founded on simplification. For optimal performance the full complexity of the system needs to be captured in the model. Any digital simulation necessarily implies deciding in advance the important interactions between parameters and the nature of these interactions. The output of such models will require verification. It is, thus, concluded that if performance is to be globally optimised, decisions should be made, where possible, based on measurements of the real system in its real environment. Where this is not possible, modelling should be undertaken with a minimum number of simplifications by using analogue models under realistic conditions.

1.1.6 Three levels of characterisation

This thesis considers the problem of characterising a complex system at three levels. At the higher level, a superficial description of a generic system-engineering problem has

just been outlined. This is considered in no greater depth, but these principles are developed at the next level in the context of the propulsion system of Autonomous Underwater Vehicles (AUVs). Finally, the propulsion system of a particular vehicle, AUTOSUB, is considered by way of an example. This leads to consideration of the measurement of one particular system parameter, that of drag. Specific means of determining this parameter in the context of the full complexity of the vehicle and its environment is addressed.

A systems engineering approach to the problem of in-service improvement of the propulsion performance of an AUV is described together with the development of a set of tools to enable the improvements sought. The tools described have been developed for, and demonstrated on, AUTOSUB. However, it is believed that the principles underlying the design are widely applicable across a range of AUVs and will help in the systematic development of current and future generations of vehicles. The approach may also find use in the wider world as part of the move from taking an idealised approach to engineering, to attempting to take a holistic view. The work described here is a step on the road towards taking into account the full complexities of reality when optimising complex systems.

1.1.7 Structure of this document

Because of the breadth of subjects covered, the thesis is divided into four parts. No separate literature review has been included. Rather reference is made to the relevant documents in each chapter, as appropriate.

The initial part considers the overall problem of the propulsion performance of a particular AUV, whose performance, on entering service, was found to be less than expected and whose performance was then found to further deteriorate with time. The propulsion system is considered as a systems engineering problem and the system analysis is described. This part concludes that, of the key parameters affecting propulsion, the drag of the hull and/or the thrust of the propulsor under operational conditions is unknown. One reason for this is that the hull-form is more complex than had been allowed for during design. Another is that the vehicle is operated in service in a different regime from that anticipated during development. The case is made for a complementary programme of laboratory experiments on a scale-model, together with trials on the full-scale vehicle in service. The intention of the scale-model trials is to characterise separately, the components of the hull over the range of conditions likely to

be met in service. This should enable the performance of different hull forms to be predicted. Additionally, a means of measuring the added mass of the vehicle is required, for use in analysis of the data from the sea trials. The sea trials are to develop and demonstrate a means of readily determining the propulsion characteristics of the vehicle whilst in service. It is also required to establish the range of values of key parameters over which the laboratory measurements need be made.

Part 2 describes the design and practice of the series of laboratory experiments to determine the contribution to drag of components of the hull and its added mass. In particular, it addresses the problem of how to determine the effects of, and interactions between, a large number of parameters in an affordable series of experiments. It concludes with a model for predicting the drag of a range of hull-forms, together with an estimate of the bare hull added mass.

Part 3 describes the design and practice of an in-service trial intended to readily enable the propulsion performance of the vehicle to be determined during deployments. It describes the data analysis process and an estimate of the drag of the vehicle is made from measurements of speed as a function of time. It also determines the range of angles-of-attack and hydroplane angles over which the laboratory experiments need to be conducted, together with the relationship between each of these and with speed.

Finally, part 4 pulls together the whole thesis and draws conclusions.

Part 1

SYSTEM ANALYSIS

Chapter 1.1

INTRODUCTION

Part 1 begins with a generic description of AUVs. The particular AUV used as an example for this work, AUTOSUB, is then described, together with the symptoms of the propulsion problem. To calibrate the problem, AUTOSUB's performance is compared with that of similar vehicles.

Attention then switches to consideration of the issues associated with systems engineering of an in-service system and definitions of complexity. The first consideration is an analysis of the propulsion system of AUVs, using AUTOSUB as an example. This analysis begins with capture of the overall requirement and the development of a parametric model to enable the sensitivity to fundamental system parameters to be established. The performance of each of the major sub-systems is then assessed and its influence determined. Conclusions are drawn as to where effort should be concentrated. In particular the need for a greater understanding of the hull drag characteristics, propeller and hull/propeller interactions is established. Of these it is argued that effort should be concentrated on further exploration of the drag of the hull under operational conditions. Because the detail of the hull-formchanges from mission to mission as a result of changes needed to payload and services, the need for a method of determining the effects of these is required. The implications and complexity of determining drag across the full range of operational conditions and hull-form options is discussed.

The need for physical modelling is discussed and the alternatives compared. The vehicle was extensively modelled during its development phase. However, as is usual, an idealised hull-formwas used. Although the models used provided an accurate reflection of the clean hull used in service, it lacked the detailed appendages, and did not reflect, for example, the surface condition that the real vehicle has when operated in the harsh environment of a seaway. In this thesis methods are described for establishing the effects of the full complexity of the vehicle as operated at sea. It addresses the problem of designing a programme of experiments to explore a large set of complex interactions. The need for both laboratory experiments and trials on the full-scale vehicle at sea is developed.

Having introduced the subject matter of this part and described its overall structure we can now move into the subject matter starting with an introduction to AUVs.

Chapter 1.2

AUTONOMOUS UNDERWATER VEHICLES

1.2.1 Introduction

The demand for knowledge of the oceans, of what they comprise, how they work, and what is in them and under them, has never been greater. In the past this quest for knowledge was driven by the need for improved navigation and by scientific curiosity. Today the major non-military drivers are the threat of climate change, resource management, exploration for new resources, and a need for a holistic appreciation of the mechanisms that influence the world's ecosystem. Unlike the atmosphere, the oceans comprise a body of fluid that is not susceptible to long range observation. Electromagnetic radiation, unless at ultra low frequency (and hence data rate) attenuates very rapidly and sonic radiation, although much more penetrative, still will not produce high-resolution information at more than a few 10's of kilometres. There is, therefore, a need to take sensors into the body of the ocean. Manned vehicles are expensive, and remotely operated vehicles necessarily limited by short-range, limited-bandwidth communications, or the length of a high-bandwidth umbilical. Hence the need for autonomous underwater vehicles.

There is a considerable history of building underwater vehicles from manned submarines to guided torpedoes and remotely operated vehicles (ROV's). However, the principal characteristic of these devices is that they have either been controlled by a man in the loop, as for submarines or ROV's, or have been single shot, one way devices, such as torpedoes and some scientific instruments. Only comparatively recently, from the mid 1980's, has the technology been developed to allow completely autonomous operation at reasonable cost. During this period most major economies have invested in this new technology. Not surprisingly the vast majority of the effort expended has been spent on the essential aspects of autonomy: automatic navigation, guidance and control. Considerable progress has been made and this progress is accelerating. In 2002 there were more than 100 vehicle types, often one-off designs,

routinely operated by more than 20 countries. The USA alone boasted 35 types of vehicle. (Funnell, 2001).

1.2.2 The essential characteristics

An AUV is an autonomous underwater transport system. Its function is to carry a payload. Normally the load is carried internally which requires dedicated volume, possibly with some form of conditioning, such as power supplies or pressure resistance.

Autonomy implies the ability to carry out tasks independent of real-time human control. This requires an on-board mission controller. At the lowest level, this implies that the vehicle be capable of storing and executing a series of pre-planned instructions. This limited capability is only useful for operation in open water, where no unplanned obstacles are expected. To operate in confined spaces more advanced designs are required, which incorporate the ability to adapt the mission to local conditions. This implies real-time decisions being made on the basis of sensor information. For example, the AUTOSUB vehicle has a collision avoidance routine based on the input from a forward looking and a downward looking sonar. For operation in still more complex environments, such as some of those encountered by the military, it is likely that future vehicles will incorporate the ability to 'learn' from their environment, that is adapt their decision making rules according to historical precedent.

In order to carry out the mission the vehicle will need to be capable of navigation. It will need some means of determining its starting point and its position thereafter. When submerged the vehicle will be incapable of receiving signals from the standard navigation beacons used for surface navigation, since these are invariably transmitted over the EM spectrum. Some form of dead reckoning will, therefore, be required, based on measurement of heading and distance. Distance will need to be measured directly by some form of log, or computed from measurement of time and velocity and/or acceleration.

Having knowledge of current location, from the navigation system, and the desired location, from the mission controller, the vehicle requires a means of locomotion and a means of controlling it in terms of speed and direction. Locomotion implies some means of interacting with the water such that motion with a forward element may be obtained. This often implies a motor and some form of propeller,

although forward motion can be obtained by passive means such as gliding. An energy supply is needed to power the means of propulsion. Normally some form of internal energy storage is essential, although in some cases, such as solar powered AUVs, this may be supplemented by energy extracted from the environment.

Direction control is usually achieved by means of trainable thrusters or by control surfaces.

Finally, to operate underwater, a means of depth control is required. This may be achieved as in manned submarines, by buoyancy control, but often the vehicles are designed to have marginal positive buoyancy for recovery purposes. In this case depth is maintained either by directed thrust and/or negative lift control surfaces.

1.2.3 Progress to date

1.2.3.1 Size and shape

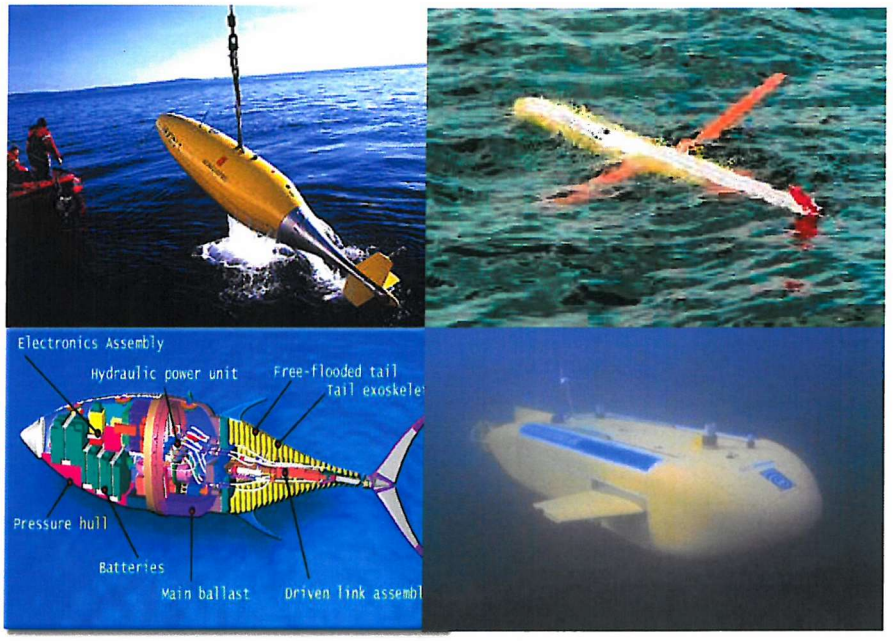

Figure 1.2.1 AUVs come in all shapes and sizes
(Clockwise from top left: Hugin, Slocum, Maridan, VCUUV)

AUVs are at that exciting stage of evolution where an enormous variety of different architectures are being tried and before the natural selection pressures of economy and efficiency have whittled these down. They come in a considerable range of sizes and shapes as illustrated in Figure 1.2.1. Sizes range from the 950 mm length of the RAO (Funnell, 2001) , to the 11 m of the Manta, with the latter having a displacement of 16

tons (French and Lisiewicz, 1999) and shapes vary from very low drag forms, through the more easily manufactured, but slightly less hull-efficient torpedo shape, to those where manoeuvrability is all. The latter may have completely inefficient hydrodynamic shapes but allow full 6 degrees of freedom movement.

1.2.3.2 Applications

The large variety of AUV forms is partly due to the drive to try out new ideas and find out what works, but is also driven by the large range of potential applications. The early AUV had much of the characteristics of a technological solution looking for a problem. Advertised ranges, payloads and navigational accuracy were suspect and reliability was insufficiently proven to justify business cases for serious investment in industrial capability. The principal areas that supported the investment were those supporting engineering research, the science community (who had no other way of obtaining some highly desirable data sets), and the military. This is now changing with the accumulated body of knowledge resulting from these first-generation vehicles and the advent of second-generation vehicles. A sample of possible applications is listed below.

- Science.
    - For use where access by other means is impossible, e.g. for obtaining extensive data on phenomena that occur under ice-shelves, where the only alternative would be bore holes, which are both expensive and intrusive.
    - Where the presence of a more intrusive vehicle would interfere with the measurement being made, e.g. for measurement of fish stocks, where it has been shown by AUTOSUB that fish will avoid a surface vessel, but apparently ignore an AUV.
    - Where the application is driven by lower cost and rapid deployment without extensive pre-planning, e.g. for the measurement of pressure waves, where the alternatives are buoy arrays, aircraft or satellites (Healey and Riedel, 1999).
- Industry
    - Survey, maintenance and laying of services (e.g. telephone cables, or oil facilities).
    - Exploration for mineral resources.

- Fish stock management.
- Environment forecasting.

- Military.
  - Reconnaissance.
  - Mine hunting.
  - Target tracking.
  - Navigation beacon.
  - Communications relay.
  - Attack of surface and submarine targets.
  - Beach survey.
  - Surveillance.

1.2.3.3 Overall AUV system performance

Many of the AUVs built to date have been considered, to a greater or lesser degree, as a total integrated system. However, the systems level work has been directed primarily at either scoping the overall AUV as an initial design study (and so has taken a mainly parametric approach (Huggins and Packwood, 1994)) or has concentrated on producing an integrated navigation and control system (D Fryxell, 1994). Few have had as its primary intent the optimisation of propulsion efficiency. Propulsion optimisation driven research has, in general, concentrated on the motor/propulsor interaction (Bradley et al., 2001) or motor/controller matching (Hunter and Stevenson, 1994) (Brown and Kopp, 1994). Such research has been directed at investigating the way in which off-the-shelf components may be integrated, rather than on determining the cost of using non-optimised components. Work has been undertaken on a number of other sets of sub-systems within the overall propulsion system (Glover and Guner, 1994), (Stevenson, 1996).

1.2.3.3.1 Endurance

In principle, those vehicles that can extract their energy from the environment are limited in endurance only by their need for maintenance. In practice all vehicles require some form of on-board energy storage, and this usually involves primary, rather than secondary, energy. A range of up to 40,000 km is claimed for the SLOCUM glider (Funnell, 2001).

However, most vehicles are entirely dependent upon the energy with which they are charged at the beginning of a mission. Proposals have been made for in-mission docking, for re-fuelling without the need for the vehicle to be recovered, but these remain at the experimental stage. Of the vehicles that carry their energy supplies with them, the maximum range is in the region of 750 km (AUTOSUB and THESEUS (Funnell, 2001)).

1.2.3.3.2 Speed

AUVs are inherently energy and power limited devices, with the power available being dependent on the characteristics of the energy supply. The power required to propel a submerged vehicle increases as the cube of the speed. Whereas high underwater speeds are undoubtedly achievable, with, for example, super-cavitating devices, these are only possible over short ranges, and even then require high energy density power supplies and propulsors. For most applications range is a higher priority than speed so AUVs tend to operate at very low speeds of around 2 m/s (4knots).

1.2.3.3.3 Depth

The technology to enable travel to great depths has been established such that the deepest oceans have received at least tentative exploration. However, engineering the vehicle to withstand the pressures at such depths is very expensive. Nevertheless, one of the attractions of AUVs is to be able to operate at much greater depths than is achievable with 'conventional' manned submarines. Many of the applications for AUVs may be achieved on or near the continental shelf and in the major ocean basins within a depth range of 1000 m. This has tended to be the maximum depth to which first generation AUVs have been designed, although some of these are now being modified to enable depths of up to 3000 m to be achieved. However, if depth can be increased to 6000m then more than 90% of the seabed area becomes accessible. Some second-generation vehicles are, therefore, being designed to this standard.

1.2.3.3.4 Positional accuracy

The ability of the AUV to be aware of its position to a defined degree of accuracy is required for three principal reasons.

1. So that collected data may be referenced and correlated with other data.
2. So that useful range may be maximised (as discussed in chapter 1.5).
3. So that the recovery area for the vehicle at the end of a mission is small.

Although GPS may be used to provide an accurate fix before diving, once submerged the vehicle is usually dependent upon on-board sensors. Accuracy is, therefore, limited to the inherent discrimination of the sensors and the rate at which their performance drifts. Positional accuracies of 0.2% of range have been claimed.

1.2.3.4 Sub-system performance

1.2.3.4.1 Mission controller

The most basic controller comprises a small, dedicated processor carrying out a list of instructions. However, this tends to be inflexible, both in terms of ability to update the controller and in terms of being able to reconfigure the system. These disadvantages are compounded by the fact that this key component forms a single point of failure node. More advanced AUVs, therefore, have opted for distributed intelligent control. This allows reconfiguration of sensor and payload systems. The intelligence enables complex tasks to be automated and the distributed nature of the system both enables new functions to be readily incorporated and critical functions to be duplicated. This type of system is used, for example on OCEAN VOYAGER as described by (Smith, 1994).

1.2.3.4.2 Navigation

The navigation problem for the submerged underwater vehicle is the unavailability of navigation information transmitted via the electromagnetic spectrum, such as that from the Global Positioning System (GPS). One way round the problem is to create an underwater equivalent of the GPS by laying a pattern of acoustic transponders at known positions, from which vehicle position can be derived. However, this is expensive and only practical for comparatively small areas. For longer range vehicles, or for those required to undertake surveys themselves, autonomous navigation is required.

Thus, on-board sensors are required to enable position to be estimated by dead reckoning. This requires measurement of distance travelled and direction of travel. Direction may be derived from a combination of accelerometers, pendulums

and/or gyro or flux gate compass (D Fryxell, 1994). Distance may be derived from measurement of time and velocity or acceleration. Velocity is usually derived from acoustic Doppler systems measuring speed over ground from bottom measurements and speed through water from specula reflections.

1.2.3.4.3 Vehicle attitude control

The aim of the control system is to be able to induce pitch, roll and yaw accelerations with sufficient accuracy to enable the required trajectory to be followed within defined error margins. The requirement is to achieve zero steady-state error with a system that demands a bandwidth that is consistent with realisable actuators, and with closed loop damping and stability margins (Fossen, 1994). There are two principal methods of generating control forces: via control surfaces, or by directional thrusters. Examples of both exist, but the additional weight and complexity of separate thrusters is only justified where very high manoeuvrability is required at low speed. Generally, for long-range vehicles only control planes are used.

Within the constraints given above, the size of the control surfaces needs to be minimised to reduce steady-state drag. However, the size required is a function of the speed of the vehicle and the minimum economic speed is determined by that at which control can be maintained. Clearly there is an interaction between speed, the size of the control surfaces and control system performance. The design of the control system and control surfaces can be optimised to minimise the overall drag (Fryxell et al., 1994) for any given mission profile. The size of control surface and whether both fore and aft planes are required depends on the agility required by the mission profile.

Where there is no requirement for high agility, it may be possible to use a propulsor that is capable of generating control forces as well as thrust and so do away with the need for separate control surfaces. This can be achieved through a steerable propeller, or more elegantly by having each propeller blade independently controllable in pitch. Pitch can then be varied both collectively to provide forward thrust, and cyclically to provide lateral thrust, in much the same way as the rotor of a helicopter.

1.2.3.4.4 Depth control

Manned submarines are equipped with ballast tanks so that buoyancy may be controlled. However, these systems are complex, expensive and consume valuable

space. AUVs, therefore, tend to be designed to be constant buoyancy devices. For security of recovery in the event of a catastrophic failure, they usually have a small margin of positive buoyancy (of the order of 0.1%). Drop weights are also often included to provide an additional margin of safety.

Pressure at depth tends to reduce the volume of the vehicle and, therefore, its inherent buoyancy. For this reason some form of stable buoyancy margin is provided in the form of syntactic foam or spherical glass vessels.

Under conditions of positive buoyancy, depth is maintained either by 'flying' the vehicle downwards, using negative lifting surfaces, or by the use of directed thrust. The thrust may be directed by means of a gimballed main thruster, by auxiliary thrusters, or by controlling the angle-of-attack of the vehicle by moving its centre of gravity.

1.2.3.4.5 Energy supplies

An ideal vehicle would extract its energy from the environment when needed. Examples in the above-water world include sailing craft utilising wind currents and gliders utilising a mixture of thermal energy stored in the atmosphere and gravitational energy stored in the mass of its structure. It is noticeable that the apertures through which they capture this energy determines the size of the vessel. However, underwater potential energy supplies such as pressure, currents and temperature have very low gradients. To use these requires a very much larger aperture compared with the size of the vessel such that they are largely impractical. However, there has been some interest in buoyancy powered underwater gliders. These are necessarily slow, and have difficulty in maintaining constant depth, but propulsion efficiencies of the order of 70% have been claimed (Simonetti and Webb, 1999).

Another source of external energy is that from the electromagnetic spectrum in terms of solar energy. Whilst this is practicable for some applications on the surface, solar radiation is attenuated so rapidly in water that it is currently of no use at any significant depth. However, a solar powered AUV has been developed that relies on returning to the surface to charge its batteries during daylight, and then using the stored energy at night. Potentially its range is unlimited, but its average speed at depth is necessarily limited by the need to spend time at the surface recharging.

Because of these limitations, except for very specialised applications, all practical AUVs carry their energy supplies with them. The key measure of goodness of an energy store is energy density. However, this needs to be balanced against other factors including cost, safety and the rate at which energy can be drawn (power density). A list of possible energy storage media and their associated energy and power densities is given in Table 1.2.1.

Table 1.2.1 shows that, by far the greatest energy density can be obtained using nuclear technology. However, cost and safety issues preclude these from use in virtually all applications. Hydrocarbon fuels also have very high energy densities. However, use of these in heat engines is invariably complex in that a source of oxygen is required, as is a sink for the exhaust products. Pressure balancing for outboard exhaust is complex and storage uses precious volume (Kumm, 1990) (Potter et al., 1998). As a consequence, the associated prime movers are bulky and net energy density low. Hydrocarbon based fuel cells appears more promising, but there is the need to crack the fuel into useable constituents and the complexity of the fuel cell itself (Sedor, 1989) (Hart and Womak, 1967).

Energy Store	Energy Density Wh/kg
Electrical super capacitor	5
Electrical superconducting electromagnet	5
Thermal storage	30 - 60
Hydrocarbon fuel	12000
Mechanical Flywheel	132 - 198
Secondary Batteries	17 - 260
Primary Batteries	20 - 660
Fuel Cells	1500
Nuclear	> 3x10^4

Table 1.2.1 Energy Source Densities

The use of Fuel cells using other than hydrocarbon fuels has been explored. Ideally a variety that operates at low temperatures is desirable for containment and safety

reasons, e.g. the polymer-electrolyte fuel cell (Tamura et al., 2000). A 1.7 kW aluminium fuel cell developed specifically for AUVs is described by Scamans, et al (Scamans et al., 1994). The energy density of this device is dependent on the form of oxygen storage used, but is of the order of 260 Wh/l for compressed oxygen and 320 Wh/l for liquid oxygen. It is generally accepted that the key to economic development of practical fuel cells lies in the speed and direction of developments in the automotive market, and until this matures purpose built fuel cells will prove an expensive option.

Because of these complications and costs, chemical batteries power the great majority of AUVs. Secondary batteries are preferable in that refuelling is simple and cheap. However, initial costs are higher and energy densities were lower than for comparable primary batteries, so for first-generation vehicles, primary batteries tended to be used. However, there is now a distinct trend to using higher energy density secondary batteries in second-generation AUVs as the costs decrease.

Affordable energy supplies, therefore, provide a severe constraint on the range of the vehicle. Foreseeable developments in battery (Sharkh et al., 2002) and fuel cell technology are unlikely to increase energy density to such an extent that available energy will not remain a severe constraint on the range performance of these vehicle.

1.2.3.4.6 Prime movers

A prime mover is required to convert the stored energy into mechanical energy for use by the propulsor. Clearly the motor must be compatible with the energy supply. Nuclear power is usually used to heat a boiler to produce steam, which may be used to drive a turbine, although in principle it could be used as the heat source for any other form of external combustion engine such as a Stirling engine. The prime mover may be connected to the propeller either directly through a gearbox, or indirectly by interposing a generator and electric motor. Because of the severe disadvantages of nuclear power these devices will be considered no further.

Hydrocarbon may be used either aerobically, employing stored oxygen, or cracked into components for use in a fuel cell. When used aerobically, they may be used in internal combustion engines, such as conventional diesels, or in external combustion engines such as steam turbines, steam reciprocating engines or Stirling engines. A principal requirement for true submarines is that they should be independent of the need for air from the atmosphere, although the Canadians have

developed a successful submersible vehicle, DOLPHIN, that is powered by a conventional diesel engine, with air supplied through a snorkel (Funnell, 2001). The Japanese have developed a true submarine driven by a closed cycle diesel engine, but it appears not to have been very successful.

A wide range of air independent Stirling engines have been developed and tested in simulations (Reader et al., 1998). A typical engine could develop 15 kW and be suitable for vehicles of 5 tons or greater (Nilsson, 1989), although there are references to engines small enough for use by individual divers (Reader et al., 1998).

Because of the cost and complexity of using heat engines, the great majority of AUVs use directly supplied electric motors, matched to conventional electric batteries.

Of electric motors by far the most popular is the permanent magnet dc machine coupled with a Pulse Width Modulation (PMW) Controller. This is partly because of the ready availability of dc power in battery-powered vehicles and partly because of its power density, ease of control and torque characteristics. The critical parameters when considering the motor and its controller are described in (Brown and Kopp, 1994) and (Kenjo and Nagamori, 1985a). This type of system is described in more detail in the chapter 1.3.

1.2.3.4.7 Motor/Propulsor Coupling

For rotating propulsors, gearboxes are aften used to match the optimal speed/torque of the motor to that of the propeller (Clower and Poole, 1992). However, gearboxes require an allocation of the volume/mass budget, are potentially noisy, and, although inherently efficient, do not pass all of the energy to the propulsor. There is, therefore, a strong incentive to provide an integrated, hard coupled, motor/propeller design.

1.2.3.4.8 Propulsors

Novel means of propulsion based on 'bio-mimicking' have been explored, including a mechanism that mimics the jet used by squid (Muggeridge, 1992) and oscillating foils which mimic tuna (Moody, 2001). Although efficiencies of greater than 70% have been claimed, these remain very much at the early exploratory stage.

The majority of AUVs, therefore, use conventional rotating propellers. Many use 'off-the-shelf' rather than purpose designed propellers, often from the model aircraft industry (MARIUS and ABE). This fact well illustrates the lack of priority

given to date to propulsion efficiency. Where propulsion efficiency has been given some priority, consideration has been given to the use of contra-rotating pairs in order to recover energy dissipated in radial motion. However, calculations undertaken by DERA (Stanier, 1992) concluded that for low speed lightly loaded propellers, the additional efficiency obtained is marginal. An alternative means of increasing efficiency is to provide a duct and either pre- or post-swirl vanes to produce a pump jet (Glover and Guner, 1994). However, again for most AUV applications there is little gain over a large diameter open-water propeller. A less complicated arrangement, where propellers are operated in smooth ducting is sometimes used, although gains can be small since improved hydrodynamics is offset by increased friction drag as a result of increase in surface area. Shrouding of the duct has been shown to improve the hydrodynamics still more, but at the expense of increased complication. (Holappa and Page, 2000)

Propellers are suitable for cruising or precise manoeuvring, but not both simultaneously. A compromise between the bio-mimicking and conventional propellers has been developed in the form of flexible fins, the so called Nektors (Moody, 2001). These have the ability to allow vehicles to translate in any direction and to yaw, pitch and role. Four of these will enable 6 degrees of freedom motion. They are claimed to be as efficient for cruising as propellers but have yet to be proven on a production vehicle.

1.2.3.4.9 Hull-form

Most designs of AUV have recognised the importance of incorporating low drag hulls. The technology for minimising drag centres on the shape, design of the body surface and modification of the boundary layer itself. A large number of low drag hull forms have been developed (e.g. that at (Kawai and Kioichi, 2001)). However, all are of complex shape. This makes them expensive to manufacture and makes the efficient utilisation of the enclosed volume difficult. It also makes no allowance for payloads and system services, which need to interact with the AUVs environment, via windows, orifices or appendages. Practical hull shapes are, therefore, nearly always a compromise.

To be effective, low drag hulls are also dependent on very smooth surfaces. These are expensive to produce and difficult to maintain in service. Alternatives to smooth surfaces, including compliant coatings and riblet films, have been explored,

but to date have only been used in special circumstances (Osse, 1998). The efficacy of the surface in reducing drag can be complemented by specific measures to change the properties of the boundary layer. These include injecting micro-bubbles (Madavan et al., 1986) or creating partial vacuums via a micro-porous skin, heating the hull surface, and injecting polymers. All of these require the AUV to carry additional consumables.

1.2.4 Bio-mimicking

There is a large body of experimental data that suggests that biological systems achieve very high overall propulsive efficiency and that, therefore, reproducing their properties may make for better AUVs. Fish and related species achieve high performance by means of a flexible, streamlined body propelled by oscillating flexible and adaptable surfaces. Understanding of the phenomena involved is increasing rapidly, but development of the technology to reproduce the effects is in its infancy. For example it is known that the flexible properties of some fish can compensate for boundary layer fluctuations in pressure and so reduce the onset of turbulence (Babenko et al., 2000). However, these properties have yet to be synthesised in the laboratory. MIT has built a robot based on the design of a tuna. This supports the belief that there is considerable potential for very high propulsive efficiencies under certain circumstances. But, at present, there are disadvantages in terms of the efficiency with which bio-mimicking prime movers convert energy, and in the practicality of the space available for the payload in any fish shaped vehicle.

In general, biological systems have evolved to be able to cope with a broad spectrum of circumstances simultaneously. Thus, a typical fish has characteristics which are a compromise between those necessary for low energy cruising, in order to find food, and those necessary for rapid linear and angular accelerations, in order to avoid becoming food. Even multi-role AUVs tend to be more specialised than this, so there is likely to be a limit to the degree to which bio-mimicking may be usefully taken. It is more likely to be useful in terms of sub-systems, rather than in providing complete system solutions.

1.2.5 The next steps

The technology for producing AUV systems is now moving from early design stage towards maturity. A first generation of reliable, capable AUV designs have now been

produced and these are being built upon. Although there remain a large variety of architectures, a number of classes of AUV, with identifiably similar features, are emerging. These include:

- Small short-range hand launched vehicles, of the order of 1 m in length, and capable of being launched from the shore or from small boats. These tend to be torpedo shaped and modular in construction so that their function may be readily changed.
- Medium range vehicles with high manoeuvrability, which tend to be of the order of 2 m in length and involve the use of a number of thrusters as well as a main propulsion propeller. These tend to be more cubic in shape to provide inherent positional stability.
- Long range vehicles of the order of 7 to 10 m in length. These tend to be torpedo shaped and to rely solely on hydroplanes for depth and directional control.

The required characteristics of the major sub-systems are now well known and further advances in, for example, navigation and control, are likely to be evolutionary. They will to some extent be dependent on advances in other technologies, such as increased processing power, reduced memory costs and improved gyroscopes.

Achieving increased depths at acceptable costs remains a challenge. Components to withstand depths of 1000 m are fairly readily available as a result, for example, of demands from the oil industry. Components such as glands and connectors to withstand depths greater than this remain problematic. The size and shape of vehicles suitable for greater depth has also yet to be finalised, with some suggestion that smaller slower vehicles may be appropriate.

The final key challenge for AUV technology, that of achieving long range at affordable cost, remains to be satisfactorily met. At present there seems to be little prospect that increased energy density energy storage systems will produce a step increase in capability. Propulsion motors are reasonably efficient, and the technology of propellers is well developed. There appears to be some scope for reduced drag hull-forms, but this again is likely to produce only small incremental improvements. The only remaining solutions are a completely new approach to the whole problem, or squeezing the maximum out of the currently available components by careful optimisation of the whole propulsion system. The approach of mimicking biological

designs may offer a fresh approach in the medium term, but the technologies are poorly understood at present. This leaves the option of propulsion system performance optimisation, which forms the subject for the remainder of this thesis.

1.2.6 Summary

It has been argued that improving the range of AUVs by optimisation of their propulsion systems is one of the major outstanding issues in AUV technology. We next consider the case of a particular AUV, that of AUTOSUB, to put this issue in context.

Chapter 1.3

AUTOSUB

1.3.1 Introduction

To this point we have described a generic issue whereby it is unlikely that the full characteristics of any system exhibiting a reasonable degree of complexity will be known on entry into service. This has two consequences. The first is that it is unlikely to have been optimised to realise its full potential performance and the second that, because of uncertainty as to its actual performance, it will be operated with a larger margin of safety than would be necessary if its full characteristics were known.

We have then focussed on a particular class of system, that of the AUV, and described its current state of evolution. We have argued that one of the outstanding issues in AUV technology is range optimisation and it is concluded that it is likely that many of the first generation of AUVs now in service are likely to be operating with sub-optimal propulsion systems.

In this chapter we focus still further on a particular AUV design, that of AUTOSUB, with a view to assessing its performance. The chapter begins by describing the purpose and construction of the vehicle. To provide a yardstick, its overall propulsion performance is then compared with that of other AUVs of similar size. This chapter concludes with a comparison between the performance actually achieved in-service and that expected at the design stage.

1.3.2 Purpose

AUTOSUB is a multi-role, re-configurable system for the collection of hydrographical and biological scientific data. It is intended for use on long transits. As such, the qualities of endurance and range are valued above those of agility and attitude control. The formal requirement is discussed further in chapter 1.5.

1.3.3 Description

The vehicle is torpedo shaped. Its form is illustrated in Figure 1.3.1.

It is 6.7m long by 900 mm in diameter and weighs 1500 kg in air, with a displacement of 1700 kg. Because of its size special handling equipment is required. An indication of its size and the handling equipment required is given in Figure 1.3.2.

Figure 1.3.1 AUTOSUB form

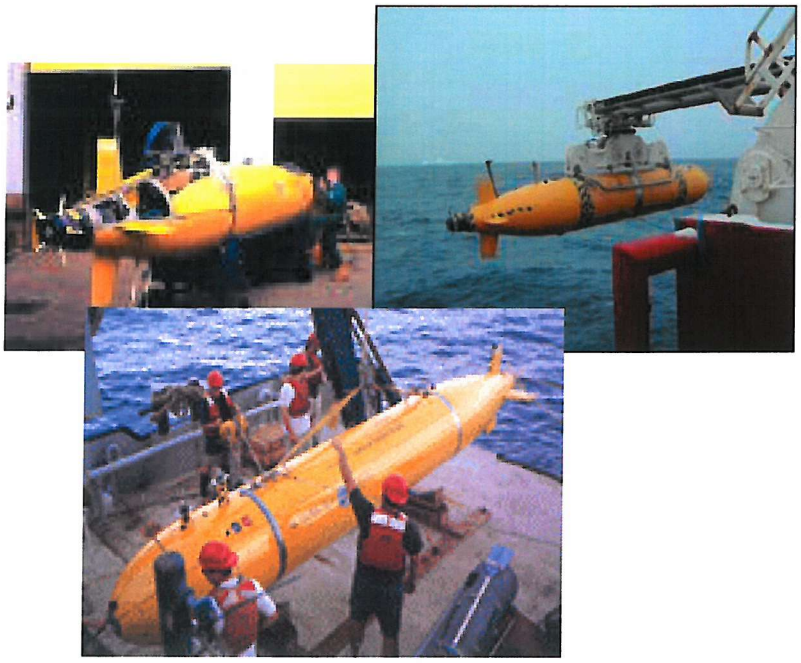

Figure 1.3.2 AUTOSUB handling

The vehicle comprises three main sections:

- A free flooding elliptical nose section reserved principally for the payload.
- A dry cylindrical central section comprising a set of pressure vessels, which contain the batteries, power distribution system and main electronics.
- A free flooding faired truncated conical tail section devoted mainly to propulsion and control.

The fore and aft sections are built on a framework of channelled aluminium which allows ready reconfiguration of the components located in these areas, as illustrated in

Figure 1.3.3. Fairing of these sections is provided by cast GRP panels fixed by countersunk screws. The fore and aft sections are connected to the central cylinder by means of stainless steel rings, which also contain the apertures to enable free flooding and drainage.

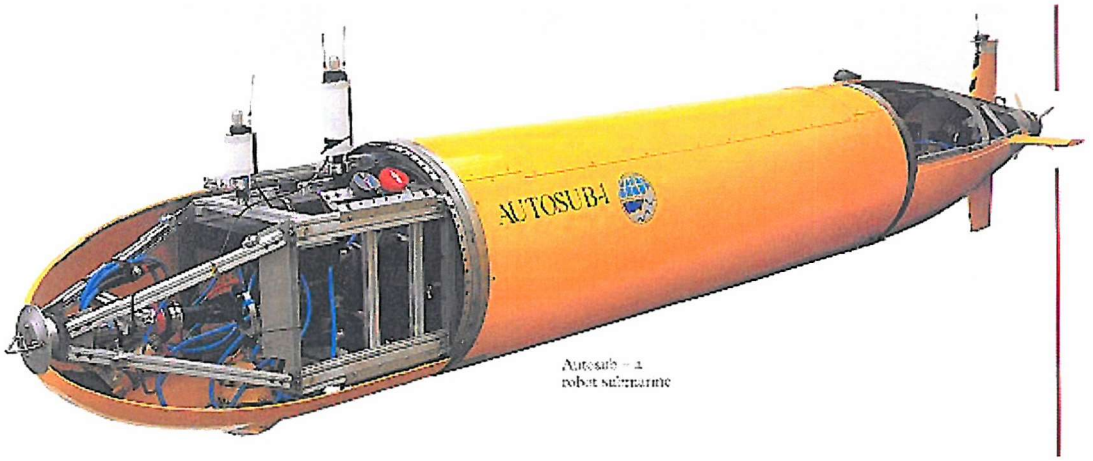

Figure 1.3.3 Construction of fore and aft sections

The central section comprises seven wound carbon fibre pressure vessels arranged to form a cylinder, with the interstices filled with syntactic foam for buoyancy purposes. Four of these cylinders are dedicated to the energy storage, one each to power distribution, and mission control and one to data logging, navigation and communication. A general schematic is given in Figure 1.3.4.

The energy supply comprises 17 battery packs in each of the four pods. Each battery pack comprises 75 alkaline manganese cells, providing a total of 5,100 cells with a mass of 600kg. The cells are arranged to provide a nominally 96 v d.c. rail.

Acoustic communication is provided for when the vehicle is submerged but close to the deployment facility. The vehicle is equipped with satcom EM links to facilitate rapid data transfer when surfaced.

Navigation fixes are provided by differential GPS when surfaced and by dead reckoning, provided from ADCP logging and fluxgate compass heading, when submerged. Mission control is by means of a series of waypoints, where the vehicle surfaces, if possible, to use GPS to correct dead reckoning errors.

Propulsion is provided by a five bladed propeller directly mounted on the rotor of a permanent magnet motor. This is described in greater depth in chapter 1.6

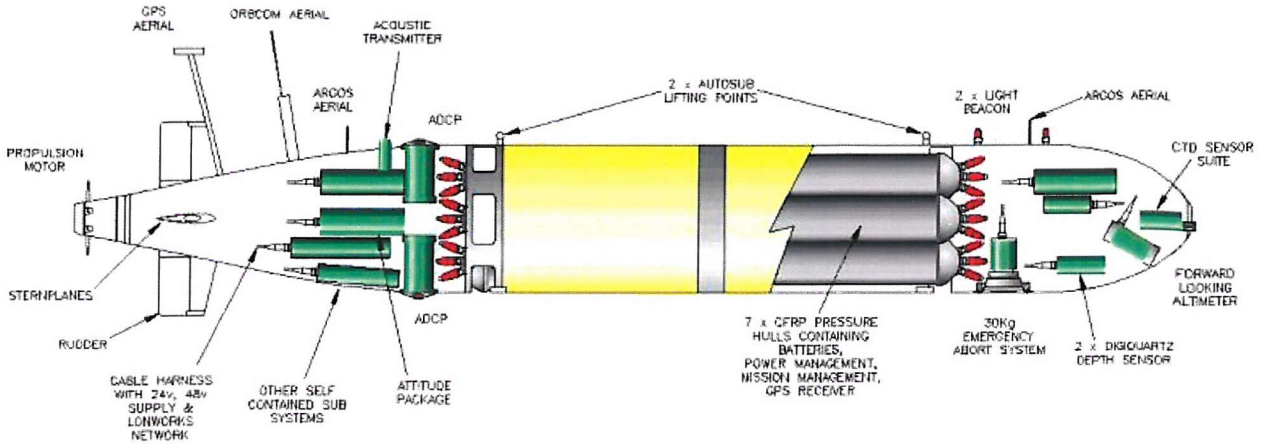

Figure 1.3.4 General schematic

Control is exercised by a cruciform set of 4 identical hydroplanes with moveable surfaces driven by stepper motors.

The vehicle is fitted with syntactic foam sections to maintain constant buoyancy with depth. It is ballasted to have a small reserve of positive buoyancy, the centre of which is designed to be above that of the C of G so that the vehicle is maintained in a stable attitude. Depth is controlled by means of the hydroplanes and the vehicle is fitted with drop-weights for use in emergency.

1.3.4 Design compared to other AUVs

For navigation purposes, most other first generation vehicles use similar combinations of sensors, i.e. a Doppler sonar log, coupled with accelerometers and a compass. Some next generation vehicles, including the latest version of AUTOSUB, are planned to have inertial navigation systems (INS) for use when submerged.

The hull shape is a compromise between cost of manufacture, ease of use of internal volume, and drag characteristics. Lower drag designs are in service, e.g. HUGIN, but most vehicles of this size and range have similar hull forms to AUTOSUB.

AUTOSUB is fitted with a specially designed, purpose built, motor tailored specifically to its requirements. The motor comprises a fixed wound stator surrounded by a permanent magnet rotor. The specially designed propeller blades are mounted directly on the rotor casing. This is unusual. Most other vehicles use off-the shelf

motors and propellers, with the motor being matched to the propeller through a gearbox.

Most vehicles of this type are battery powered, although there are examples using combustion engines and fuel cells. Many vehicles use secondary batteries to enable rapid recharging. AUTOSUB has remained with alkaline primary batteries for cost-effectiveness reasons.

1.3.5 Performance relative to comparable AUVs

Before a worthwhile comparison between the performance of AUTOSUB and that of other AUVs can be made we need to determine a measure of goodness. AUTOSUB is a long-range vehicle, designed for the collection of scientific data throughout the world. Clearly the size of the payload that can be carried, together with the depth to which it can be taken, and the accuracy with which its position can be measured are all important. The climates under which it has been proven to operate are also relevant

There are vehicles that have been designed for extreme range and which scavenge a large portion of their energy requirements from their environment. Examples of this include the SLOCUM glider and the Solar-powered Autonomous Underwater vehicles (SAUV). However, none have been built in the same class as AUTOSUB. That is the scavengers are small (< 2 m long) and consequently have little volume available for payloads. Similarly, the amount of on-board energy is extremely limited and so their ability to service the payload is restricted. For these reasons, we shall restrict out comparison to those vehicles that carry their own energy supply.

Self-contained vehicles are necessarily energy limited. The discussion on energy densities in chapter 1.2 demonstrated that it is reasonable to assume that all contending vehicles are likely to have energy storage system of roughly equivalent energy densities. Like-for-like range, coupled with payload carrying ability is, therefore, directly related to the size of the vehicle. Thus, comparison is only made with vehicles of similar size. According to Janes *(Funnell, 2001)* there are 8 such vehicles. These are listed in Table 1.3.1. One of these, HUGIN, has first and second generation versions with different depth capabilities, as does AUTOSUB. This issue will be addressed shortly. A second, Dolphin, is air breathing through a snorkel. It is , therefore, incapable of diving to any significant depth and is considered no further. A

third, Test Bed AUV, has been built as a technology demonstrator only, and so is also considered no further.

	Hull Dimensions			Performance				Payload
Name	Length (m)	Diameter (m)	Volume	Range (km)	Endurance (hrs)	Depth (m)	Speed Cruising (m/s)	Volume (m^3)
DOLPHIN	7.3	0.99	5.62	550	26		6	
AUTOSUB 1	6.82	0.9	4.34	800	100	600	2	1
AUTOSUB 2	6.82	0.9	4.34	800	100	1600	2	1
ISE-ARCS	6.5	0.7	2.50	37	4	400	2.5	
ISE-THESEUS	10.7	1.3	14.20	500	70	1000	2	1
REDERMOR	6	1	4.71	70	7	200	2.7	
R-One Robot	8.27	1.15	8.59	120	25	400	1	0.6
HUGIN	4.8	0.78	2.29	200	6-8 hr or 36 hr	600		
HUGIN 3000	5.3	1	4.16	290	40	3000	2	
Test Bed AUV	6.6	0.533	1.47					

Table 1.3.1 Vehicles of similar size

Data on deployments of the remaining vehicles is not readily available. However, AUTOSUB has undertaken to date in excess of 100 scientific missions worldwide. It has been deployed in temperate, tropical and Antarctic waters: in the North Sea, in the South West Approaches, the Mediterranean, and the Wedel Sea. AUTOUB's deployments are illustrated in Figure 1.3.5. It is unlikely that any of the other vehicles has better demonstrated its ability to operate in all climates.

The remaining parameters selected for comparison are range, depth, payload-volume and navigation accuracy. Where data are available on the internal volume available for the payload, it can be seen (Table 1.3.1) that all of the types are comparable. Where data are published, navigation accuracy, of the order of 1% of distance travelled, is also found to be comparable. This leaves range and depth. These are compared in Figures 1.3.6 and 1.3.7.

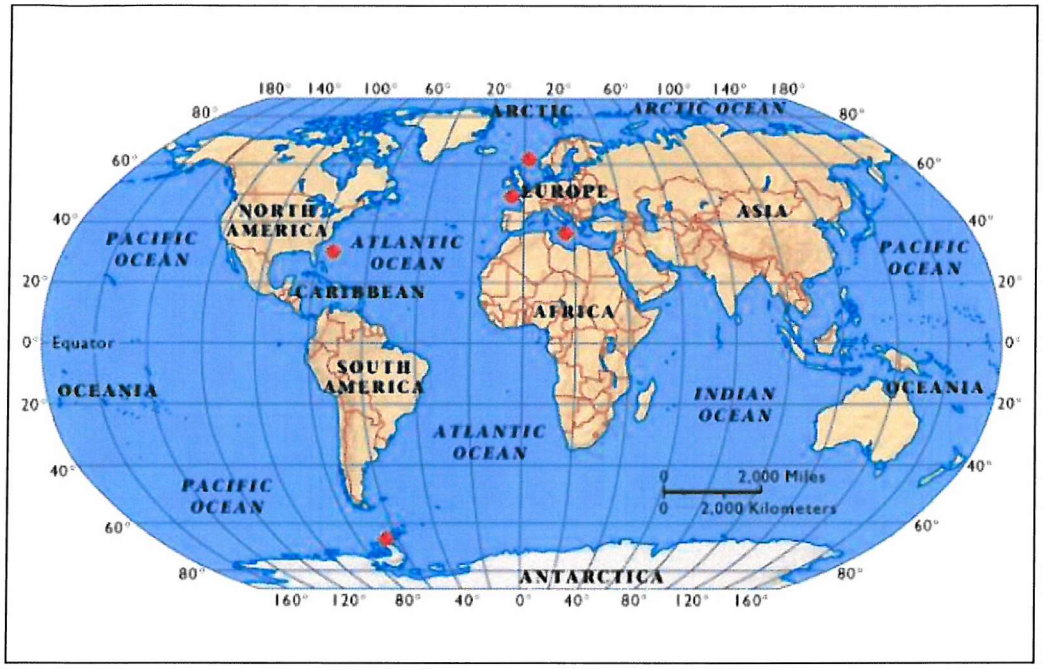

Figure 1.3.5 AUTOSUB deployments

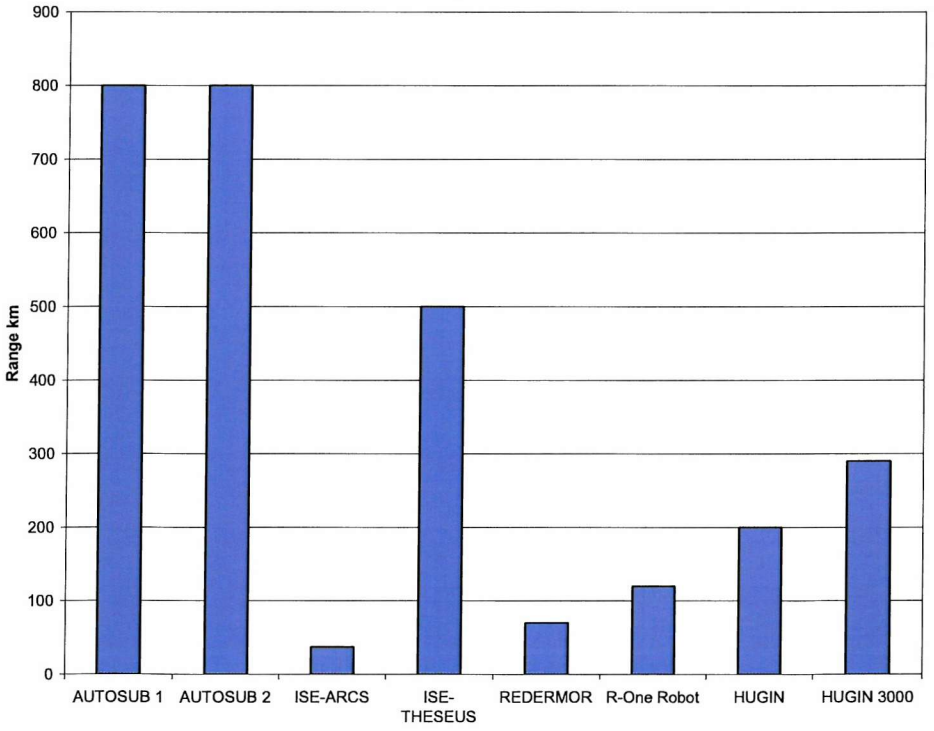

Figure 1.3.6 Range comparison

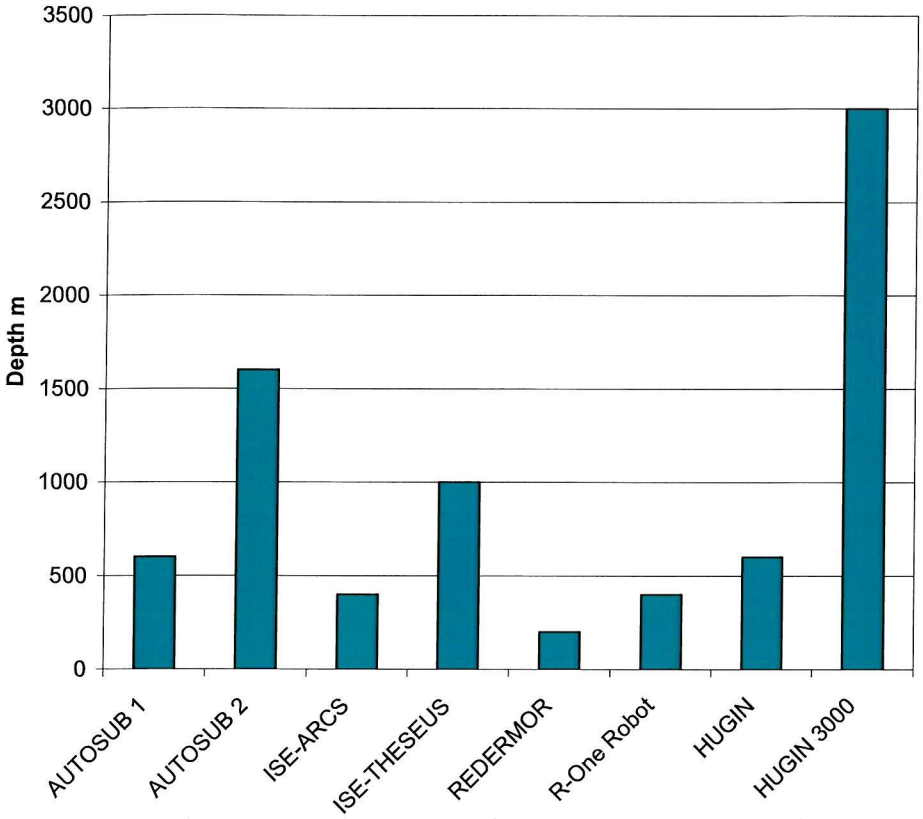

Figure 1.3.7 Depth comparison

To produce a design capable of propelling a vehicle at greater speed for a given range and depth enables a mission to be completed more rapidly and, therefore, has value. However, all of the vehicles chosen travel at about the same speed, so this parameter is not an effective discriminator. Equally, diving to great depth requires either a more massive structure or a more elegant engineering solution than an equivalent design capable of lesser depth. Thus, one would expect a trade-off between range and depth. For a rational comparison, these two parameters, therefore, have to somehow be combined. The weighting to be applied to each is a matter for judgement. Since, all else being equal, depth is the more difficult to achieve, one would expect this to be given a greater weight. However, in the absence of any agreed yardstick, they are taken as equal for the purposes of this comparison, and the straight product of range and depth taken as the measure of goodness. A comparison of the performance of the contenders on this basis is shown in Figure 1.3.8. The two versions of AUTOSUB and HUGIN are included to show the effect of improving the depth parameter in this comparison.

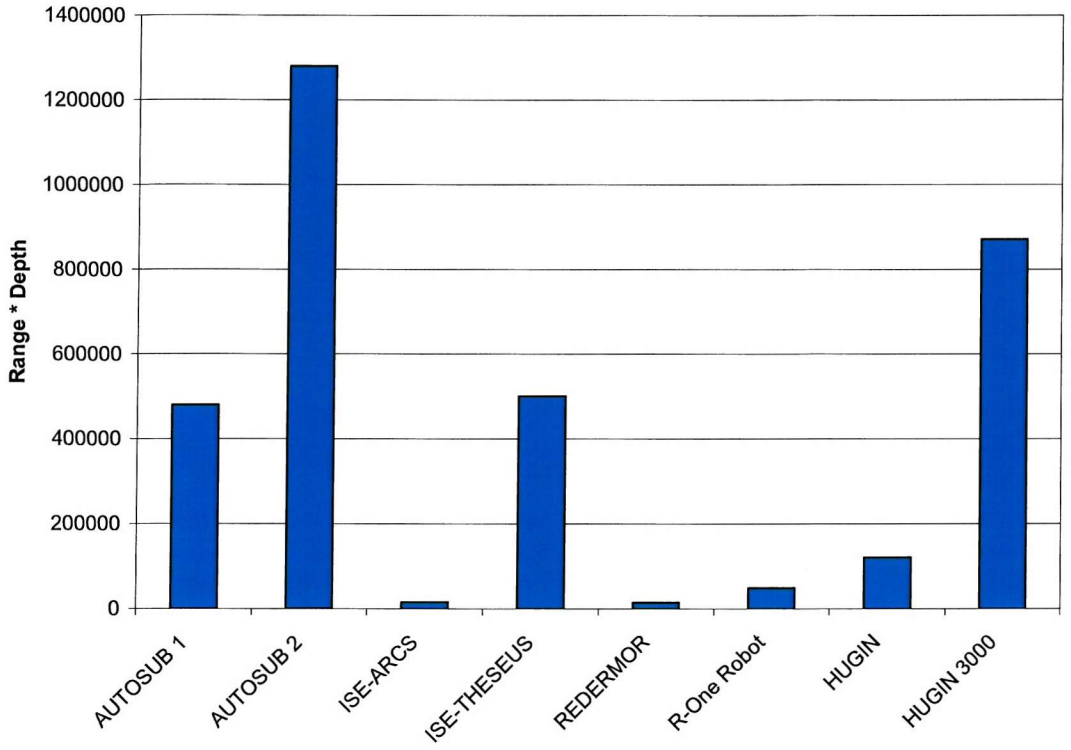

Figure 1.3.8 Range x depth comparison

The measurement of total propulsion performance is complex. However, the objective of the system is to maximise range for a given vehicle within a defined performance envelope of speed and depth. For submarines, unlike surface vessels, volume and weight is expensive, so a reasonable measure of effectiveness might be range per unit volume. Since only vehicles of comparable volume have been considered, the analysis presented indicates that the performance of AUTOSUB is comparable with that of similar vehicles. The next step is to compare its performance with that which may be possible, by comparing the performance of the vehicle in-service with that expected when the vehicle was being designed.

1.3.6 Comparison of actual and anticipated performance

The performance of the AUTOSUB vehicle in service is readily monitored since the vehicle is well instrumented and is equipped with a comprehensive data logging facility. Change of performance with time can, therefore, be determined.

The vehicle is intended to cruise at 2 m/s and the key system components were designed to achieve maximum range under this condition. It was expected that the vehicle would need to expend energy at the rate of about 70 J/m (i.e. 140 W) to

achieve this cruising speed. In fact the energy required has been consistently higher. Furthermore, it has been found to increase with time such that, during one deployment in the year 2000, it was found to be consuming 700 J/m (i.e. approaching 1 kW) to achieve a speed of only 1.4 m/s. Clearly, either one or more of the components of the propulsion system was not performing as expected or there were unanticipated interactions between sub-systems causing a reduction in performance at the system level. Furthermore, either the original cause of reduction in performance was worsening with time, or additional detrimental mechanisms were evolving. An analysis of the propulsion system to determine the causes of this effect is the subject of the remainder of this part.

The requirement to improve the performance of an in-service AUV is by no means unique to AUTOSUB. For example, exercises similar to that undertaken for AUTOSUB has been taken on a comparable, albeit much smaller vehicle, REMUS, (Prestero, 2002) and on a vehicle of completely different layout, ABE (Bradley et al., 1995).

Summary

It has been demonstrated that AUTOSUB is a rugged, reliable, effective and adaptable vehicle for the gathering of scientific data, and at least as good as designs worthy of comparison. Nevertheless, it is clear that the propulsion system is performing sub-optimally, leading to reduced speed, duration and range. Recovery of range, speed and voyage duration would clearly lead to greater opportunities to investigate more remote locations, as well as to sample larger volumes of the ocean per mission. The remainder of this thesis is devoted to providing an analysis of the causes of sub-optimal propulsion performance in order to facilitate an improved AUTOSUB operational window. This begins with an analysis of the performance of the current system. However, before undertaking this analysis, we need to consider some of the issues associated with formal analysis of a potentially complex system and one that is already in service.

Chapter 1.4

SYSTEMS ENGINEERING CONCEPTS

1.4.1 Introduction

Because of the inevitable compromises in manufacture and the simplifying assumptions made at the design stage, the performance of systems once in-service seldom match that aspired to during the design stage. Calculations based on data derived from full-scale trials of an in-service AUV (AUTOSUB) at sea indicated that, although the performance of the vehicle was comparable to others of its type, the energy required to propel it was considerably greater than that expected from the results of scale-model tests undertaken during the design stage. Furthermore, it was noted that overall propulsion performance was decreasing with time. Thus, one or more of the components of the propulsion system was either not performing as expected, or was producing unanticipated interactions. Additionally, either the performance of one or more of the major sub-systems had been decreasing with time, and/or the effect of an undesirable interaction between sub-systems had increased with time.

Considerable investment has been made in developing and building the vehicle. By analysing the system to determine the causes of performance shortfall it is possible that significant improvement in performance may be obtained at comparatively small additional investment. This chapter considers some of the concepts that underly the subsequent analysis. It begins by discussing why we need to consider the issue of propulsion efficiency as an integrated system problem and looks at what this approach implies. It then debates the implications peculiar to the application of systems engineering disciplines to a system that is already in service. It ends by considering the issue of system complexity, how this may be defined and some implications.

1.4.2 An integrated system

The net effectiveness of an AUVs propulsion is dependent upon the individual performances of a large number of components. However, the performance of the

parts does not provide the whole picture. Total performance is also a consequence of the interactions it and the environment in which it finds itself. It is a consequence of interactions with other components of the overall AUV, i.e. its internal environment and with elements of the external environment within which the AUV operates. Any explanation of sub-optimal in-service performance needs, therefore, to begin with an analysis of the total energy conversion system.

So let us consider what we mean by 'system' and the characteristics that this implies. A system implies a device designed to produce a set of outputs in response to a pre-determined set of inputs. The system comprises a set of sub-systems, each of which also have pre-determined characteristics and are in some way self-contained. Another characteristic of many systems is that the net functional value of the system is greater than that of the sum of its sub-systems (Roza, 2001). This implies beneficial interactions between sub-systems, although there is a corollary, addressed later, that there may also be unintended detrimental interactions.

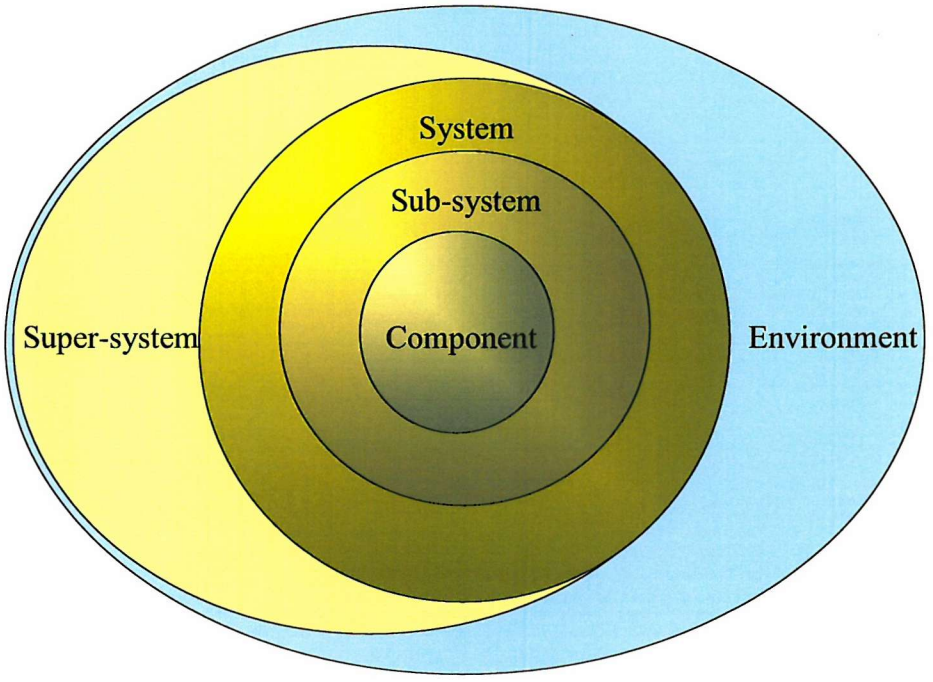

Figure 1.4.1 System hierarchy

The system will interact with its environment. The environment may comprise in part or whole, other defined systems. In this case it may be possible to exert some control over that part of the environment. Alternatively, the environment may have a larger or smaller element of uncontrolled features, such as, for example, a radar,

which needs to interact with the atmosphere. This implies a hierarchy of elements. For the purposes of this thesis the hierarchy is defined in Figure 1.4.1.

The initial step in analysing a system is to define the requirement that the system is designed to meet. The requirement will comprise a series of functions that the system needs to perform. Functional decomposition is usually required to arrive at a level of understanding sufficient to enable analysis.

To perform an analysis, an understanding of the required outputs of the system is needed so that a measure of goodness can be devised. The parameters that define goodness may be derived from the requirement. From the requirement a system boundary may be drawn, which defines the interface between the system and its environment. The definition of the environment will include the specification of any super-system within which the system must operate.

The system may now be partitioned into sub-systems. The connections between sub-systems can be specified and the consequent interfaces defined. The connections between sub-systems falls into two categories, those that are intended as part of the system functionality, and those that are an unavoidable consequence of the characteristics of the sub-systems. The unplanned interactions (cross-talk in electronic systems jargon) are not always obvious. It is often difficult to identify in advance all of the interconnection mechanisms, e.g. parasitic capacitance in electronic circuits. A dedicated investigation is often required to identify where they occur. The investigation will need to consider, not only the system, but also the critical sub-systems. The latter often need to be characterised in some detail. This is a general engineering problem that tends to emerge with the need to optimise systems after their initial development. For example, in the manufacture of 'system-on-chip' electronic components, until recently it was entirely satisfactory to use cell libraries that gave standard characteristics for a cell type. However, as designers seek to obtain greater and greater performance from the technology, they are finding that they need to characterise the individual cells as they have been built, rather than as they were conceived (Pezzati, 2003).

Once the critical interactions have been identified, they need to be controlled, preferably by isolating one sub-system from another. In rf systems, for example, this may be achieved by Faraday shielding. If this is not possible, then each interaction needs to be characterised so that it can be allowed for in performance prediction.

The number of possible interactions increases with complexity. The subject of complexity is discussed later in this chapter, but for now it can be considered as the number of possible interactions between sub-systems. The number of interactions can increase as a result of two non-exclusive causes: an increase in the number of sub-systems; and/or an increase in the number of possible interactions between sub-systems.

Another characteristic of systems engineering is the need to consider holistically, not just the system as it exists at any point in time, but also its existence throughout its life. In terms of the propulsion system problem, this implies, for example, consideration of the maintenance and operation regime as it applies to propulsion efficiency, as much as to the initial design.

Not only the state of maintenance of the system changes with time, but so inevitably does its build state. There will be a need for modifications as a result of obsolescence or in an attempt to improve system performance through life. The introduction of new sub-systems can lead to unexpected changes in performance. It is, therefore, necessary to maintain control of the build state during the system's life.

The application of systems engineering implies the need for a process model as well as a performance model. (A process model is analogous to a performance model but it applies to people and organisations rather than electro-mechanical components.) This will become clear as the thesis develops. A process will emerge whereby performance is continually monitored through life and modelling capabilities evolved, so that performance may be continually optimised.

The analysis of a system already in service brings a set of constraints additional to those experienced during the initial design. These difficulties are addressed prior to undertaking the intended analysis.

1.4.3 Concept of systems analysis of an in-service vehicle

Systems engineering involves a process whereby the needs of the customer are satisfied throughout the life cycle of the system. To achieve this, the following tasks are undertaken (ANSI/EIA632, 1999).

- State the problem: capture the requirement and define the system.
- Investigate alternatives: evaluate different combinations of sub-system.
- Model the system.
- Integrate: characterise the sub-systems, interfaces and interactions.

- Produce the system.
- Assess performance
- Iterate.

Problems in systems engineering are normally formulated at the beginning of the system design process. However, the required improved performance in this case became evident after a fully operational and very successful system was already extant.

Now a key characteristic of systems engineering is that it is fractal in at least two aspects, i.e. the same functions may be performed at any level in the system. The first aspect of this is in the process of design, illustrated in Figure 1.4.2. This process may be carried out at any level within the system, at system level, at sub-system level, or at component level.

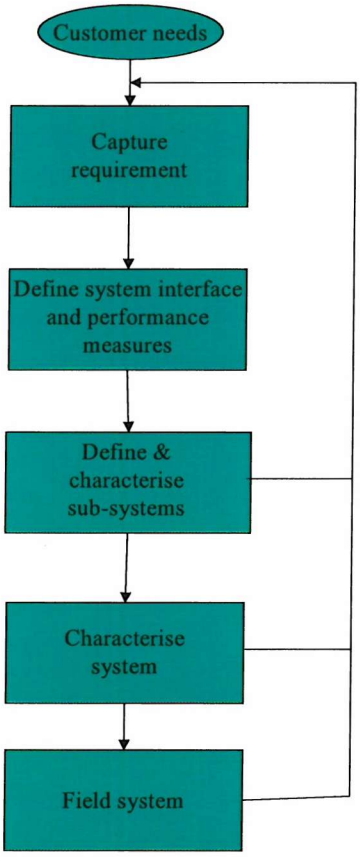

Figure 1.4.2 System design process

The second condition under which the fractal nature of systems engineering is manifest is that of the systems engineering process. This process is defined in Figure 1.4.3, and it may be carried out at any point in the system life cycle. Thus, the

process may be carried out on initial build, or at any time once the system has entered service.

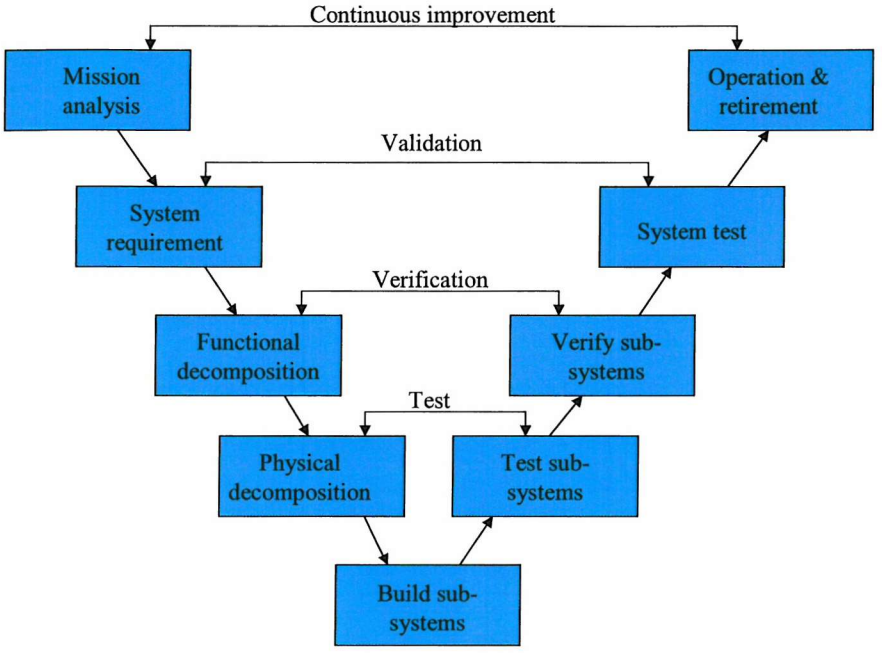

Figure 1.4.3 Systems engineering cycle (Bahill and Dean, 2001)

Whilst all of the elements of system analysis are pertinent, the undertaking of a post-production type systems analysis necessitates a modified approach (Bahill and Briggs, 2001). In particular there is a need to:

- Capture both the original and the current requirement at a time when the customer's views will have changed in the light of experience.
- Understand the original design process when records may be incomplete.
- Characterise the system and sub-systems as built, rather than as conceived.
- Acknowledge the fact that the systems engineer is likely to work to the project manager, not the customer.
- Recognise that the role of the systems engineer will be that of an investigator rather than instigator.
- Realise that resources will be necessarily more limited, whereas the task may be more complex.
- Accept that such investment will already have been made that many of the sub-systems and/or interfaces will be immutable.

The advantages of undertaking the analysis post hoc include:

- The availability of archived data.
- The availability of a complete working system.
- The fact that many of the more complex issues will already have been addressed.
- Ready acknowledgement by those who control resources that there remain difficult issues that need to be investigated.

There are also a number of disadvantages, namely:

- Strong ownership of the current design resulting in the original designers being defensive of the status quo.
- The need to change management systems that are already in place and so challenge vested interests, or the need for the implementation of new systems where the requirement for them has not previously been recognised, e.g. the introduction of strict build state control.
- The need to work within the existing management structure, rather than design it to fit the system.
- The scope for innovation is constrained by investments already made, both in financial and intellectual terms.

1.4.4 Approach adopted for this investigation

The approach adopted for the AUTOSUB propulsion system investigation is based on the principles outlined above and is summarised in Figure 1.4.4.

AUTOSUB is a vehicle designed to undertake a broad spectrum of scientific missions. Consequently the configuration of the vehicle is altered according to its mission. A primary aim of this work is to enable the propulsion performance of the AUV to be optimised for the particular configuration required for each mission. The hub of the analysis is, therefore, configuration management. The system configuration is defined and assessments are made of its expected performance. These are compared with measurements made on the full-scale vehicle and on laboratory simulations. As a result an optimal configuration can be predicted that maximises propulsion efficiency within the operational and mission payload constraints. The process loop continues from mission to mission.

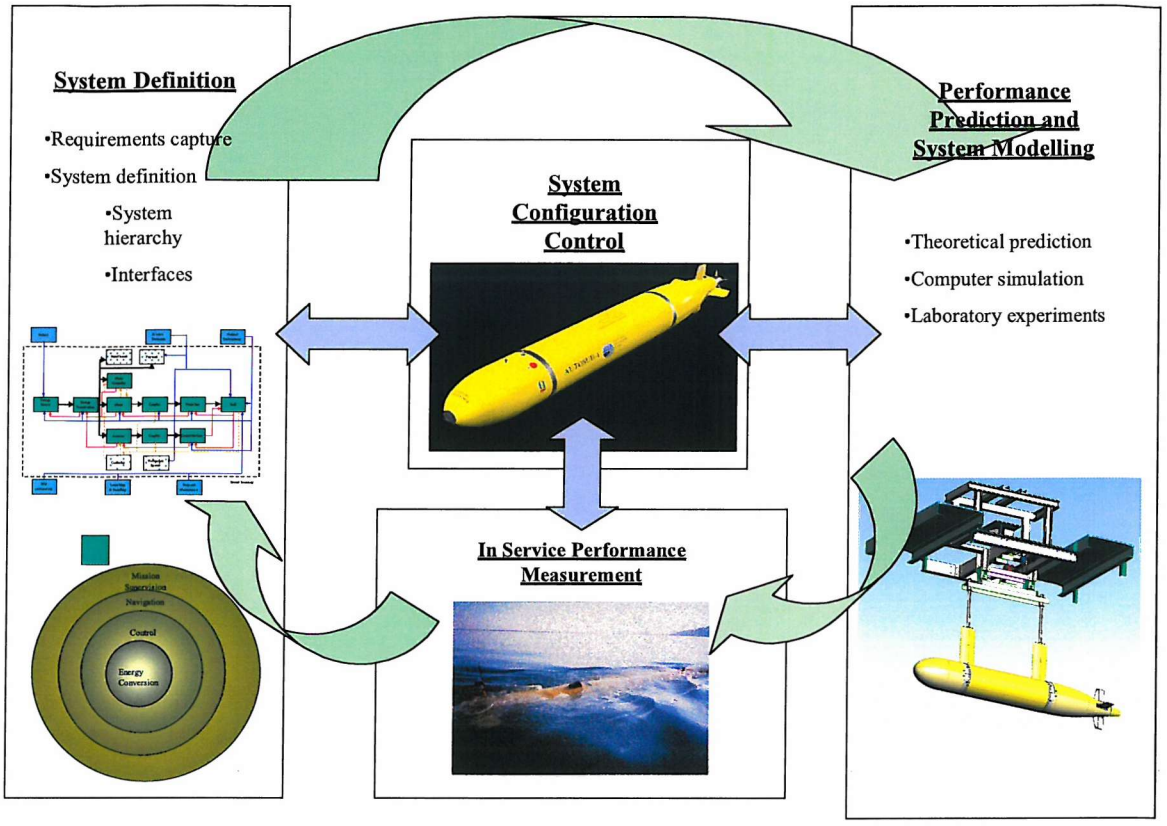

Figure 1.4.4 Systems engineering approach

1.4.5 Complexity

For simple systems the problem of system design and improvement is trivial. It will be established in chapter 1.7 that an AUV propulsion system, within the context of the problem set here, is complex. Before we are able to make this assertion we have to be able to define complexity and derive some method of measuring it. There are two particular fields where complexity as a subject has been studied, that of the biological sciences, such as physiology (Mikulecky, 2004), and that of computer programming (Beckerman, 2000), (Abu-Sharkk, 2003), where the complexity of programmes is now a limiting factor on further development.

As with many qualities the world may be divided into two: those that have it and those that don't. Thus, in principle, the world may be divided into those features or processes that are complex and those that are simple. However, in practice, everything in the real world is inherently complex. All things and events are connected to all other things and events. Complexity is, therefore, not a quality of the subject, but rather a quality of how we choose to view the subject. We may choose to

consider a problem such as the position of a simple pendulum in an idealised form, (say imagining that its bearing is frictionless, that its mass does not change with time, and that it is operated in vacuo) in which case the solution is susceptible to a simple harmonic equation. Alternatively, we may wish to dive a little deeper by including friction and air resistance, in which case we find that the motion, far from being simple, rapidly becomes chaotic, and is impossible to predict for more than a short period ahead (Gleick, 1998). The degree of complexity we allow is a function of the model we adopt, i.e. of the encoding we use to describe the problem and facilitate the analysis (Mikulecky, 2004). Mikulecky defines complexity as follows.

> 'Complexity is the property of a real world system that is manifest in the inability of any one formalism being adequate to capture all its properties. It requires that we find distinctly different ways of interacting with systems. Distinctly different in the sense that when we make successful models, the formal systems needed to describe each distinct aspect are NOT derivable from each other.'

This implication of disconnectedness between consideration of systems at different levels of complexity seems intuitively sound. Thus, it is inconceivable to describe interactions at the level of a biological system, such as an animal, on the basis of quantum physics, although the latter may well play a part in describing specific processes, such as part of the functioning of the nervous system. However, this concept is not directly helpful in describing the complexity of intermediate systems such as that under consideration here.

Alternatively, Beckerman (Beckerman, 2000) suggests that the final state of the system, in terms of whether it is likely to be steady state, dynamic, non-linear or chaotic, can be used to describe system behaviour. Complex systems exhibit dynamic and non linear behaviour, and are able to exist in a large number of possible system states. This is readily applicable to digital systems where the number of states is finite, but is not readily applicable to systems where possible outputs are described by a continuum.

Another approach has been used in computer science where parameters have been sought to enable the effects of complexity to be forecast in terms of cost and program development time (Abu-Sharkk, 2003). Such parameters as execution time and program storage requirements are not of direct use in the type of investigation

under consideration here, but we may be able to develop thoughts along these lines to determine the complexity of a continuous system.

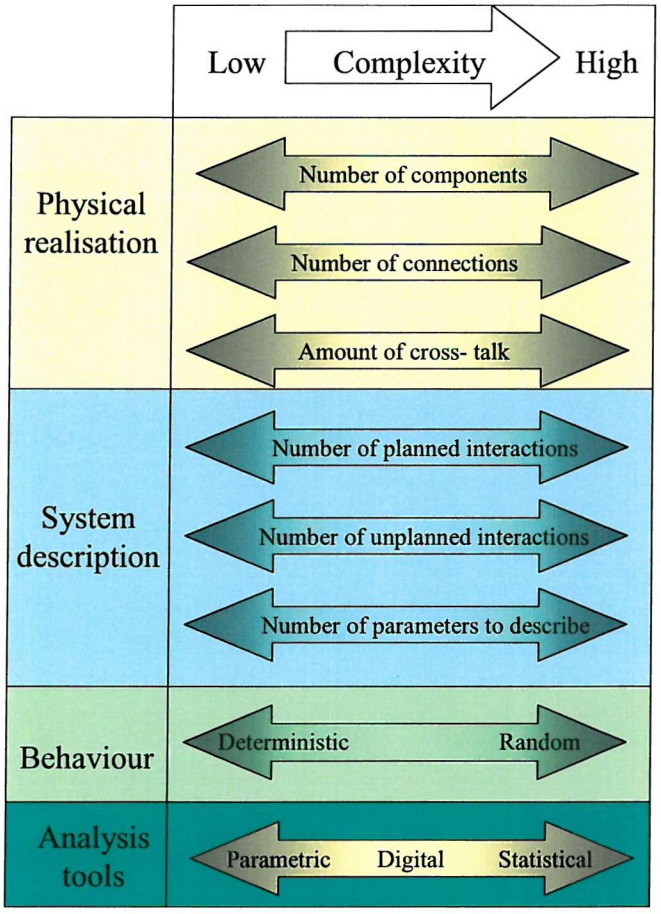

Figure 1.4.5 Characteristics of system complexity

We can combine the two approaches by considering the degree of reductionism required to define the system sufficiently well to be able to analyse it to the level required. This approach is illustrated in Figure 1.4.5.

Thus, for the purposes of this thesis, a complex system is defined as one that comprises many components or sub-systems, has many interactions between each set of components, has many interactions between sub-systems and components, and has a significant number of unplanned interactions. Such a system is likely to require many parameters to describe it. It is likely to exhibit random rather than deterministic behaviour and require statistical methods to describe its characteristics. We now have a set of tests that can be readily applied to measure the degree of complexity of the system.

Summary

Chapter 1.1 described a problem common to many types of system. Chapter 1.2 focussed on a particular problem associated with the in-service propulsion performance of AUVs. Chapter 1.3 concluded by defining the requirement for the analysis of the propulsion system of a particular AUV.

This chapter has described some of the general systems engineering concepts that will underpin any analysis. It has discussed how these concepts need to be adapted to cater for the case of a system that has already been introduced into service and concludes by proposing a set of metrics by which the complexity of the system to be analysed may be established. This will help in deciding which analysis tools are appropriate.

Chapter 1.5

THE SYSTEM BOUNDARIES

1.5.1 Introduction

Before looking at the detail of performance of the sub-systems to establish where shortfalls may be, we first have to define the system under consideration. This is the subject of this chapter. The process involves 5 principal steps:

1. Capture the requirement that the system is designed to satisfy and establish the measure of goodness by which its performance may be assessed.
2. Define the system in terms of :
    a. Its boundaries.
    b. Its component sub-systems
    c. The environment within which it has to operate.
3. Produce a system level model based on the gross parameters that define the system.
4. Run the model for the parameters applicable to the values of the key parameters assumed at the design stage and determine the expected overall system performance
5. Establish the sensitivity of the performance of the system to variation in the key parameters.

Having done this, we will then be in a position to examine the performance of the individual sub-systems in order to determine the effect of their actual performance compared with that assumed at the design stage. This will be the subject of the following chapter.

1.5.2 Requirements capture

Requirements capture is the means whereby the needs of the customer are defined in a non-prescriptive manner. They need to be stated in such a way as not to imply any particular material means of satisfying the need. The output is a series of logically connected statements that define the functionality required of the system. For complex requirements formal means are required to ensure that all of the

requirements have been elucidated and that they are stated within a logically consistent framework. There are many tools marketed for this purpose, although, since the formal process of requirement capture evolved in the software industry, many are specifically tailored for that market (INCOSE, 2001). A manual process based on functional decomposition will be sufficient for present purposes.

The process for determining the requirement is summarised in Figure 1.5.1. Interviews with, or documents from, the customer provide the initial set of requirements. These are checked for inconsistencies or gaps in the specification and integrated into a single Statement of Requirements document. This is checked to establish whether the statement is in sufficient detail to enable design solutions to be derived. Once a sufficiently detailed set of requirements is established the Statement of Requirements may be formally issued. The process is iterative throughout the life of the project with the Statement of requirement being maintained under formal issue control.

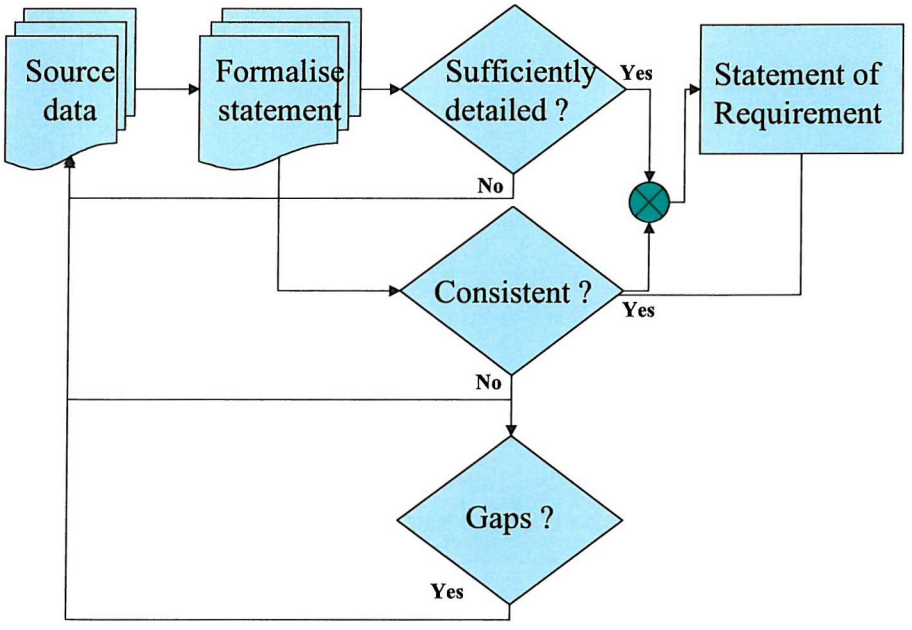

Figure 1.5.1 Requirements capture process

A requirements document is usually stated in a hierarchical form, with broad statements being qualified by ever more detailed statements. *Functional decomposition* is a means of ensuring that the statement is logically consistent between successive levels of the requirement and that sufficient detail is obtained. It is

a process whereby the higher-level functions of a system are progressively decomposed into their component parts. An example, based on the requirement for the AUTOSUB AUV, is illustrated in Figure 1.5.2. The top level requirement is the ability to deploy scientific payloads, within the body of the ocean, throughout the world. This need is readily decomposed into *constituent* parts including the ability to accommodate scientific instruments, the ability to move within the body of the ocean and the ability to deploy throughout the world. Taking one of these, the ability to take measurements throughout the oceans of the world, implies the ability to deploy worldwide and the ability to be able to withstand a wide range of environment. Each of these requirements may, in turn, be further decomposed.

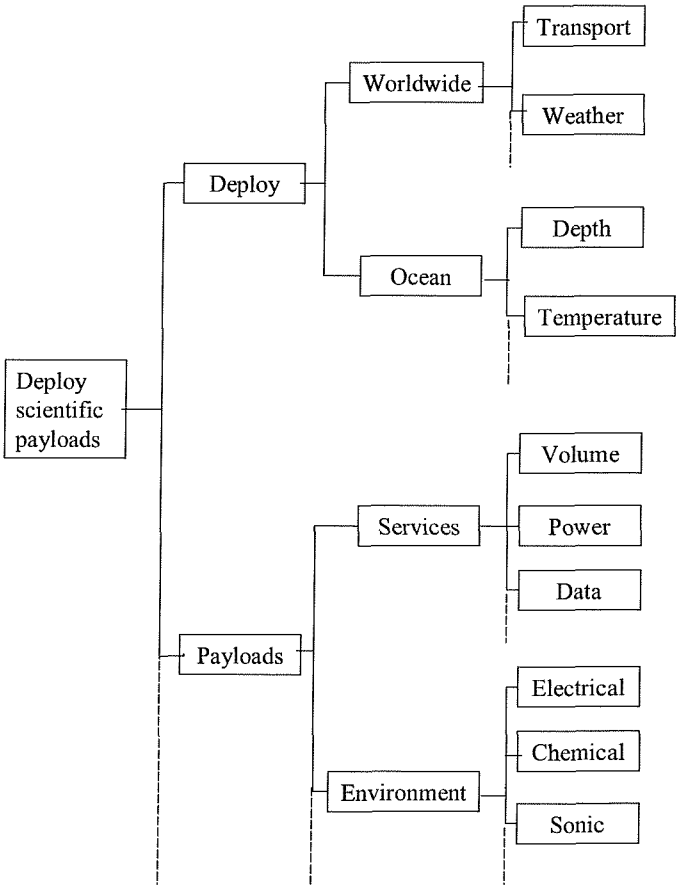

Figure 1.5.2 Example of functional decomposition

An outline of a statement of requirements for the AUTOSUB propulsion system based on these principles is given by (Fallows, 2005).

The key requirements of the propulsion system may be derived from such an exercise. Thus, speed is comparatively unimportant, but range and duration are

critically important, limited only by the dimensions of the Oceans. Similarly, because the vehicle is intended to serve the whole scientific community, there is no discernable limit to the payload size, shape or power needs. However, the need to be able to deploy worldwide imposes a size constraint determined by the transport system: in this case the reasonable size that can be handled on, and deployed from, a NERC research vessel. Budgetary constraints determine the type of energy storage and maximum depth. The requirement, therefore, reduces to the need to achieve the maximum range obtainable within the constraints of the vehicle size, and the energy and power density limits of the energy storage system.

1.5.3 Definition of the system for analysis purposes

Having defined the requirement, the next step in the analysis is to bound the problem by:

a. Defining the system boundaries.
b. Defining the sub-systems and their interfaces.
c. Fixing the interfaces between the system and the outside world.

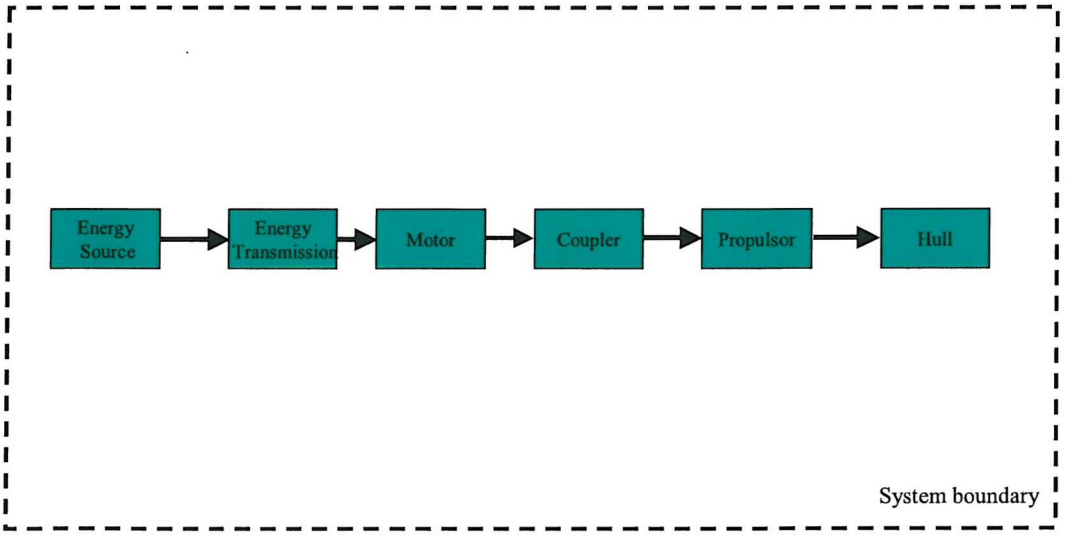

Figure 1.5.3 Propulsion system core

The heart of the propulsion system must be the propulsor itself together with that which it propels, the complete vehicle. For an underwater vehicle, the net resistance that the propulsor must overcome may be represented by the drag of the hull. The propulsor requires a prime mover, which in turn requires an energy supply. The energy needs to be transmitted at each stage from the primary supply through to the hull. We can thus, represent the core of the propulsion system as in Figure 1.5.3, where the dark arrows represent the energy flow.

The architecture of AUTOSUB is that it has a single energy supply that serves the whole vehicle. AUVs of the AUTOSUB class are energy-limited devices. Since we are defining the system with a view to establishing its range, and this parameter, for any given system, is entirely dependent on the energy available, then we need to include within the system all energy sinks. Energy is required to control the vehicle and for the navigation system. All other energy sinks are categorised as either payload or hotel load. The payload is the energy requirement of the instruments for which the mission is being undertaken. The hotel load is defined as the load imposed by all other services in the vehicle. The complete energy conversion system with the energy flows is shown in Figure 1.5.4.

Now although the energy flows from left to right in the system as defined, under steady state conditions (i.e. when travelling at a constant speed) the cause of the energy dissipation flows from right to left. Thus, the propulsor only has to deliver power because it has to overcome the drag of the hull. Likewise the motor only requires a supply of power because of a demand put upon it by the propulsor, and so on. The principal energy feedback paths are shown in red in Figure 1.5.5.

The flow of information required to control the energy conversion system is shown in brown in Figure 1.5.6.

The propulsion system sits within a higher-level system, that of the complete self-contained vehicle, the energy consumption consequences of which are contained within the system as defined. This in turn exists within a vehicle operating system and the natural environment. The impact of this environment on the energy conversion system is illustrated in Figure 1.5.7., which provides a complete definition of the energy conversion system, its sub-systems, the system boundary and its environment.

Having defined the energy conversion system based on an appreciation of AUTOSUB, an assessment of performance may be undertaken.

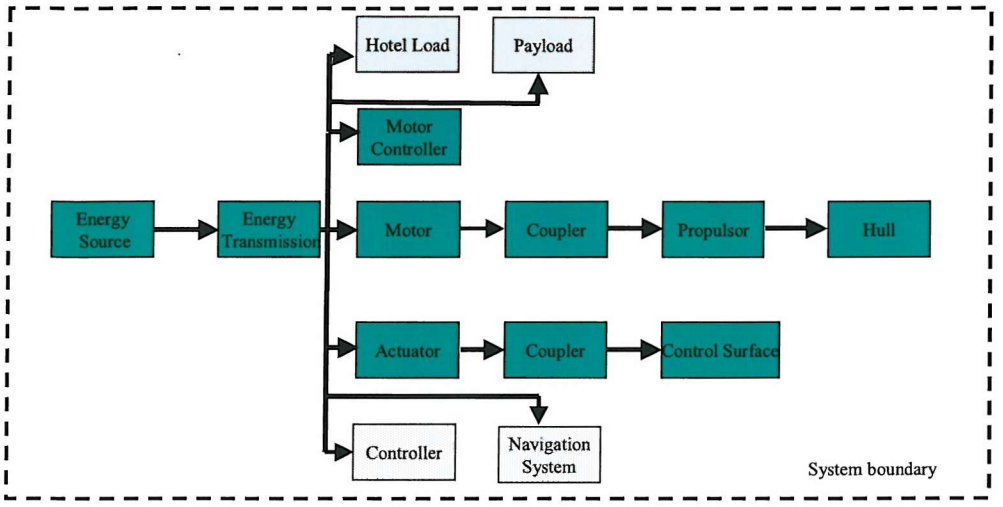

Figure 1.5.4 Energy conversion system

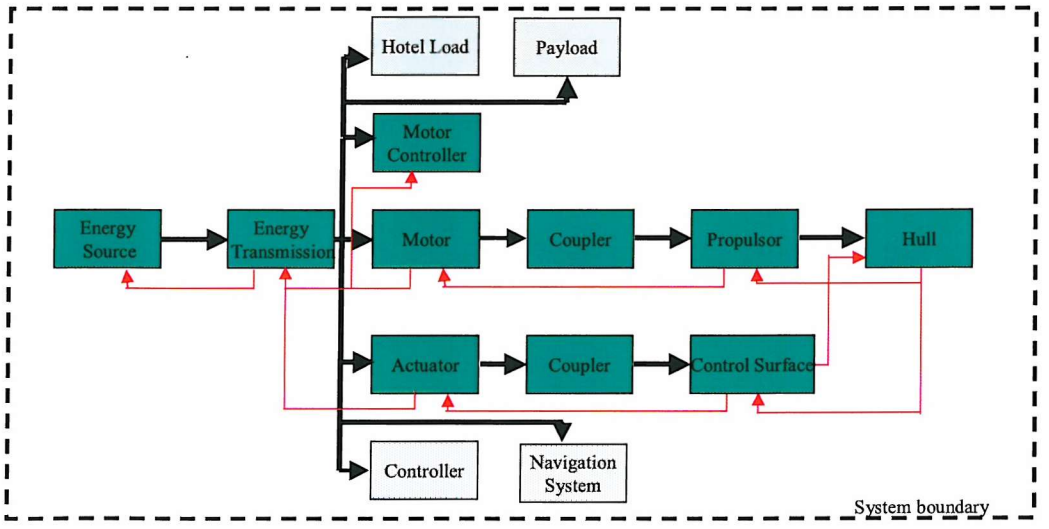

Figure 1.5.5 Energy feedback paths

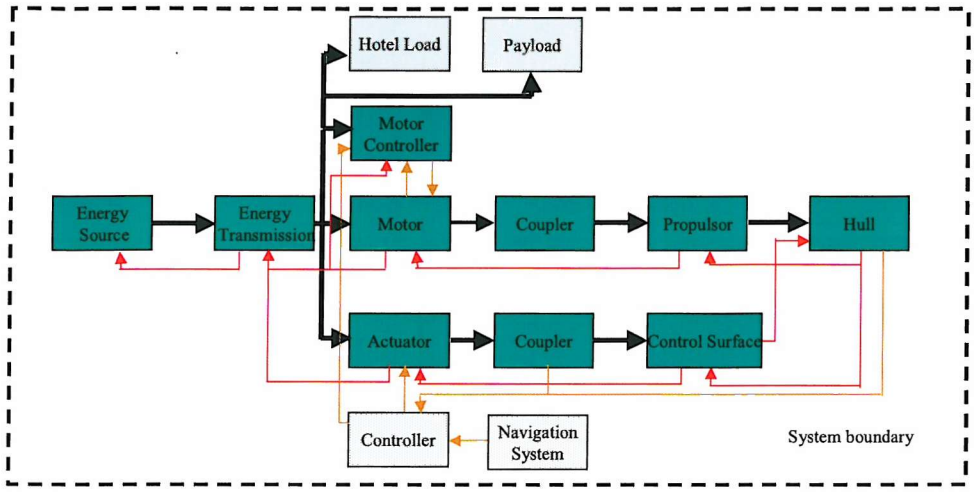

Figure 1.5.6 Information paths

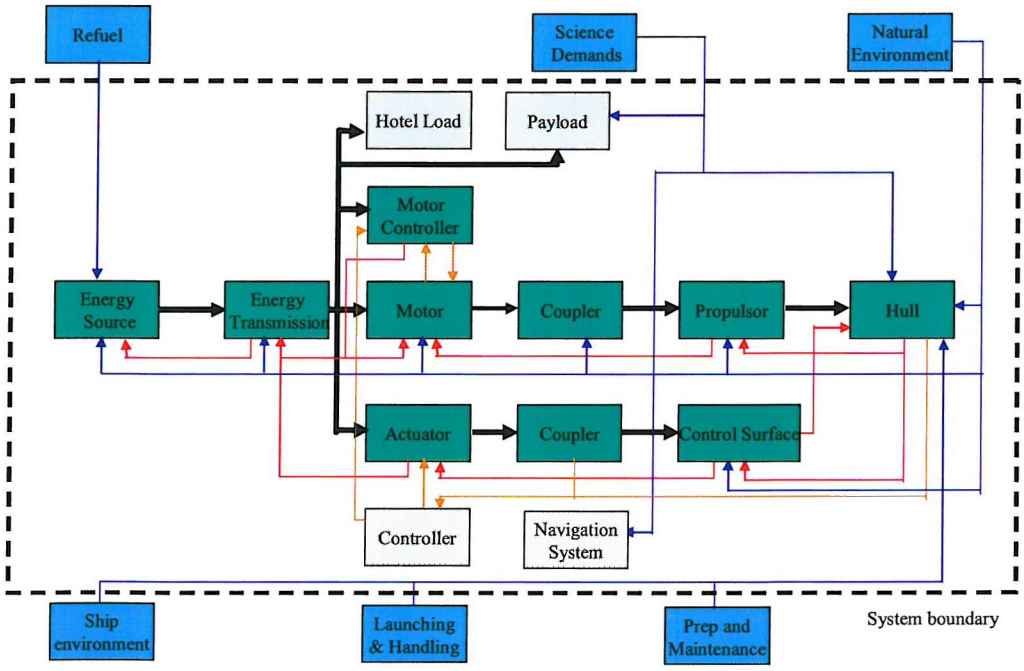

Figure 1.5.7 Energy conversion system.

1.5.4 Initial performance assessment

The measure of goodness of the propulsion system, derived from the statement of requirements, is range. An initial estimate of the expected range of an AUV, from a specified energy store, can be made based on the principal parameters of each of the sub-systems defined in the system definition. Some of these parameters are defined by the performance required of the vehicle. Others are a consequence of design decisions.

The following vehicle parameters are set by the performance requirement:

- Total volume of vessel as defined by ship handling and cost constraints, v_t.
- Cruising speed, u, (or mission time, t) set by the operational need.
- Payload volume, v_{pl}, mass, m_{pl}, and power requirement, P_{pl}, set by the operational need.

It is useful to introduce the concept of payload density, defined as:

$$\rho_{pl} = \frac{m_{pl}}{v_{pl}}$$

Range, R, is the product of cruising speed and mission time:

$$R = ut \quad . \tag{2.1}$$

Similarly duration of the mission is a function of total energy available and the power required to achieve the mission:

$$t = \frac{E}{P_t} \quad . \tag{2.2}$$

Now the energy source may be characterised by two parameters: volume energy density, ρ_e; and volume available for energy storage, v_e. The energy available may be stated as:

$$E = \rho_e v_e \, . \tag{2.3}$$

The volume available for the energy source is the total volume of the vessel less that required for the payload, v_{pl}, the services and the propulsion, v_p, that is:

$$v_e = v_t - v_{pl} - v_s - v_p \quad . \tag{2.4}$$

Clearly the volume required for propulsion is the power required to drive the vehicle divided by the volume power density of the propulsion plant, namely:

$$v_p = \frac{P_p}{\rho_p}. \tag{2.5}$$

The total power required is the sum of that required for device propulsion, the support of the payload operation and the hotel load. This can be expressed as:

$$P_t = P_p + P_{pl} + P_s. \tag{2.6}$$

The power required by the propulsion system is dependent upon the efficiency of the propulsion train, the force required to overcome vehicle drag, F_d, and the required cruising velocity, that is

$$P_p = \frac{F_d u}{\eta}. \tag{2.7}$$

The force required to overcome drag is a function of the drag characteristics of the hull-form and is generally expressed in the form:

$$F_d = \frac{1}{2} v_t^{2/3} C_d u^2 \rho_{sw}. \tag{2.8}$$

Here C_d is the drag coefficient and ρ_{sw} is the density of the water.

Having appreciated the different interdependencies of the parameters defining the principal sub-systems, Equations (2.1) to (2.8) may be combined to provide the relationship between these parameters and the range of the vehicle, namely:

$$R = u\rho_e \frac{(v_t - \frac{v_t^{2/3} C_d u^3 \rho_{sw}}{2\eta\rho_p} - (v_{pl} + v_s))}{(\frac{v_t^{2/3} C_d u^3 \rho_{sw}}{2\eta}) + (P_{pl} + P_s)}. \tag{2.9}$$

The Matlab script at (Fallows, 2005) 1.5.2 was written to explore the performance as a function of the principal system parameters. The consequences of the vehicle parameters derived from experiments and calculations undertaken during its design phase were explored using this to scope the possible performance. The values of these parameters are given below.

- Hull
  - Volume, v_t = 3.7 m^3
  - Drag coefficient Cd = 0.0275 (Kimber and Scrimshaw, 1994)
- Payload characteristics
  - Volume v_{pl} = 1 m^3
  - Mass = 100 kg

- Power consumption p_{pl} = 150 W

- Hotel Load
  - Volume v_h = 1m^3
  - Power consumption p_s = 100 W
- Energy source
  - Energy mass density ρ_e = 150 Wh/kg (DURACELL, 2001)
- Propulsion plant
  - Power density ρ_p = 1000 W/m^3
  - Motor efficiency = 70 % (McPhail, 1993)
  - Propeller efficiency = 75 % (Clark and Wiltshire, 1997)
  - Net efficiency η = 52.5 %

The results showing the effect of speed on performance are presented next. Figure 1.5.8. indicates the drag force as a function of speed assuming a drag coefficient of 0.0275. This indicates that the drag force at 2 m/s is 135 N, which is consistent with the value derived from trials of a scale model during development (Kimber and Scrimshaw, 1994).

The power consumption of the vehicle is derived from Equations (2.7) and (2.8) as a function of steady state speed. The total power consumed allows for 150 W averaged over time for the payload and 100 W for the hotel load. The predictions are shown in Figure 1.5.9. The propulsion power consumption at 2 m/s is 515 W.

The volume allocation of the vehicle, derived using Equations (2.4) and (2.5) with (2.7) and (2.8), is shown in Figure 1.5.10 as a function of speed. As already indicated, 1 m^3 is allocated to the payload and 1 m^3 for the hotel load. The volume required by the hotel load includes that required for the structure of the hull and for less than perfect volume utilisation. The volume required for the propulsion system as a function of speed is calculated assuming the power density characteristics of the propulsion system used in AUTOSUB. Thus, if the vehicle is operated at a lower speed, the volume required for the propulsion system decreases and more volume is available for the energy storage system. All remaining volume is assumed to be allocated to the energy supply.

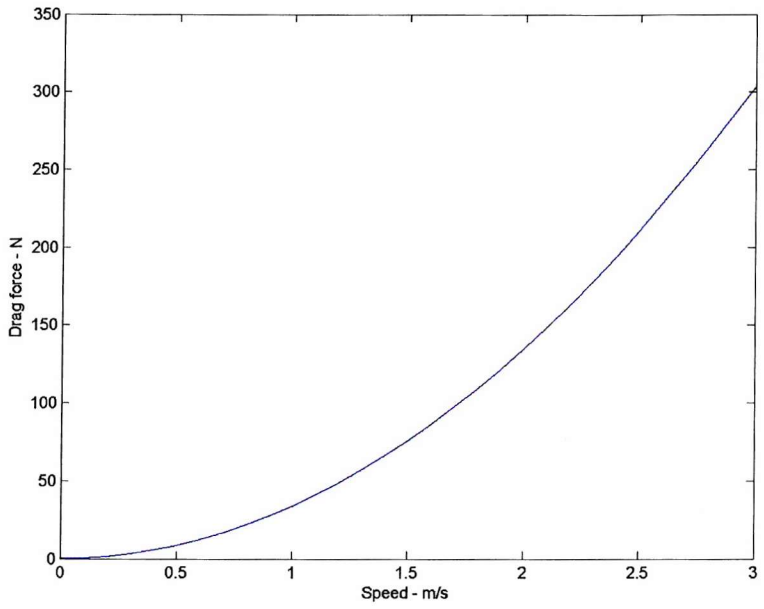

Figure 1.5.8 Drag force as a function of speed

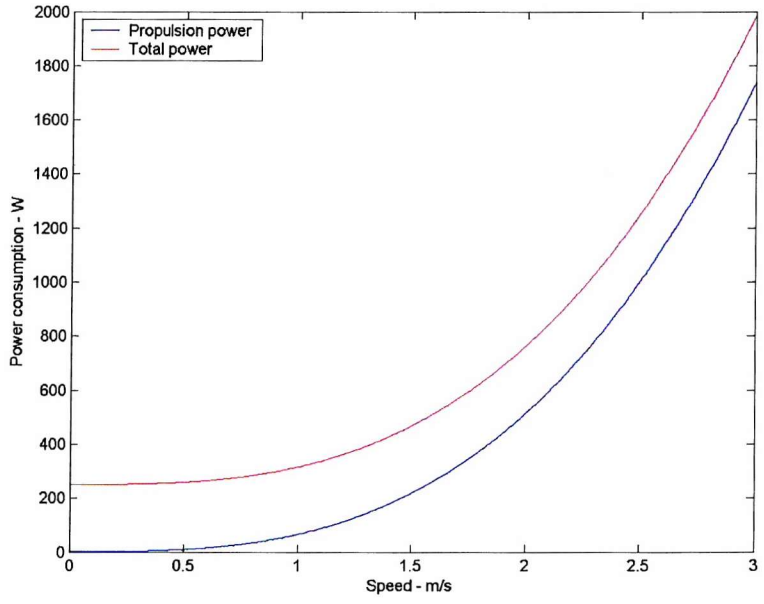

Figure 1.5.9 Power consumption

The energy density assumed for the energy supply is based on the alkaline battery technology used in AUTOSUB. Figure 1.5.10 suggests that for a speed of 2.3 m/s as much volume is required for the propulsion system as for the energy supply and that it is not possible to drive the vehicle faster than 3 m/s since for this speed all available volume needs to be devoted to the propulsion plant.

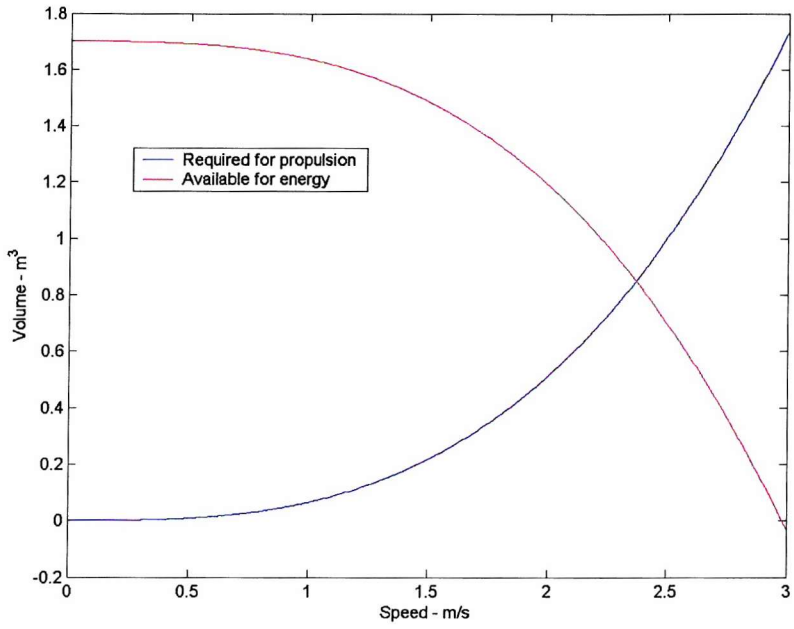

Figure 1.5.10 Volume allocation

The calculated maximum mission duration and range as a function of the selected design cruise speed of the vehicle is given in Figures 1.5.11 and 1.5.12 respectively. As already observed, range falls to zero for a speed of 3 m/s. The optimal design for a vehicle with these characteristics would propel it at about 1 m/s, when a range of up to 2,700 km could be expected, with a duration of about 1 month.

For AUTOSUB's design speed of 2 m/s, this design of vehicle can be expected to produce a range of 1700 km and a duration of 10 days, Thus, confirming that the design as conceived should be capable of meeting the requirement. However, the maximum range achieved in service is of the order of 800 km. It is clear that the vehicle in service is not performing as intended and that, therefore, one or more of the sub-systems does not have the characteristics assumed.

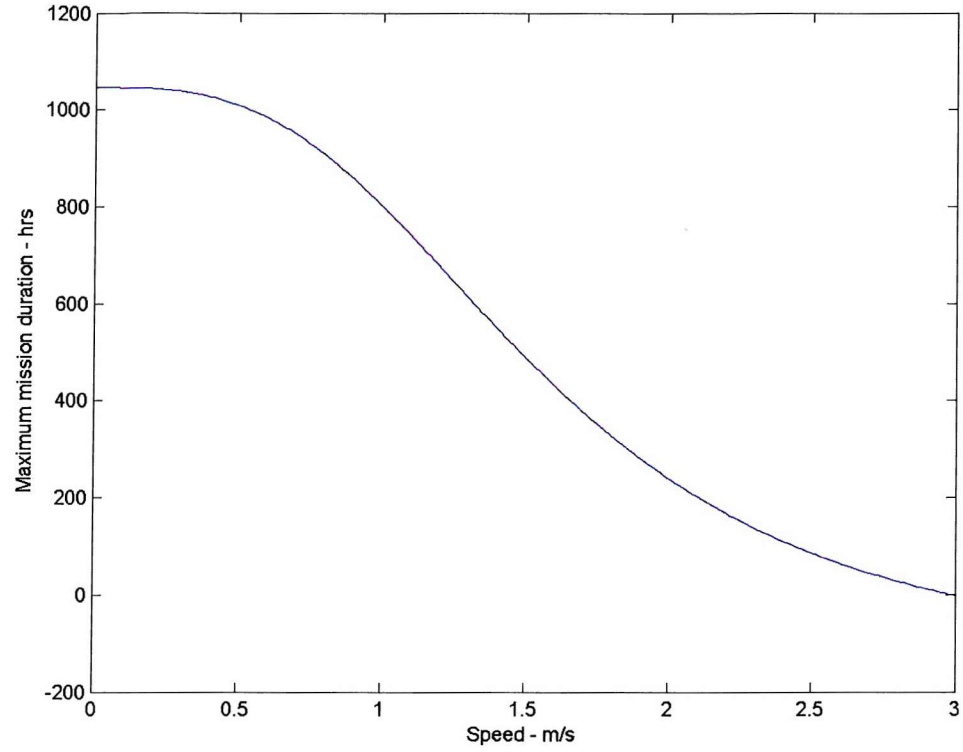

Figure 1.5.11 Maximum mission duration as a function of speed

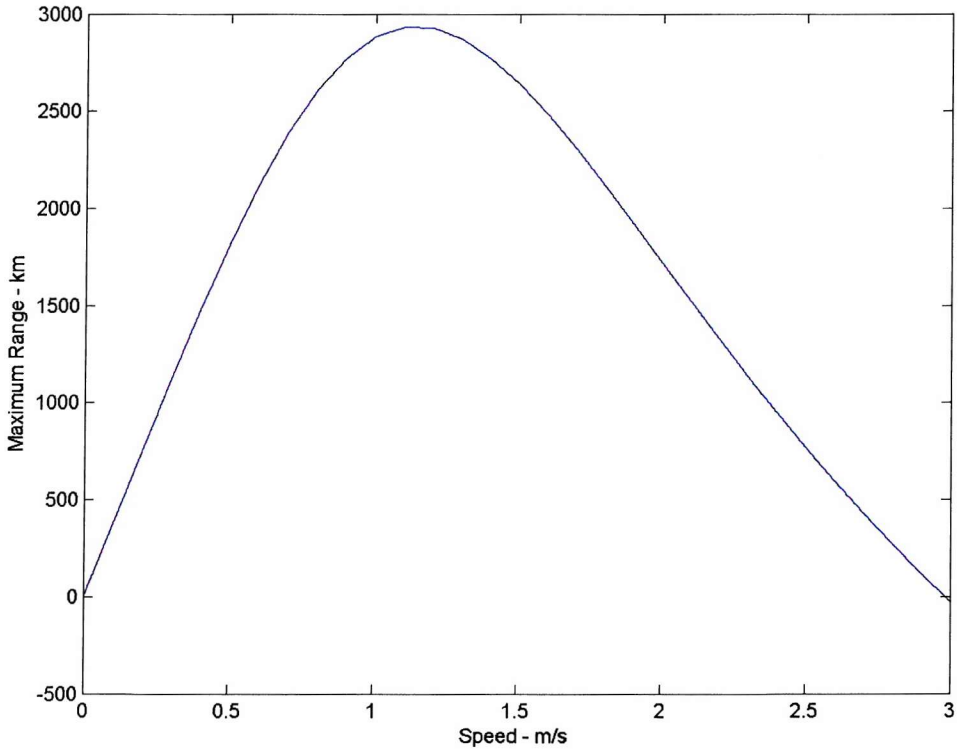

Figure 1.5.12 Maximum range as a function of speed

1.5.5 Sensitivity Analysis

The model at (Fallows, 2005) may be readily adapted to indicate the sensitivity of performance to a number of parameters. For reasons that will become apparent in the next chapter, the sensitivity to drag coefficient and propeller efficiency are shown in Figures 1.5.13 and 1.5.14. These assume that the vehicle is designed to cruise at the required speed of 2 m/s. Thus, if the drag factor doubles from 0.0275 to 0.055, the maximum range at this speed is reduced to less than 600 km.

If the propeller efficiency falls to 50% of the assumed value, all other parameters remaining unchanged, Figure 1.5.14 indicates that the maximum range reduces to less than 600 km. Should efficiency drop to less than 20%, then all available space is required by the propulsion plant and the vehicle becomes non-viable.

Clearly the sensitivity to other parameters may equally be derived.

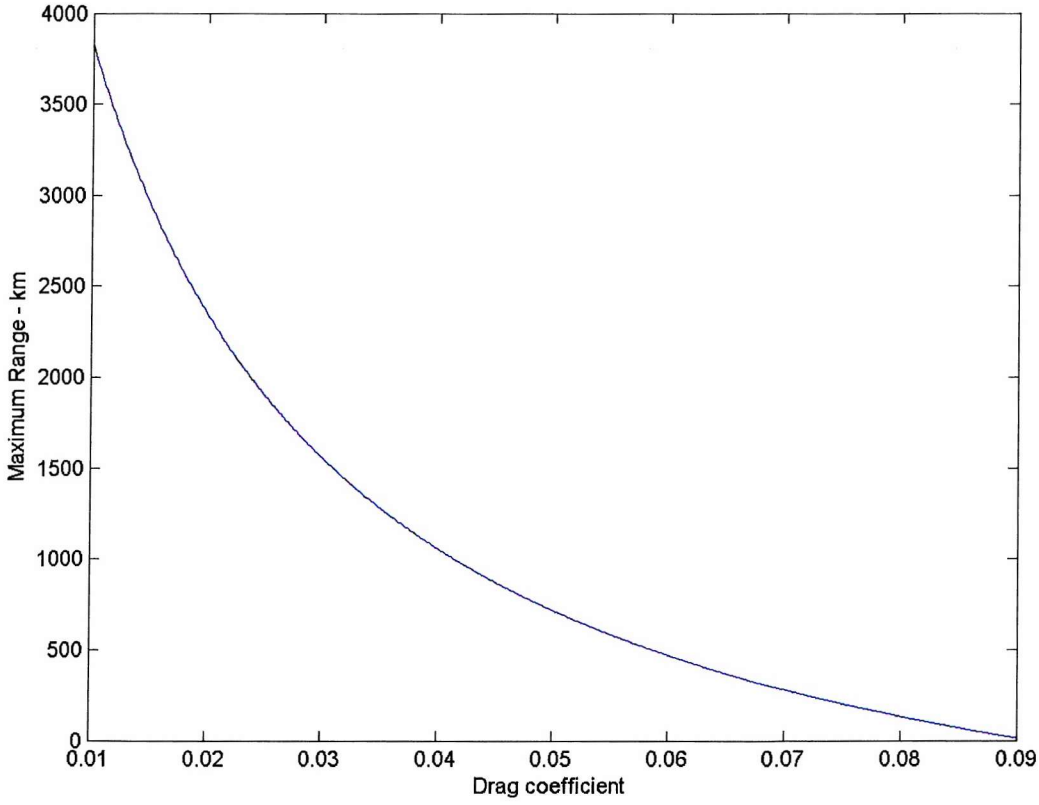

Figure 1.5.13 Range sensitivity to drag coefficient

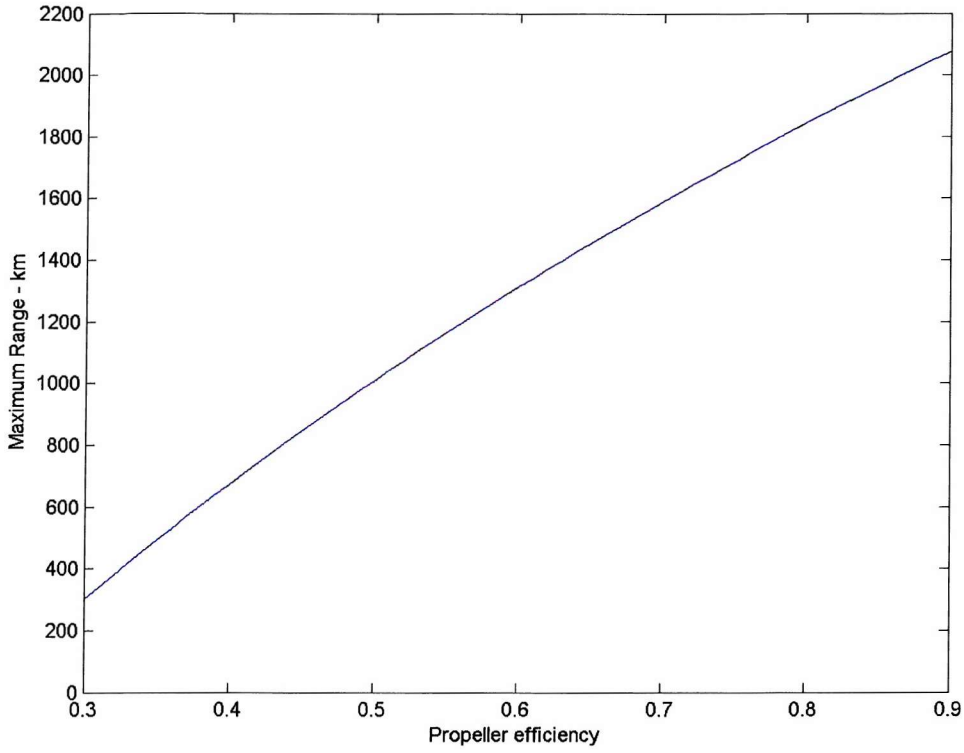

Figure 1.5.14 Range sensitivity to propeller efficiency

Summary

In this chapter we have defined the boundaries of the system under discussion in terms of:

- The system requirement, that is the functions that the system is designed to perform.
- A definition of the system, its components and the environment within which it must work, for analysis purposes.
- The performance that may be expected from the system in terms of the fundamental parameters that describe it.

The concepts behind requirements capture have been discussed and the process demonstrated in the context of AUTOSUB. This has shown that the essence of the requirement is to achieve the maximum range possible within the constraints of the vehicle size, and the energy and power density limits of the energy storage system.

The system has been described in the terms necessary for the purposes of determining the maximum range. Because the vehicle is an energy-limited device, and because the key output parameter is a direct function of energy consumption, it has been concluded that all sub-systems that effect the consumption of energy need to be

included within the system. The sub-systems and system boundary have been defined in this context.

The total system may be described in terms of the key parameters that describe the performance of each of the sub-systems. An analytic expression that relates the output parameter, range, to the sub-system descriptors, has been derived. A parametric model has been produced based on this. The model has been used to show that a system based on the values for the key parameters used in the AUTOSUB design should be capable of producing the performance required.

Finally, we have used this model to indicate the sensitivity of performance to some of these parameters.

Having demonstrated that the AUTOSub-system as conceived should be capable of achieving the required performance and armed ourselves with a tool to enable the effects of trade-offs to be determined, we are now in a position to examine the performance of each the sub-systems in an attempt to isolate the causes of performance shortfall.

Chapter 1.6

SUB-SYSTEM PERFORMANCE

1.6.1 Introduction

In the last chapter the key performance requirement was established as that of maximum range within the constraints of overall size of the vehicle and the chosen energy supply technology. Further, it was shown that the overall architecture of the vehicle should be adequate to meet range aspirations at the design cruise speed of 2 m/s. However, performance in service has fallen short of that expected. This chapter reports the results of an analysis of the performance of each of the major sub-systems to assess their contribution to performance shortfall. In doing this, the performance expected at the design stage of each of the principal components is compared with the actual performance achieved in–service. The in-service performance has been obtained from trials and from specific experimental data.

1.6.2 Sub-systems

The sub-systems to be assessed are those contained within the energy conversion system (as defined in chapter 1.5) that directly affect the propulsion system performance. One major interaction, that between the propulsor and hull, is also considered.

1.6.2.1 Energy source

AUTOSUB uses manganese alkaline secondary cells arranged in batteries. Each battery comprises 75 cells connected in series, creating a nominal 96 volt supply. An investigation of these energy modules (Sharkh et al., 2002) (Griffiths et al., 2002), has indicated that there have been problems resulting from shorting, heating effects, and some cells not performing to specification. Additionally the energy that can be recovered from the batteries has been shown to be dependent on the battery ambient temperature, which is important when operating in low temperature environments, such as the Antarctic.

The variability in battery performance has been corrected by changing the battery supplier. The shorting and local heating effects have been overcome as a result of modifying the method of assembly of the battery packs.

Two means of overcoming the problem of being able to extract less energy from the batteries at low temperature have been proposed. The first is to maintain the batteries at closer to their optimal temperature by means of improved insulation., which allows the heat generated by the batteries as they discharge to be retained. The second is to monitor its performance and assess the remaining charge: effectively fitting a fuel gauge. This will enable the mission controller to optimise the vehicle's range as a function of the operating conditions. The gauge would be based on a model of the battery and assess remaining charge based on temperature and terminal voltage history (Sharkh et al., 2002), (Bradley et al., 2001).

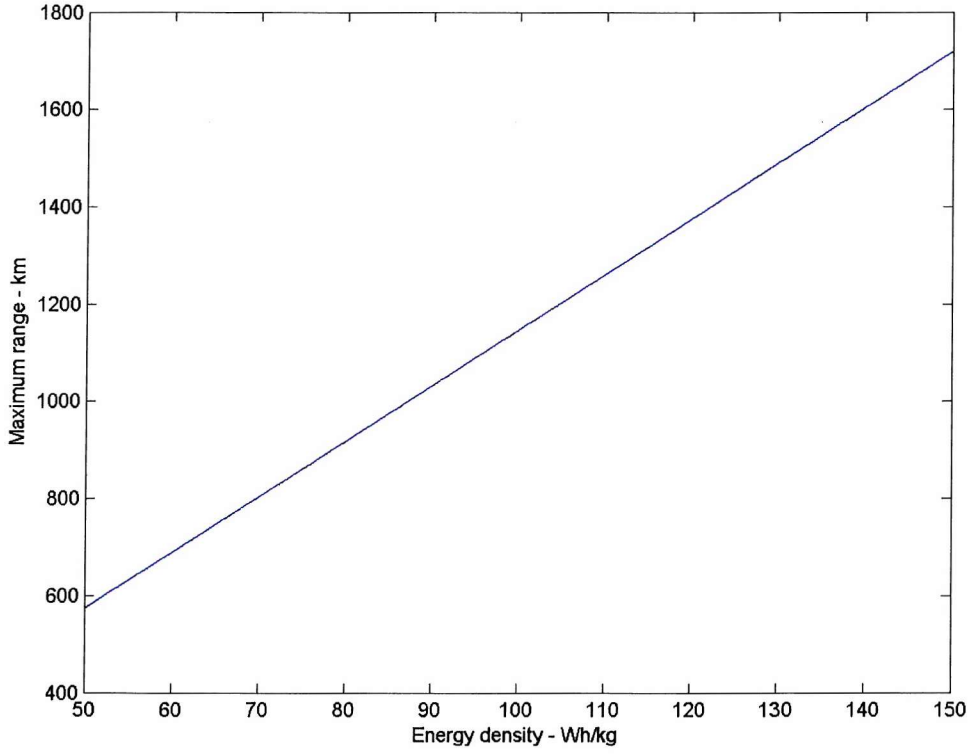

Figure 1.6.1 Range as a function of energy density

Even without these improvements, the battery energy density remains within a few per cent of that assumed in the model at an assumed speed of 2 m/s. Figure 1.6.1, shows that range is directly proportional to energy density. To account for a reduction in range from 1700 km to 800 km would require a reduction of energy density of 50% from the 150 Whr/kg assumed. It is, therefore, concluded that the small shortcomings

in battery effectiveness cannot constitute the main cause of vehicle performance shortfall.

1.6.2.2 Energy transmission

In generic AUVs there are two main energy transmission sub-systems within the overall energy conversion system.

- An electrical distribution system, whose primary purpose is to deliver power from the energy supply to the prime mover, but also supplies energy to the control system, payload and hotel load.
- A mechanical transmission system to transfer power from the prime mover to the propulsor

1.6.2.2.1 Electrical transmission system

The present system utilises low voltage dc transmission. Low voltage is inherently energy inefficient compared with using higher voltage for two reasons. First, for any given power a low voltage necessitates a high current. For any given resistivity of conductor, high currents require larger diameter cables for the same resistance/unit length (although this is partly offset by a lower requirement for insulation). These larger diameter cables require greater volume within the vehicle and imply greater mass. Secondly, for any given resistance, power dissipated within the cable is proportional to the square of the current carried, whereas it is only directly proportional to the voltage. Both of these effects determine that high voltage distribution systems are inherently more energy efficient than low ones. Additionally, any component that involves induction, is smaller the higher the supply frequency.

These facts together suggest that increasing both voltage and frequency by the adoption of aircraft style 400 Hz components operating at 208 V could reduce both Ohmic losses and the volume of the vehicle required for energy transmission. However, analysis of trials results indicate that electrical transmission losses are insignificant (less than 10 W). This, together with concerns about, for example, safety in handling higher voltages at sea, means that there is no case for changing the status quo.

1.6.2.2.2 Mechanical transmission system

Most AUVs are fitted with general purpose, off-the-shelf motors and propellers. The speed torque characteristics of the two are generally matched by means of a mechanical gearbox. This will inevitably result in some insertion loss. However, the current design of AUTOSUB has the propeller hard coupled to the motor. Such an arrangement, whilst eliminating transmission loss between components, does require the motor and propeller torque and speed characteristics to be precisely matched. This requirement is examined later in this chapter, but as the design currently stands the mechanical transmission is virtually 100 % efficient.

1.6.2.3 Prime mover

1.6.2.3.1 Description

Primary motive power is provided by a purpose designed brushless d.c. permanent magnet motor. It is unusual in that it comprises an external permanent magnet rotor, on which the propeller blades are directly mounted. The rotor surrounds a wound stator with the two being separated by ceramic-ring saltwater bearings. The arrangement is illustrated in Figure 1.6.2.

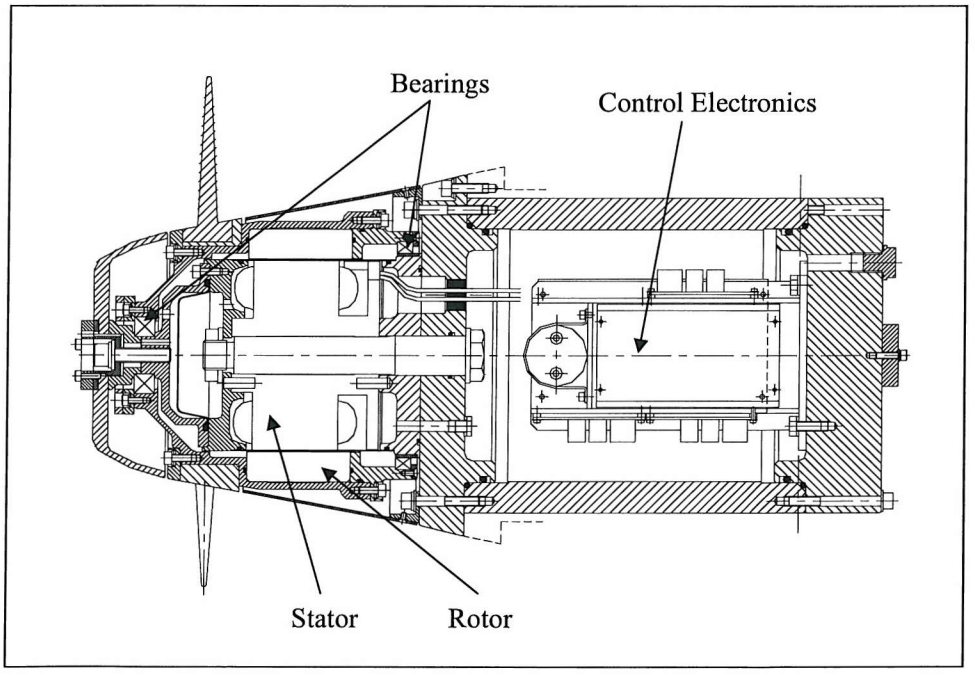

Figure 1.6.2 Main propulsion motor

Commutation is provided by low loss MOSFET control electronics (Kenjo and Nagamori, 1985b), which are located in a pressure proof housing attached to the end of the motor (Stevenson, 1996). These provide a three phase rotating magnetic field in the stator windings by means of the motor control switching circuit shown in Figure 1.6.3. Speed and torque are controlled by pulse width modulation.

1.6.2.3.2 Specification

The motor is designed to run from a supply voltage of 80 v, at a speed of 350 rpm. At this speed it should produce an output power of 1000 W at an efficiency of 70% (McPhail, 1993).

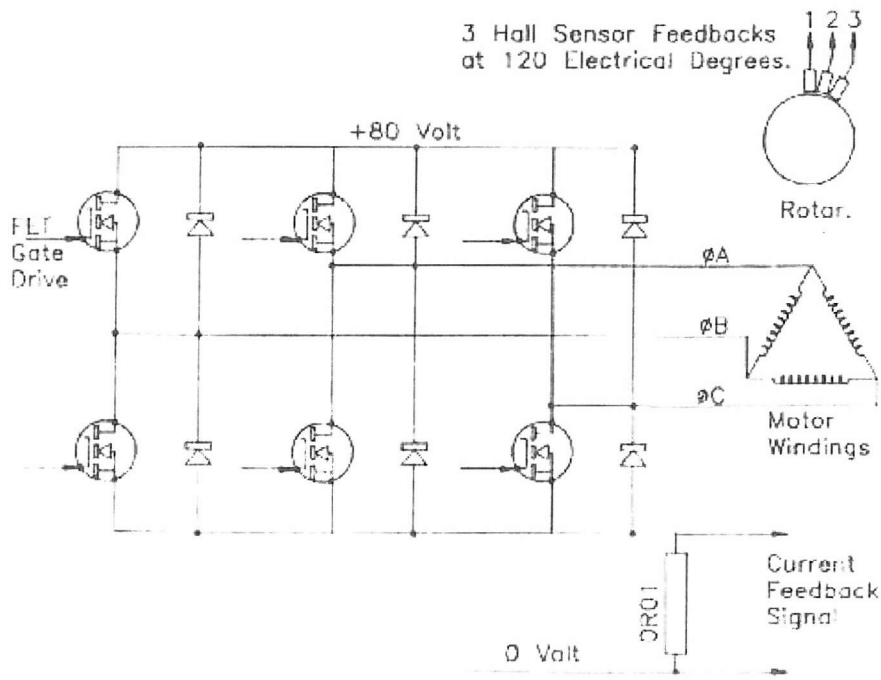

Figure 1.6.3 Motor control (Stevenson, 1996)

1.6.2.3.3 Measured performance

The motor test results indicate that with an 80 v supply and at a rotation rate of 350 rpm, the motor delivers 660 W at an efficiency of 68%. The analysis in chapter 1.5 indicated that this power output should be more than adequate. In fact the vehicle should only require 350 W at its cruising speed if the other parameters are as designed. At this power the efficiency of the motor falls to 60% at 350 rpm. Figure 1.6.4 shows how range varies with change in motor efficiency. This indicates that a

reduction in motor efficiency of 10% will reduce range from 1700 to 1450 km. Clearly this reduction in efficiency is not the major contributor to range shortfall, but, nevertheless, any increase in motor efficiency would contribute to recovery of range. Possible improvements to the motor were investigated (McPhail, 1993), including the diameter of the wire used in the motor windings and static and viscous friction losses. It was concluded that no significant improvement could be made by modifying the windings and that viscous losses were also very small. An investigation was, therefore, conducted into static friction losses.

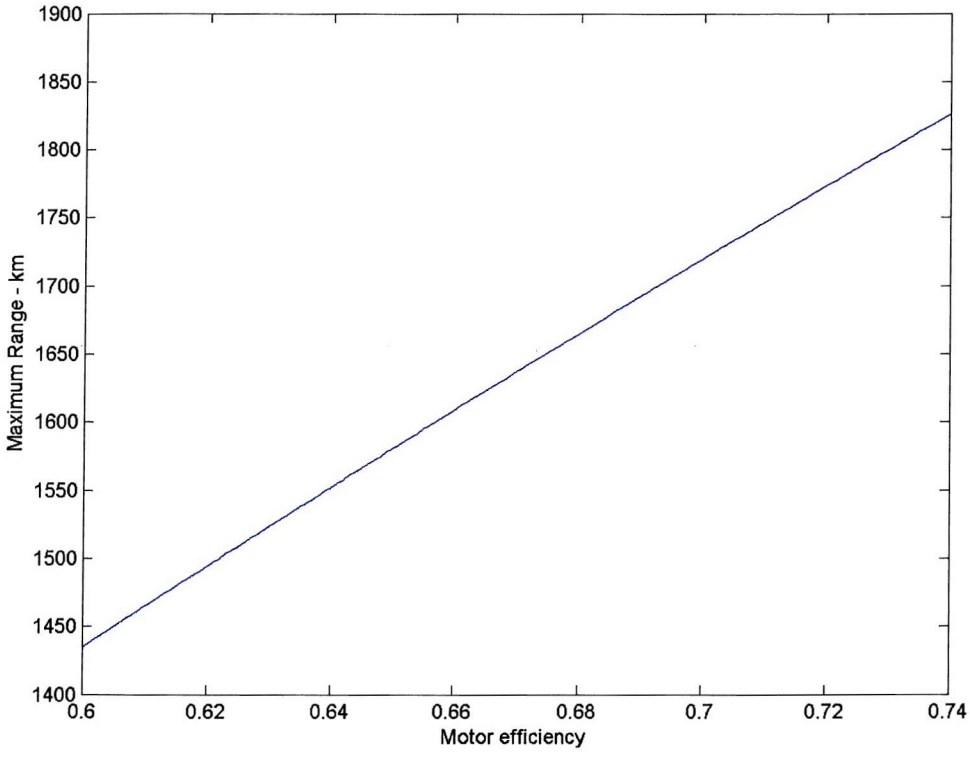

Figure 1.6.4 Range as a function of motor efficiency at a vehicle speed of 2 m/s

The motor runs on salt-water bearings. A stainless steel ball-race running in sea water is fitted at the rear end, to take the thrust loads, and a large diameter Xzylan-coated aluminium bronze ring at the forward end (Stevenson, 1996). These have the advantage over standard ball races in that they require no lubricant retention pressure glands. This makes the design both simpler and easier to maintain. However, they produce greater friction losses (and noise) than oil lubricated bearings and in the event these proved greater than anticipated. As a consequence, other bearings have been assessed (Figure 1.6.5) (Stevenson, 2001) and the motor was re-engineered to

accept stainless steel ball races, packed with grease but otherwise running in salt water (Stevenson, 1996). The reduced losses at the operating speed of interest of 350 to 400 rpm are of the order of 10 W. This improvement is sufficient to recover the motor efficiency to 70%. Thus, the motor is not the cause of performance shortfall.

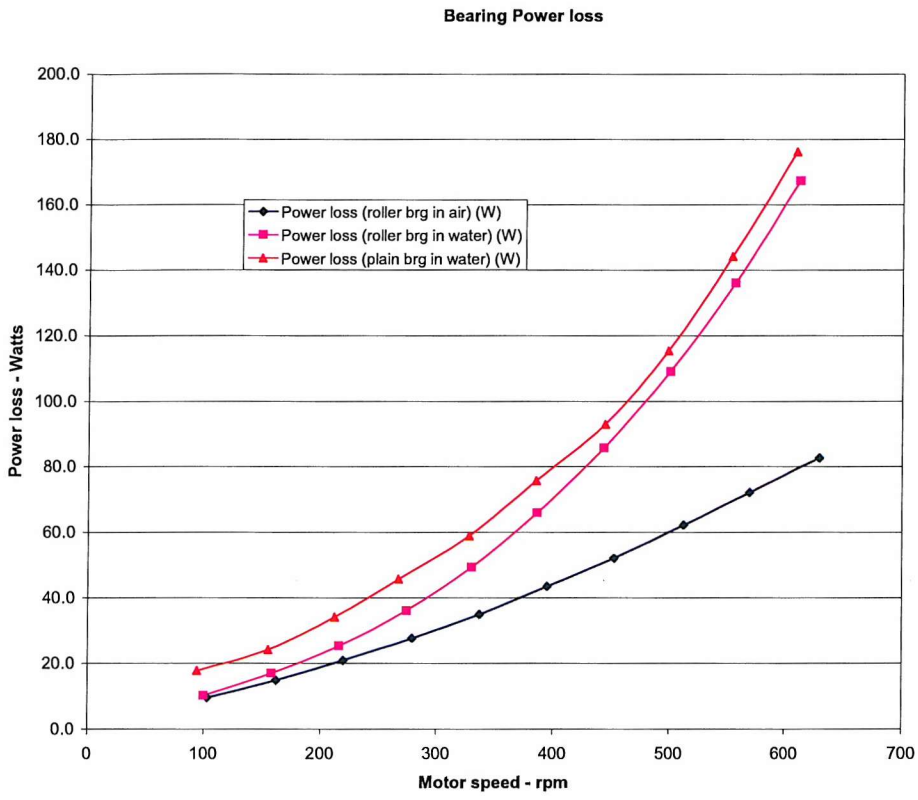

Figure 1.6.5 Motor bearing power loss

1.6.2.4 Propeller

The vehicle is driven by a 5-bladed, purpose-designed propeller, with the blades being mounted directly on the motor casing. The blades are made of a tough plastic material to reduce the effect of impact damage. In the event of damage, they are designed to be easily replaceable. Examination of reports on the design process (Stanier, 1992) (Wills, 1994) and the results of experiments undertaken at the design stage on the propeller (Clark and Wiltshire, 1997) indicate that the propeller in service may not be operated in the regime for which it was designed.

Because the blades are constructed of plastic, rather than a more rigid material, experiments were run during the design phase to determine the effect of deflection for a range of materials. The results of these trials are reported at (Clark and Wiltshire, 1997). These trials were undertaken for a range of conditions of water inflow and

rotation rates, determined from estimates of water flow over the hull and wake fraction made prior to finalisation of the hull design. Regrettably very few measurements were made under the conditions actually experienced in operation.

Since the water flow into and approaching the propeller plane were not measured questions arise concerning the matching of the propeller geometry and inlet flow conditions. These were explored in the report at (Fallows, 2001). The Matlab script at (Fallows, 2005) 1.6.1 was written to analyse the data (Clark, 1997) applicable to the operating conditions. The results suggest that the propeller is operated in a region of rapidly decreasing efficiency (Figure 1.6.6 and 1.6.7).

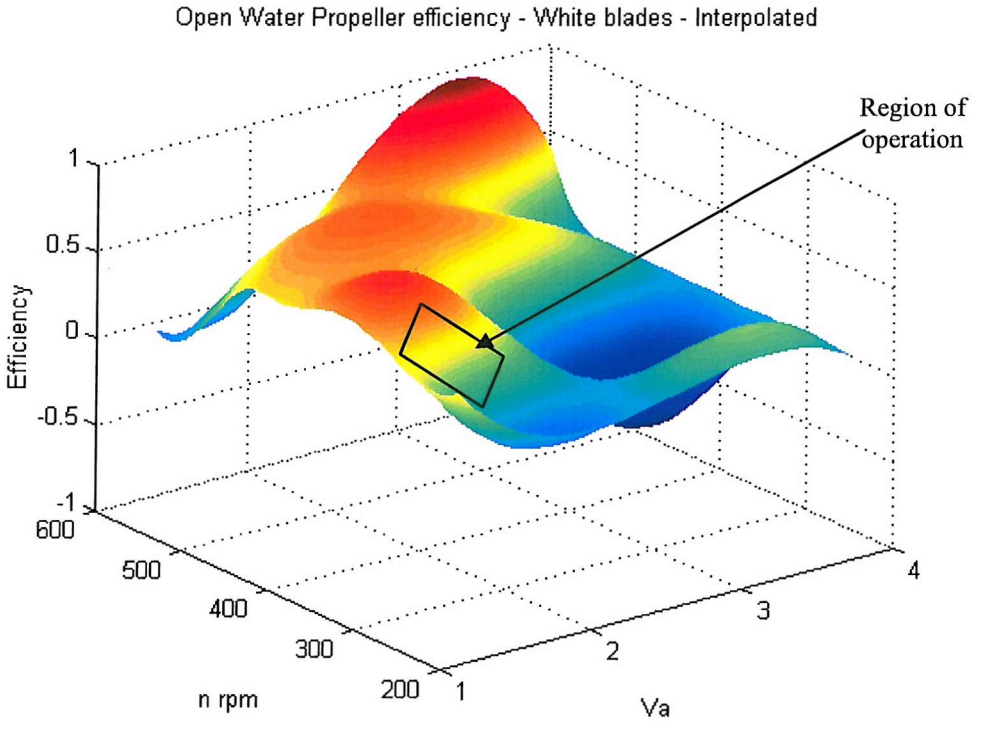

Figure 1.6.6 Propeller efficiency surface

From the marked contours (Figure 1.6.7), it can be seen that, according to these results, if the propeller is operated at the original design rotation rate of 550 rpm and an inflow of 2 m/s the expected efficiency is only 55% compared with the 75% assumed. Under the actual operating conditions of around 350 rpm, efficiency could be as low as 30 to 45%. The effect of such a shortfall on range performance is likely to be dramatic (Figure 1.6.8).

It is, therefore, concluded that the performance of the propeller should be further investigated to establish its performance under realistic operating conditions.

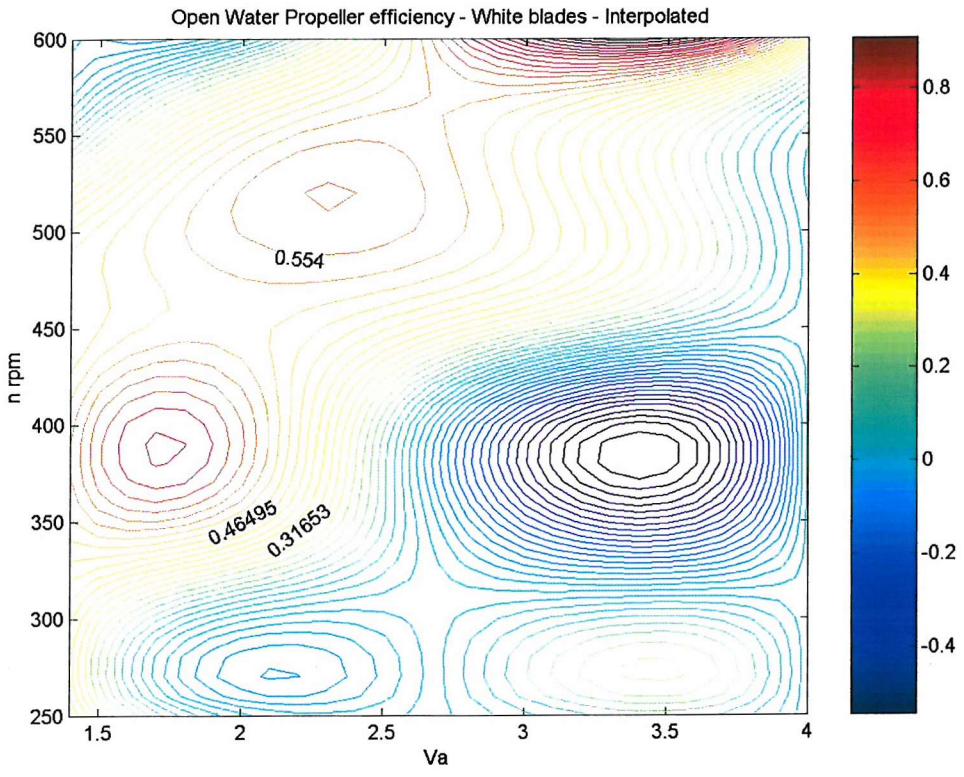

Figure 1.6.7 Propeller efficiency contours

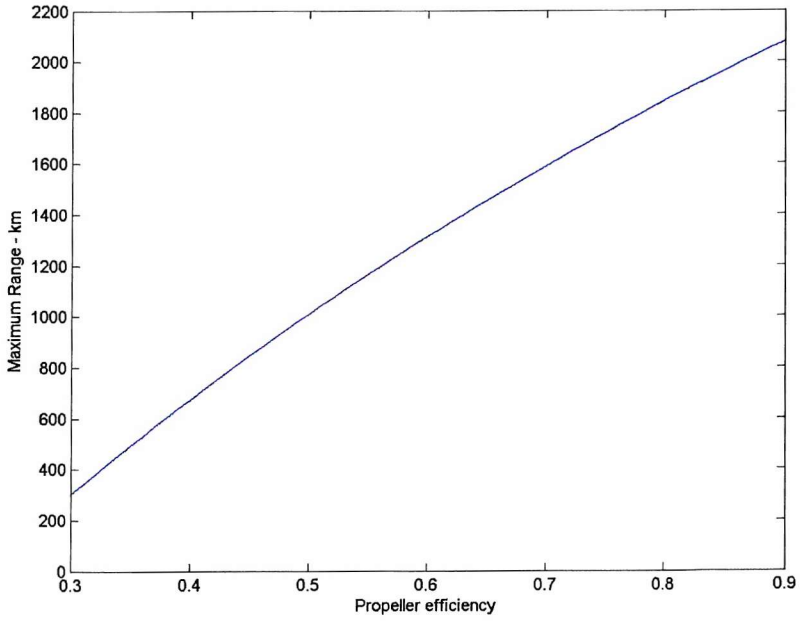

Figure 1.6.8 Range as a function of propeller efficiency

1.6.2.5 Hull

During early investigations into the design of AUTOSUB's hull, very low drag laminar flow forms were examined and tested (Babb, 1994). These designs were not adopted in the event due to reasons of cost and practicality, but the eventual hull-formchosen was still designed to exhibit low drag, albeit within constraints of ease of manufacture and high utilisation of internal volume, as illustrated in Figure 1.6.9. However, once in service, the requirement to fit a range of mission payloads, and the results of maintaining the vehicle under the harsh conditions of a research ship in a seaway soon resulted in a degraded hull form.

The build state and degree of damage changes with each operation. These are illustrated in Figure 1.6.10. The effects of these changes between missions make them the most likely candidates for the causes of performance decreasing with time.

Figure 1.6.9 AUTOSUB hull as conceived

A preliminary analysis of trials results (see chapter 3.2) indicated that the in-service drag of the vehicle could be of the order of twice that envisaged during the design stage. The effect that an increase in drag coefficient from 0.03 to 0.06 would have on range may be ascertained from Figure 1.6.11.

It is, therefore, concluded that the performance of the hull warrants further investigation to establish its performance under realistic operating conditions, particularly with respect to the effects of appendages and damage.

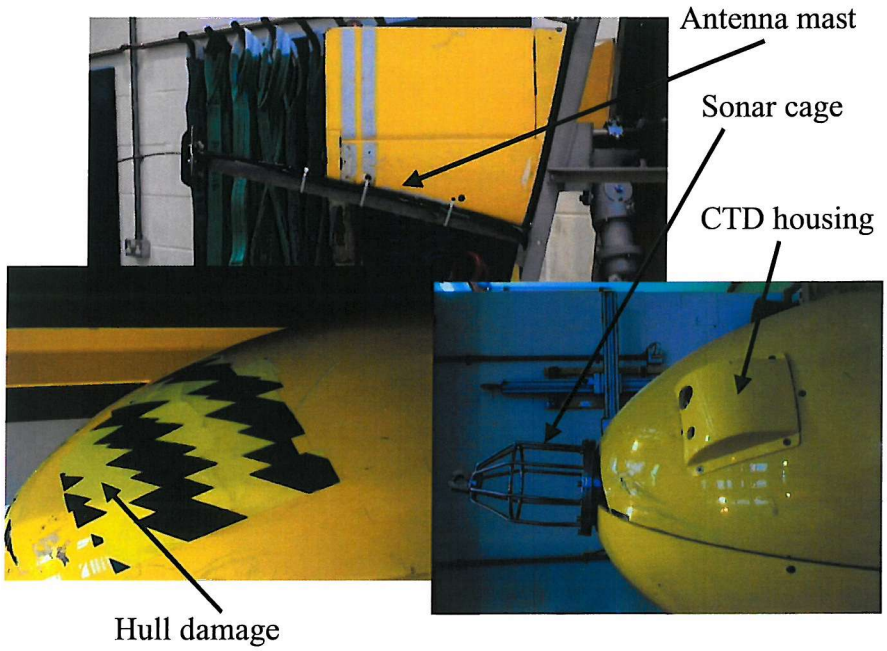

Figure 1.6.10 Details of in-service hull form

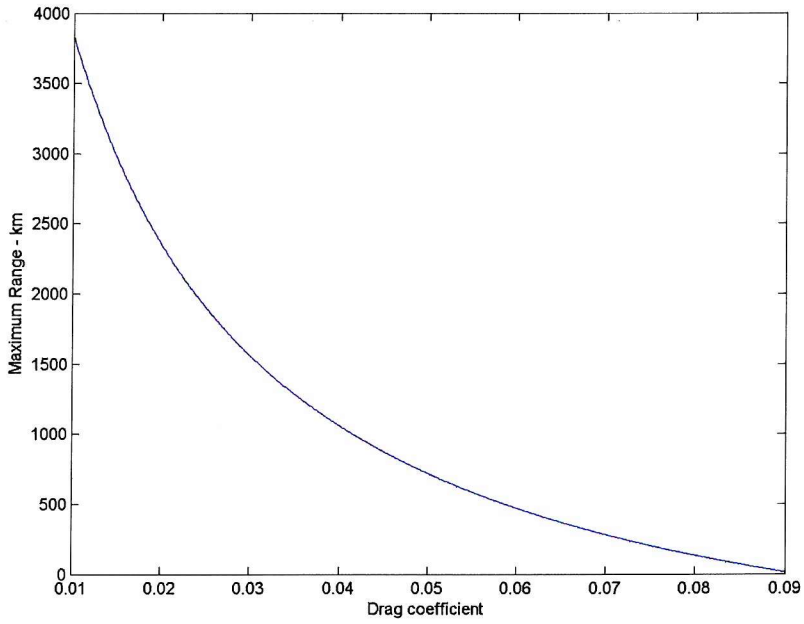

Figure 1.6.11 Effect of drag coefficient on range

1.6.2.6 Hull/Propulsor Interaction

At the time that the propeller was being designed, the hull-form had not been finalised. Assumptions as to the flow regime into the propeller disc were, therefore, made based on an existing torpedo hull form. It is possible that the actual environment

experienced by the propeller is different from that assumed. This interaction therefore requires examination.

1.6.2.7 Control System Influences

AUTOSUB has no active buoyancy control. A passive buoyancy system based on the use of syntactic foam blocks is used. These blocks automatically compensate for some of the change in buoyancy under pressure at depth. A small margin of positive buoyancy is maintained for safety. This is overcome at depth by negative lift obtained from the hull and control surfaces. The forces generated to maintain negative lift will necessarily increase drag. The level of drag experienced depends upon body and hydroplane forms and relative angles to the direction of forward motion.

(Abbott and Doenhoff, 1959, p16) indicates that the induced drag coefficient for aircraft wings has a quadratic dependence upon the lift coefficient, C_L, that is

$$C_{Di} = \frac{C_L^{\,2}}{\pi A u} + C_L \varepsilon a_e v + (\varepsilon a_e)^2 w .$$

Here the following notation applies:

A is the aspect ratio of the lifting surface.

u, v and w are factors dependent upon the taper and aspect ratios, and may be obtained for standard wing section series from published charts (Abbott and Doenhoff, 1959, pp 16-18).

ε is the aerodynamic twist.

a_e is the lift/curve slope for the section under consideration.

C_L is the coefficient of lift, and is itself a function of the angle-of-attack of the lifting surface or body given by:

$$C_L = a(\alpha_s - \alpha_{los} + J\varepsilon)$$

Where:

α_s is the angle-of-attack.

α_{los} is the angle of zero lift.

J is a factor that may be obtained for standard wing section series from published charts (Abbott and Doenhoff, 1959, p 17).

Clearly calculating the drag from this equation is only possible when the various factors have been established for the geometry under consideration. Such data are available for standard wing geometries (Abbott and Doenhoff, 1959), and so could be

applied to the AUTOSUB hydrofoils (since their geometry conforms to NACA 0015 sections with defined aspect ratios and taper). However, standard data does not exist for the AUTOSUB hull-form, so, either estimates must be made using lifting surface panel codes, or direct experimental measurements made on a model. This subject is addressed further in chapter 2.4.

1.6.2.8 Navigation and control

The distance travelled is not the sole determinant of overall system range effectiveness. For optimal use of energy the navigation system needs to be able to provide the most energy efficient course and the control system needs to be able to accurately follow it. However, such scope for improvement in overall system performance is being addressed separately and will not be considered further here.

1.6.2.9 Conclusions

Chapter 1.5 established that the system should be capable of significantly greater range and endurance than that experienced in service, provided that all of the sub-systems perform as anticipated. The analysis of sub-system performance in this chapter has indicated that some aspects of the vehicle as built warrant further characterisation to provide a basis for the development of improvements. The principal areas for further investigation include:

- Performance of the actual as-built hull under in-service conditions in terms of:
    - Drag coefficient as a function of hull-formand speed.
    - Sources and causes of hull-formdrag.
    - Drag forces as a function of hull attitude, hydroplane angle and speed.
    - Flow conditions into propeller disc.
- Performance of the in-service propeller in situ and under operational conditions.
- The possibility of the vehicle control system being improved so as to minimise hull and control surface angles.

Work on the propeller and control system is being undertaken elsewhere. The task of determining the drag characteristics of the hull and its appendages is the subject of the remainder of this thesis.

CHAPTER 1.7

HULL DRAG – A COMPLEX PROBLEM

1.7.1 Introduction

Because AUVs are energy-limited devices, efficient propulsion is critical. For any given size of vehicle, energy source, motor and propeller, propulsion efficiency is dependent upon minimising the force needed to overcome the hydrodynamic drag of the hull and matching of the flow over the hull into the propeller. AUV hull-forms are hence designed to be hydrodynamically efficient within the constraints of economic manufacture and practical payload spaces. However, two factors result in degradation of the hull-form:

- The vehicle requires to interact with the outside world. It, therefore, needs to be fitted with communication devices and sensors. These often necessitates changes in the detail of the hull-formby the addition of aerials, ray-domes and orifices.
- Practical vehicle control systems, particularly for lighter than water vehicles, necessitate the hull and control surfaces travelling at sub-optimal angles to the direction of motion.

In the case of the class of AUVs designed to collect scientific data, this phenomenon is complicated by the need to tailor the payload to the mission. Changes to the detail of the hull form, resulting from in-service wear and tear, compound these effects. The net effect of this is frequent changes in hull-form and hence propulsion efficiency.

For AUTOSUB in particular, analysis of the performance of the propulsion system (chapter 1.6) has identified an apparent discrepancy between the expected drag of the hull and that experienced in practice.

There is, therefore, a need to:

- Characterise the hydrodynamic performance of the basic hull.

- Derive guidance as to the optimal shape, size and location, of payloads and services that need to penetrate beyond the normal hull surface, in order to minimise the effect on propulsion efficiency.
- Propose affordable modifications to the hull that would improve propulsion performance.

Items that may be readily modified include:

- Shaping and sighting of services, such as beacons and aerials.
- Improved maintenance of the hull surface such as repair of abrasion, or careful fitting of panels.
- Changes to the hydroplanes should these be found to produce an adverse effect on the inflow to the propeller or cause undue drag.
- Changes to the propeller blades should they be found to be operating in a sub-optimal regime.

It has been demonstrated that the hull in-service has significantly different drag from that of the idealised form assumed during development. Further, experience has shown that propulsion performance is reducing with time. Together these indicate that the detail of the hull form, not considered during the design phase, is having a significant effect on overall hydrodynamic performance. Furthermore, changes in the detail of the hull-form from mission to mission appear to affect the performance. An investigation is, therefore, required that takes account of the full complexity of the actual hull as deployed at sea.

Because of these differences between idealised and real performance, the vehicle operates in a regime not expected, and, therefore, not characterised, during development. For example drag was calculated (Kimber and Scrimshaw, 1994) for the expected operating speed of 2 m/s. The drag of the actual in–service speed, in the region of 1.5 m/s, was unknown. The vehicle operates at an angle-of-attack in the region of 2°, whereas drag was only measured at 0°. There was, thus, a need to characterise the performance of the hull across a range of operational conditions as well as for a variety of appendages and other detail of the hull form. This would enable the causes of drag to be derived and enable design and operating guidance to be formulated.

Finally, because of uncertainty in the actual performance of the vehicle, it is necessarily operated with a safety margin to ensure that it has sufficient fuel to return

to its rendezvous for recovery. A simple means of measuring its actual in-service propulsion performance would reduce the margin required, and effectively enable increased range for the cost of the measurement.

1.7.2 Alternative approaches

There are four broad methods by which the investigation may be made:

- Theoretical modelling.
- Computer simulation.
- Analogue simulation. (Laboratory experiments using physical models)
- Real world trials. (On the full-scale vehicle at sea).

Theoretical calculations underpinned the original design. Methods are available to provide a broad indication of the level of drag and the analysis in chapter 1.5 has confirmed that, taking a broad parametric approach, the vehicle as built should be capable of meeting the original performance aspirations. A more detailed assessment is possible by taking into account the effects of angle-of-attack and hydroplane angle, although as shown in chapter 2.4, data is not readily available for non-standard geometries such as the hull forms usually adopted for AUVs. This approach is outlined in (Fallows, 2005). These methods are suitable for producing an indication of the performance of the bare hull. Extending the analysis, to include the effect of appendages, is possible, but necessarily increases its complexity. There is a considerable literature (Hoerner, 1965) providing empirical guidance on specific appendages, although these are often for highly idealised geometries. Formulae that take into account combinations of appendages and allow for their relative positions in sufficient detail have not been found. A theoretical approach will, therefore, become increasingly unreliable with increase in the level of detail sought and is unlikely, on its own, to provide a sound basis for a detailed examination of the issue.

Theoretical modelling and computer simulations using hydrodynamic code has been undertaken elsewhere (Chettleborough, 2002). An investigation into the drag of the bare hull has been undertaken using a panel code, 'PALISUPAN', devised by Turnock (Turnock, 2000). This explored the transition point, and boundary layer thickness, and from this derived the drag force. However, adding increasingly fine detail to the model to produce the answers required of this investigation is both time consuming and conceptually difficult. To include the fine detail a much larger number of panels than has been used to date is required. There will be a tendency for the

number of panels to increase geometrically as the level of detail increases and for the time required for the consequent computation to increase at an even greater rate. The stability of the programme is uncertain under these conditions. Additionally it will be difficult to assess the detailed interactions between appendages and any attempt to do so will increase the complexity still further.

Part of this investigation is to assess how drag varies with angle-of-attack and hydroplane angle. This necessitates modelling the vehicle as a lifting body. Whilst PALISUPAN will allow this, there will be uncertainty on the nature of the Kutta condition for the detailed model. Thus, the success of such detailed modelling could only be ascertained once it had been validated by comparison with measurements made in the real world. Physical modelling is, therefore, indispensable.

1.7.3 Requirement

Experiments are required to met the following objectives:

a) To quantify the total drag of the basic vehicle for a range of cruising conditions and configurations.
b) To determine how changes to the detail of the hull-form effect drag, i.e. establish which factors and combinations of factors most contribute to drag.
c) To determine the actual in-service drag of the real vehicle.

The only convincing means of satisfying objective (c) is to derive the effects from operation of the real vehicle at sea, preferably immediately before its deployment, and accept that there is little control over the environment. However, in order to meet the remaining objectives it will be essential both to either control the environment or monitor it, and to be able to readily change the configuration of the vehicle. The options for achieving this are considered further in Section 1.7.8.

The measurements required from within a known environment may be obtained from the following experiments:

1. To determine the components of drag of the basic vehicle (bare hull and hydroplanes).
2. To determine the effect of angle-of-attack and corresponding control surface angle on the drag of the clean hull.

3. To determine how the size, shape, orientation, position and combinations of orifices and attachments contribute to drag.
4. To determine how changes to surface finish contribute to drag.

1.7.3 Effects and factors

The first step in designing a set of experiment is to determine what effects are to be measured, and which factors will effect these measurements

1.7.3.1 Principal effect

The objectives of the experiments are to determine the overall drag of the vehicle hull under operational conditions and to determine the sources and causes of that drag. The measurable parameter quantifying drag is the force opposing motion in the direction of travel.

1.7.3.2 Secondary effects

Although not required to meet the main objectives of this investigation, two additional effects are of interest.

- The lift generated by the vehicle across a range of angles of incidence will be of interest to those designing the control system. This parameter can be easily measured at no extra cost.
- As will become apparent later, knowledge of the added mass of the vehicle is of interest and can be measured.

1.7.3.3 Primary factors

Two sets of factors will influence the results of the experiment: those that directly determine the fluid flow, and hence drag; and those that determine the performance of the measurement system. Each of these may further be categorised into those factors that are under control in the experiment and those that remain uncontrolled. Some of the uncontrolled factors may be measured. For example it may not be possible to ensure that the temperature of the body of fluid in which the experiment is conducted is maintained constant and uniform, but it should be possible to sample the temperature at various times and positions. On the other hand, it may be considered uneconomic to measure and record the sources of noise within an electronic amplifier used in the measurement system.

Designation	Main factor	Related factors		
		level 1	level 2	level 3
1	Motion			
1.1		Direction		
1.2		Speed		
2	Attitude			
2.1		Angle-of-attack		
2.2		Hydroplane angle		
3	Model			
3.1		Size	Scaling	
3.2		Shape		
3.2.1			Bare hull	
3.2.2			Fins	
3.2.3			Features	
3.2.3.1				Type
3.2.3.2				Size
3.2.3.3				Shape
3.2.3.4				Position
3.2.3.5				Relative position

Table 1.7.1 Primary factors

Because of the connectedness of all things it is not possible to provide an exhaustive list of the factors that may influence the results. The best that can be done is to list those that are considered most important and group the remainder under unidentified sources of noise. Some factors, termed here the primary factors, are a direct consequence of the aims of the experiment. Primary factors identified by the author are listed in Table 1.7.1. Other factors flow from the particular design of the experiment undertaken and are considered in part 2, chapter 2.2.

1.7.4 Dealing with detail

The detailed form of the vehicle is according to the payload and services required. In addition, it varies as a result of damage sustained in the harsh environment of a ship in a seaway. Understanding is, therefore, required of the effects of comparatively fine detail, such as that of appendages and orifices needed for sensors, and that which results from in-service handling, such as ill-fitting panels, and dents and abrasions on the hull surface.

The detailed form of the vehicle may be considered under three headings.

a) Common services. These are present on every mission and allow the vehicle to perform its basic task. These include for example, control surfaces, lifting lugs and communications antennae.
b) Mission-specific services and mission payload. The latter usually requires hull-penetrating sensors.
c) In-service damage.

Item (a) is constant: (b) changes from mission to mission: and (c) changes with time according to the maintenance state.

It is necessary to understand the effects of each of these individually, together with their interactions. From this knowledge a model and set of rules may be developed to guide the design and positioning of orifices and appendages and enable analysis of the cost effectiveness of improved vehicle handling strategies.

1.7.4.1 The form of the basic hull

The bare hull of AUTOSUB comprises a central cylinder with an ellipsoid nose and a conical tail blended into the central cylinder as shown in Figure 1.7.1. Four identical fins are mounted on the tail. These provide the control surfaces and constitute port and starboard hydroplanes and dorsal and ventral rudders.

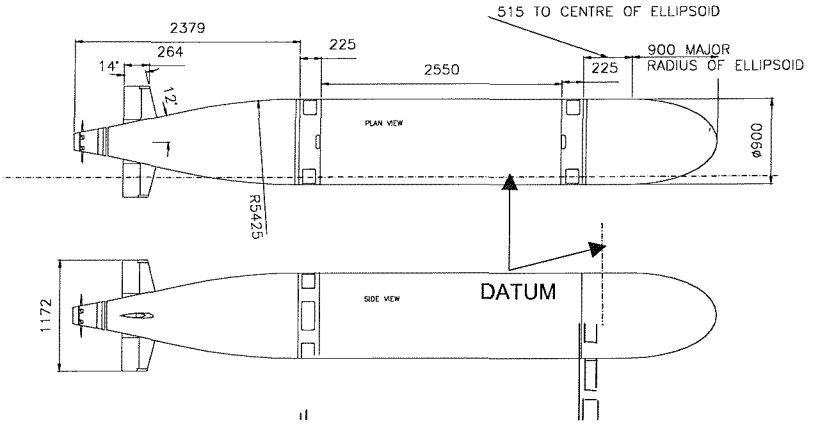

Figure 1.7.1. AUTOSUB bare hull form

This simple shape is complicated by the presence of a number of features that modify the basic form.

1.7.4.2 Baseline features

These provide essential services and are present on all missions. Examples are illustrated in Figures 1.7.2. A full listing is given in Table 1.7.2.

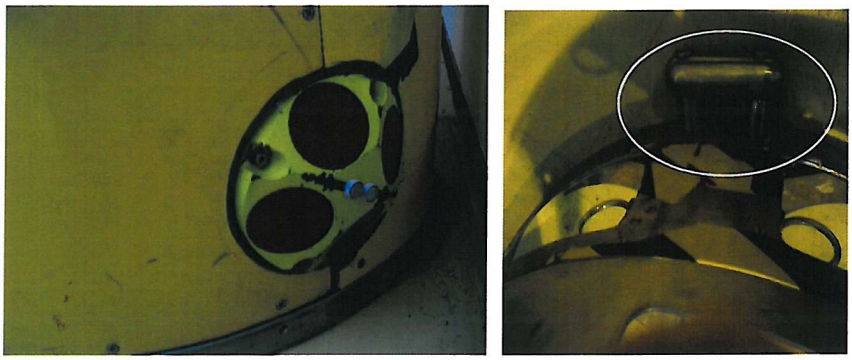

ADCP Lifting Eye

Figure 1.7.2 Examples of baseline features

1.7.4.3 Mission specific features

These comprise payload specific modifications and service sensors whose position changes according to the need of the sensor and the availability of space. Examples are illustrated in Figure 1.7.3 and a listing included in Table 1.7.2.

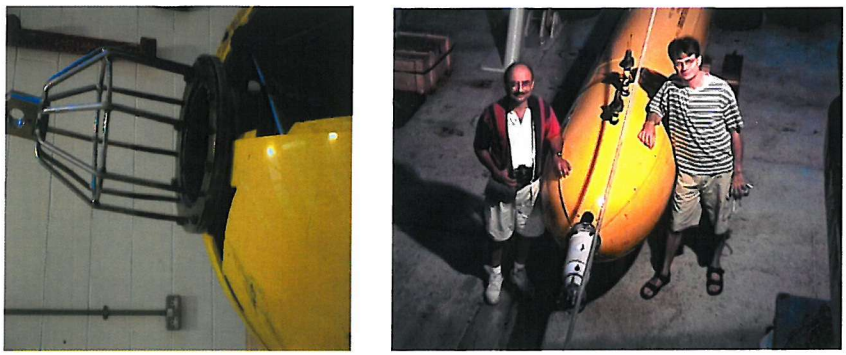

Figure 1.7.3 Examples of mission specific features (IF Sonar Cage and Turbulence Probe)

1.7.4.4 Wear and tear features

These result from in-service degradation and are illustrated in Figure 1.7.4 and listed in Table 1.7.2.

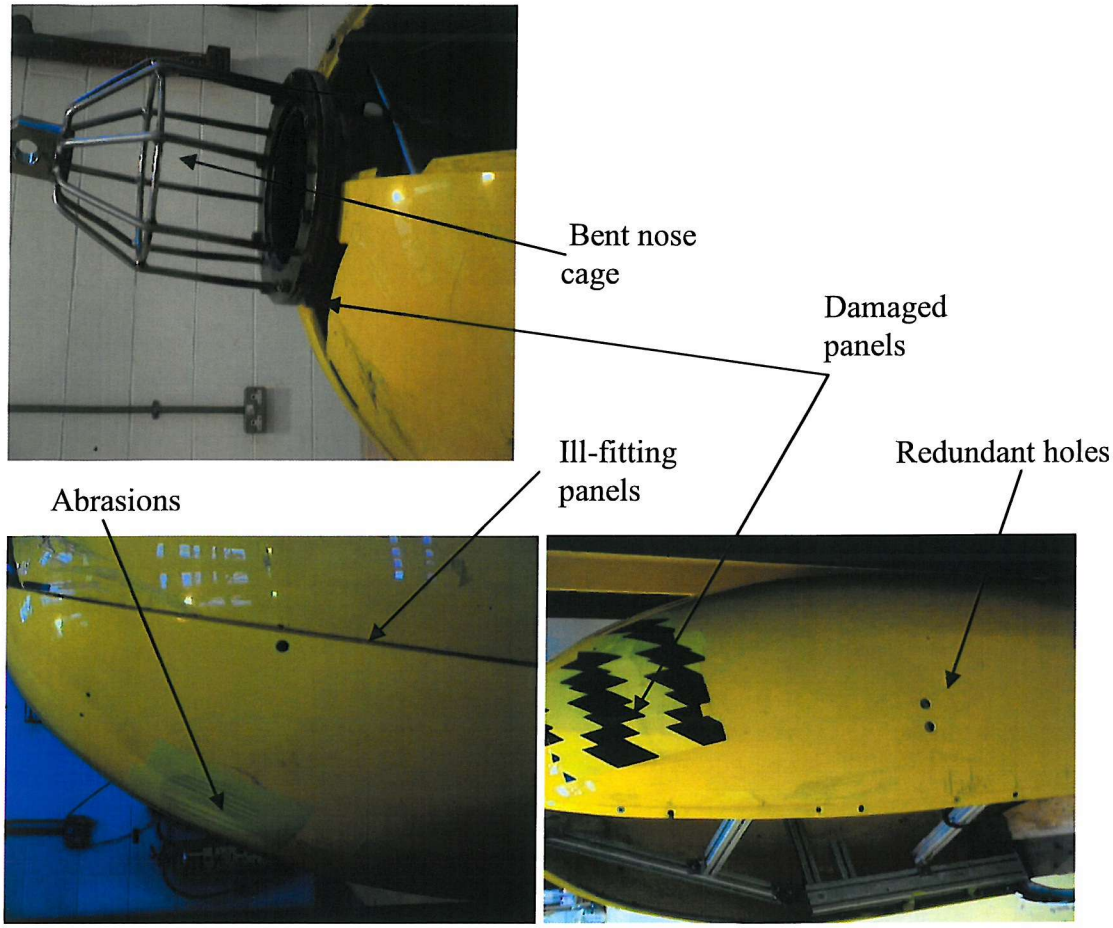

Figure 1.7.4 Examples of in-service damage

1.7.5 Specifying location

A vehicle measurement datum and notation system is required to enable the location of hull features to be specified. This is defined in Figure 1.7.5, with the fore and aft datum plane being located at the forward bulkhead and the radial datum projecting from the axis of the vehicle to starboard. Location on the surface of the hull is defined by distance x, and angle ϕ, with x being positive aft of the vertical datum, and ϕ being positive clockwise from the horizontal datum looking from the bow.

1.7.6 Levels

Drag is a consequence of the nature of the flow round the vehicle and the interaction between the fluid and the vehicle surface. The primary factors of motion, attitude, shape, size and position may all be expressed as continuous functions and can take an infinite number of levels. However, each is, in practice, limited in range to that which is feasible for the in-service vehicle. For experimental purposes they will need to be

restricted to a practical number of predetermined levels within that range. The number of levels chosen will depend on the maximum number of measurements that can be made within resource constraints and the complexity (number and location of inflections) of the effect surface expected.

Baseline	Payload		Damage	
Description	Variety	Representative of:	Variety	Representative of:
Argos Aerial	Cylinders & rods		Surface roughness	
Beacon lamp A		Large sonar dome (AUI)		Scratches
Beacon lamp B		Small sonar dome (Navigator size)		loss of jellcoat
CTD Sensor (port)		Small sonar dome (AUI)	Poorly fitting panels	
CTD Sensor (stbd)		Comms antenna (Argus)		Channels
Lifting line stow hole		Strut (GPS support)		longtitudinal
Flooding hole A (fwd)	Domes			circumferential
Flooding hole B (fwd)		Small housing (Beacon)	Spot features	
		Large housing (Navigator)		screw/rivet heads
Lifting lug (fwd)	0015 NACCA Section beams			longtitudinal
Lifting line (fwd)		Long strut (GPS support)		Circumferential
Lifting line (aft)		Short strut (1/2 size support)	Annuli	
Lifting lug (aft)		Large streamlined Housing (Navigator)		Poorly fitted sensors
		Small streamlined Housing		
Flooding hole A (aft)			Holes	
Flooding hole B (aft)	Tubes: Horizontal			
Top fin mast, GPS antenna & Argos aerial		ctd sensor		
ADCP 1	Vertical			
		sensor		
	Cage			
	Dome - 0.5cm rod - large	LF Sonar protective cage		
	Dome - 0.3cm rod - small	1/2 size protective cage		

Table 1.7.2 AUTOSUB Features

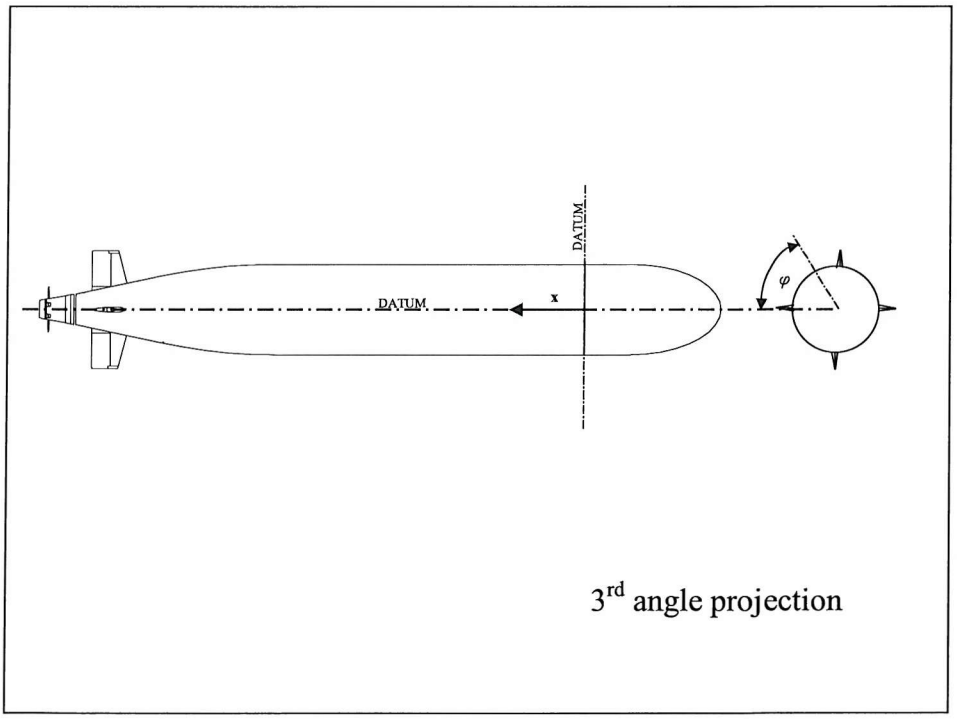

Figure 1.7.5 Positional measurement

Levels for motion and attitude are comparatively easily specified. However, the specification of shape and size of the vehicle down to a significant level of detail presents a greater problem. An analysis of the patterns of features that occur in AUTOSUB gives the total array of levels for each of the primary controlled factors in Table 1.7.3.

	Factors					Unit	Range	Number of levels
	main	level 1	level 2	level 3	level 4			
1	Motion							
1.1		Direction				deg		1
1.2		Speed				m/s	1 - 2.4	8
2	Attitude							
2.1		Pitch angle				deg	0 - 15	5
2.2		Hydroplane angle				deg	0 - 15	
3	Model							
3.1		Size	Scaling				fixed	1
3.2		Shape						
3.2.1			Bare hull				fixed	1
3.2.2			Fins				0 - 4	3
3.2.3			Detail					
3.2.3.1				Baseline				
3.2.3.1.1					Number			16
3.2.3.1.2					Shape			9
3.2.3.1.3					Size			1
3.2.3.1.4					Position			4
3.2.3.2				Mission				
3.2.3.2.1					Number			5
3.2.3.2.2					Shape			5
3.2.3.2.3					Size			3
3.2.3.2.4					Position			17
3.2.3.3				Wear and Tear				
3.2.3.3.1					Number			3
3.2.3.3.2					Shape			6
3.2.3.3.3					Size			3
3.2.3.3.4					Position			4

Table 1.7.3 Primary controlled factors and levels

1.7.7 The magnitude of the experimental space

Even with this restricted number of levels a complete exploration of all of the factors at all levels would take of the order of 10^{10} measurements for a single datum at each point. Should additional data be required to give statistical significance then the number of measurements required becomes larger still.

To explore a sample space of this size in a reasonable time requires a high sample rate. From Figure 1.7.6 it can be seen that to take this number of samples within 1 year, taking measurements 8 hrs/day for 300 days, would require a mean data rate of 100 kHz. Such rates are readily achieved with electronic measurement systems

such as radar but the maximum data rate achievable, for example, in a towing tank is 3 mHz (1 measurement every 10 minutes), and the worst, when changing hull configuration, is 250 μHz. Thus, to achieve statistically significant results over the entire experimental space would take of the order of 10^{11} years. (To put this figure in context, it is estimated that the Earth was formed some 4.6 x 10^9 years ago. Obtaining funding for such an experiment was considered to be a challenge too far, so an alternative approach was sought.

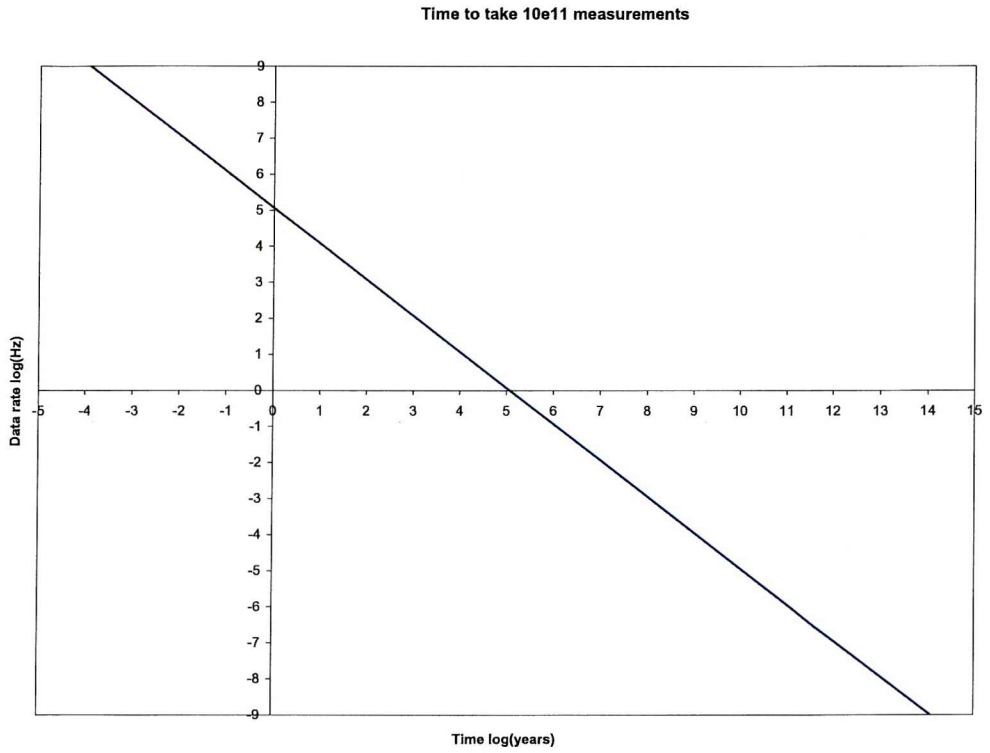

Figure 1.7.6 Time vs. data rate for 10^{11} data points

The issue of the design of an affordable experimental programme is addressed in chapter 2.2.

1.7.8 Experiment options

Three options were considered for the experiments:

- On the full-scale in-service vehicle at sea.
- On a scale model in a wind tunnel.
- On a scale model in a towing tank.

Using the full-scale in-service vehicle at sea has the advantage of measuring the real effects experienced in service. However, drawbacks include: the cost of employing the only in-service vehicle or producing another, the inability to control

the environment and difficulty in measuring it, and the difficulty in deploying the required instrumentation.

The option of using a scale-model in a wind tunnel had been pursued during the early design phase and readily facilitates flow visualisation and measurement. The higher data rate, when compared with that obtainable from a towing tank, was also attractive. However, the non-availability of a wind tunnel ruled it out.

Finally the possibility of using a scale-model in a towing tank was considered. The properties of the 'fresh' water used in a towing tank approximates to the seawater in which the in-service vehicle operates. Scaling to retain the flow patterns experienced by the full-scale vehicle is, thus, straightforward.

The availability of facilities determined that the experiments had to be conducted either in a towing tank and/or on the full-scale vehicle. It was established that limited experiments could be performed on the in-service vehicle provided that they did not require significant modification and could be contained within the extant deployment programme. These constraints, together with the limitations of control over the environment at sea and the difficulty of deployment of instrumentation, meant that some controlled laboratory experiments would be essential. A complementary set of experiments was, therefore, devised. Exploration of the fundamental performance of the vehicle would be undertaken in the laboratory. The results would be verified by experiments on the full-scale vehicle at sea, which would also be used to determine the ranges over which the factors needed to be explored. It was hoped that a strong relationship between velocity, angle-of-attack and hydroplane angle could be found from the experiments at sea so that these need not be treated as independent variables in the tank experiments. In the event it was found that correlation between hydroplane-angle and angle-of-attack was weak. These, therefore, had to be treated as separate factors.

An additional output sought from the at-sea trials is a standard process that will allow rapid and economic determination of the effect on propulsion performance of future modifications to the form of the hull. As described in part 3, the designed trial requires knowledge of the added mass of the vehicle. This was to be measured in the laboratory.

Summary

For a full understanding of the causes of the vehicle not performing as envisaged at the design stage, and for the changes in its performance observed in-service to be understood, it is necessary to determine the implications of the full complexity of the hull, down to a lower level of detail than had been considered during the design phase, and across a range of operating conditions not investigated during development. To do this a range of experiments is required to completely characterise the hull and hull/control-system interaction. This can only be achieved in the laboratory, but the results will need to be tested against the results derived from trials on the in-service vehicle at sea. The problem of the design of laboratory experiments focuses on how to capture the effects of this level of complexity within an achievable set of experiments. This is addressed in part 2, which takes into consideration facility availability, affordability and time. The at-sea trials are described in part 3.

Chapter 1.8

CONCLUSIONS FROM THE SYSTEM ANALYSIS

1.8.1 Introduction

A generic issue concerning the characterisation and optimisation of complex systems was posed in the opening part of the thesis. The issue was discussed at three different levels: that of the generic system; that of a family of systems, AUVs; and that of a specific system, AUTOSUB. As a consequence, a specific problem concerning the propulsion system of AUTOSUB has been identified. The solution to this particular problem requires argument at a different level of detail to that used in this part. This will be undertaken in parts 2 and 3.

1.8.2 The evolution of systems

The required increase in functionality of man-made machines, coupled with the desire to make them operate in ever more challenging environments, results in the need for machines to be constructed as systems. As time progresses, these systems become ever more complex and assessing their performance under all conditions becomes increasingly difficult.

When designing complex systems, simplifying assumptions are necessarily made so that estimates of overall performance may be more readily derived. Because of economic pressures of cost and time, and because of the sheer difficulty of measuring the performance under the more extreme conditions, it is likely that the system will not have been fully characterised when it enters service. It is probable that it will only have been characterised to the extent necessary to demonstrate that the most important requirements, such as overt safety and key performance parameters, have been met. This will have two consequences. Firstly, its net performance is unlikely to have been fully optimised and, therefore, enhancement should be possible at a cost small in comparison to the investment already made. Secondly, because the full performance envelope will be unknown, the vehicle will be operated with a larger safety margin than would otherwise be necessary. Again an effective increase in

performance should be possible for modest outlay. The subject of this thesis is to describe a process for achieving a better understanding of the characteristics of an in-service system so that these improvements may be made. The process is developed by considering a particular system, that of an in-service AUV of proven effectiveness.

1.8.3 Autonomous Underwater Vehicles

The essential characteristic of an AUV is to be able to carry a payload within the body of the ocean, to meet a pre-defined mission requirement, without real time human intervention. This implies the need for a means of propelling in three dimensions, a navigation system and some means of controlling itself.

The first generation of practical vehicles did not enter service until the end of the last century. These have demonstrated that the main problems of autonomous movement underwater have been solved, although there remains much room for improvement. The major outstanding issues are: enabling greater depth to be achieved economically ;and affording greater range/endurance/speed at acceptable cost. This thesis concentrates on the latter issue.

1.8.4 AUTOSUB

In examining the issue of range in the context of a complex system, the thesis uses the example of an in-service AUV, AUTOSUB. Its performance has been found to compare favourably with other AUVs of its class. Despite this, it has still been found to have a significantly shorter range than had been expected during its design stage: for any particular cruising speed, the propulsion system is found to consume energy at an order of magnitude greater rate than anticipated. The process for achieving improved performance of an in-service system through a greater appreciation of its characteristics is developed in the context of this problem.

1.8.5 System engineering concepts

Before considering the particular issue of the AUTOSUB propulsion system a number of system engineering concepts required development. The characteristics that distinguish a system from other classes of mechanism, include: the fact that it comprises a number of sub-systems; each of these provide their own functions and are in some way self contained; each contributes to a system functionality that exceeds that of its constituent sub-systems. A system also invariably sits in a hierarchy of

systems, with it being a sub-system of a super-system as well as comprising sub-systems itself. The interfaces between these levels as well as between the subsystems require specification and control. The environment within which the system operates may be considered under two categories: those that are under human control, the super-system, and those that are not, the natural environment. Each requires definition. The interaction of a system with its environment requires description and characterisation.

A system is not a static entity. Rather its characteristics change with time as its build state changes due to obsolescence and improvements. Its performance Thus, has to be anticipated and managed on a whole life basis. System engineering requires conscious design of models on three levels: performance, operation and process. The analysis of a system already in-service provides opportunities, in terms of availability of information, and imposes constraints, in terms of sunk costs that need to be taken into account.

1.8.6 Complexity

Systems are often described as being complex without a clear understanding of what is meant by this term. Complexity is considered here to be a quality of the way in which the entity is considered rather than of the entity itself, i.e. all mechanisms may be considered to be complex if they are considered in sufficient detail.

The characteristics that imply complexity are defined for the purposes of this thesis at four levels: the overall behaviour of the system; the way in which it is described; its physical realisation; and the analysis tools appropriate to its investigation. A complex system is characterised at the physical realisation level by a large number of sub-systems, with many interconnections, a number of which are unintentional and produce unwanted side effects. A large number of parameters and many interfaces are needed to describe a complex system. Its behaviour has some elements of unpredictability that require statistical tools for its analysis.

1.8.7 System boundaries

The concepts summarised above have been applied to the AUTOSUB propulsion system. The overall problem is scoped by analysing the system to determine its boundaries. These are defined in terms of: the requirement the system is

designed to satisfy; the interface between the system and its environment; the sub-systems of which it comprises and the fundamental characteristics of each of these; and a parametric assessment of the performance that may be expected from such a system. As a result of formal requirement capture it has been established that the essence of the requirement for AUTOSUB is to achieve the maximum range possible, within the constraints of chosen vehicle size and the energy and power density constraints of the chosen energy storage system. The boundary of the system to be considered was, therefore, drawn so as to include all sub-systems that affected energy consumptions. The results of parametric modelling of the system confirm that, as conceived, it should be capable of considerably greater range than that observed in service, provided that the sub-systems exhibit in service the characteristics anticipated during development. The characteristics of each of the sub-systems were, thus, considered, in order to identify which may be responsible for the performance shortfall.

1.8.8 Sub-system Performance

Shortfalls in the performance of the energy storage and prime mover sub-systems have been identified together with means of correcting them. The shortfalls, however, were insignificant in terms of the overall system shortfall. The same applies to the energy transmission system, where alternatives have been considered but found to offer no significant improvement. However, the performance of the hull and propeller, under in-service conditions, has been demonstrated to be poorly understood and is likely to be significantly different from that expected at the design stage. Their characteristics, together with the effects of their interactions, are likely to provide the main contributions to the overall system performance shortfall. The issue of the propeller is being pursued elsewhere. Further characterisation of the hull is the subject of the remainder of this thesis.

1.8.9 The hull drag problem

Measurements were made on a scale-model during vehicle development to determine the drag of the hull at the expected cruising speed. However, the measurements were taken at zero angle-of-attack and with the hydroplanes feathered. More importantly, the form of the model was idealised, in that it assumed a perfect surface finish and replicated no appendages. In practice the vehicle travels at a range

of speeds different from those anticipated, and with constant hydroplane incidence and hull angle-of-attack. Its hull-form is far from ideal, including a significant number of appendages. These change from mission to mission. Due to wear and tear, the surface finish of the vehicle when in service is often far from perfect and changes with time. There is, therefore, the need to characterise the hull under more realistic circumstances. The level of detail required to describe the hull under these conditions means that characterising it is a complex problem within the definition derived earlier. Ideally measurements will be made on the real vehicle under operating conditions. A means of doing this is described in part 3. However, because of the difficulty of controlling and measuring the environment, and of gaining a sufficient number of samples of the varying hull form, some degree of modelling is required. The degree of complexity being considered rules out exclusive use of theoretical modelling and computer simulation. Complete complexity is best captured by use of the real vehicle in the real environment. However, the difficulty of controlling and/or measuring the real environment precludes this from providing a complete solution. It is, therefore, concluded that analogue modelling using scale-models is required as a complement to full-scale trials. The large number of parameters required to be investigated, coupled with the large range over which each needs to be explored implies an extremely large experimental space. The experiments will, therefore, need careful design.

Summary

Part 1 of this thesis has identified a generic systems-engineering problem. It has set this in the context of the propulsion system of an in-service AUV, AUTOSUB. An analysis of the AUTOSUB propulsion system has identified two components that warrant further investigation to establish their performance characteristics under in-service conditions, the propeller and the hull. The propeller is being considered elsewhere. Further characterisation of the hull is the subject of the remainder of this thesis. Scale modelling is described in part 2 and measurements on the full-scale vehicle under operational conditions in part 3.

Part 2

LABORATORY EXPERIMENTS

Chapter 2.1

INTRODUCTION

Part 1 concluded that a series of laboratory experiments is required to complement trials on the full-scale vehicle at sea in order to determine the drag characteristics of the hull and its appendages. This part describes the formulation and conduct of the laboratory experiments. The full-scale trials are discussed in part 3.

The principles underpinning the experiment design are discussed (Fallows, 2005). In particular it derives the means chosen to address how complexity may be handled in an affordable programme of experiments. It concludes, that for the full complexity to be explored in a realistic timescale, three conditions must be met. Firstly the experiments require careful design so that the maximum amount of information may be derived from a realisable number of runs. Secondly, the apparatus needs to be carefully designed so as to minimise the noise on the signal. Finally, the residual noise in the measurement system must be carefully characterised so that it can be distinguished from anomalies caused by unexpected interactions between apparently controlled factors.

The design of the experiments is described in chapter 2.2, which concludes with a set of experimental programmes to explore the key aspects determining hull performance. The design of the apparatus required to conduct these experiments is explained in chapter 2.3.

Accuracy in measurement of the key parameters is essential to facilitate extraction of the required information from an affordable number of measurements. This requires that the apparatus is characterised in detail so that variation in measurements due to uncontrolled factors are quantified and the sources of the variations identified. A report (Fallows, 2005) describes how key aspects of the apparatus are characterised. Pre-processing of the data resulting from the measurements is also required to remove as many residual sources of variation as possible. The process for doing this is described in (Fallows, 2005).

The drag of the vehicle is considered in two parts: that of the basic hull; and the additional drag caused by appendages to the hull. The concepts underpinning the theory of the hydrodynamic drag of an axi-symetrical submerged body as a function

of speed, angle of attack and appendages is summarised at the Appendix to this thesis. In this part, chapter 2.4 derives the drag of the bare hull as a function of speed, angle-of-attack and hydroplane angle. It also examines the corrections that need to be made to the results of experiments performed on fully immersed models, in order to predict effects on the full-scale vehicle in the open ocean.

Knowledge of the added mass of the hull is required for processing of the results of the full-scale trials discussed in part 3. This is derived from measurements of force during periods of acceleration of the scale-model. Chapter 2.5 describes the process.

Finally, derivation of the additional drag of individual appendages and combinations thereof is discussed in chapters 2.6, 7 and 8.

Overall conclusions are drawn in chapter 2.9, which also summarises lessons learned.

Chapter 2.2

DESIGN OF LABORATORY EXPERIMENTS

2.2.1 Introduction

As described in chapter 1.7, towing tank experiments are required to characterise the AUV hull using a captive model in a towing tank. The aim is to accurately determine the total drag of the hull over a range of potential operating conditions and the additional drag of specific key components. Additionally, determination of the added mass of the vehicle is required as an input to the full-scale vehicle trials described in part 3.

The number of factors and levels to be explored is large. For tank experiments acquisition of data is both slow and resource intensive. For these reasons exploration of the total experimental space is not possible. The concepts underpinning the design of experiments that efficiently sample a large experimental space are described in (Fallows, 2005). This concludes that where large numbers of factors need to be investigated, each of which can occupy a significant number of levels, then it is not viable to adopt the normal experimental technique of varying one parameter at a time. The one factor at a time approach is adopted to avoid the results being contaminated by unanticipated interactions between factors. By adopting techniques developed for the natural sciences and quality engineering, particularly those of (Taguchi, 1988), it is possible to design experiments where the levels of many factors are changed simultaneously. This allows the required information to be obtained from a viable number of measurements. The technique is based on the use of orthogonal arrays and assumes that factors act orthogonally, and that any interactions between factors may themselves be considered as independent variables. Any unanticipated interactions will appear as additional noise on the measured signal. It is therefore critical that the apparatus is designed for minimum noise, and is carefully calibrated such that remaining sources of noise are quantified (Fallows,2005).

This chapter explains how the ideas expounded in (Fallows, 2005) may be applied to enable adequate sampling of the response surface within resource limitations. The process results in an affordable programme of measurements that allows the required relationships to be established.

2.2.2 Requirement

Experiments are required to establish two principal relationships:

1. That between the speed, angle-of-attack and hydroplane angle of the vehicle and its drag.
2. That between the size, shape, position and relative position of detailed hull features and the hydrodynamic performance of the hull.

The experiments must be designed such that these needs are met within an achievable number of measurements and yet need to describe the response surface with sufficient accuracy to be able to provide dependable guidance on the optimal size, shape and disposition of appendages and their effect on mission range and duration.

2.2.3 Partitioning

The total number of measurements made depends upon the number of combinations of factors and levels that need to be considered simultaneously. This number may be kept within reasonable bounds by partitioning the total investigation into a number of self-contained activities. The experimental programme reflects the following strategy (Figure 2.2.1):

1. Set a firm baseline by establishing the performance of the bare hull from a well-sampled velocity/angle-of-attack/hydroplane-angle space.
2. Determine the effects of adding the baseline features detailed in Table 2.2.1 to identify the total additional drag and the principal sources.
3. Add a defined set of payload detail (representative of those used in the 'AUTOSUB Under Ice' science mission) to enable comparison with at-sea experience.
4. Establish the effect of damage on bare hull performance.
5. Establish the relationship between the shape, size and position of detail and the resultant additional drag.

Two major campaigns of experiments, therefore, need to be conducted:

1. To determine the drag performance of the bare hull.

2. To determine the additional drag cause by adding appendages.

Baseline	Payload		Damage	
Description	Shape	Representative of:	Shape	Representative of:
Argos Aerial	Cylinders & rods		Surface roughness	
Beacon lamp A		Large sonar dome (AUI)		Scratches
Beacon lamp B		Small sonar dome (Navigator size)		loss of jellcoat
CTD Sensor (port)		Small sonar dome (AUI)	Ill fitting panels	
CTD Sensor (stbd)		Comms antenna (Argus)		Channels
Lifting line stow hole		Strut (GPS support)		longtitudinal
Flooding hole A (fwd)	Domes			circumferential
Flooding hole B (fwd)		Small housing (Beacon)	Spot features	
		Large housing (Navigator)		screw/rivet heads
Lifting lug (fwd)	0015 NACCA Section beams			longtitudinal
Lifting line (fwd)		Long strut (GPS support)		Circumferential
Lifting line (aft)		Short strut (1/2 size support)	Annuli	
		Large streamlined Housing		Poorly fitted
Lifting lug (aft)		(Navigator)		sensors
		Small streamlined Housing		
Flooding hole A (aft)			Holes	
Flooding hole B (aft)	Tubes:			
	Horizontal			
Top fin mast, GPS				
antenna & Argos aerial		ctd sensor		
ADCP 1	Vertical			
		sensor		
	Cage			
	Dome - 0.5cm rod - large	LF Sonar protective cage		
	Dome - 0.3cm rod - small	1/2 size protective cage		

Table 2.2.1 AUTOSUB Features

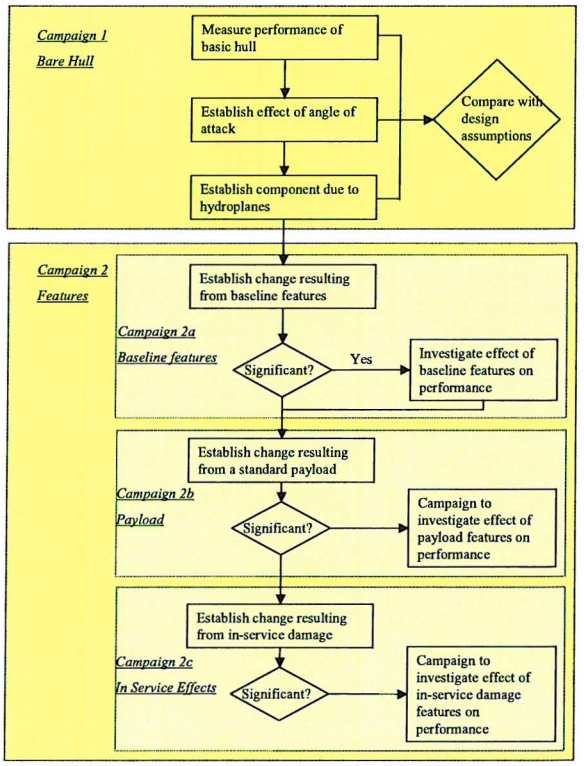

Figure 2.2.1 Campaign Logic

Because of the number of parameters involved in determining the additional drag of appendages (size, shape and aspect ratio of individual appendages, numbers of each type, position and relative position of each, etc.), Campaign 2 is divided into

three Sub-Campaigns to establish separately the effects of each of the major groupings of hull-form detail described in chapter 1.7: baseline, payload and damage.

A fourth Sub-Campaign is added to assess the effects of *sets* of appendages and allow comparison of total drag with that achieved on the real vehicle at sea.

A programme of experiments is now derived for each of the Campaigns and Sub-campaigns.

2.2.4 Campaign 1 – Performance of the bare hull

Campaign 1 explores the effect of four factors on the drag of the bare hull: the number of fins, angle-of-attack, hydroplane angle and speed. The number of levels to be explored for each factor depends on the expected shape of the response curve.

It is initially assumed that there is little interaction between each of the fins. The relationship between the number of fins present and total drag is, therefore, expected to be linear. Consequently it should be possible to determine the relationship by measuring the effect of only 3 levels for this factor. The levels chosen are: all 4 present, one missing and none present. If the results prove not to sum then an interaction effect may be assumed and further work will be required to quantify it.

An assessment of the likely shape of the responses to the remaining 3 factors was undertaken and is reported in (Fallows, 2005). This indicates that there is likely to be at least one, and possibly 2 degrees of curvature, even allowing for no interactions. Thus, to provide a sound assessment of the basic hull, 5 levels are required for each of these 3 factors. The levels for the angle-of-attack (α) and hydroplane angle (δ) factors are chosen to cover the full range that it is reasonable for these parameters to take under operational conditions, and to be biased towards the region where the operational vehicle spends most time. Thus, the levels for α are 0, 2, 5, 7 and 10 ^{o} and those for δ are 0, 3, 6, 9, 15 ^{o}. The levels for the factor 'speed', u, are chosen to produce Reynolds numbers for the scale-model corresponding, so far as possible, to those of the full-scale vehicle in service, viz: 2.7, 3.2, 3.75, 4 and 4.1 m/s.

The minimum size orthogonal array that will enable exploration of 4 factors at 5 levels is the $L_{25}(4^5)$ Array (detailed in (Fallows, 2005)). The experiment plan based on this array is outlined in Table 2.2.2.

The array allows for the effects of a maximum of 6 factors to be determined. However, we are interested in the effects of only 4 factors. The first 4 columns of the array only are, therefore, used for the allocation of levels to runs. The allocation of

levels for factor α, δ, and u is trivial. However, it is only necessary to explore the first factor, number of hydroplanes, across 3 levels. The in-service condition, all 4 hydroplanes present, has, therefore, been assigned to levels 1, 2 and 3 in column 1 of the array, Table 2.2.2.3, with the remaining 2 configurations being allocated to levels 4 and 5.

The order of runs in the programme of experiments needs to be changed from that shown in the array for reasons of practicality. Changing the number of fins is time consuming, so the order is arranged to minimise the number of changes required. Runs have been added to provide an initial set of runs across the full range of speeds with no other changes required. This allows exploration of the force envelope in a controlled manner to ensure that the dynamometer is not inadvertently overloaded.

Factor	Hull form, *h*			Angle of Attack, alpha					Control surface angle, delta					Carriage Speed, *u*				
				Deg					Deg					m/s				
Level	H1	H2	H3	A1	A2	A3	A4	A5	G1	G2	G3	G4	G5	U1	U2	U3	U4	U5
	Hull + 4 hydroplanes	Hull + 3 hydroplanes	Hull without hydroplanes	0	2	5	7	10	0	3	6	9	15	2.7	3.2	3.75	4	4.1
Run No.																		
1	*			*					*					*				
2	*			*					*						*			
3	*			*					*							*		
4	*			*					*								*	
5	*			*					*									*
6	*				*					*					*			
7	*					*					*					*		
8	*						*					*					*	
9	*							*					*					*
10	*			*						*									*
11	*				*						*			*					
12	*					*						*			*				
13	*						*						*			*			
14	*							*	*								*		
15	*			*							*						*		
16	*				*							*							*
17	*					*							*	*					
18	*						*		*						*				
19	*							*		*						*			
20		*		*								*				*			
21		*			*								*				*		
22		*				*			*									*	
23		*					*			*				*					
24		*						*			*				*				
25			*	*									*		*				
26			*		*				*							*			
27			*			*				*							*		
28			*				*				*								*
29			*					*				*		*					

Table 2.2.2 Experiment design for Campaign 1

2.2.5 Campaign 2 – The effect of features on hull performance

2.2.5.1 Feature Definition

The features that modify the shape of the bare AUTOSUB hull are grouped into 3 categories (baseline, payload and damage) according to their function and how they change with time. The baseline features, that provide basic services to the vehicle, evolve only slowly with time. They can be well defined, and, for the purposes of this work, are assumed to be constant. The payload features vary from mission to mission, and are, therefore, more difficult to generalise. And clearly the effect of damage on shape, being a function of the environment and maintenance regime, is impossible to predict with any accuracy. For these reasons only the baseline features attempt to mimic the actual shapes present. For the payload and damage features a variety of idealised representative shapes have been devised.

The categories of detailed feature are defined in Table 1.7.2 (reproduced for convenience as Table 2.2.1). The baseline category lists the devices present, and the payload and damage categories provide lists of representative shapes and the sorts of payload or damage that these might represent.

Originally four types of shape are chosen to represent the payload features (cylinders, domes, NACA section beams, and wire cages). This was subsequently reduced to three because of unexpected manufacturing issues, as described in chapter 2.7. For each type initially up to 3 different aspect ratios are defined: squat, average and lean, although this was also modified later. Each shape is defined in 3 sizes: small, medium and large. They are illustrated in Figures 2.2.2 to 2.2.5.

Cylinders ***Full scale - cm***

Aspect ratio	Size	Description	Geometry
Squat	Large	Ser.No. C1	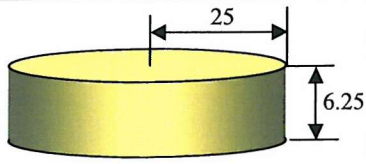
	Average	Ser.No. C2	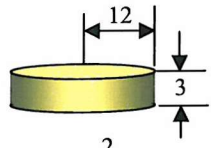
	Small	Ser.No. C3	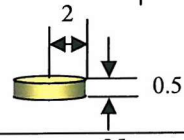
Average	Large	Ser.No. C4	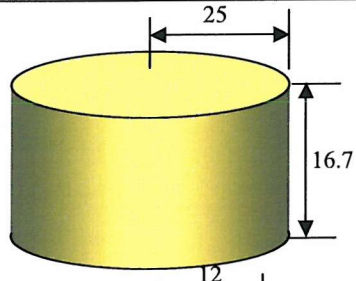
	Average	Ser.No. C5	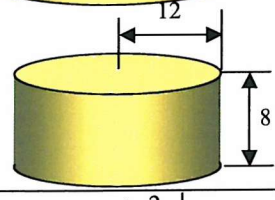
Lean	Small	Ser.No. C6	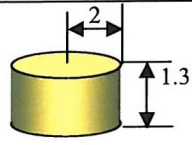
		Ser.No. C7	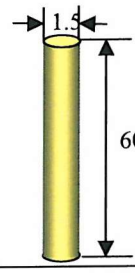

Figure 2.2.2 Payload features 1

Domes

Aspect ratio	Size	Designation	Geometric form
Squat	Large	Ser No D1	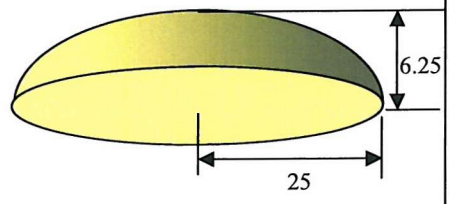
	Average	Ser No D2	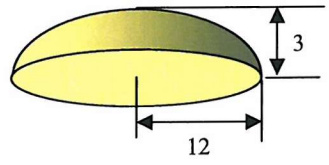
	Small	Ser No D3	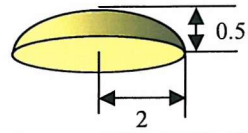
Average	Large	Ser No D4	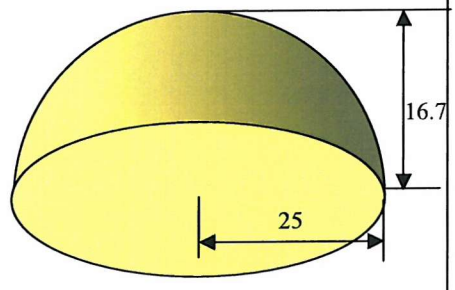
	Average	Ser No D5	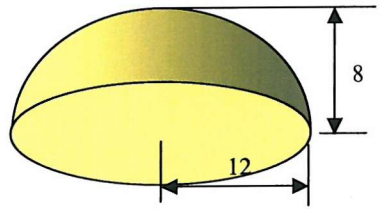
	Small	Ser No D6	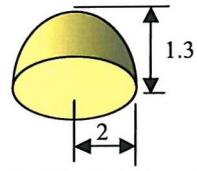

Figure 2.2.3 Payload features 2

NACA0033 Section Beams

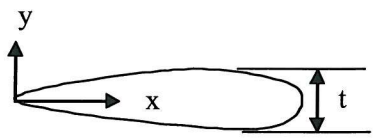

$$y_t = \pm 5t(0.2969\sqrt{x} - 0.126x - 0.3156x^2 - 0.2843x^3 + 0.1.15x^4)$$

Aspect ratio	Size	Designation	Geometric form
Squat	Large t = 050	Ser No N1	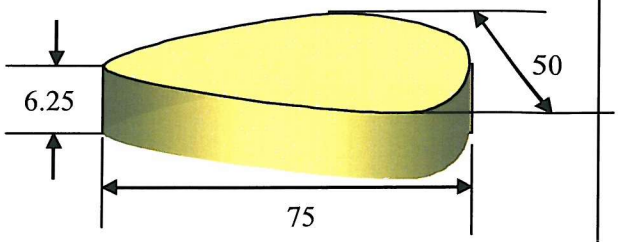
	Average t = 24	Ser No N2	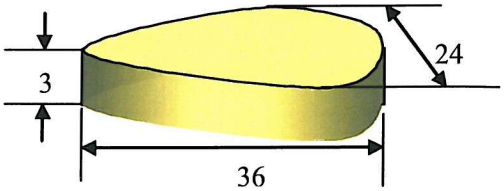
	Small t = 4	Ser No N3	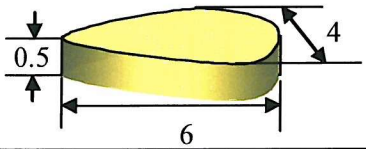
Average	Large t = 50	Ser No N4	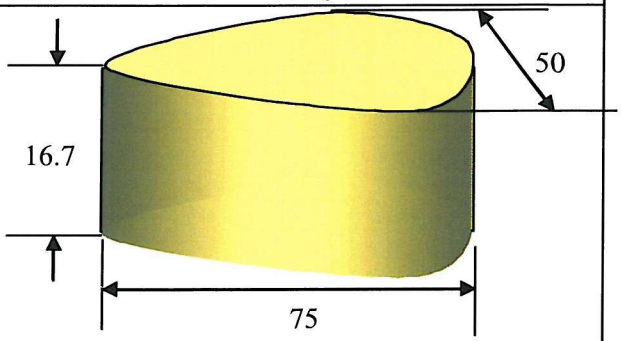
	Average t = 24	Ser No N5	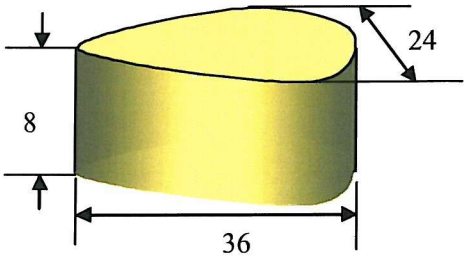

Figure 2.2.4 Payload features 3 (Continued overleaf)

Aspect ratio	Size	Designation	Geometric form
	Small t = 4	Ser No N6	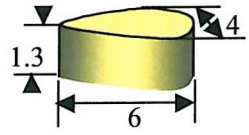
Lean	t = 3	Ser No N7	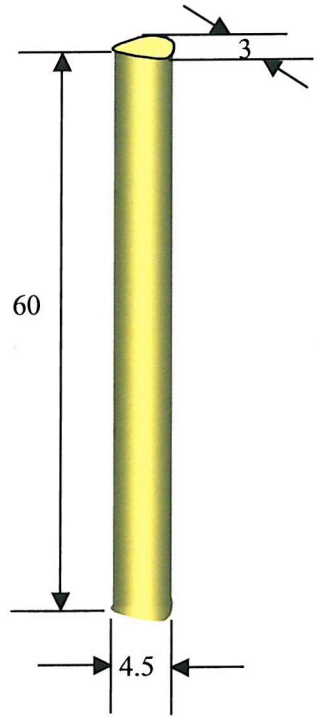

Figure 2.2.4 Payload features 3 (continued)

Cages

Manufactured at model scale of 2mm wire

Aspect ratio	Size	Designation	Geometric form
Squat	Large	Ser No C1	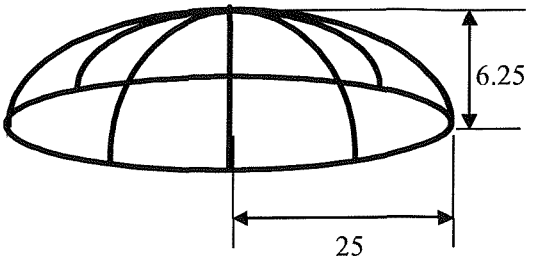
Nose Cage	Large	Ser No C2	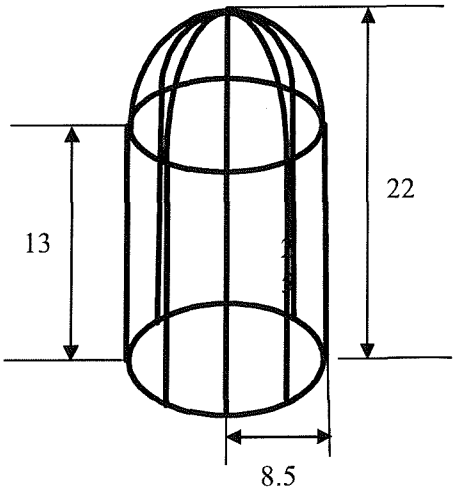
	Small	Ser No C3	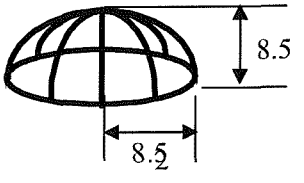

Figure 2.2.5 Payload features 4

Similarly damage features are represented by idealised shapes. Four varieties of imperfection have been identified: surface roughness due to surface abrasion; longitudinal and circumferential channels due to ill fitting panels; spot arrays due to un-faired screw and rivets; and holes or annuli penetrating the surface as a result of fitting payload appendages. Each of these is defined in terms of a shape and size as defined in Table 2.2.3.

Type Number	Type	Representative of:	Shape		Size	
			Definition	Shape ratio	Definition	Size
1	Surface Roughness	Scratches/Loss of jellcoat	Sheets of coarse abrasive		Large:	l = 30 ,b = 10
1.1			of area	l x b	Average:	l = 20,b = 5
1.2					Small:	l = 10,b = 1
1.3						
2	Channels				Wide	w = 0.05
2.1	Longitudinal	Poorly fitting panels	width	(note 3)	Narrow	w = 0.01
2.2					Wide	w = 0.05
2.3	Circumferential	Poorly fitting panels			Narrow	w = 0.01
2.4						
3	Spot arrays				Large/distant	r = 1.3,p = 33
3.1	Longtitudinal	Lines of screw/rivet heads		r/p	Small/Close	r = 0.7,p = 10
3.2					Large/distant	r = 1.3,p = 33
3.3	Circumferential	Lines of screw/rivet heads			Small/Close	r = 0.7,p = 10
3.4						
4	Annuli / Holes					
		ll fitted sensors (ADCP)			Large gap = 1.5cm	r = 13.5, ri = 12
4.1				r/ri	Small gap = 0.5cm	r = 12.5, ri = 12
4.2				r/ri		
		Holes left after modification			Large hole	r = 11.5
4.3		Unplugged drain hole (note 3)		r	Small hole	r = 2
4.4		Small hole (note3)		r		

Notes:
1. Symbols
b = breadth in circumferential direction
l = length in longtitudinal direction
p = pitch
r = external radius
ri = internal radius
2. Channels are of scale depth equivalent to full-scale skin thickness
3. Holes are treated as annuli with zero internal radius
4. Dimensions are full scale cm

Table 2.2.3 Damage features

2.2.5.2 Feature location

Having defined the features to be fitted to the model, we now need to consider their locations. The location of each feature of the baseline fit is well defined and is illustrated in Figure 2.2.6. However, it is not possible to predict where payload or damage features may occur. The positions that these features may take on the model

have, therefore, also been idealised. They have been selected to conform to those that are feasible and to approximate to actual positions that have occurred to date. Thus, for the purposes of the experiments, the positions of the features are limited to pre-set defined locations. These are illustrated in Figure 2.2.7.

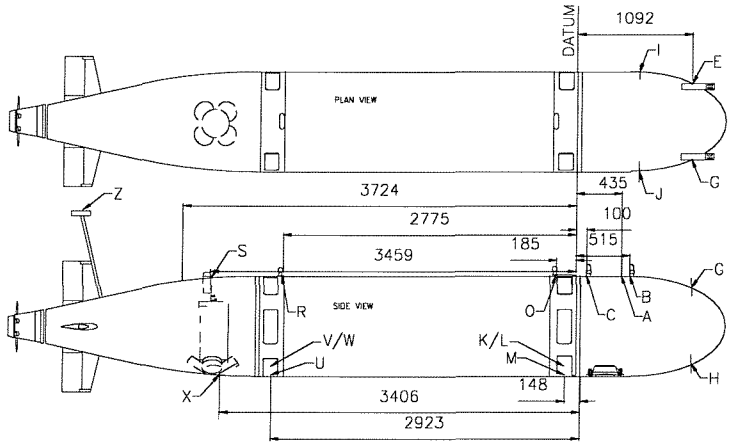

Figure 2.2.6 Baseline feature stations

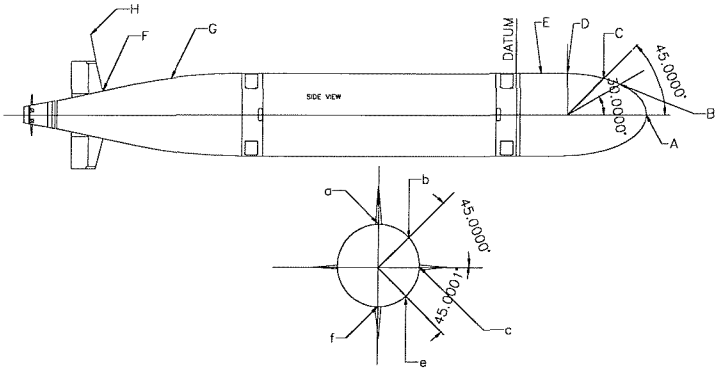

Figure 2.2.7 Payload feature stations

2.2.5.3 Feature Sets

Because of the large number of factors and levels to be explored, the campaign has been divided into 4 phases. Campaign 2a investigates the effect of various combinations of baseline features and position on hull performance. Campaigns 2b and 2c do the same for payload and damage features respectively. Finally, campaign 2d examines the total effects of combinations of predetermined sets of payload, baseline and damage features as a function of speed and angle-of-attack. The standard sets are defined in Table 2.2.4. For economy in both manufacture and experiment set up time, each set is selected to represent only those features expected to have the most effect. Thus, the baseline set comprises only the 5 most significant items of the 16 listed in Table 2.2.1. The payload combination comprises a series of appendages representative of the special-to-mission items fitted for AUTOSUB Under Ice (AUI) science mission. Similarly the damage set is chosen to represent the damage that was observed on that mission.

Baseline				Payload				Damage			
Number	Type		Position	Number	Type		Position	Number	Type		Position
	Description	Idealised Ser. No.			Description	Idealised Ser. No.			Description	Idealised Ser. No.	
B1	Argos Aerial	C7	A	P1	CTD Sensor (port)		Cc	D1	Flooding hole A (fwd)	4.3	M
B2	Beacon lamp A	D6	B	P2	CTD Sensor (stbd)		C-c	D2	Flooding hole B (fwd)	4.3	U
B3	Beacon lamp B	D6	C	P3	ADCP 2		Df	D3	Anulus round sonar cage	4.2	A
B5	Top fin mast, GPS antenna & Argos erial	N7	Z	P4	IF sonar cage		A	D4	Abrasion f'w'd	1.2	Cf
B6	ADCP 1	D2	X	P5	Dorsal sonar		Da				

Table 2.2.4 Standard feature sets

2.2.6 Campaign 2a – Baseline features

The aim of the campaign is to examine the effect of baseline features on hull performance, to establish the overall drag of the features in their standard positions and then to assess the effect of moving them to a number of alternative positions. To minimise the number of variables in the experiment, the alternative positions are restricted to a maximum of two, each of which must comprise a realistic option. The features, positions and alternative positions are defined in Table 2.2.5.

Type		Position		Station			
Number	Description	Current	Alternative	Current	Alternative		
				a	b	c	d
1	Argos Aerial	Fwd Hull		A			
2	Beacon lamp A	Fwd Hull	Aft Hull	B	C	D	Z
3	Beacon lamp B	Fwd Hull	Aft Hull	C	D	Z	
4	CTD Sensor (port)	Fwd Hull	Fwd Hull	E	G	I	
5	CTD Sensor (stbd)	Fwd Hull	Fwd Hull	F	H	J	
6	Lifting line stow hole	Fwd Hull		G			
7	Flooding hole A (fwd)	Fwd Conecting ring		K	M		
8	Flooding hole B (fwd)	Fwd Conecting ring		L	M		
9	Lifting lug (fwd)	Centre Section		O			
10	Lifting line (fwd)	Centre Section		P			
11	Lifting line (aft)	Centre Section		R			
12	Lifting lug (aft)	Centre Section		Q			
13	Flooding hole A (aft)	Aft Conecting ring		V	U		
14	Flooding hole B (aft)	Aft Conecting ring		W	U		
15	Top fin mast, GPS antenna & Argos aerial	Aft Hull		Z	Within fin		
16	ADCP 1	Aft Hull		X	Y	T	

Table 2.2.5 Baseline feature positions

To further reduce the number of factors, all runs are to be made at the same speed, and at zero angle-of-attack and hydroplane angle. Despite this, to examine the effects of all baseline features would require the assessment of nominally 16 different factors, with each occurring at up to 3 levels. Even using factorial designs, a complete evaluation of this number of factors and levels is impractical. However, the number of runs required can be reduced to a realisable level if the set of features to be considered is reduced to only those expected to have the greatest effect. The experiment is, therefore, designed to concentrate on these. This is done by conducting the Campaign in three logical stages.

- Stage 1. The drag with all features present is established. Those features suspected of having little effect on drag are then removed. If the measurement confirms the suspicion then the experiment moves on to the next stage. If not, items are added back until the set of significant features is identified.
- Stage 2. In the second stage the feature identified as having the greatest effect is selected and the effect of moving this between its alternative positions is determined.
- Stage 3. The final activity is to take those features demonstrated at Stage 1 as being the most significant and run a factorial experiment based only on these. It was expected that only four features would be in this set, based on an

assessment of size, shape and feasible positions. Of these, one cannot be moved and so is a constant throughout the experiment. The remaining features can each occupy one of three stations. This part of the experiment has, therefore, been based on an $L_9(3^3)$ array (see (Fallows, 2005)).

The complete design is given in Table 2.2.6.

Campaign 2a - Determination of the Effect of Baseline features on Hull Performance

Stage	Run	Factor - Type / Level - Station	Feature Type and Station																																
			1	2				3			4			5			6	7		8		9	10	11	12	13		14		15		16		
			a	a	b	c	d	a	b	c	a	b	c	a	b	c	a	a	b	a	b	a	a	a	a	a	b	a	b	a	b	a	b	c
	Number	Description																																	
1	1	All features present - original stations	*	*				*			*			*			*	*		*		*	*	*	*	*		*		*		*		
	2	Remove features not expected to have significant drag									*			*									*								*			
2	3	Only feature with most significant drag									*												*											
	4	Move										*											*											
	5	Move											*										*											
3	6	Move all significant features									*			*									*								*			
	7										*				*								*									*		
	8										*					*							*										*	
	9											*		*									*											*	
	10											*			*								*								*			
	11											*				*							*									*		
	12												*	*									*									*		
	13												*		*								*											*
	14												*			*							*								*			

Note: All done at a single representative speed (3.75 m/s corresponding to 1.4 m/s full scale) and angle of attack

Table 2.2.6 Campaign 2a. Exploration of the effect of baseline features on hull performance

2.2.7 Campaign 2b - Payload

The aim of the campaign is to examine the effect of each of a range of appendages of varying shape, aspect ratio and size on overall drag as a function of position and relative position. Four different shapes have been chosen (cylinder, dome, NACCA section and cage), each of which may take one of three aspect ratios and three sizes. Four representative positions have been selected, three on the forward hull and one on the aft. These are positions Aa, Ca, Ea and Ga as defined in Figure 2.2.7. The relative positions are defined as: only one appendage present; two present and separated by more than 2 diameters (where 'diameter' is defined as fore to aft length for shapes of non-circular cross section); two present and separated by less than 2 diameters.

Again, to limit the number of variables, all runs are to be made at the same speed and zero angle-of-attack and hydroplane angle.

Thus, this campaign involves 4 factors with factors 'shape' and 'position' each having 4 levels, and the other two factors each having 3 levels. The plan is, therefore, based on an $L_{16}(4^4)$ orthogonal array (see (Fallows, 2005)) with the 'average' level of factors 'size' and 'shape' being allocated to levels 2 and 3 in columns 3 and 4. The complete design is given in Table 2.2.7.

2.2.8 Campaign 2c – Damage Effects

In a similar manner to that of campaign 2b, this campaign is to examine the effect of each of a range shapes representative of surface imperfections. These will also come in a range of types, aspect ratio and sizes. Four different types are to be tested (surface roughness, channel, spot arrays and hole), each of which may take one of three shape/size combinations and one of four positions, all on the forward hull since this is most susceptible to damage and surface effects here are expected to have the greatest effect.

The runs will be made at the same speed, angle-of-attack and hydroplane angle as campaigns 2a and 2b.

This campaign involves 4 factors each of which can take one of 4 levels. The plan is, therefore, based on an $L_{16}(4^4)$ array (Fallows, 2005). The factors and levels

are defined in Table 2.2.1. Allocation of factors and levels results in the design at Table 2.2.8.

2.2.9 Campaign 2d –Effects of sets of appendages

This Campaign is to examine the effect of the baseline, payload and damage Sets of appendages defined in Table 2.2.4 as a function of speed and defined combinations of angle-of-attack and hydroplane angle. Three combinations of feature sets have been chosen such that it will be possible to determine whether the effects of combinations of sets comprises the sum of the effect of individual sets. The combinations are: baseline alone; baseline + payload; baseline + payload + damage. Three speeds representative of in-service Reynolds Number have been chosen, together with three combinations of angle-of-attack and hydroplane angle (0,0), (3,2) and (10,15).

Thus, this Campaign also involves 3 factors each of which has 3 levels. The design given in Table 2.2.9 is, therefore, based on an $L_9(3^3)$ array (Fallows 2005).

Summary

The conclusions of the systems analysis (part 1) was that an investigation into the characteristics of the hull was required that would take into account the effects of not just the basic hull shape, but also the detail of its appendages, surface finish and so on. Chapter 1.7 argued that the investigation would require a mixture of laboratory experiments and trials at sea. Further, it indicated that the laboratory experiments would require the consideration of so many different factors and levels that the normal one-factor-at-a-time approach would not be sustainable. The report at (Fallows, 2005) described an alternative approach, which offered the prospect of describing the expected complex response surface within a realisable number of experiments. This has been applied in this chapter to derive such a set of experiments.

Before describing the experiments themselves, we need to consider the characteristics of the equipment required to do make the necessary measurements. This is done in the following chapter, whilst the method by which the measurement system is characterised together with the results achieved is given in (Fallows, 2005).

Campaign 2b - Determination of the Effect of Payload features on Hull Performance

Factor	Shape				Aspect ratio			Size			Position				Relative Position		
Level	Cylinder 1	Dome 2	NACCA 3	Cage 5	Squat	Average	Lean	Large	Average	Small	Nose Aa	Frd of break Ca	Aft of break Ea	Stern Ga	Single	>2d separation	<2d separation
Run																	
1	*				*			*			*				*		
2	*					*			*			*				*	
3	*					*			*				*				*
4	*						*			*				*			*
5		*			*				*				*				
6		*				*				*				*			*
7		*				*		*			*					*	
8		*					*		*			*			*		
9			*		*					*				*		*	
10			*			*			*				*		*		
11			*			*			*			*					*
12			*				*	*						*	*		
13				*	*				*			*					*
14				*		*		*			*						
15				*		*				*				*	*		
16				*			*		*				*			*	

Table 2.2.7 Campaign 2b. Exploration of the effect of payload features on hull performance

Campaign 2c - Determination of the Effect of In Service Damage on Hull Performance

Factor	Type				Size/shape				Position			
Level	Roughness 1	Channel 2	Spot 3	Annulus/ Hole 4	1	2	3	4	Aa	Ba	Ca	Da
Run												
1	*				*				*			
2	*					*				*		
3	*						*				*	
4	*							*				*
5		*			*					*		
6		*				*			*			
7		*					*					*
8		*						*			*	
9			*		*						*	
10			*			*						*
11			*				*		*			
12			*					*		*		
13				*	*							*
14				*		*					*	
15				*			*			*		
16				*				*	*			

Table 2.2.8 Campaign 2c. Exploration of the effect of damage features on hull performance

Campaign 2d. Determination of the Effects of Features on Hull Performance

Factor	Hull Form Feature Set			Velocity m/s			Angle of Attack and related control surface angle Deg		
Level	F1 Baseline	F2 Baseline + payload	F3 Baseline + Payload + Damage	U1 2.7	U2 3.75	U3 4.1	A1 0,0	A2 3.2	A3 10,15
Run No.									
1	*			*			*		
2	*				*			*	
3	*					*			*
4		*		*				*	
5		*			*				*
6		*				*	*		
7			*	*					*
8			*		*		*		
9			*			*		*	

Table 2.2.9 Campaign 2d. Exploration of the overall effect of sets of baseline, payload and damage features on hull performance

CHAPTER 2.3

DESIGN OF THE LABORATORY APPARATUS

2.3.1 Introduction

Having defined in the previous chapter the experiments required, it is now possible to consider the apparatus needed to undertake the measurements. In this chapter we will first consider the requirements that the equipment must satisfy. The facility to be used is then described, together with the constraints that this puts on the experiment and hence the remaining apparatus. The means for measuring the critical parameters is then addressed and finally the design of the model on which measurements are to be made is considered.

2.3.2 Requirement

The requirement that the apparatus is to fulfil is determined by the specification of the experiments described in the previous chapter and may be divided into 3 Categories:

- The conditions required for the experiment. This includes the specification for the model and the facility required to move it.
- The means of measuring the principal parameters under investigation.
- The means for monitoring the environment in which the experiment is conducted.

2.3.2.1 Experiment conditions

A model is required to provide an accurate representation of the shape of the real vehicle. It must be re-configurable so that it can represent the range of payloads, services and in-service damage required. The hydroplane angles need to be capable of adjustment across the range that occurs in service (+/- 15°). It must be able to move at a range of angles to the direction of motion.

A body of isotropic fluid through which the body may be moved is required. The availability of facilities determines that this will be the water in the Southampton Institute (S I) Towing Tank.

A means of drawing the model through the water, at a range of scaled speeds and angles relative to motion representative of the in-service vehicle, is required (ideally 1.5 to 2.5 m/s full scale).

The angle-of-attack at which the model is drawn through the water needs to be adjustable across the in-service range (+/- 10°).

For measurement of added mass, a means of accelerating the vehicle over a scale range corresponding to 0 to 2m/s full-scale is required. To facilitate the calculation, linear acceleration is desirable.

2.3.2.2 Measurement of principal parameters

The speed at which the model is drawn through the water needs to be measured. Since a standard facility is to be used there is no advantage in attempting to specify the accuracy require. However, the accuracy of the measurement needs to be established.

For the determination of added mass, acceleration needs to be measured with an accuracy of at least 0.1g.

Measurement of the force experienced by the model in both the longitudinal and transverse direction, across the range expected to be experienced in the experiment, is required (0 to 200 N for the model plus up to 200 N for the model support posts). Again the accuracy of the measurement will be dependent upon the equipment available but will need to be established.

The configuration of the vehicle under test will need to be recorded.

The angle-of-attack will need to be set as accurately as possible, but no worse than +/- 0.5°. When zero angle-of-attack is required accuracy of alignment will need to be measured in terms of minimising model transverse force and moment.

Force is required as a function of speed and acceleration. For correlation of measurement each needs to be established as a function of time. Time, therefore, needs to be measured.

The noise throughout the measurement systems needs to be minimised and quantified.

Finally a means of logging the data is required.

2.3.2.3 Environment monitoring

For scaling results to the real vehicle in sea water, and for comparison with results achieved by others and on other bodies, it is desirable that they should be described in non-dimensional terms. This requires that speed should be converted to Reynolds number. To enable this, the kinematic viscosity of the water needs to be established. This is a function of temperature and density. Therefore, the temperature and specific gravity of the water will need to be recorded. Fluctuation of these parameters will affect the hydrodynamic forces. Measurements will, therefore, ideally need to be recorded at a number of positions within the body of the water and as a function of time.

2.3.3 Experimental facility

For reasons of availability, the Southampton Institute Towing Tank was used for these experiments (Figure 2.3.1). It comprises an 80 m long channel of water 3.7 m wide by 1.8 m deep. A towing carriage straddles the tank and runs on steel wheels mounted on rails. It is propelled by an electric motor driving through a gearbox. The speed of the carriage is calculated from measurement of time between two fixed points and is variable in 100 steps between the limits of 0 and 4.5 m/s.

Figure 2.3.1 Southampton Institute towing tank

A number of factors that will affect the results of the experiment arise from the use of the tank. Under normal operating conditions, the AUV travels remote from both the free surface and any solid boundary. The dimensions of the tank mean that the model may need to travel sufficiently close to the surface and at sufficient speed to experience wave induced drag. Similarly, the cross sectional area of the model may be such that it experiences blockage effects, which again will appear as additional drag.

Finally the carriage transmission will be more or less noisy, which in itself may influence the force measurement system. This effect will be amplified should it couple with any natural harmonics of the model support structure.

2.3.4 Instrumentation

Drag is measured by means of a purpose built dynamometer (Figure 2.3.2). This comprises a rigid frame, which attaches to the towing tank carriage. The model is supported by fore and aft posts attached to a beam in such a manner that the model's immersion depth can be adjusted to pre-set heights. The model support beam is isolated from the carriage attachment frame by two sets of force blocks. Each set comprises 2 linear force transducers, mounted orthogonally. The output signals, therefore, enable the measurement of the drag force, side force and yaw moment incident on the model as it is towed through the water. Each force block can be calibrated within the range 0 to 500 N.

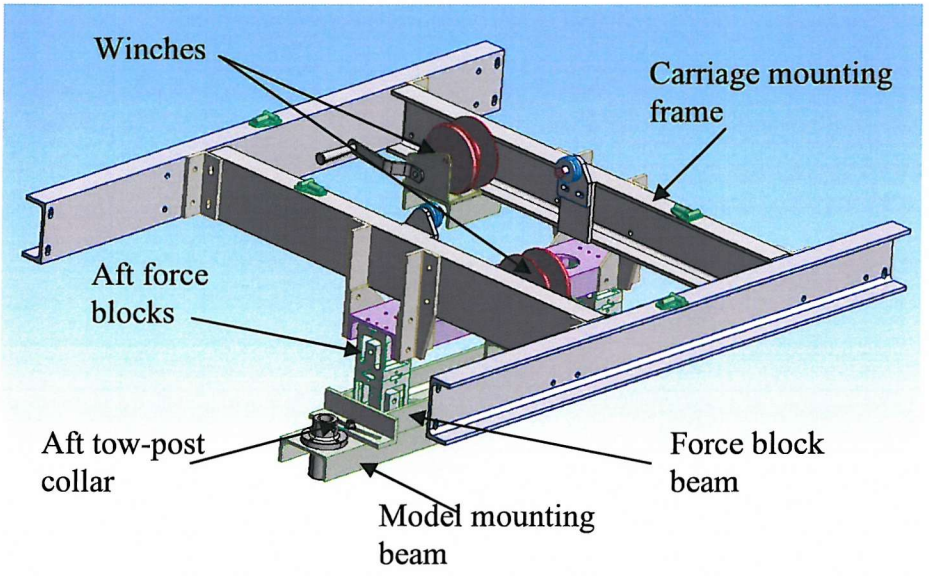

Figure 2.3.2 Dynamometer

The signals from the force blocks are amplified and passed through an analogue filter before being recorded as a function of time by a PC based data logger.

Analysis of the signals will need to take count of the noise of the amplifiers and force block calibration will need to take account of the insertion loss of the filters.

The model mounting-beam is able to rotate relative to the force block beam (Figure 2.3.2) by means of a central pivot point. The angle of the model relative to direction of travel may be adjusted by +/- 10 °.

Acceleration of the model is measured by means of an accelerometer fitted to the carriage.

Speed, force block signal and accelerometer readings are recorded as a function of time by a computer-based data logging system mounted on the carriage. It is an integral part of the towing tank facility.

It is possible that the model will, of necessity, be sufficiently close to the free surface that it will generate waves. The energy taken to do this will be expressed in the form of additional drag. The profile of the waves is measured using a set of wave probes. A record is taken of wave height as a function of time at four stations in the tank, as illustrated in Figure 2.3.3.

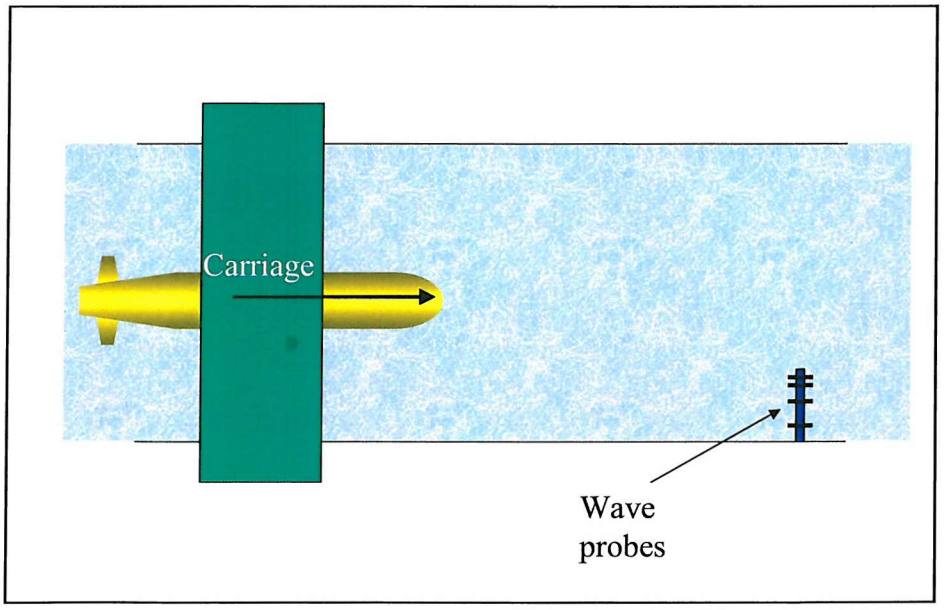

Figure 2.3.3 Wave measurement

If the model induced wave heights are found to be significant, then the induced drag may be calculated using software developed by Insel (Insel, 1990a) (Insel, 1990b), which uses multiple longitudinal cut data and has been demonstrated to produce stable results for waves higher than 3 mm in amplitude.

A standard hydrometer is used to measure the specific gravity of the water and the temperature of the water is measured at 3 depths and 2 positions along the length of the tank.

2.3.5 The AUTOSUB Model

A 2.5 m scale model representative of the shape of the bare hull, together with a representative selection of attachments was designed. The design is constrained by the requirement to be operated in the Southampton Institute Towing Tank. In order to maintain flow patterns over the model that are representative of those of the full-scale vehicle, the model is designed such that, so far as possible, it may be operated at speeds consistent with the Reynolds Number experienced by the vehicle in service.

The bare hull of AUTOSUB (Figure 2.3.4) comprises three main sections, fore, centre and aft, with the fore and aft sections being connected to the centre sections by connecting rings. Attached to the aft section are four hydroplanes and the propulsor comprising motor, propeller and end cap. The fore and aft sections and connecting rings are free flooding. The fore-section comprises a short cylinder faired into an ellipsoid nose. The centre section and connecting rings are cylindrical. The aft section comprises a 12^{o} truncated cone faired into the centre section by means of a large radius arc. The motor fairing, propeller disc and end cap comprise a 10^{o} truncated cone. The four hydroplanes are identical NACA0015 aerofoils.

A variety of attachments as defined and illustrated in Figures 2.2.2 to 2.2.5 can be fitted across a range of stations as defined in Figures 2.3.6 and 2.3.7. Various attachments will simulate damage features. The fore and aft sections of the model are free flooding to enable internal circulation of water. This will enable simulation of phenomena experienced by the real vehicle as a result of orifices in the fore and aft sections, and the flooding and drainage holes in the connecting rings.

In order to preserve the nature of the flow round the body, and similarity of force coefficients, it is intended to run the model at the Reynolds number (R_e) appertaining to the full-scale vehicle. Now,

$$R_e = \frac{ul}{\nu}$$

Where:

u = velocity of the vehicle

l = characteristic length of the vehicle

ν = kinematic viscosity of the fluid at the appropriate temperature

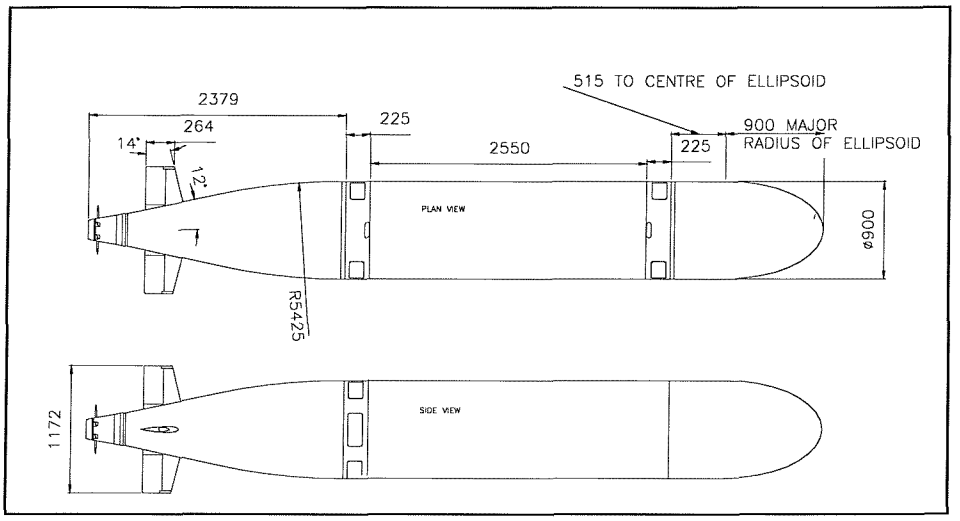

Figure 2.3.4 AUTOSUB Hull

Assuming that the model is run in water, then ν_{model} is approximately equal to $\nu_{vehicle}$, and the model will need to be run at a speed approximately inversely proportional to the scale of the model. This implies building a model of a scale consistent with the range of carriage speeds available on the chosen towing tank.

The towing tank is limited both in the size of model that can be accommodated and in the velocity with which it can be propelled. For the Southampton Institute tank these parameters are:

$$u_{max} = 4.5 \text{ m/s}, \qquad l_{max}(model) = 2.5 \text{ m}$$

The limitations that the tank restrictions impose on the experiment are explored in Table 2.3.1. The experiment is to be run at constant R_e. The R_e for AUTOSUB for a range of speeds is calculated from the first 4 columns. The length of model required to achieve the equivalent Rn with the towing tank operating at maximum speed is given in column 9. From this it can be deduced that the maximum size model will allow exploration of up to equivalent full scale velocities of 1.7 m/s, assuming that the tank is filled with fresh water at a temperature of 15° C and that AUTOSUB's normal environment is seawater at 15° C.

A maximum scale length of 2.5 m implies a body diameter of 0.321 m and a maximum draught from fin to fin of 0.419 m. The tank is 3.7 m wide by 1.8 m deep.

Assuming that the model is run submerged, equidistant between the tank walls and the water free surface and tank bottom, then clearance of the hull from the walls will be ~1.67 m (> 5 diameters) (with the fins clearing by 1.64 m (~ 4 diameters)) and clearance from the bottom and free surface will be 0.74 m (2.3 diameters) (with the fins clearing by 0.69 m (1.6 diameters)).

	AUTOSUB				Model				
T deg C	l m	u m/s	Nu(T) seawater	Rn	Nu(T) freshwater	Max size l Model	u m/s	l Model	Max velocity u m/s
15	7	1	1.19E-06	5.88E+06	1.14E-06	2.5	2.68	1.49E+00	4.5
15	7	1.1	1.19E-06	6.47E+06	1.14E-06	2.5	2.948	1.64E+00	4.5
15	7	1.2	1.19E-06	7.06E+06	1.14E-06	2.5	3.216	1.79E+00	4.5
15	7	1.3	1.19E-06	7.65E+06	1.14E-06	2.5	3.484	1.94E+00	4.5
15	7	1.4	1.19E-06	8.24E+06	1.14E-06	2.5	3.752	2.08E+00	4.5
15	7	1.5	1.19E-06	8.82E+06	1.14E-06	2.5	4.02	2.23E+00	4.5
15	7	1.6	1.19E-06	9.41E+06	1.14E-06	2.5	4.288	2.38E+00	4.5
15	7	1.7	1.19E-06	1.00E+07	1.14E-06	2.5	4.556	2.53E+00	4.5
15	7	1.8	1.19E-06	1.06E+07	1.14E-06	2.5	4.824	2.68E+00	4.5
15	7	1.9	1.19E-06	1.12E+07	1.14E-06	2.5	5.092	2.83E+00	4.5
15	7	2	1.19E-06	1.18E+07	1.14E-06	2.5	5.36	2.98E+00	4.5
15	7	2.1	1.19E-06	1.24E+07	1.14E-06	2.5	5.628	3.13E+00	4.5
15	7	2.2	1.19E-06	1.29E+07	1.14E-06	2.5	5.896	3.28E+00	4.5
15	7	2.3	1.19E-06	1.35E+07	1.14E-06	2.5	6.164	3.42E+00	4.5
15	7	2.5	1.19E-06	1.47E+07	1.14E-06	2.5	6.7	3.72E+00	4.5

Table 2.3.1 Velocity Scaling

Since the objective is solely to represent the dimensions of the vehicle, the model is machined from Cibetool BM5461. This is a polymer specifically designed for pattern making and space models. It is well characterised and is dimensionally stable under its planned conditions of use.

The model comprises a clean hull, which may be readily modified to represent the addition of standard instrumentation and mission-particular items. It may also be modified to represent the realities of a real hull, including form changes resulting from in-service wear and tear.

The clean hull comprises 3 main sections, representing the fore-body, aft body and mid section as shown in Figure 2.3.5.

The mid section is of solid construction and the fore- and aft bodies hollow such that they may be flooded. Free flooding is achieved by means of a hatch in the upper side of the fore and aft sections. Once flooding has occurred, these holes may

be blanked by means of a hatch cover to achieve a smooth hull contour. These holes also enable rapid draining of the model when lifted from the water. The fore and aft sections are dimensioned such that they also represent the connection rings, which, in the full-scale vehicle, contain the orifices that allow free flooding.

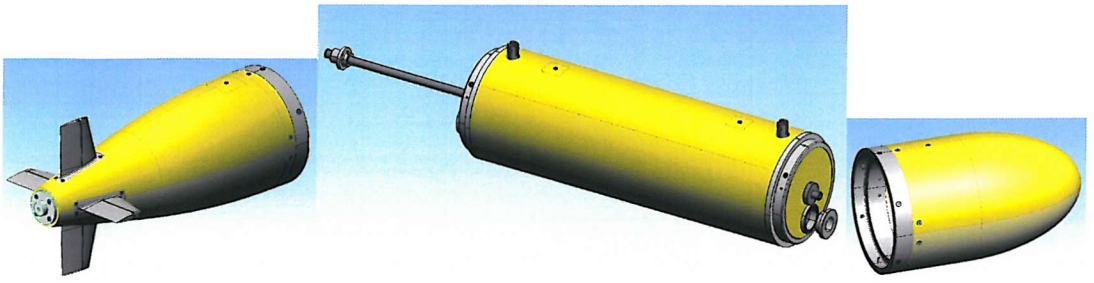

Figure 2.3.5 Model aft, centre and fore sections

The model has also been designed so that the water-flow into the propeller disc may be ascertained. The form of the vehicle is, therefore, accurately represented in this region and designed such that different forms may be tried. Solid truncated cones bolted to the main after-body section, therefore, represent the detail of the motor housing, propeller ring and end cap.

The 4 hydroplanes, made of machined aluminium, are formed in 2 parts to simulate the fixed and moving surfaces as shown in Figure 2.3.6. The fixed parts are bolted directly to the aft body. The hydroplanes are removable and may be replaced by conformal blanking plates. This is to facilitate measurement of the effect of the hydroplanes on the drag of the bare hull. The moveable control surfaces may be fixed at any angle between +/- 15°. The angle of each pair of hydroplanes may be adjusted by means of a screw slot located in the surface of the body. These screws drive a gearbox and shafting, hard coupled to the hydroplane control surfaces.

A set of solid geometric shapes, representative of the various instruments and payloads, may be attached to pre-determined stations on the bare hull. Representative orifices may be cut as necessary into the fore and aft bodies and blanked as necessary. Similarly areas representing in service wear and tear may be attached to the surface. Finally, ill-fitting panels may be represented by attaching strips of defined width and thickness to the surface of the model.

The completed model is illustrated in Figure 2.3.7.

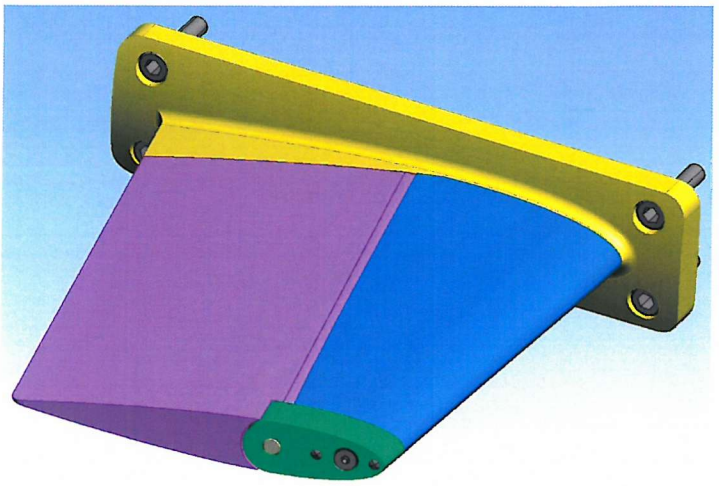

Figure 2.3.6 Model hydroplane

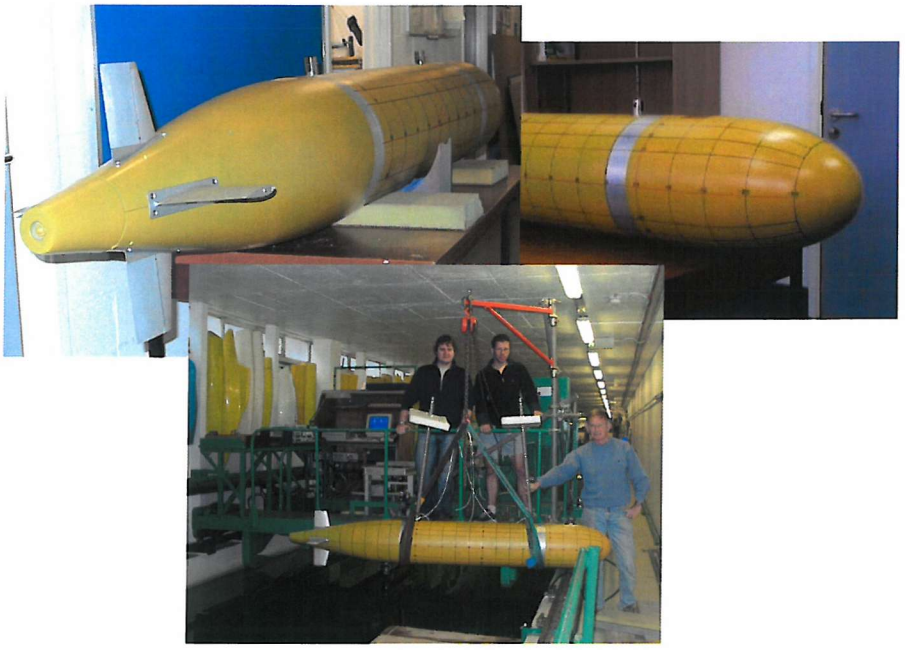

Figure 2.3.7 Completed Model

The model is 2.5 m long and weighs of the order of 100 kg in air. Because the principal material from which it is made has a specific gravity less than 1 it will naturally exhibit about 10 kg of buoyancy even when flooded. To ease handling in water the model is, therefore, designed to be ballasted such that it has virtually neutral buoyancy and to be trimmed fore and aft. Two sets of spaces are, therefore, included in the design of the centre section for the addition of lead shot. Each set comprises a cavity fore and aft to allow trim as well as ballast. The main set is placed low in the model to provide coarse ballast and trim and to provide vertical stability. A second, smaller set is accessible from the top of the model to enable fine-tuning (Figure 2.3.8).

2.3.5.5 Model to carriage attachment

Force measurement is made by means of the dynamometer described above. The dynamometer also provides the interface between the model and the carriage. The model is required to be attached to the carriage such that it may be run at a defined depth and angle-of-attack in the testing tank, whilst minimising interference with the drag force, streamlines, and water velocity field. It will, therefore, be attached to the dynamometer by means of a pair of stiff struts. These locate in receptors at the fore and aft ends of the mid-section. Originally it was intended that these struts would be streamlined to minimise the effect on the flow of water over the model and to minimise the wave generating effect of the struts themselves. However, it proved too difficult in practice to produce stable streamlining that could be readily adjusted to match changes in angle-of-attack. The struts, therefore, comprise turned stainless steel cantilevers of circular cross-section. Some interference effects between the streamlines round the struts and that over the model is inevitable. Most attachments and orifices are expected to occur on the centre line of the vehicle. Therefore, the model is mounted at a notional angle of 90° to the vertical to minimise the effect of the struts on the most important streamlines. The model is mounted in the tank with the port side uppermost. The angle-of-attack of the model may then be simply adjusted by means of the alignment of the struts.

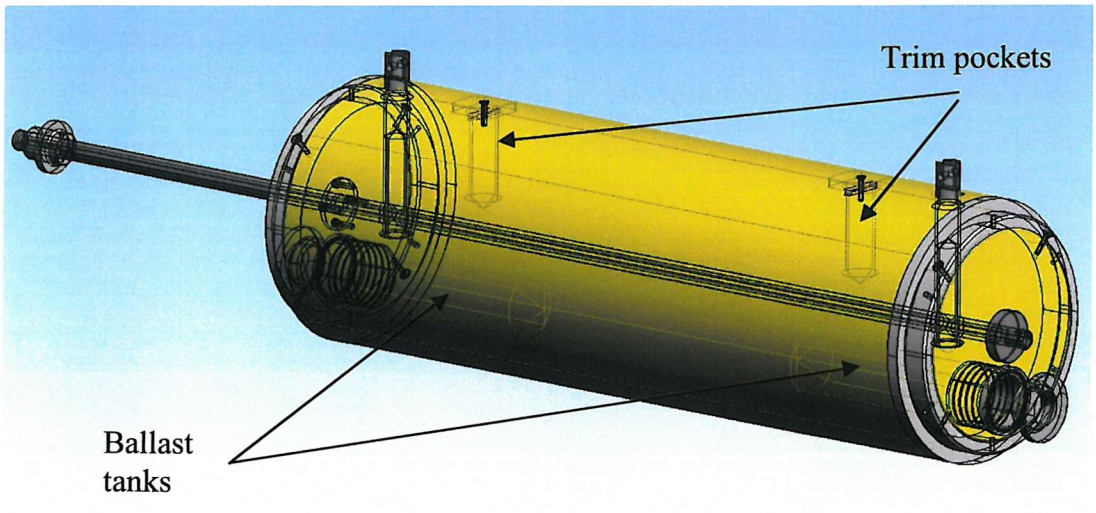

Figure 2.3.8 Model ballast and trim

Summary

A suitable facility for the laboratory experiment has been described together with the instrumentation required to measure the principal parameters and to enable the environment under which the experiments are conducted to be recorded. A space model has been designed and built. The model has been designed such that it can be run within the facility identified across a range of Reynolds numbers, angles of attack, hydroplane angles and configuration representative of the in-service vehicle.

Chapter 2.4

BARE HULL DRAG CHARACTERISATION

2.4.1 Introduction

The analysis undertaken in part 1 demonstrated that the drag of the hull was probably greater than that expected as a result of the design process. Further it was established that no measurements had been made of the drag of the naked hull under the conditions that the vehicle is actually operated. Only a single drag measurement was made, at zero angle-of-attack, with feathered hydroplanes, and at the design cruising speed. The last condition was seldom achieved in service.

Further, the drag effects of differences in the detail of the form between the idealised hull and that used in service was unknown. In order to isolate the effects of these a detailed knowledge of the drag of the basic hull-form is required.

An experiment was, therefore, designed (chapter 2.2) to:

- Characterise the drag performance of the basic hull across the full range of steady state operating conditions likely to be experienced by the vehicle at sea. The operating conditions may be specified in terms of the range of angles of attack, hydroplane angles and speed experienced during missions.
- Establish the contribution to drag made by the hydroplanes to determine whether there would be any advantage in reducing their number.

The campaign of experiments to investigate the drag of the bare hull was the first of a series of experiments looking at the effects of ever-more detail of the hull-form. As explained in chapter 1.7, as the detail with which the form is described increases, the number of factors needed for the description increases. The experiments described in this chapter are at the least detailed level considered here, but the bare hull needs to be characterised to the greatest level of confidence, since it provides the foundation on which the subsequent experiments are based. The confidence with which the effect of changes to the basic hull-form may be stated is entirely limited by the confidence with which the drag of the basic hull-form is known. The experiments performed, therefore, incorporated all of the measurements derived from the Taguchi type design

described in (Fallows, 2005), augmented by additional measurements to give greater confidence in critical areas of characterisation, such as that at zero AoA, with the hydroplanes feathered.

The chapter is divided into three principal parts. The first examines the corrections that need to be made to the data to remove the consequences of effects that are felt by the model in the towing tank, but would not be felt by the full-scale vehicle in open water. The second derives the drag effects that would be experienced by the bare hull of the full-scale vehicle at sea, as a function of speed, angle-of-attack and hydroplane angle. And finally, comparisons are made between the results obtained here, and those derived for similar vehicles and for this vehicle but by an alternative method.

2.4.2 Data Corrections

The objective is to be able to reliably establish the drag that a full-scale, clean hull would experience under its normal operating conditions. There are a number of influences on the force measurements made in the laboratory that are not relevant to the drag force that would be experienced by the vehicle at sea, even after pre-processing the data as described in (Fallows, 2005), viz:.

- The force measured in the laboratory is augmented by the drag of the model support posts, modified by the consequences of any interaction between them.
- The model travels in a constrained channel producing two effects not experienced at depth at sea:
    - The proximity of the model to the surface may enable wave-induced drag to affect the total force measured.
    - The need for water to flow from ahead of the vehicle to behind, because of the constraining nature of the channel, increases the difference in speed between that of the model and the surrounding water, above that registered by measuring the speed of the carriage alone: the so-called blockage effect.

Both of these effects are exacerbated by the need to move the model at constant Reynolds number in order to reproduce the flows over the real vehicle. The scaling effect means that the model must be propelled significantly faster than the full-scale vehicle. The corrections necessary to allow for each of these effects are discussed in the following sections.

2.4.2.1 Support post tare drag

The model is connected to the carriage by support posts, at the forward and aft ends of the model centre body. As described in chapter 2.3, it was originally intended to mitigate the effects of the support posts by providing them with fairings. These were intended to both reduce their contribution to the measured force and, equally important, to reduce their wave-making effect. However, it proved unduly complex to produce a fairing that would be both stable in the water and not produce significant lift, whilst retaining the ability to easily change the angle-of-attack of the model. The supports used were, therefore, simple cylindrical posts. Because they had to be able to withstand both the forces inherent in handling the >100 kg weight of the model in air and the bending moment of the expected maximum 500 N load during runs, they had to be of substantial construction. They, therefore, comprised 3 cm diameter, thick walled, stainless steel tubes.

For purposes of wave drag determination it was necessary to be able to run the model at a range of depths. The poles were, therefore, attached to the dynamometer through two colleted sleeves with locating pins to determine the depth. The poles had a series of holes drilled along their length, corresponding to the standard depth settings. Hole numbering convention and dimensions are defined in Figure 2.4.1. Hole 1 could not be used because of interference with the dynamometer frame.

To establish their contribution to the total force measured, they were run alone at an immersion depth corresponding to the model being run at mid tank depth for a range of speeds and offset angles corresponding to the model experiment speeds and angles of attack. The results are given in the form of a mesh surface in Figure 2.4.2 and as a contour plot in Figure 2.4.3. The effect of offset angle is given in Figure 2.4.4.

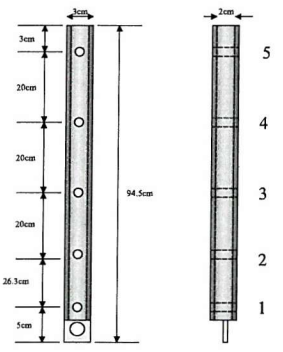

Figure 2.4.1 Model Mounting Poles

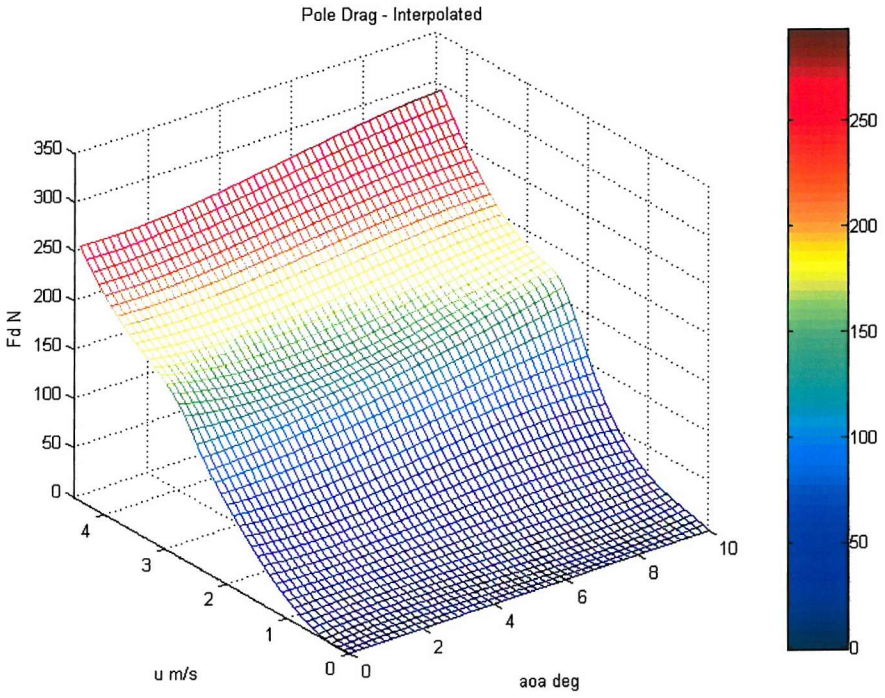

Figure 2.4.2 Pole drag as a function of speed and angle-of-attack, depth 5

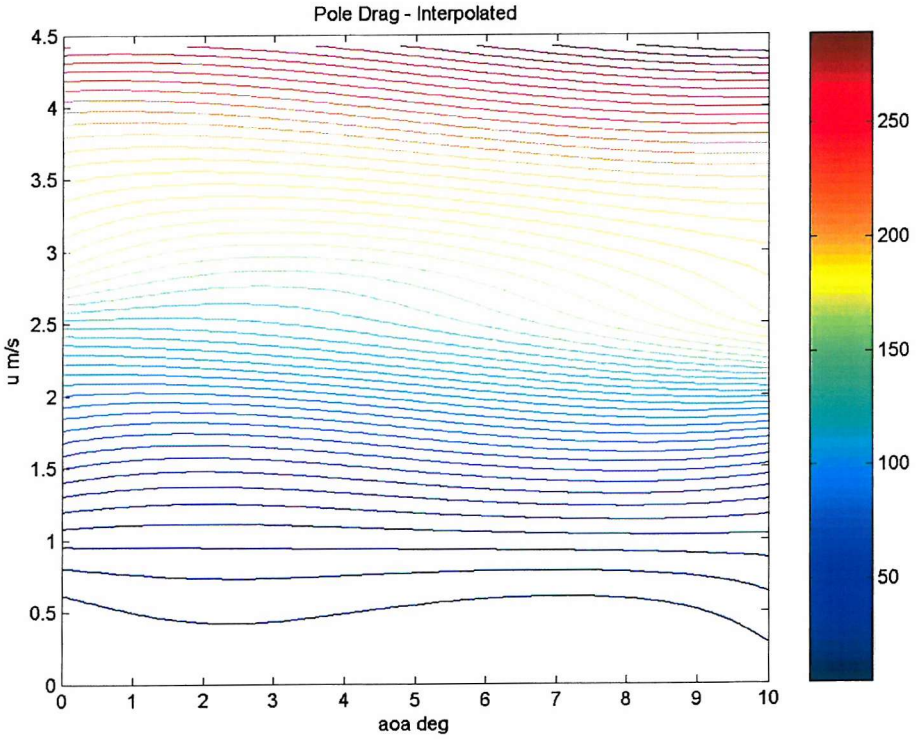

Figure 2.4.3 Pole drag contour plot

The effect of pole drag vs. speed for a range of offset angles is given in Figure 2.4.4

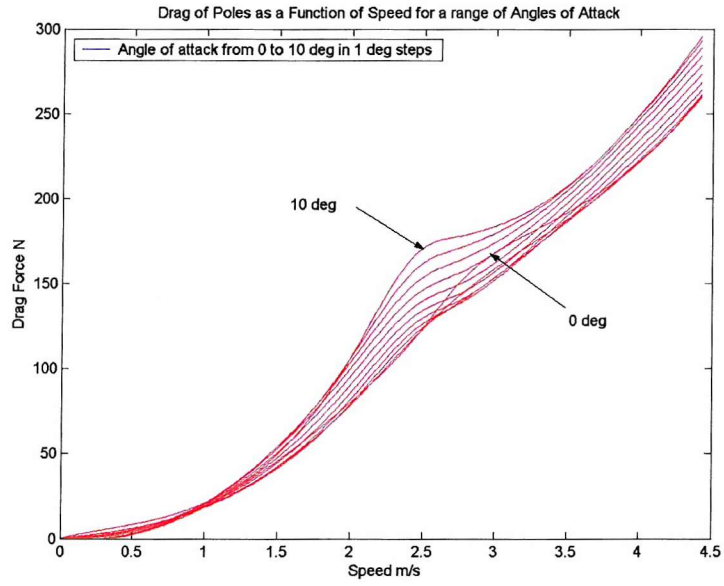

Figure 2.4.4 Effect of offset angle on pole drag

The script for processing the data is given at (Fallows, 2005). This produced a three dimensional interpolation as a data file. A look-up function (Fallows, 2005) enables the pole drag for any combination of the three parameters to be produced. A function to determine the accuracy with which the interpolation tracks the input data is given in (Fallows, 2005). The ability of the process to follow data used in the interpolation is given in Figure 2.4.5.

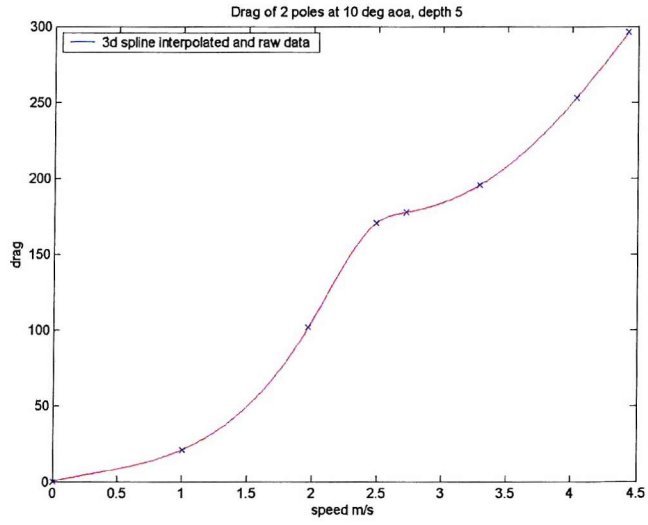

Figure 2.4.5 Interpolation accuracy

Accuracy of the predictions obtained from this model were compared with measurements not used in formulating the model with the results shown in Figure 2.4.6. The mean difference between predicted and measured was 0.3% with a standard deviation of 3%.

One method of determining the wave drag of the model is to run it at different depths as described in Section 2.4.3.3. To enable pole correction to be made, the pole drag was also measured at zero angle-of-attack for a range of depths and speeds. The results are illustrated in Figure 2.4.7.

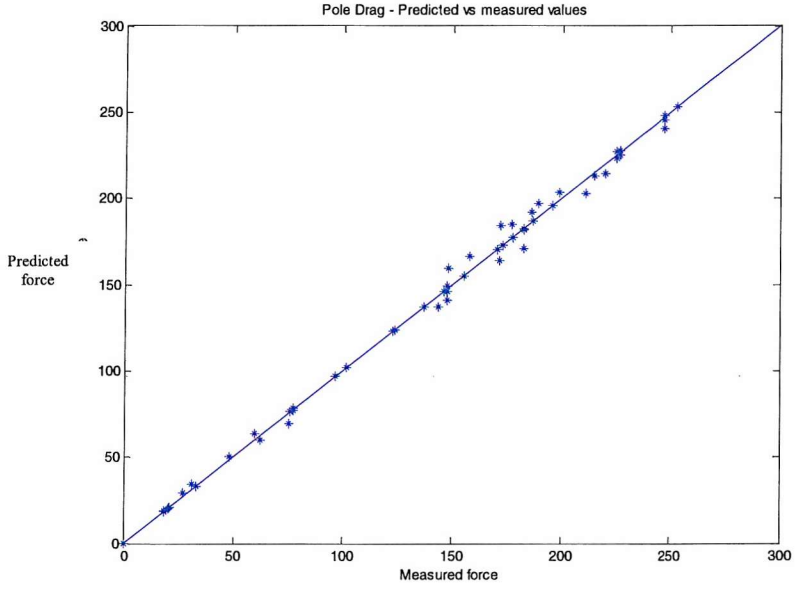

Figure 2.4.6 Pole drag model prediction accuracy

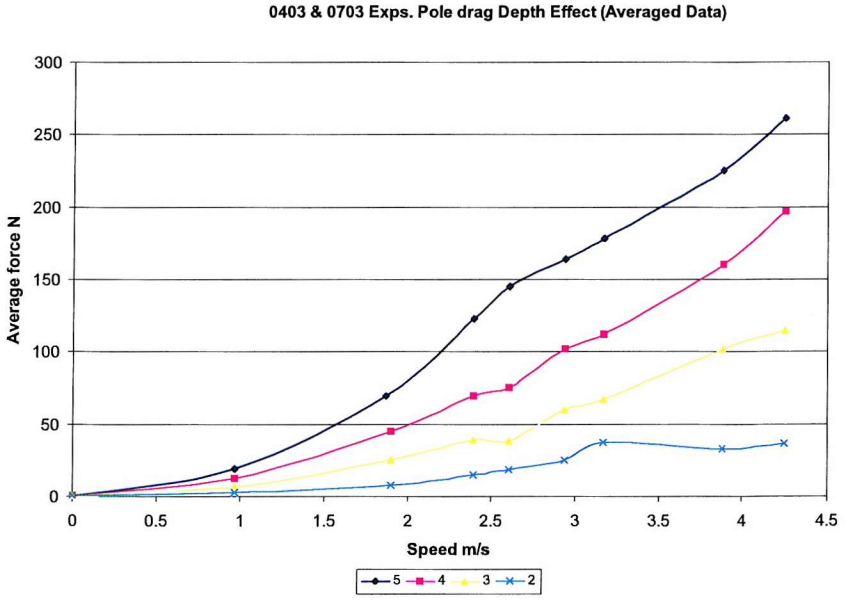

Figure 2.4.7 Effect of immersion depth on pole drag

The poles generated considerable waves, especially at high speed. The effect of wave generation on their drag can clearly be seen, with maxima at about 2.5 m/s at depth 5 through to about 3.2 m/s at depth 2.

2.4.3 Wave Drag Correction

2.4.3.1 Introduction

In order to produce good estimates of full-scale drag, AUV model experiments are designed to reproduce the flow lines and drag experienced by the full-scale vehicle. The experiments are, therefore, conducted on fully immersed large-scale models, travelling at speeds equivalent to the Reynolds Numbers experienced by the vehicle in service. As a consequence, the experiments are conducted at high Froude Numbers (Fn = 0.9 at full model speed of 4.5 m/s). The model may, therefore, experience drag induced by wave-making that it would not experience travelling at depth in the open ocean. Hoerner pp 11-17, 11-18 (Hoerner, 1965) indicates that wave-making of submarines is unlikely to be significant at immersion depths greater than 5 diameters. The geometry of the AUTOSUB model and SI Tank dictates that the model, when run at mid depth, is at a depth of approximately 3 diameters.

Since wave drag cannot be directly measured, three approaches to estimating this effect were taken. Two methods were based on the analysis of direct measurements undertaken in the tank and these were to be checked by comparison with a theoretical approach based on the geometry of the model. The three methods were:

- Measuring the surface disturbance and from this calculating the force that the model and support structure would need to exert in order to generate the disturbance.
- Deriving wave induced drag from measurements of drag as a function of immersion depth.
- Calculating wave drag from thin-ship theory.

2.4.3.2 Wave geometry

Insel (Insel, 1990a) describes a method for determining the wave drag exerted on both symmetrical and asymmetric hull forms based on analysing the wave pattern generated by the model. The waveform is measured by means of a series of longitudinal cuts taken by a number of wave probes. For a symmetrical hull, as used

here, only one set of wave cuts on one side of the tank is required. The apparatus for measuring the wave profile is shown schematically in Figure 2.4.8. Four resistance wave probes placed asymmetrically along a mounting post feed Churchill wave monitors which in turn are connected to a data logger to produce the wave cuts. The wave cut records are analysed using a Fortran programme written by Insel for the purpose (Insel, 1990a). This uses an iteration method to determine the wave coefficients and from these calculates the implied drag. The method is stable and has been used successfully for a number of surface ship models in the SI Towing Tank across a range of Froude numbers.

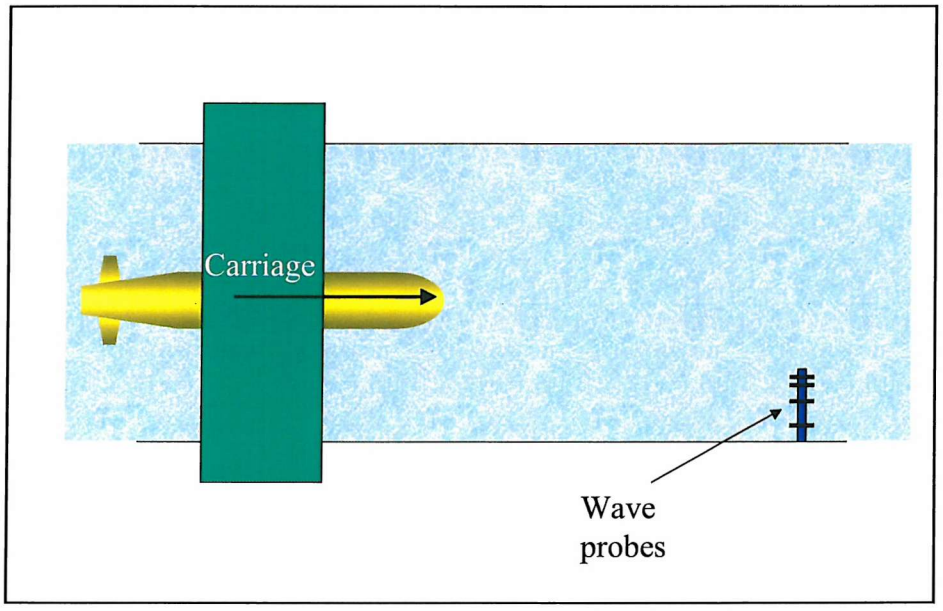

Figure 2.4.8 Wave cut measurement

Unfortunately the un-faired cylindrical support poles travelling at high speed caused large breaking waves. These swamped the wave probes and prevented the collection of usable wave cut records. This rendered the direct measurement approach untenable. Recourse was, therefore, taken to the second method of deriving wave drag, from measurements of drag across a range of depths.

2.4.3.3 Measurement of drag as a function of immersion depth

2.4.3.3.1 Theory

At depth, d, total drag, $F_t(d)$, comprises the sum of model form drag, F_f, pole drag (including its wave-making resistance), $F_p(d)$, model wave drag, $F_w(d)$, and forces resulting from blockage effects, F_b. For a given speed, both form and blockage effects (see Section 2.4.4) are purely a function of model and tank dimensions and are independent of depth. Only pole drag and model generated wave drag will change as a function of depth., therefore, for a given speed,

$$F_t(d) = F_f + F_b + F_p(d) + F_w(d)$$

let $k = F_f + F_b$

and $y(d) = F_t(d) - F_p(d).$

Then $F_w(d) = y(d) - k.$

The form of $y(d)$ for a range of speeds, u, may be found by fitting a curve to measured values of $F_t(d)$ and $F_v(d)$ as illustrated in Figure 2.4.9.

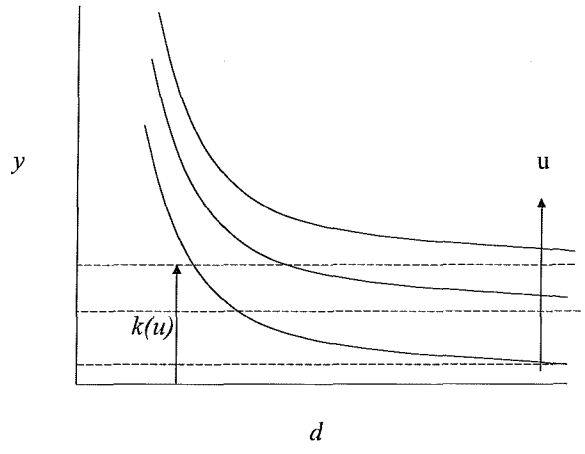

Figure 2.4.9 Wave drag by depth

For a given u, as $d \to \infty$, $y \to k$, and so $F_w(d)$ may be calculated.

2.4.3.3.2 Measurements

The model was run in a standard configuration (with no angle-of-attack, all 4 hydroplanes attached, and with the control surfaces feathered) across a range of speeds and for a series of immersion depths corresponding to the fixed positions provided by the mounting post location holes. The model centreline depths below the free surface for which $F_t(u)$ was measured are given in Table 2.4.1.

Hole Number	Depth
2	0.28
3	0.48
4	0.68
5	0.88

Table 2.4.1 Centreline depth of model in metres

A corresponding set of measurements was made for the mounting posts alone. The net drag of the model, after removing the effect of the poles is illustrated in Figure 2.4.10.

Figure 2.4.10 demonstrates that the net drag has reached a constant value at all speeds by 0.68m depth. Subtracting the constant value from the net force and plotting the residual against speed gives the curve for model wave drag for the range of depths considered, in Figure 2.4.11.

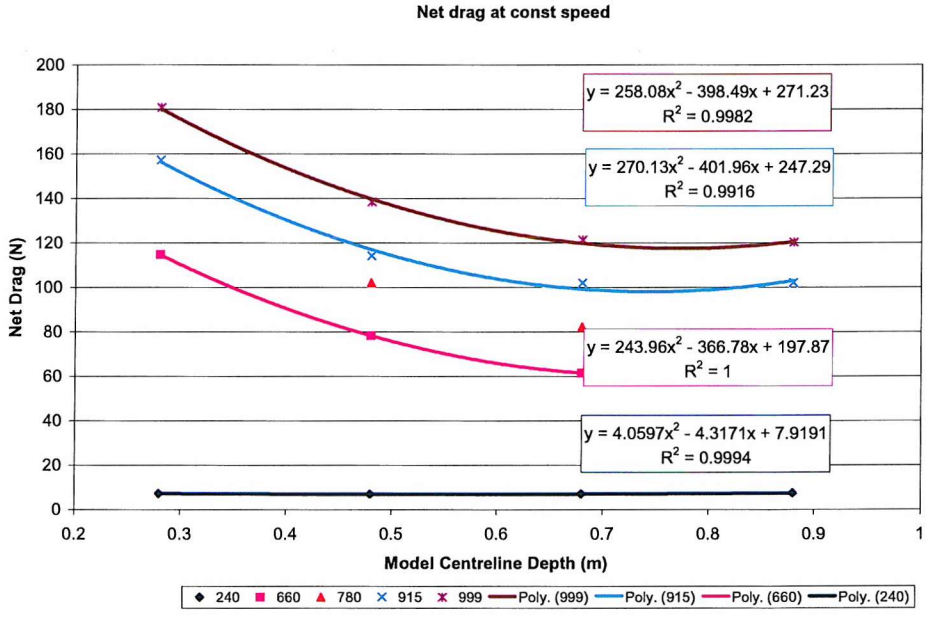

Figure 2.4.10 Model drag as a function of depth for a range of speeds

From Figure 2.4.11 it can be seen that at the depth at which the experiments were conducted (0.88m), the wave component of drag is negligible (< 0.5 N).

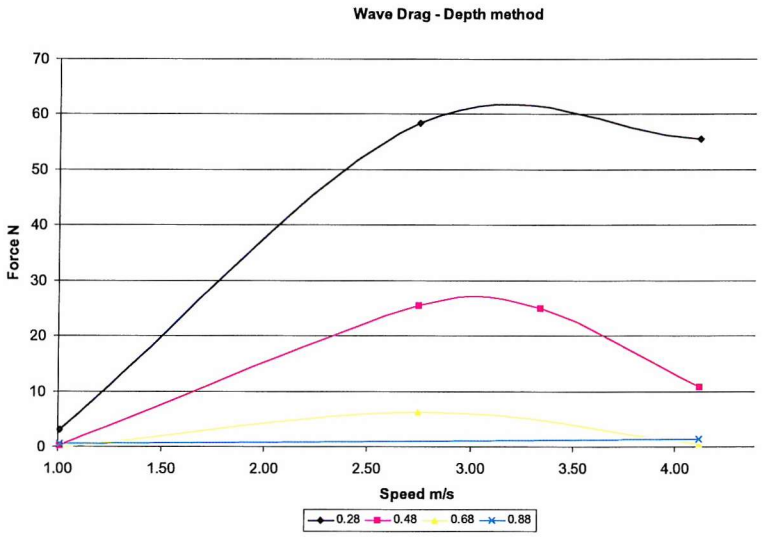

Figure 2.4.11 Model wave drag for a range of depths

2.4.4 Thin-Ship Modelling

As a check, the wave drag was calculated using a model based on Thin-Ship Theory. Thin-Ship Theory is generally considered to be applicable to vessels of length to breadth ratio greater than 7. AUTOSUB's is 7.5.

2.4.4.1 Theory

Thin-ship theory was developed by Michell (Eggers et al., 1967) (Newman, 1977) as a method of calculating the wave resistance of ships. Its basis is described at (Fallows, 2005).

Michell represents the body by a centre plane source distribution, proportional to its longitudinal rate of change of thickness. The only condition for its validity is that the rate of change be small: hence thin ships. The theory is Thus, applicable to submerged bodies as well as surface ships. In general, there is no restriction on beam/draft ratio, so long as the beam/length ratio is small. Thin-ship theory is, therefore, applicable to submerged bodies of revolution as considered here.

2.4.4.2 Modelling

The components of drag for the bare AUTOSUB hull-formwere calculated using a Fortran programme written by Hearn et al. Friction resistance is calculated using the ITTC '57 formula, assuming form factor to be negligible, and wave resistance based on thin-ship theory. The input file requires the form to be defined by the waterline profile at a number of stations. It assumes the hull to be symmetrical

about the centre line. A wire model of AUTOSUB was constructed. The details of the geometry used are given in (Fallows, 2005). The time to compute is necessarily a function of the number of panels in the model. To adequately capture pressure change, more panels are required in areas of high curvature (such as at the bow and around the circumference) than in constant sections. A satisfactory level of definition was found with 17 waterlines, 9 stations for the ellipsoid, 3 stations for the cylinder, 1 for the transition and 1 for the frustum. The resulting model is illustrated at Figure 2.4.12.

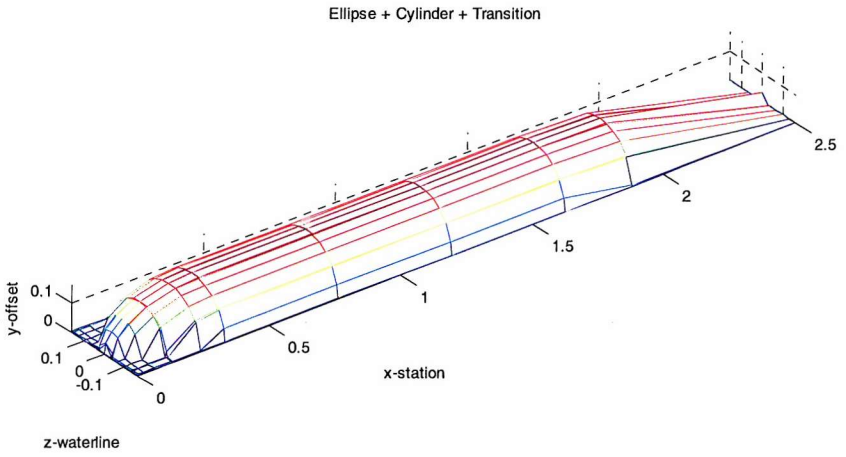

Figure 2.4.12 AUTOSUB space model

Wave resistance as a function of speed calculated for the depths used in the experiments is given in Figure 2.4.13.

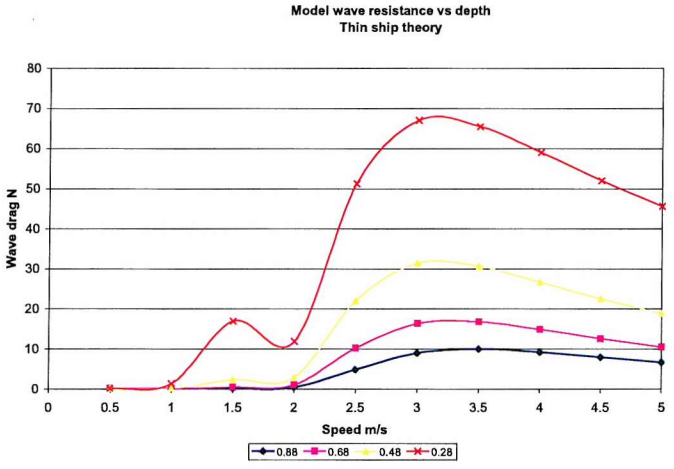

Figure 2.4.13 Wave resistance for a range of depths

2.4.4.3 Wave drag conclusions

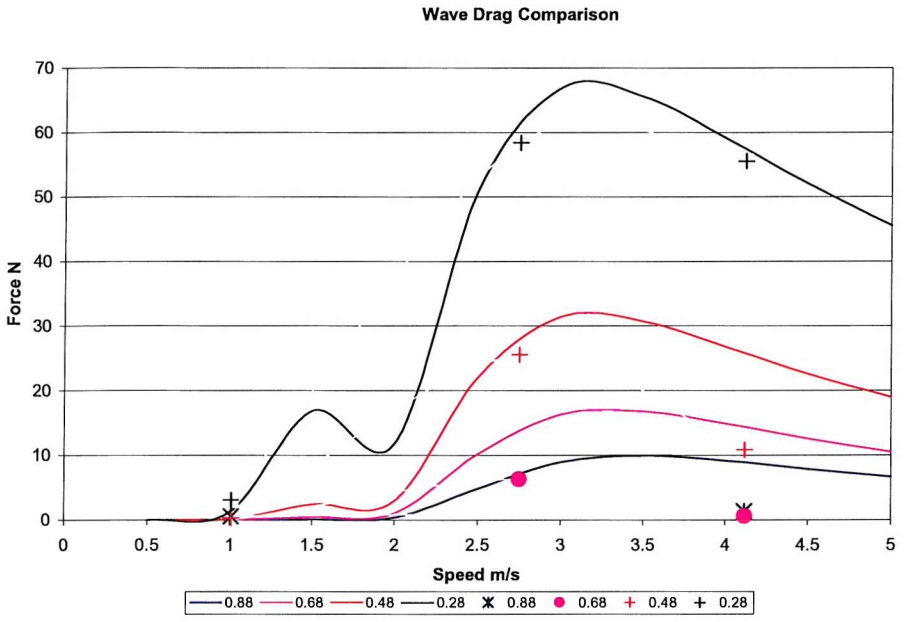

Figure 2.4.14 Comparison between theory and measured data

A comparison between wave drag calculated from measured data and that from Thin Ship Theory is shown in Figure 2.4.14. This shows a remarkably good fit at shallow depths when wave drag may be expected to produce the greatest effect. It also shows reasonable agreement at low speeds at other depths, but less so at high speeds. Both methods conclude that wave drag at the operating depth of 0.88 m is small.

2.4.5 Blockage Correction

The velocity of the flow around a body travelling in a body of water constrained within the confines of a shallow, limited width, finite length channel, will be different to that experienced by the same body travelling in deep water in mid ocean. An adjustment to the results obtained from models in towing tanks, therefore, needs to be made to allow the results to be extrapolated to those that would be experienced by a similar body in mid-ocean. This adjustment is expressed as a modification to the towing speed.

2.4.5.1 Causes of blockage

Blockage is the result of three complementary effects (Scott, 1965):

1. The tank walls and floor exert viscous drag on the fluid flows established as a result of the passage of the model. The model, therefore, experiences an apparent increase in relative fluid flow close to the hull over that which it would experience in open water.
2. The velocity, v, of a wave of wavelength, λ, in water of depth, d, is given by:

$$v = \sqrt{\frac{g\lambda}{2\pi}\tanh\left(2\pi\frac{d}{\lambda}\right)}$$

Therefore, waves naturally travel more slowly in shallow water than in deep. But the velocity of the wave is effectively increased by the propulsion mechanism.

Now velocity is related to frequency by:

$$v = f\lambda .$$

But wavelength is a function of the length of the model and so may be considered constant. Hence, for constant speed, the frequency of the wave must be maintained higher than it would otherwise be.

The energy of a wave of mass, m, frequency, f, and amplitude, d, is given by (Giancoli, 1988).

$$E = 2\pi^2 m f^2 d^2 ,$$

Where m is the mass moved by the wave:

$$m = \rho A v t$$

A is the cross sectional area through which the wave moves, v is its velocity and t time.

Thus, greater energy is required to generate a wave in a shallow tank than in deep water and so the wave resistance experienced by the model is greater than it otherwise would be.

3. Wave reflections from the tank wall will in principle affect the model, although in practice this effect is considered to be small and is usually ignored.

2.4.5.2 Critical parameters

The methods described below are applicable provided that:

Tank width to depth ratio $\frac{w}{d} = 2$, i.e. a surface piercing model is equidistant from the tank walls and floor.

Model length $3.5 < l < 9m$

Froude number $F_r = 0.08 < \frac{u}{\sqrt{gl}} < 0.4$

Blockage Ratio $m = \frac{A_m}{A} < 0.03$

Where, A_m = model cross sectional area

A = tank cross sectional area

Depth Froude number $F_{nd} = \frac{u}{\sqrt{gd}} < 0.7$,

where h = water depth of tank.

Reynolds number $R_e = \frac{ul}{\nu}$, where ν = kinematic viscosity m^2/s

For the AUTOSUB model:

Tank width to depth ratio $\frac{w}{d} = \frac{3.7}{1.85} = 2$

Model length $l = 2.5\ m$

Froude number $F_n = 0.1 < \frac{u}{\sqrt{gl}} < 0.92$

Blockage Ratio $m = \frac{A_m}{A} = \frac{0.086}{3.7x1.85} = 0.013$

Max depth Froude number $F_{ndmax} = 1.07$

The largest problem is the high F_n experienced by the AUTOSUB model due to running it at constant R_e. This is likely to lead to the need for a large correction due to blockage resulting from additional wave-making.

2.4.5.3 Alternative methods

A number of methods are recommended by the ITTC for blockage correction in towing tank experiments. Each is stated below and subsequently compared. It should be noted that these are primarily intended for experiments relating to displacement hulls rather than fully submerged bodies

2.4.5.3.1 Young and Squire

Young and Squire propose the following formula for speed correction, based on inviscid fluid theory applied to a fully submerged body:

$$\frac{\delta u}{u} = 0.15VA^{-\left(\frac{3}{2}\right)} \tag{1}$$

where V = immersed volume of model.

and A = tank cross sectional area *in feet.*

The advantage of this method is that it takes account of a fully submerged body, rather than a partial displacement hull, and is simple to apply. However, for the AUTOSUB experiments it has the significant disadvantage that it only allows for the frictional component of blockage and makes no allowance for interaction with the free surface.

2.4.5.3.2 Schuster

The Schuster blockage formula is:

$$\frac{\delta u}{u} = \frac{m}{1-m-F_{rh}^{\ 2}} + \left(1-\frac{R_v}{R_T}\right)\frac{2}{3}F_{rh}^{\ 10} \tag{2}$$

where R_T = total resistance

R_v = viscous resistance obtained from the ITTC '57 correlation line,

And $m = \frac{A_m}{A_T}$

Where A_m is the cross sectional area of the model and A_T is the cross sectional area of the tank.

2.4.5.3.3 Scott

Blockage correction according to Scott (Scott, 1965) is given by:

$$\frac{\delta u}{u} = k_1 VA^{\frac{-3}{2}} + BL^2 k_2 A^{\frac{-3}{2}} \tag{5}$$

Factor k_1 is a graphical function of a, where:

$$a = \frac{C_B V^{\frac{1}{3}}}{L} \tag{6}$$

and the block coefficient (C_B) is the ratio of the immersed hull volume at a particular draught to that of a rectangular prism of the same length, breadth, and draught as the ship.

$$C_B = \frac{V}{BTL} \tag{7}$$

where, B = beam, T = draught and L = length.

For AUTOSUB model $C_B = 0.6$ and $a = 0.15$. From [Ref: ITTC, Fig 2]:

$$k_1 = 1.3 \text{ for } 2 \times 10^{-6} < R_e < 4.8 \times 10^{-6}$$

and then decreases linearly until $k_1 = 0.85$ at $R_e = 8.3 \times 10^{-6}$.

Factor k_2 is a function of F_n. For the speed of interest for the AUTOSUB model (>1m/s), $F_n \geq 0.2$ and so:

$$k_2 = 2.4(F_r - 0.22)^2$$

The first term in Equation (5) reflects the effect of skin friction and is Reynolds number dependent. For low values of R_n, ($R_n < 2 \times 10^6$) it is identical to that provided by Young and Squire. The second term provides the wave generated effect and is a function of Froude number.

2.4.5.3.4 Tamura

Tamura's speed adjustment also includes shallow water effects. It is given by:

$$\frac{\delta u}{u} = 0.67m\left[\frac{L}{B}\right]^{\frac{3}{4}} \frac{1}{(1 - F_{nd}{}^2)} \tag{8}$$

Where B = breadth of tank.

2.4.5.4 Discussion

All four methods are in reasonable agreement at low speeds, but vary significantly at higher F_n. With the exception of Young and Squire, all have an empirical element and assume a surface penetrating hull.

Scott is the standard method recommended by the ITTC and so results prepared on this basis will more readily be comparable with those published elsewhere. Its derivation is founded on Equation (1) proposed by Young and Squire, which is derived from inviscid flow theory for a fully submerged body. This formula is only applicable for small back flow effects and makes no allowance for wave-making, boundary layer or wake effects. Scott has, therefore, modified this equation to take account of these. It is assumed that the effect of reflected waves will be very small and so only backflow and wave retardation are included.

Consider first wave retardation. This is manifest in the form of a surface disturbance. The net surface disturbance over the whole tank sums to zero. It is assumed that this condition also applies locally over areas of the order of the square of the tank breadth.

The local surface disturbance may be derived from Bernoulli's theorem:

$$\frac{\delta d}{d} = \frac{u^2}{gd}\left(\left(\frac{u_u}{u} + \frac{\delta u}{2u}\right)\frac{\delta u}{u} + \frac{1}{2}\left(\frac{u_u{}^2}{u^2} - 1\right)\right). \tag{9}$$

Where u_u is the mean local speed in unrestricted flow, δu is the increase in speed over u caused by blockage and u is the mean speed in the tank.

Now $\frac{\delta u}{u}$ is small, so (9) reduces to:

$$\frac{\delta d}{d} = -\frac{u^2}{gd}\left(\frac{1}{2}\left(\frac{u_u{}^2}{u^2} - 1\right)\right). \tag{10}$$

Scott quotes Schlichting as recording 3 diagrams that suggest that $\frac{u_u}{u}$ is of the order of 1.3 for a surface penetrating model. Therefore:

$$\frac{\delta d}{d} = \frac{u^2}{gh}\left(\frac{1}{2}\left(1.3^2 - 1\right)\right) = 0.35\frac{u^2}{gd}. \tag{11]}$$

However, for a submerged body of revolution, Schlichting indicates

$$\frac{u_u}{u} = 1.05. \tag{12}$$

Substituting this value in [10] gives:

$$\frac{\delta d}{d} = \frac{u^2}{gh}\left(\frac{1}{2}\left(1.05^2 - 1\right)\right) = 0.05\frac{u^2}{gd}. \tag{13}$$

Thus, in the vicinity of the model, the effective cross sectional area of the tank is reduced by the Bernoulli depression, $\frac{\delta d}{d}$, as given by equation (13).

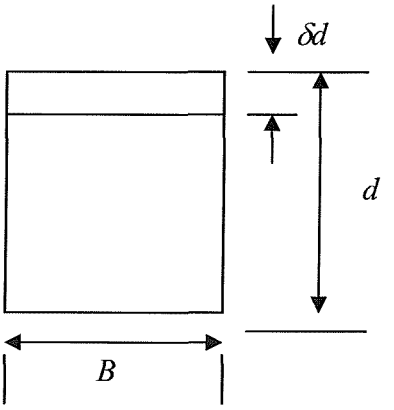

Figure 2.4.15 Tank cross section

The effective tank cross sectional area in the vicinity of the model (Figure 2.4.15), therefore, becomes:

$$A' = A - B\delta d\,. \tag{14}$$

Equation (13) in (14) gives:

$$A' = A - Bd\left(0.05\frac{u^2}{gd}\right) = A\left(1 - 0.05\frac{u^2}{gd}\right) \tag{15}$$

Equation (1), therefore, becomes:

$$\frac{\delta u}{u} = 0.15VA^{-\left(\frac{3}{2}\right)}\left(1 - 0.05\frac{u^2}{gd}\right)^{-\left(\frac{3}{2}\right)} \tag{16}$$

Now consider the effective volume of the model. The layer of fluid immediately adjacent to the model surface is usually considered to move at the same velocity as the model. The velocity of succeeding layers slips relative to this layer and becomes progressively slower, until at a sufficient distance from the surface of the model the fluid travels at the free stream velocity. This effect is amplified in the wake of the vehicle as it drags fluid along with it. The effective volume of the model when travelling at speed is, therefore, greater than its displacement volume. For a given cross sectional area, the effective volume is unlikely to be much affected by form, but will be dependent on length. The thickness of the boundary layer and the volume of the wake will also be dependent on speed and is, therefore, likely to be a function of Reynolds number. Scott, therefore, hypothesises that the backflow in the region of the model is likely to change by an amount:

$$\delta V = L^3 f(\mathrm{Re}). \tag{17}$$

Substituting Equation (17) into Equation (16) gives:

$$\frac{\delta u}{u} = 0.15\left(V + L^3 f(\mathrm{Re})\right)A^{-\frac{3}{2}}\left(1 - 0.05\frac{u^2}{gd}\right)^{-\frac{3}{2}} \tag{18}$$

Finally consider the effect of wave retardation. The ratio of the wave speed in a fluid of depth h, to that in infinitely deep fluid is given by:

$$\frac{u_{wh}}{u_{w\infty}} = \sqrt{\tanh\frac{gd}{u_\infty^{\,2}}} \tag{19}$$

From this, Scott derives that the effect due to wave retardation is given by:

$$\frac{\delta u}{u} = \left(1 - \frac{1.82C_v}{n_t C_t}\right) f\left(\frac{u^2}{gd}\right) \quad , \tag{20}$$

where,

$$n_t = 2 + \frac{R_n}{C_t}\left(\frac{dC_t}{dR_n}\right) \tag{21}$$

and $\frac{dC_t}{dR_n}$ is derived from the ITTC'57 line and has the value 1.82.

The total blockage effect, as derived by Scott, but adjusted for a submerged body of revolution rather than a conventional surface piercing hull form, is, therefore, the sum of the flow constriction , equation (18), and wave effects, equation (20), viz:

$$\frac{\delta u}{u} = 0.15\left(V + L^3 f(\mathrm{Re})\right)A^{-\frac{3}{2}}\left(1 - 0.05\frac{u^2}{gh}\right)^{-\frac{3}{2}} + \left(1 - \frac{1.82C_v}{n_t C_t}\right) f\left(\frac{u^2}{gd}\right) \tag{22}$$

Comparing Equation (22) with the form advised by ITTC, Equation (5), (which omits the wave retardation term) yields modified forms of the two constants used in Equation (5):

$$k_1' = 0.15\left(1 - 0.05\frac{u^2}{gd}\right)V \tag{23}$$

compared with

$$k_1' = 0.15\left(1 - 0.35\frac{u^2}{gd}\right)V \tag{24}$$

and

$$k_2' = 0.15L^3\left(f(R_e)\right)\left(1 - 0.05\frac{u^2}{gd}\right)A^{-\frac{2}{3}} \tag{25}$$

rather than $$k_2' = 0.15L^3\left(f(R_e)\right)\left(1 - 0.35\frac{u^2}{gd}\right)A^{-\frac{2}{3}} \quad (26)$$

Thus, the blockage effect experienced by a model of an underwater body of revolution will be smaller than that predicted by Scott.

2.4.5.5 Comparison

The Matlab script at (Fallows, 2005) was written to calculate the blockage corrections for the AUTOSUB model according to each of the four methods, amended to allow for a fully submerged body as described above.

Young and Squire produce a very small linear speed correction of < 1%, as shown in Figure 2.4.16

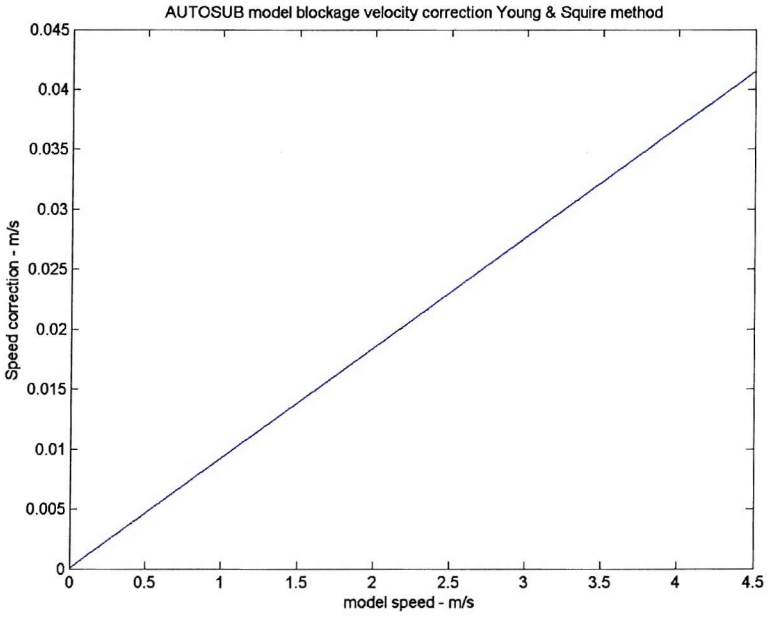

Figure 2.4.16 AUTOSUB Model blockage correction according to Young & Squire

The correction calculated using Schuster's method is given in Figure 2.4.17. This takes account of the wave effect above 3 m/s, although the correction rapidly becomes excessive at higher speeds.

Total blockage correction according to Scott is the sum of two terms, that due to friction effects and that due to wave effects. The friction term is a function a factor *k1*, which itself is a function of the dimensions of the vehicle and its R_e. The factor *k1* for the AUTOSUB Model is given in Figure 2.4.18.

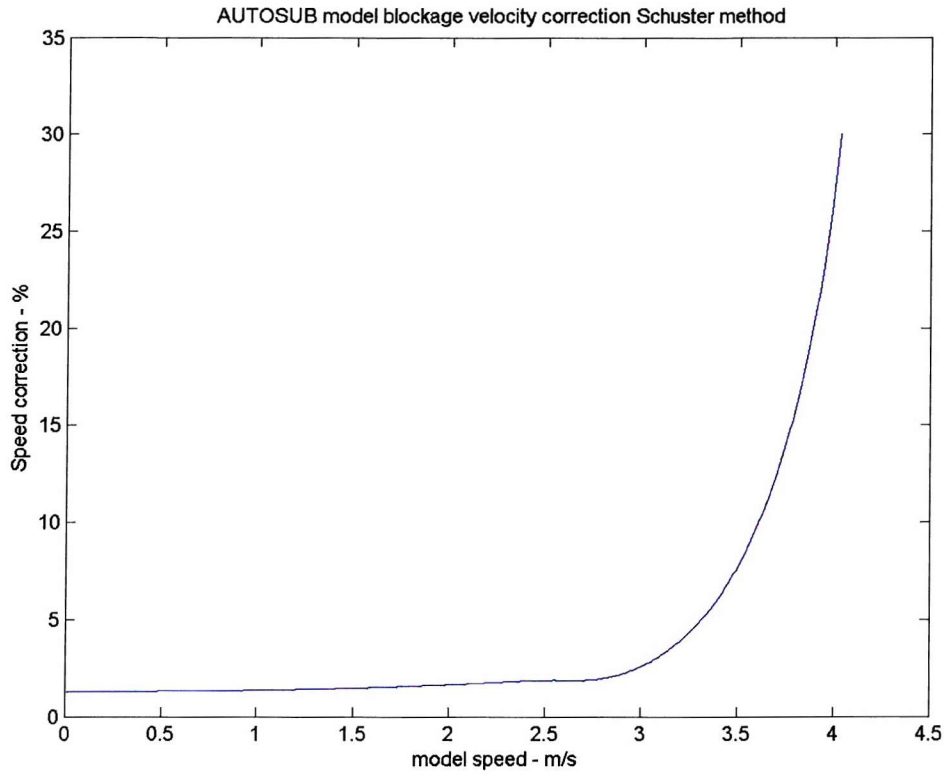

Figure 2.4.17 AUTOSUB Model blockage correction according to Schuster

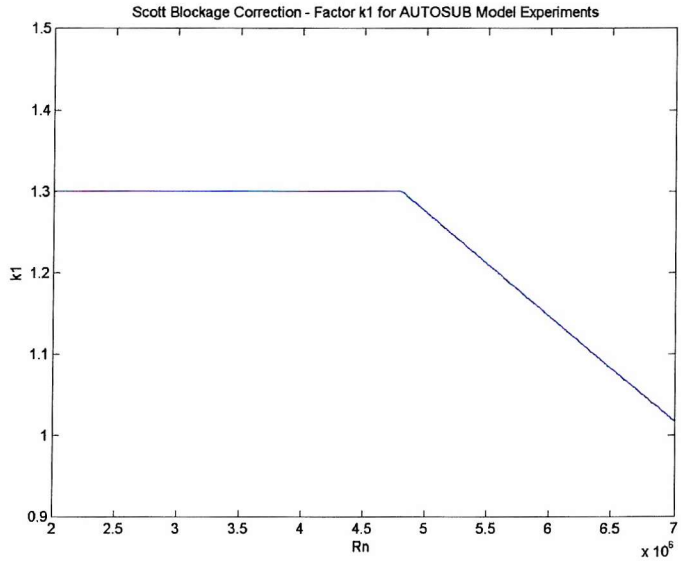

Figure 2.4.18 Scott factor k1 for the AUTOSUB Model

The friction component of Scott's correction derived from this factor is small, as can be seen from Figure 2.4.19.

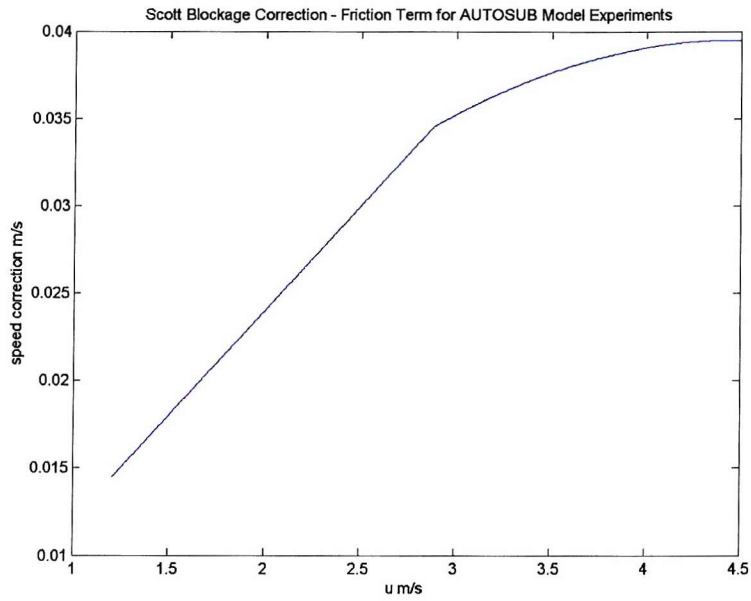

Figure 2.4.19 Scott correction friction term for AUTOSUB Model

The component relating to the wave retardation term of for Scott's blockage correction is a function of a factor, *k2*, which, for the AUTOSUB Model, is given in Figure 2.4.20.

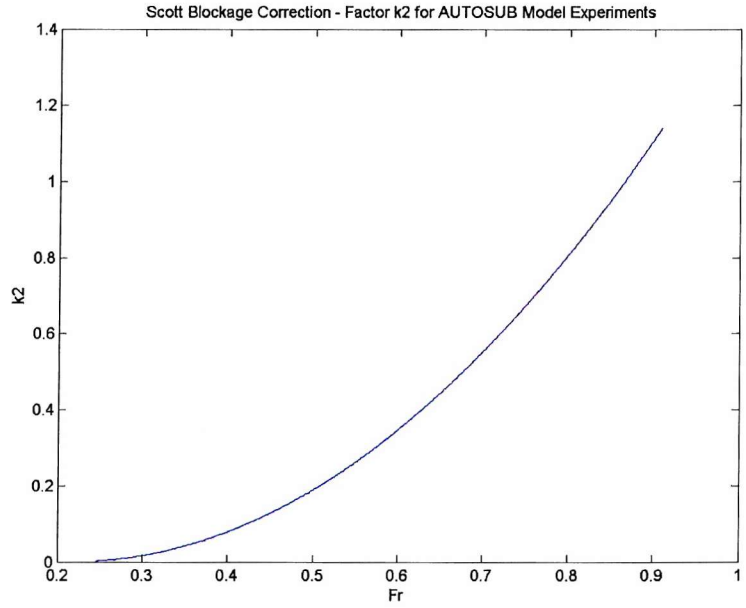

Figure 2.4.20 Scott factor k2 for the AUTOSUB Model

The wave retardation component of Scott's correction is given Figure 2.4.21.

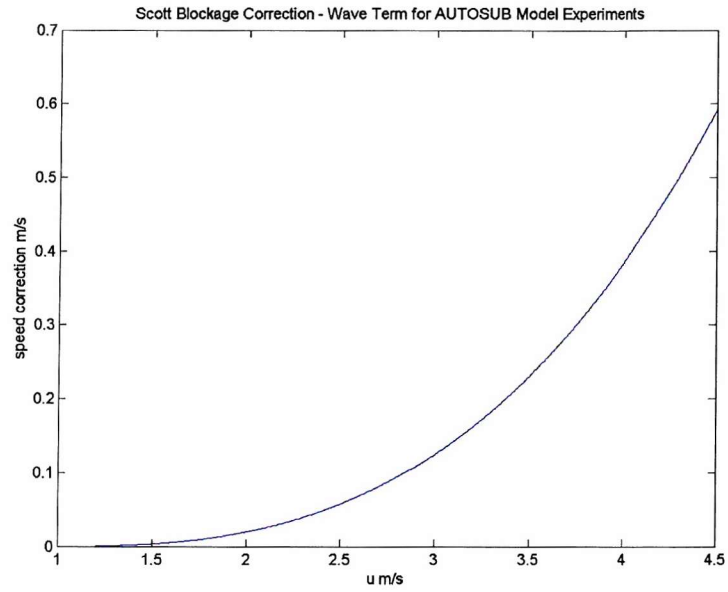

Figure 2.4.21 Scott wave retardation component of blockage for the AUTOSUB Model

As can be seen from Figure 2.4.22 the wave term dominates the total Scott correction.

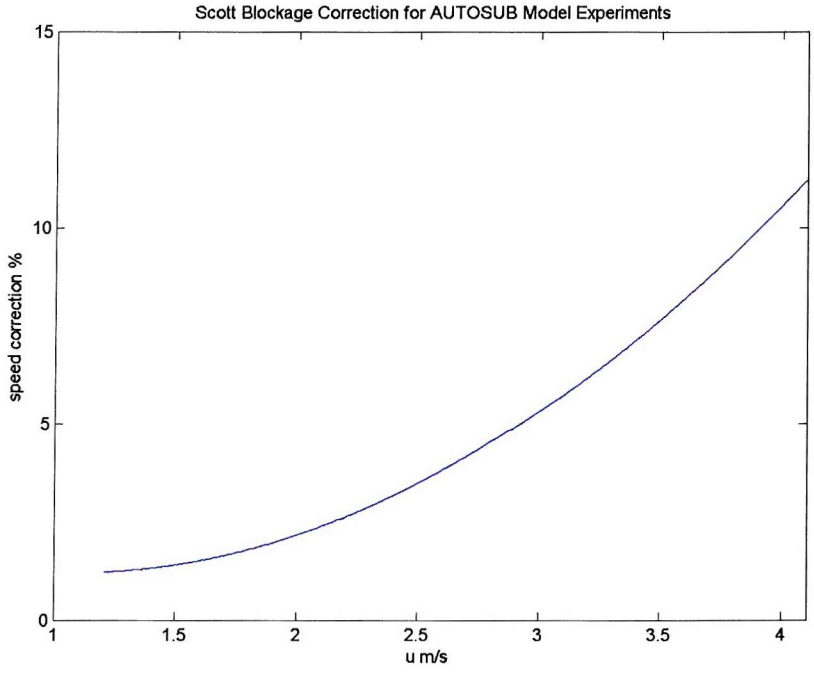

Figure 2.4.22 AUTOSUB Model total blockage correction according to Scott

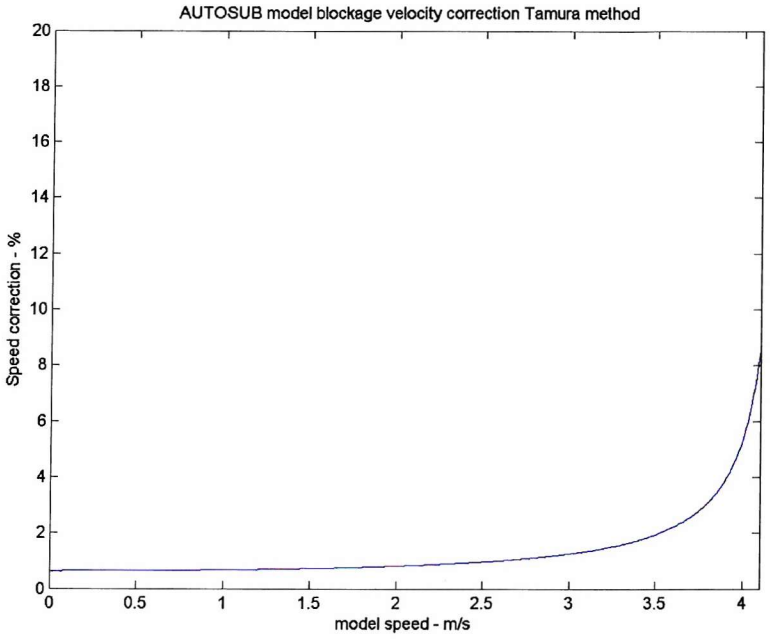

Figure 2.4.23 AUTOSUB Model blockage correction according to Tamara

The correction according to Tamara is given in Figure 2.4.23. This proves to be more stable at high speeds than either Schuster or Scott, but again there is a rapid rise in correction for speeds > 3.5m/s.

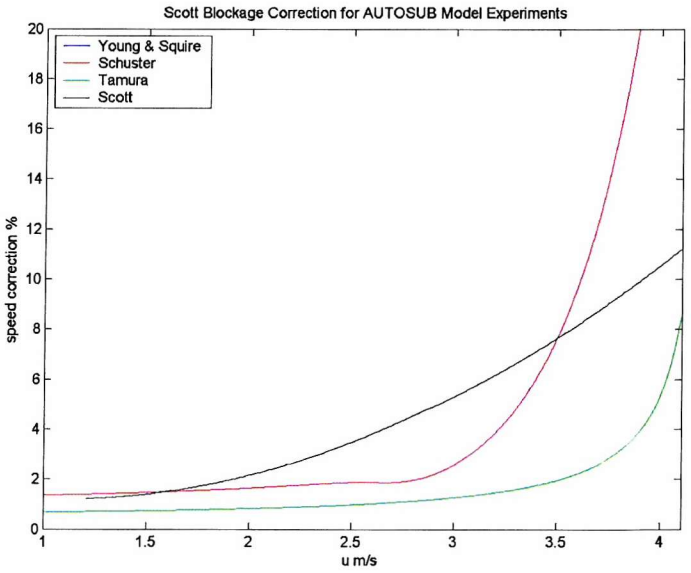

Figure 2.4.24 Comparison of the results of 4 blockage corrections for the AUTOSUB Model

Figure 2.4.24 provides a comparison between all methods discussed. Tamara's method provides the most likely for the AUTOSUB model, but ITTC cautions that

even this method is unreliable for $F_n > 0.7$ (which equates to speeds greater than 3.4 m/s for the AUTOSUB model in the SI towing tank). The blockage factor, m, for the AUTOSUB model is very small. It is, therefore, reasonable to assume that back flows, even when travelling at high F_n will be small compared with that experienced by large surface models. It is, therefore, reasonable in this case to use simple extrapolation for speeds higher than 3.4 m/s. A Matlab script (Fallows, 2005) was written to do this and second and third order polynomials fitted to the resultant curve as shown in Figure 2.4.25. The third order polynomial produces an excellent fit and was used to generate a blockage correction look-up table for use in subsequent analysis.

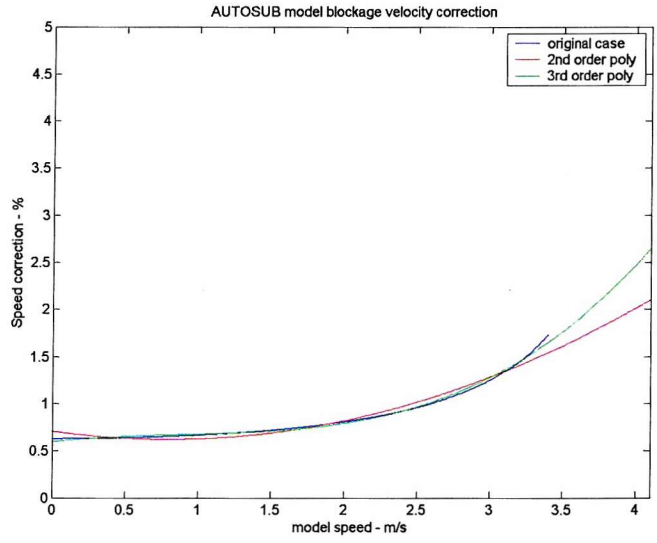

Figure 2.4.25 Blockage correction for the AUTOSUB Model in the SI Towing Tank

2.4.5.5 Blockage correction - conclusions

As a result of the above analysis it is concluded that:

a) The formula proposed by Young and Squire, although derived for a fully submerged body of revolution, will result in too small a correction due to no allowance being made for the boundary layer or Bernoulli depression effects.

b) Scott's approach will result in too large a correction since it is derived for a surface penetrating conventional hull form, rather than a submerged body of revolution.

c) Schuster and Tamura's method both result in lower blockage corrections than Scott and there is a large measure of agreement between them for

speeds up to 2.5 m/s. However, above this speed the Schuster prediction becomes unstable due to the F_n^{10} term.

d) Thus, Tamara is likely to produce the most accurate prediction. However, ITTC cautions that even this method is unreliable for $F_r > 0.7$ (which equates to speeds greater than 3.4 m/s for the AUTOSUB model in the SI towing tank).

e) The blockage factor, m, for the AUTOSUB model is very small. It is, therefore, reasonable to assume that back flows, even when travelling at high F_n will be small compared with that experienced by large surface models. It is, therefore, reasonable in this case to use simple extrapolation for speeds higher than 3.4 m/s.

The blockage correction applicable to the AUTOSUB model is, therefore, that of Tamura up to speeds of 3.4 m/s, with a polynomial extrapolation to cover the remainder of the speed range used for AUTOSUB model testing, i.e. to 4.1 m/s.

2.4.6 Characterisation of the bare Model hull

Having established the magnitude of those effects that are experienced by the model in the towing tank that would not be experienced in unconfined water, we can now establish the open water characteristics of the model.

That set of data containing measurements of the drag force experienced by the bare model hull mounted at depth 5 (0.88m centre line depth), with the support poles penetrating the water surface and with hydroplanes fitted but feathered was selected. This data contains force measurements across a range of speeds and angles of attack. The Matlab script given at Annex 2.4.4 was written to analyse this data.

A 3-d piecewise cubic spline interpolation may be fitted to the data to enable estimation of gross drag at points not measured. The results are shown in Figure 2.4.26.

This process may be repeated for the gross pole drag data to produce a 3-d interpolated model of pole drag as a function of speed and angle-of-attack. Provided that the same interpolation grid is used for both the gross and pole drag data, the pole drag may be subtracted from the gross drag at each data point to produce an interpolated net drag as a function of speed and angle-of-attack. The effect of this process is shown in Figure 2.4.27.

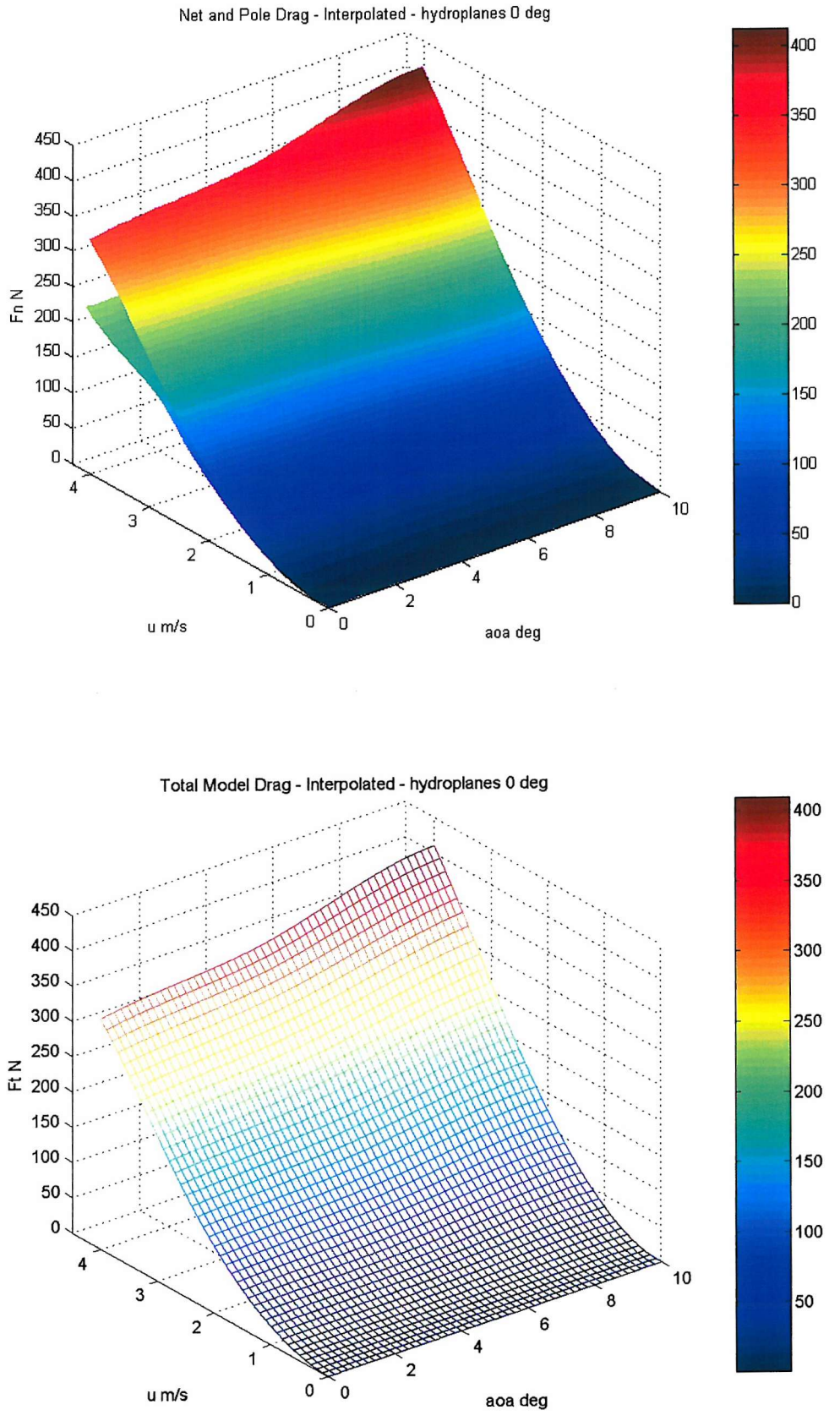

Figure 2.4.26 Total model drag

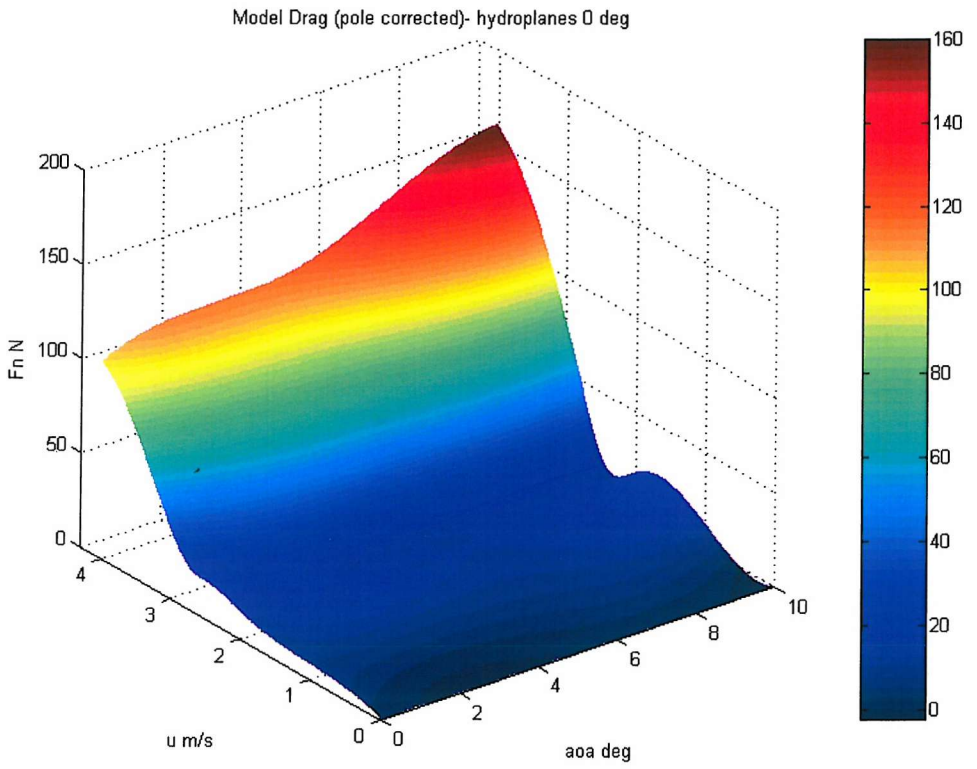

Figure 2.4.27 Effect of removing pole drag

Because the gross pole drag includes its wave-induced drag, the net drag comprises only the sum of the friction plus form drag of the hull, the wave induced drag of the hull and the hull blockage effect. (It is assumed that the blockage effect of the poles is negligible).

The wave drag is calculated using a thin-ship model (see Section 2.4.4). The simplifying assumption is made that wave drag is independent of the angle-of-attack. A 3-d interpolated model is made of wave drag, to the same mesh as that applied to the gross and pole drag data (Figure 2.4.28). Wave drag may then be subtracted from the net drag to produce the drag that the model would have experienced in unconfined water (Figure 2.4.29).

Finally the results need to be adjusted to produce force as a function of the speed that would have been experienced in open water by allowing for the blockage effect. The blockage effect is calculated using Tamara's method (see Section 2.4.5.4). The speed adjustment required is shown in Figure 2.4.30.

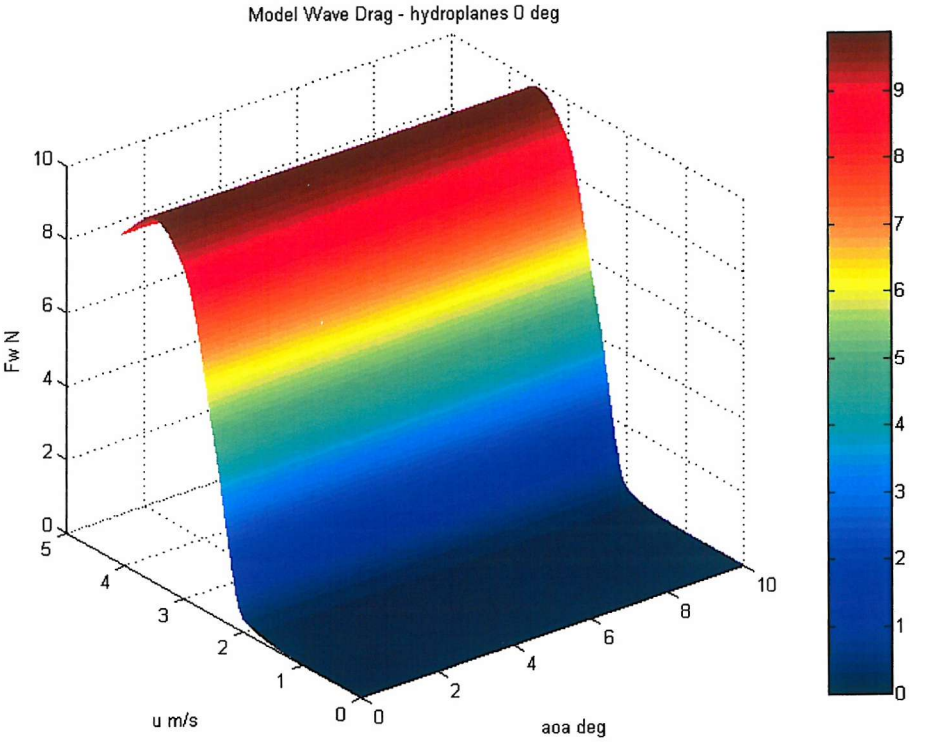

Figure 2.4.28 Interpolated wave drag

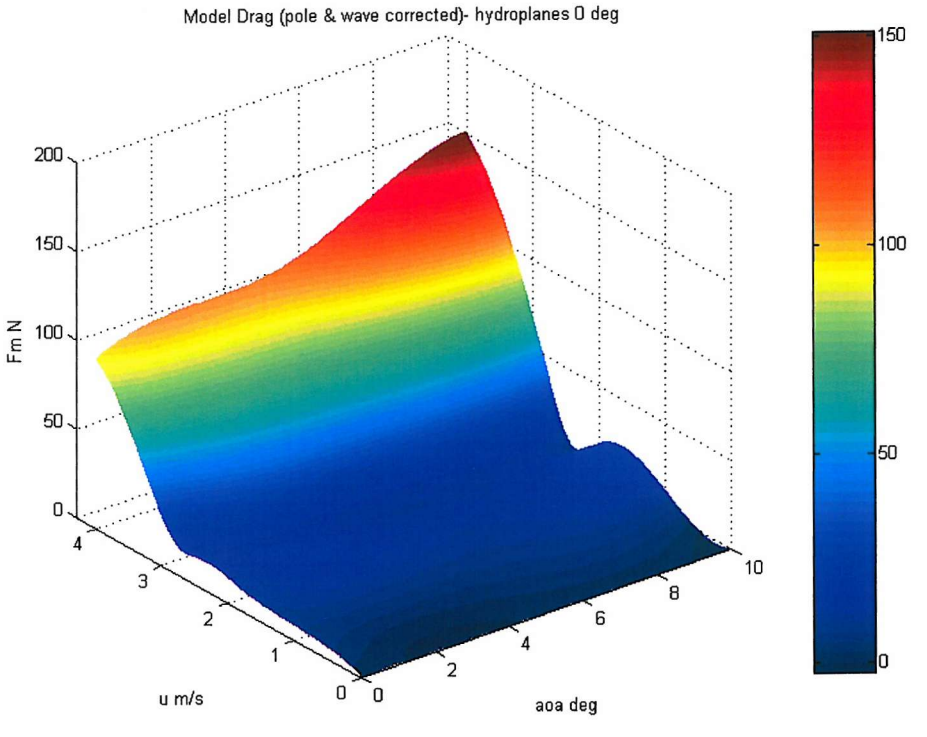

Figure 2.4.29 Drag that the model would have experienced in unconfined water

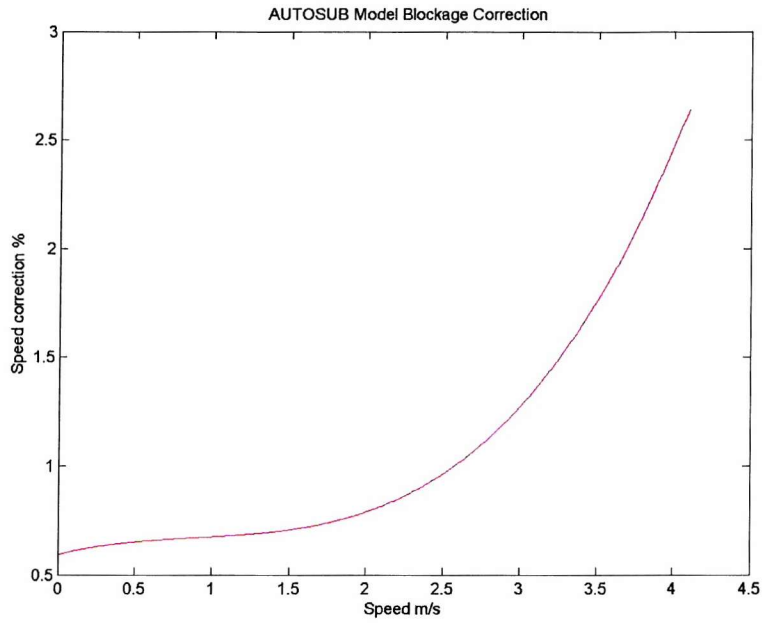

Figure 2.4.30 Model blockage correction for SI Towing Tank

The above process results in a 3-d model (Figure 2.4.31) of the drag force acting on the model, as a function of its speed and angle-of-attack, that would be experienced by it if it were travelling unsupported, in deep water, remote from any boundary. This is shown as a contour plot in Figure 2.4.27

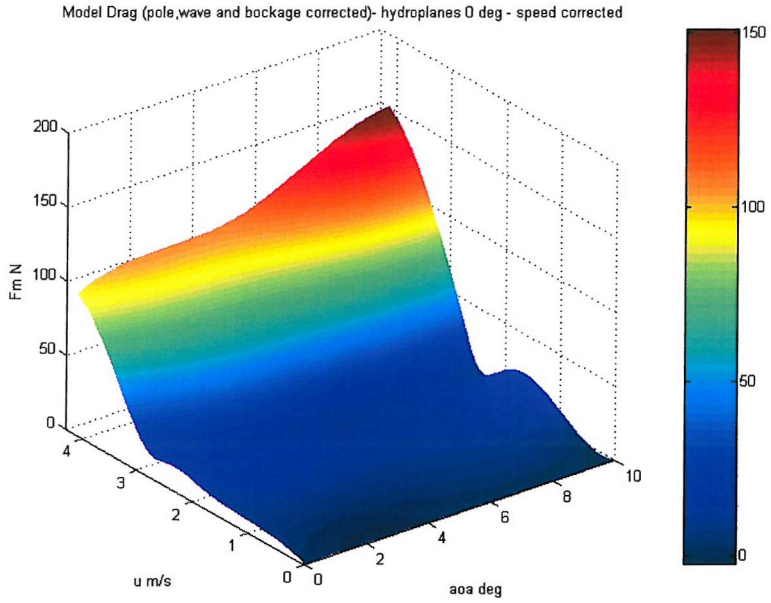

Figure 2.4.31 Open water model drag

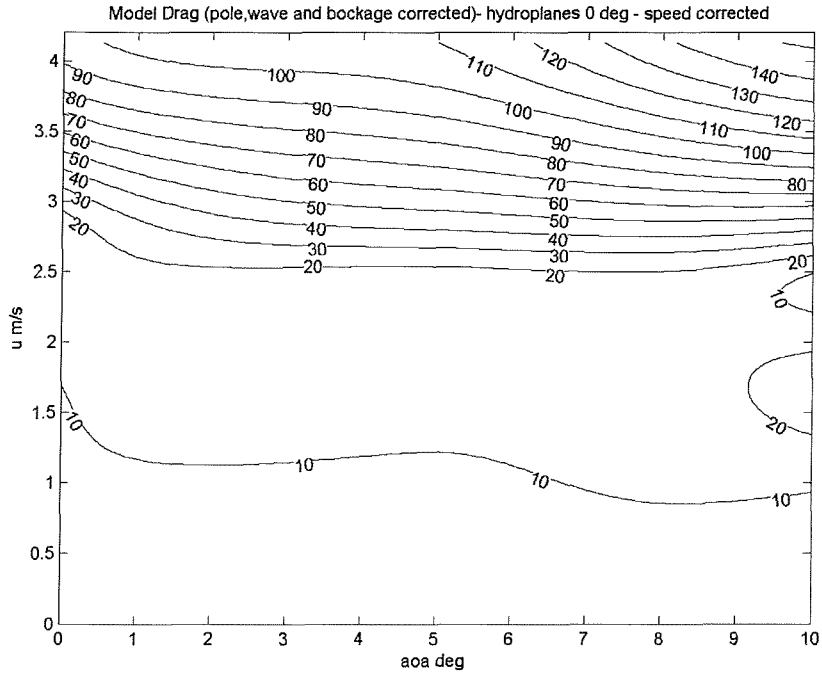

Figure 2.4.32 Model drag contour plot

2.4.7 Drag of the Full-scale vehicle

A further Matlab script has been produced to scale the results from the model to full-scale (Annex 2.7.4). The results from the model are transformed to non-dimensional form to produce the drag coefficient (based on $V^{2/3}$) for that shape of body as a function of angle-of-attack and Reynolds number (Figure 2.4.33).

For added clarity, families of curves of C_d vs. R_e for a range of angles-of-attack, and C_d vs. angle-of-attack for a range of speeds are given in Figures 2.4.34 and 2.4.35 respectively. The dimensions of the full-scale vehicle, together with the properties of seawater (as compared to those of fresh water used in the experiment), may then be applied to the de-dimensioned data to produce estimates of the drag forces that would be experienced by the full-scale vehicle under operational conditions (Figures 2.4.36 and 37).

A contour plot is given in Figure 2.4.37.

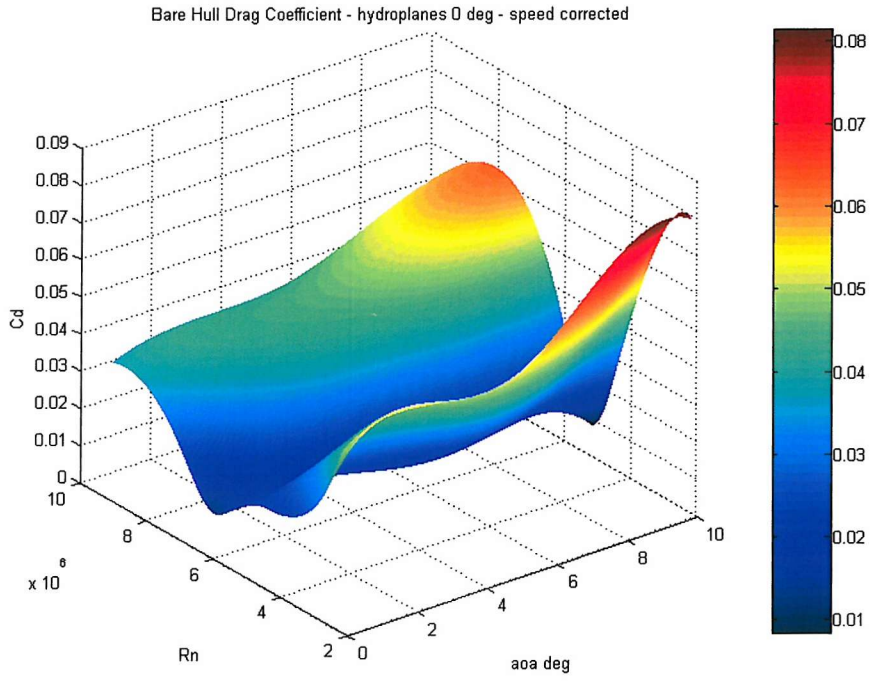

Figure 2.4.33 Drag coefficient as a function of Reynolds number and angle-of-attack

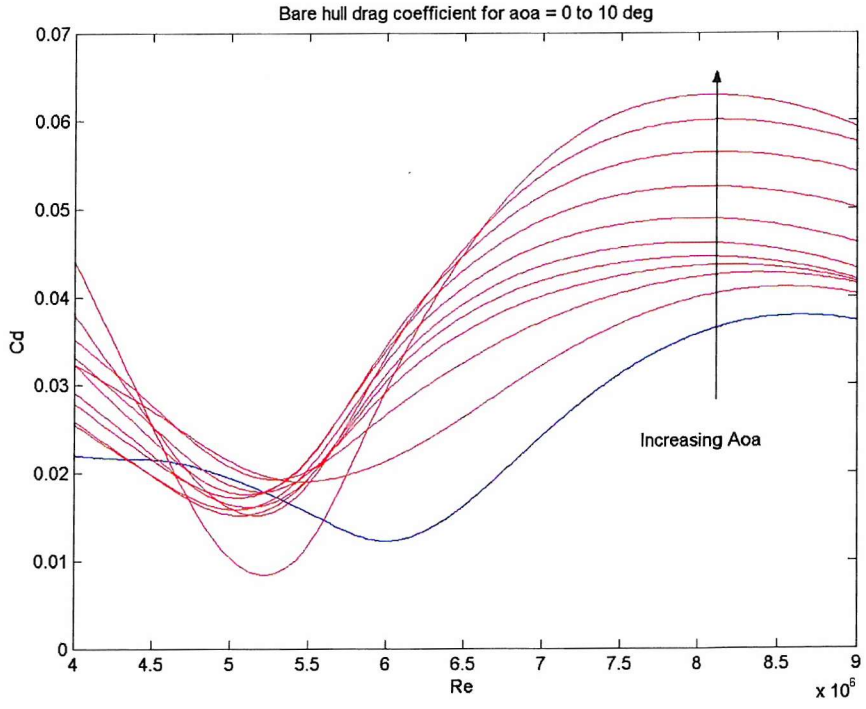

Figure 2.4.34 Drag coefficient as a function of Reynolds number for a range of angles-of-attack

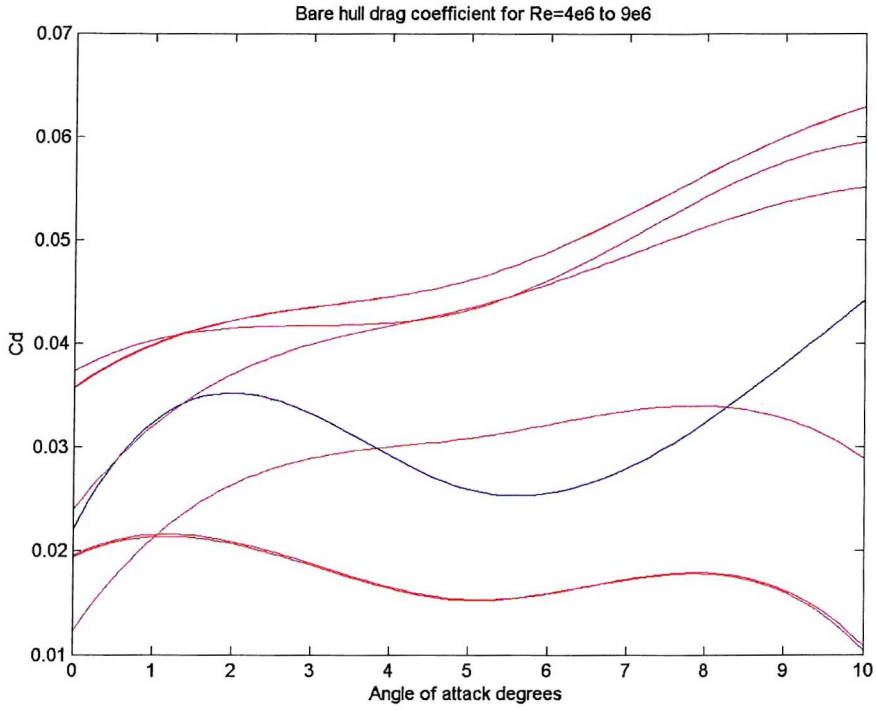

Figure 2.4.35 Drag coefficient as a function of angles-of-attack for a range of Reynolds number

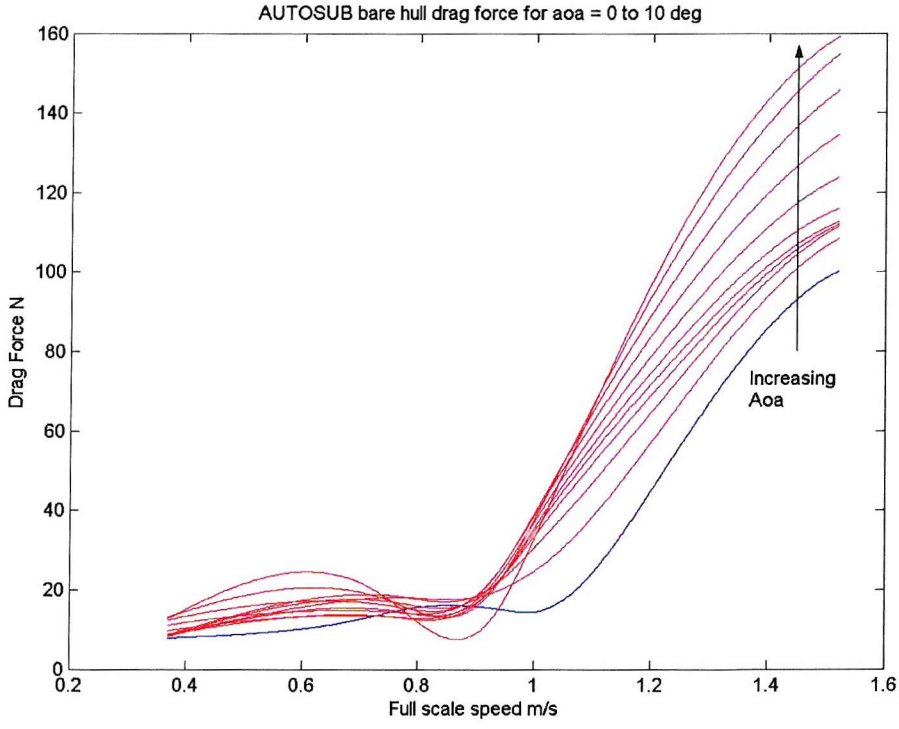

Figure 2.4.36 Full-scale vehicle drag

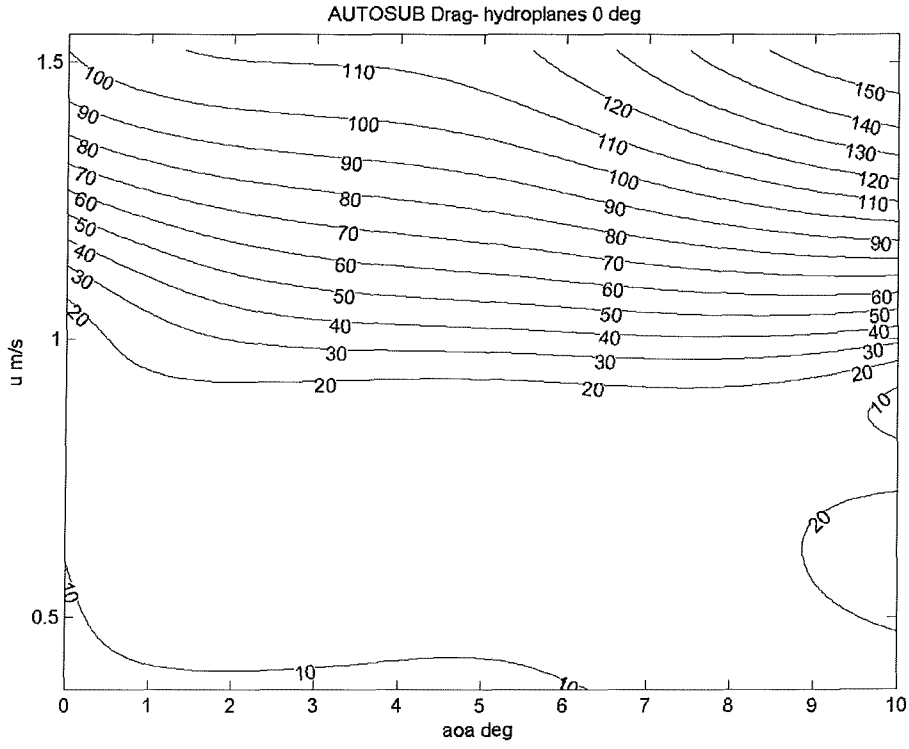

Figure 2.4.37 Full-scale vehicle drag contours

2.4.8 Reality check

No data on torpedo shaped vehicles was readily available, but data on vehicles of similar length to breadth ratio and travelling at similar R_e was found for Airships (Hoerner, 1965). The results obtained for AUTOSUB are compared with the airship drag data in Figure 2.4.38.

The drag characteristics for a torpedo-shaped body, as derived here, appear to be significantly different from that for a similar dimensioned, but cigar-shaped, airship. The drag characteristics of a low drag body optimised for a Reynolds number of $5x10^6$ (Osse, 1998) indicates a rapid rise in Cd in the region of $R_e = 10^7$, similar to that observed here. Nevertheless, an investigation was undertaken into the effect of possible inaccuracies resulting from the method described above to confirm the reality of the derived drag curve. The Matlab script at (Fallows, 2005) was written for this purpose.

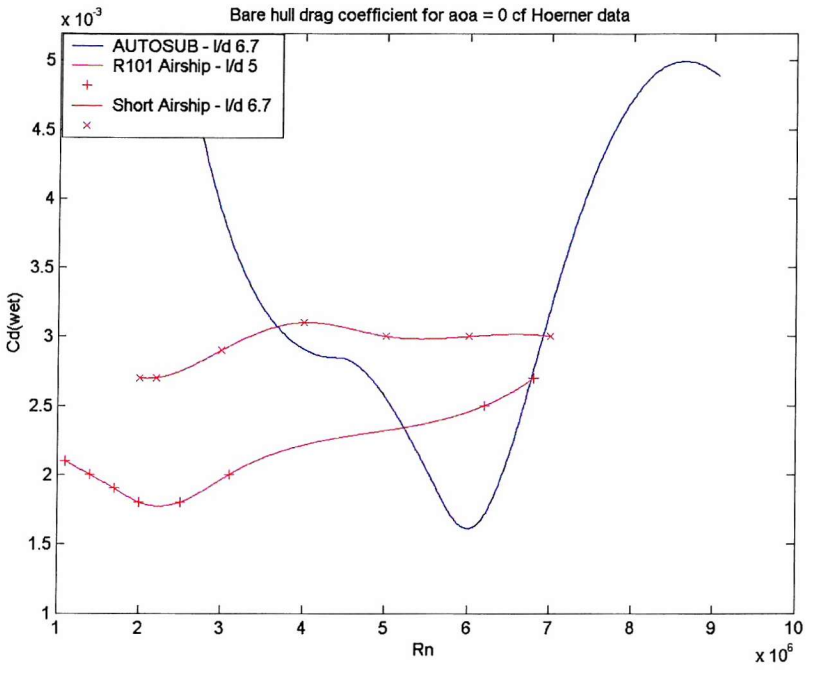

Figure 2.4.38 AUTOSUB drag coefficient compared with that of airships of similar shape

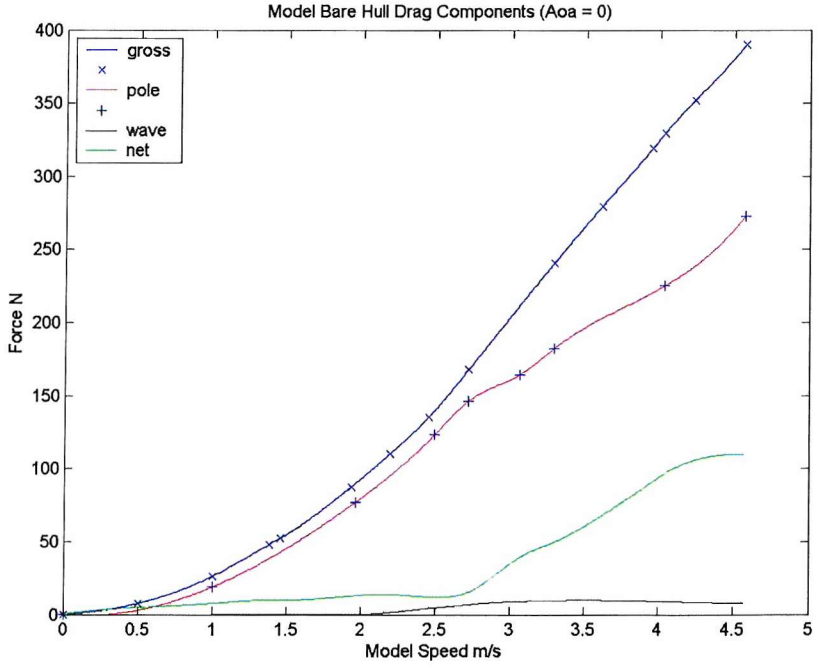

Figure 2.4.39 Components of the total measured drag force signal

To establish their relative importance, the various components of the total measured drag force were plotted on the same graph (Figure 2.4.39) and a separate graph was drawn to illustrate the effect of the blockage correction (Figure 2.4.40).

The consequence of the blockage effect is so small, that any error in its calculation is unlikely to explain the difference.

The graph at Figure 2.4.41, shows the cumulative effect of the components of the force block signal. This illustrates that the size of the drag caused by induced waves is also insignificant. But indicates that the drag of the model mounting posts is greater than that of the model itself and dominates the signal (Figure 2.4.42).

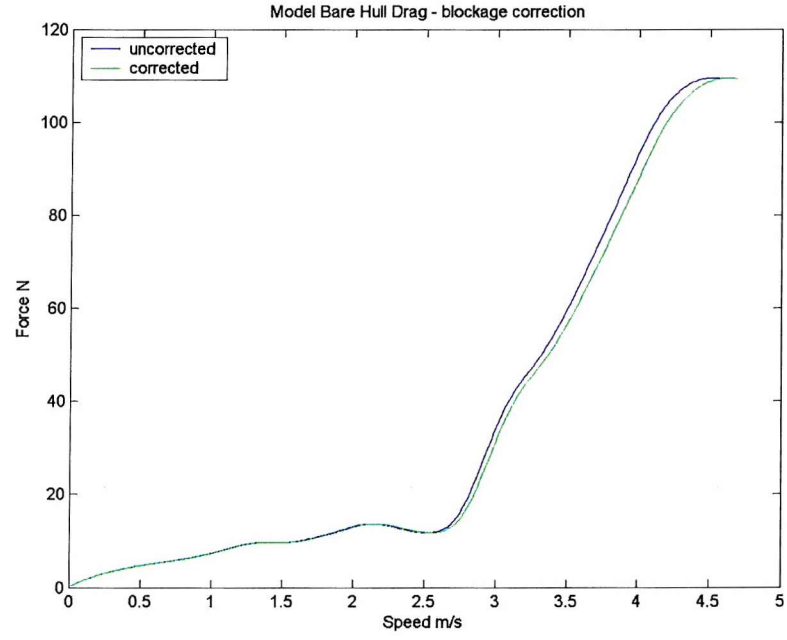

Figure 2.4.40 Consequences of blockage correction

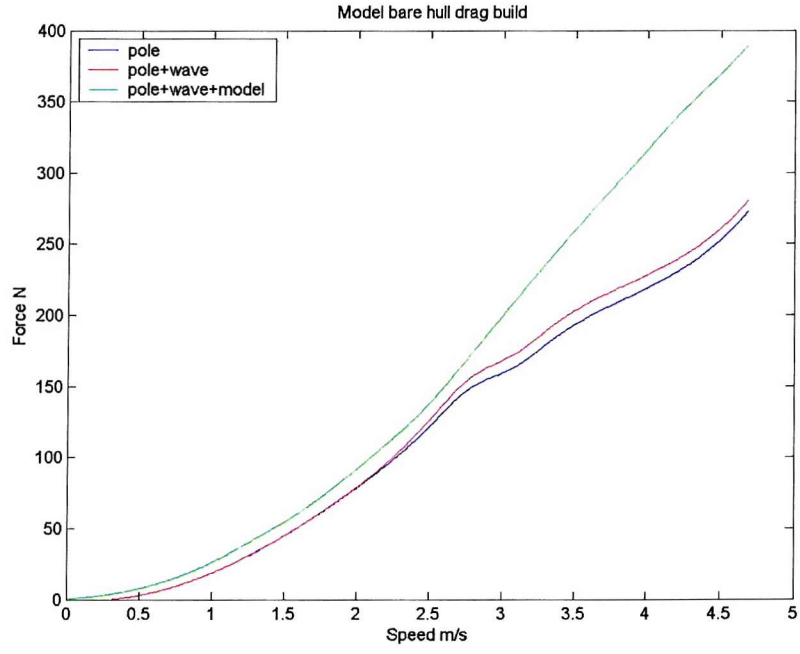

Figure 2.4.41 Build of drag force signal

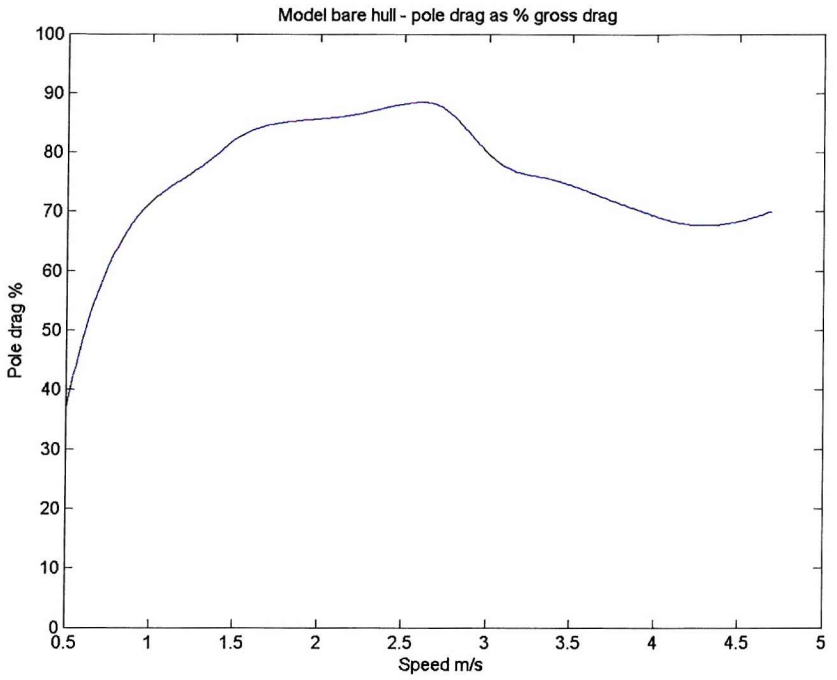

Figure 2.4.42 Pole drag as a percentage of the total drag signal

This observation led to additional measurements being made of the drag of the poles alone, to ensure that they were as well characterised as possible. As a consequence, it is considered unlikely that this is the cause of the difference.

A significant part of the data processing involves interpolation, so the implications of the method used was examined. Because the spline interpolation function requires full matrices, a significant number of data points are discarded. The richest data set exists for the base case of the bare hull at zero angle-of-attack. This set was, therefore, taken and used for a 2-d interpolation of drag as a function of speed, using all of the data available. Although some detail is missed in the 3-d interpolation, the close agreement in the results obtained by the two methods (Figure 2.4.43) indicates that inaccuracies in interpolation can be discarded as the reason for the difference.

Finally, the results obtained from the scale-model laboratory experiments were compared with those obtained from at-sea trials on the full-scale vehicle (described in part 3) (Figure 2.4.44). The shapes of the curves match extremely well. The higher drag of the full-scale vehicle at sea may be explained by the fact that:

- Its angle-of-attack is of the order of 2° at high speeds and much greater than this at low speeds, as the vehicle attempts to maintain depth. 2° adds ~10 N to drag across the speed range and 7° adds 30 N at 1.4 m/s.
- A similar response occurs for the hydroplane angle.
- The full-scale vehicle has a number of appendages not present on the scale-model. The added drag of these is discussed in chapters 2.7 to 2.9.

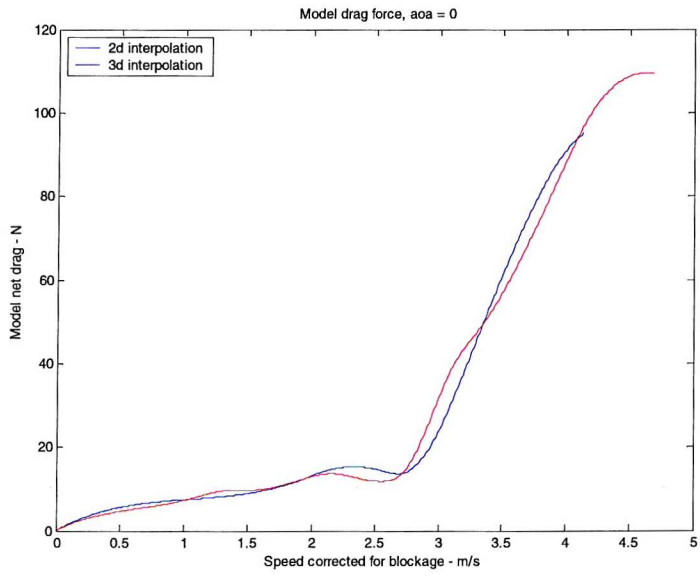

Figure 2.4.43 Comparison of 2-d and 3-d models

A full reconciliation of the curves is given in chapter 3.7.

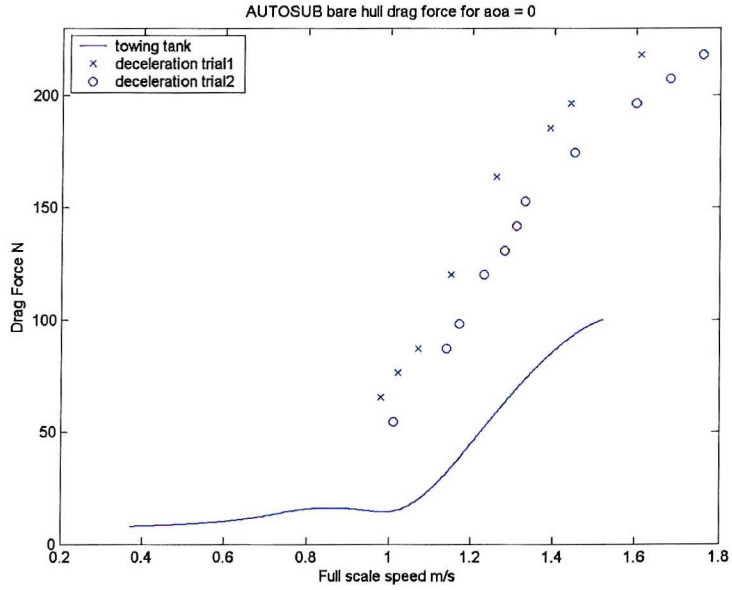

Figure 2.4.44 Comparison of experimental and trial results

2.4.9 Conclusions

The following conclusions are derived from this chapter:

- The model support posts generated the major part of the force block signals, thereby swamping the model signature and degrading the overall signal to noise ratio. To overcome this, significant effort had to be diverted to characterising the posts so that their effect could be reliably subtracted.
- Running a large-scale model at a Reynolds number equivalent to the full-scale vehicle generates considerable waves from the model mounting posts and makes a small but discernable difference to total drag.
- The wave cut method of determining the wave drag of the model is unsuited to conditions where large and breaking waves are created.
- There is good agreement between the values for wave-induced drag determined from measurement of change in drag with depth and those obtained from Thin Ship Theory.
- Conducting experiments at a range of Reynolds number equivalent to those of the full-scale vehicles implies running at high Froude number and, for a towing tank, high depth Froude number. The normally accepted methods for calculating the effects of blockage do not apply at these high speeds.
- From a comparison of a number of methods of determining the effects of blockage, that proposed by Tamara appears to be most easily adapted for use with fully-submerged models, but this had to be adapted to cater for the high Froude numbers encountered in these experiments.
- The drag characteristics of a torpedo shaped body differ significantly from those of an airship cigar-shaped body of similar length to breadth ratio travelling at similar Reynolds number.
- There is good agreement obtained on the drag characteristics obtained for AUTOSUB from laboratory experiments on a scale-model and those obtained from trials on the full-scale vehicle at sea. The differences between the two may be explained in terms of angle-of-attack, hydroplane angle and appendage effects.
- Since two different methods for determining the drag characteristics (the laboratory method by direct measurement of drag force, and the sea trials

method by inference from dynamic behaviour), there is considerable confidence in the results.

- Confidence in the laboratory method and results is reinforced by an investigation into possible causes of error. This indicated that the only major potential source of error would be the large mounting pole drag effect swamping the desired signal. Investing additional effort in characterising the poles ameliorated this.

Chapter 2.5

MEASUREMENT OF ADDED MASS

2.5.1 Introduction

A simple process for deriving the drag of the AUV directly from the performance of the full-scale vehicle at sea is described in part 3, chapter 3.3. An essential component of this is an accurate assessment of the added mass of the vehicle. This may be derived from measurements made on the scale-model.

2.5.2 Theory

When the model is accelerated along its axis the applied force must overcome inertial forces, drag forces and, if the vehicle penetrates or is sufficiently near to the free surface, a force resulting from wave-making. Inertial forces are proportional to acceleration, and drag and wave forces to velocity. The total forces acting upon the body, as measured by the force blocks, may, therefore, be expressed as:

$$F_t = f_1(\frac{du}{dt}) + f_2(u) + c\,.$$

Knowledge of total 'steady' force as a function of 'steady' velocity has been derived in chapter 2.4 and so, provided that instantaneous velocity is known, $f_2(u) + c$ is known. Instantaneous velocity may be derived from knowledge of acceleration as a function of time, *a(t)*, since:

$$u(t) = \int (a(t))dt$$

Hence, $f_1(\frac{du}{dt})$ may be determined from knowledge of F_t, *a(t)* and $f_2(u) + c$.

Now:

$$f_1(\frac{du}{dt}) = m_t(\frac{du}{dt})\,.$$

Thus, knowledge of acceleration will enable the total apparent mass, m_t, to be calculated.

The apparent mass comprises two components. The force required to accelerate a body in a vacuum, is directly proportional to its inertial mass. However, additional force is required to accelerate a body in fluid, since the fluid displaced by the passage of the body must be accelerated. This force is proportional to acceleration

and, therefore, has the dimension of mass. It is generally termed 'Added Mass'. Thus, for a model in a towing tank,

$$m_t = m + m_a .$$

Where m is the inertial mass, i.e. the mass of the apparatus below the force blocks, and can be measured. Thus, measurement of force and acceleration as a function of time will enable added mass, m_a, to be derived. A period of constant acceleration makes the calculations less arduous.

2.5.3 Acceleration measurement

To measure acceleration, an accelerometer was attached to the towing tank carriage. The instrument was less than ideal in so far as its range was of the order of 10 g, whereas the maximum acceleration of the carriage was expected to be of the order of 1 m/s^2 (approximately 0.1g) and no suitable amplifier was available to improve its resolution. As a consequence, the maximum discrimination obtained was of the order of 0.1 m/s^2 and the signal (Figure 2.5.1) was found to be noisy. Nevertheless, it can clearly be seen that the initial acceleration of the carriage is remarkably linear and was found to be constant between runs. As a consequence this time interval was selected for further processing.

Force as a function of time is given in Figure 2.5.2, with that over the period of constant acceleration marked.

Total force as a function of acceleration is shown in Figure 2.5.3. The constant acceleration portion is shown in Figure 2.5.4 during which the mean acceleration is 0.92 m/s^2.

Force during the period of constant acceleration is shown at Figure 2.5.5, with linear and quadratic terms fitted to the data.

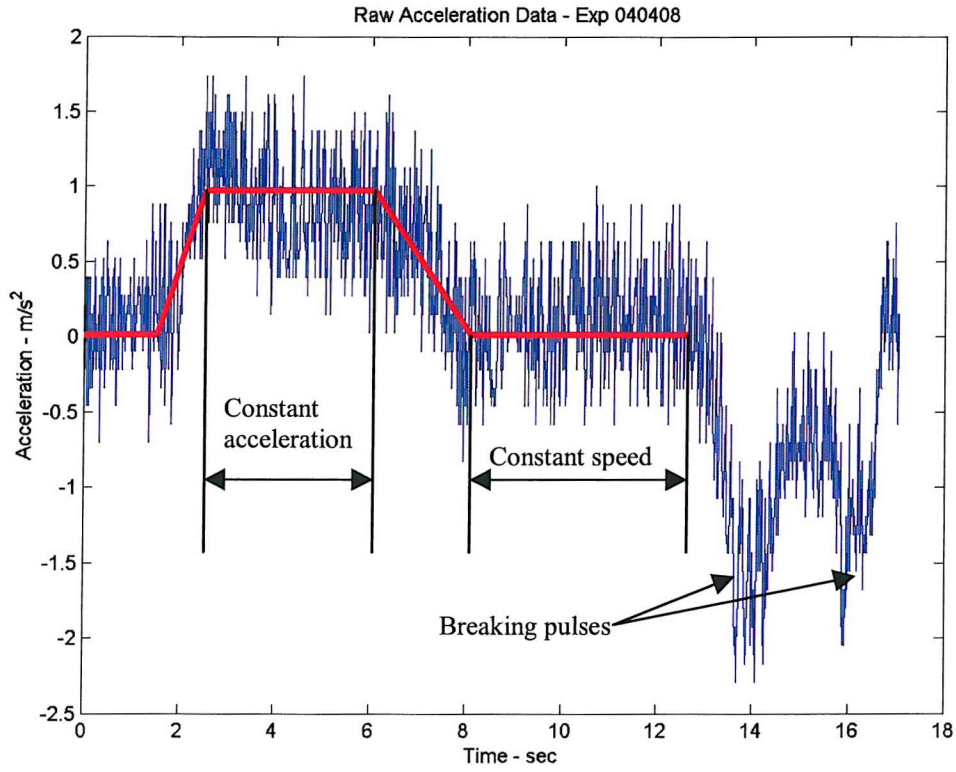

Figure 2.5.1 Raw acceleration data

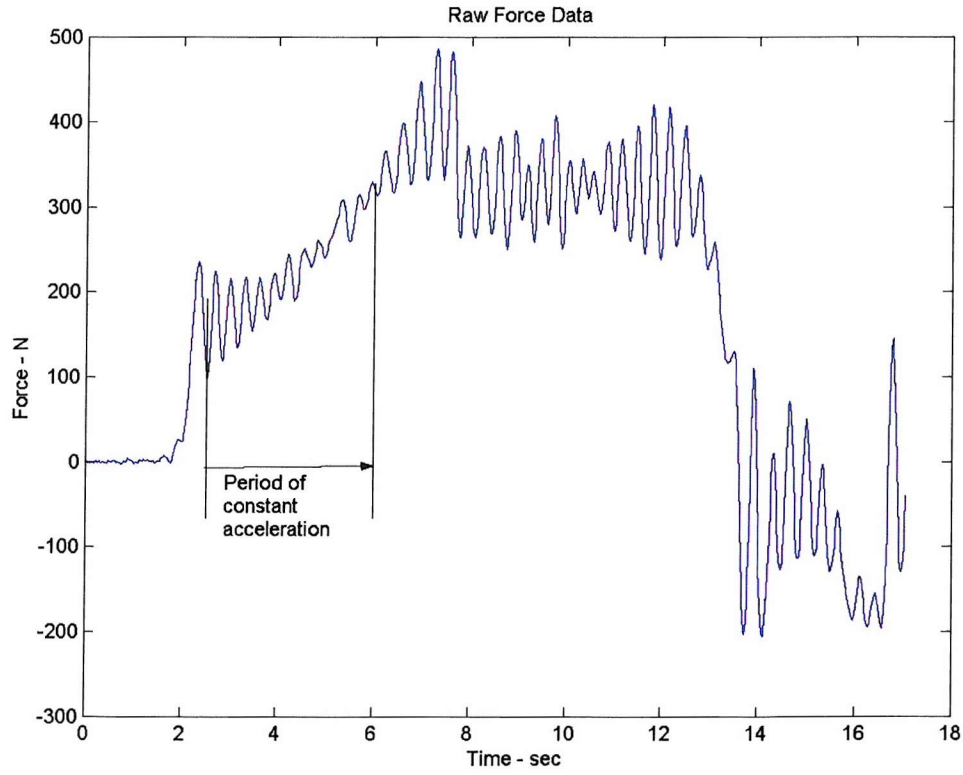

Figure 2.5.2 Raw Force data

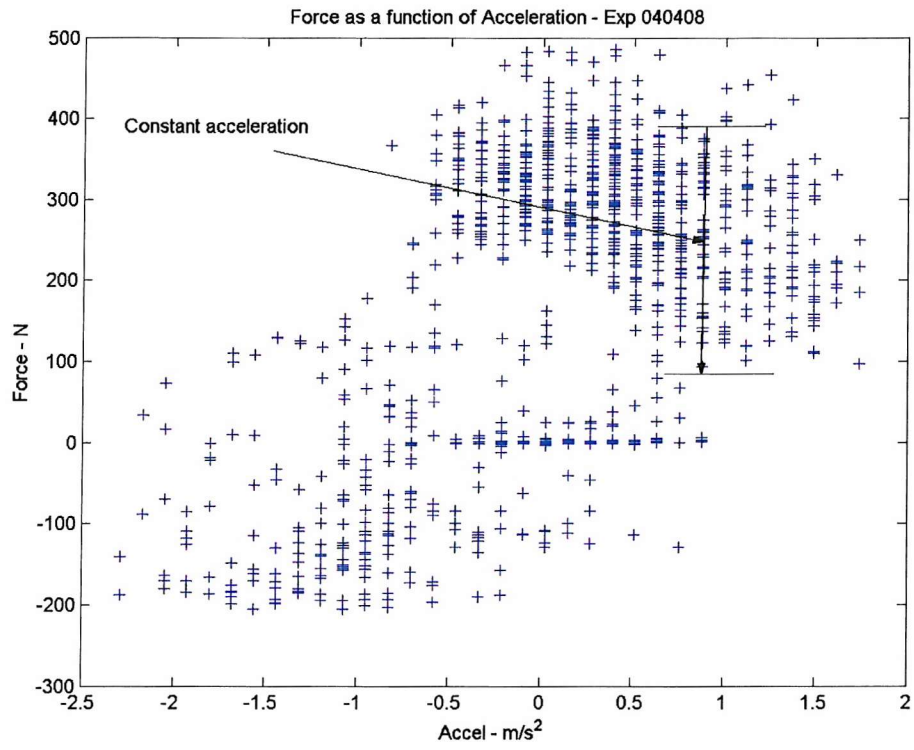

Figure 2.5.3 Force as a function of acceleration

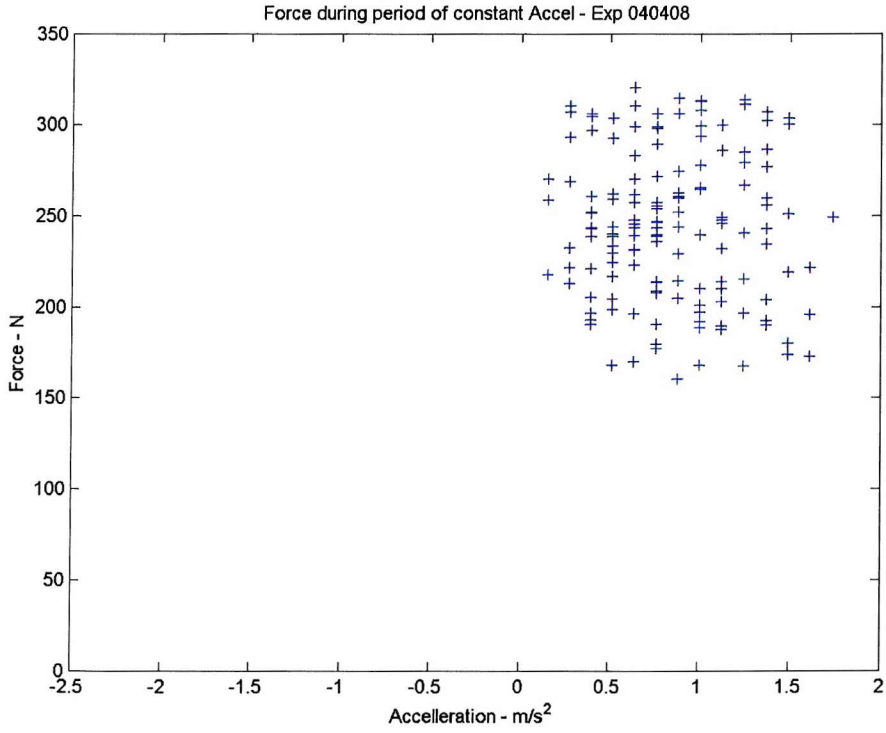

Figure 2.5.4 Force during period of constant acceleration

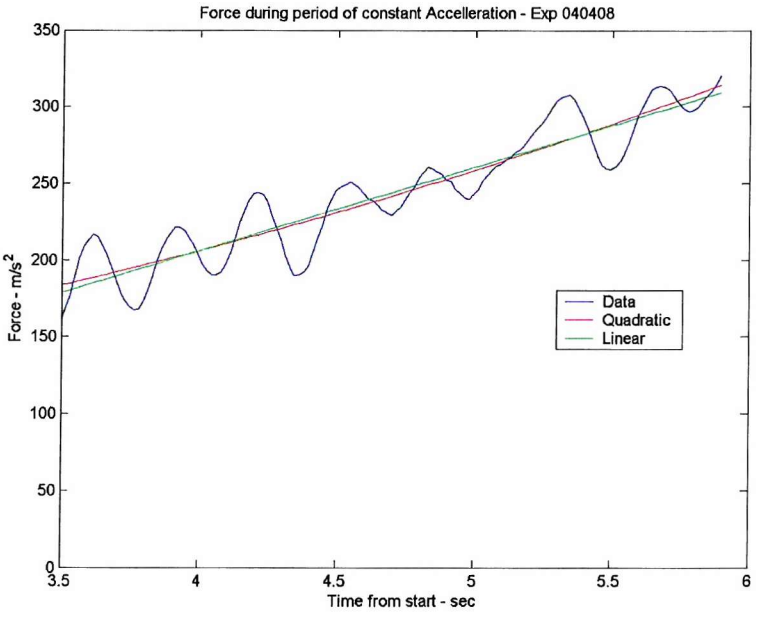

Figure 2.5.5 Force during constant acceleration

Velocity is derived from acceleration using simple numeric integration:

$$u(n) = u(n-1) + (\frac{a(n) + a(n-1)}{2})(t(n) - t(n-1))$$

The effectiveness of this approach is demonstrated by Figure 2.5.6, which confirms that velocity increases linearly over the period of constant acceleration.

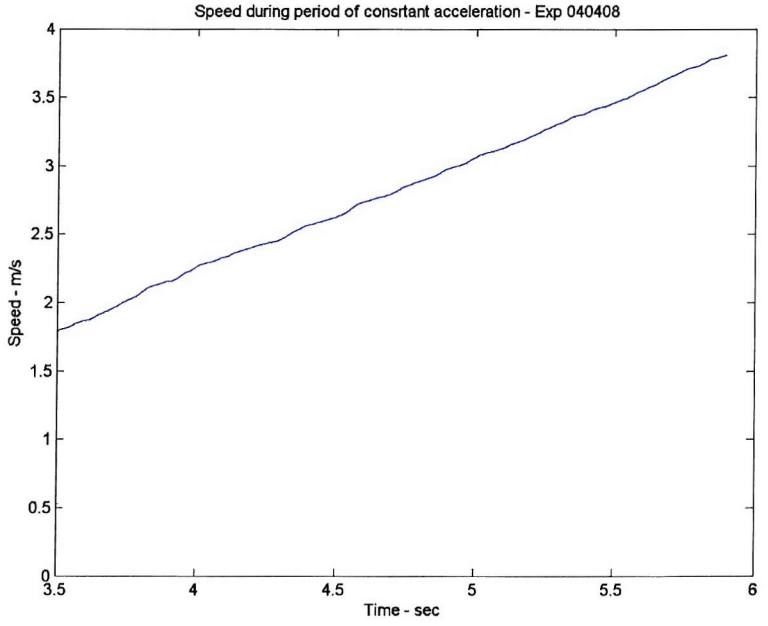

Figure 2.5.6 Speed derived from acceleration data for period of constant acceleration

Speed as a function of time during the period of constant acceleration may be derived from Figure 2.5.6. The relationship between the drag force of the model and speed is known from the analysis described in chapter 2.4 to be:

$$F_d(u) = 8.46u^2 + 6.65u$$

Thus, drag force as a function of time may be established. This can be subtracted from total force to reveal the total inertial force, $F_i(t)$, as in Figure 2.5.7. The inertial force is demonstrated to be reassuringly constant with time.

Dividing $F_i(t)$ by $a(t)$ gives $m(t)$, which, for experiment 040408a5 is 185 kg. The equipment below the force block comprises the model, the support posts and part of the dynamometer. Together these weigh 116 kg. Subtracting this from the apparent mass reveals an added mass for the AUTOSUB model hull of 69 kg. When scaled by volume, this gives an estimate of the added mass of the bare hull of the full scale vehicle of 1547 kg.

The Matlab script, written to undertake the above analysis, is given at (Fallows, 2005) and was used for the analyses in the subsequent reality checks.

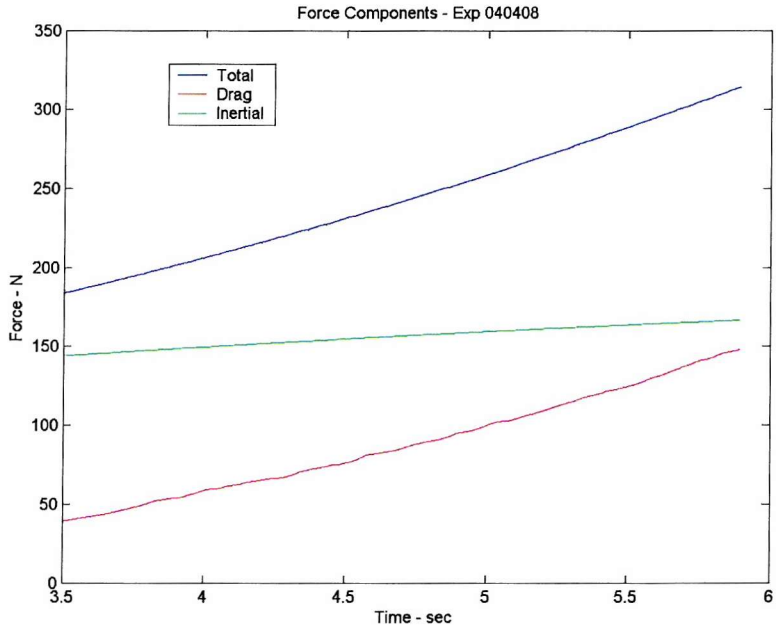

Figure 2.5.7 Components of force during constant acceleration

2.5.4 Reality check

Two checks were undertaken to establish the method and three more to determine the specific value of added mass for AUTOSUB. The two to check the method were as follows:

1. The method was used with the mounting poles travelling in air to assess the accuracy with which the acceleration data could be interpreted in terms of the mass of the poles.
2. The process described in Sections 2.5.2 to 2.5.4 was repeated for the mounting poles alone to determine their added mass.

The three checks on the value for added mass for the AUTOSUB hull-form were:

1. Comparison with theoretical predictions of added mass made for a similar shape.
2. Repeating the experiment described above twice more to determine repeatability.
3. Comparison with results from other vehicles.

2.5.4.1 Weighing the mounting poles

The mounting poles, with no model attached, were fully retracted so that they travelled above the surface of the water. The carriage was run down the tank and acceleration and force data recorded as before. The force record is shown in Figure 2.5.8, with the only force felt by the poles being during periods of acceleration and deceleration at the beginning and end of the run.

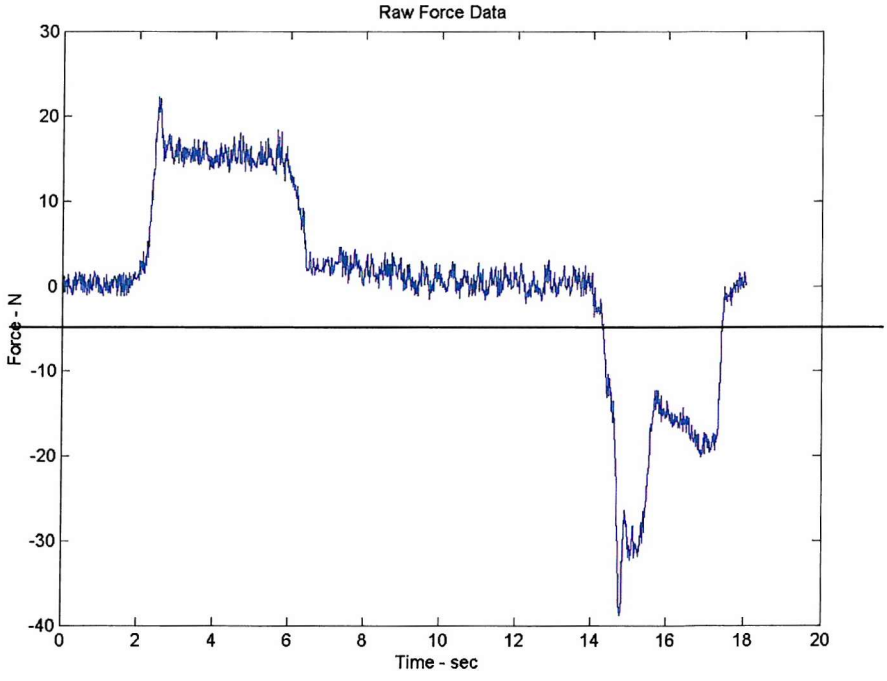

Figure 2.5.8 Force exerted on two mounting poles run clear of the water

Analysis using the same Matlab script as that used above (Fallows, 2005) revealed the force over the period of constant acceleration to be as illustrated in Figure 2.5.9. Acceleration during this period was 0.75 m/s^2, resulting in a net mass of 20.4 kg. This compares favourably with the weighed value of 19.9 kg, Thus, giving confidence in the method.

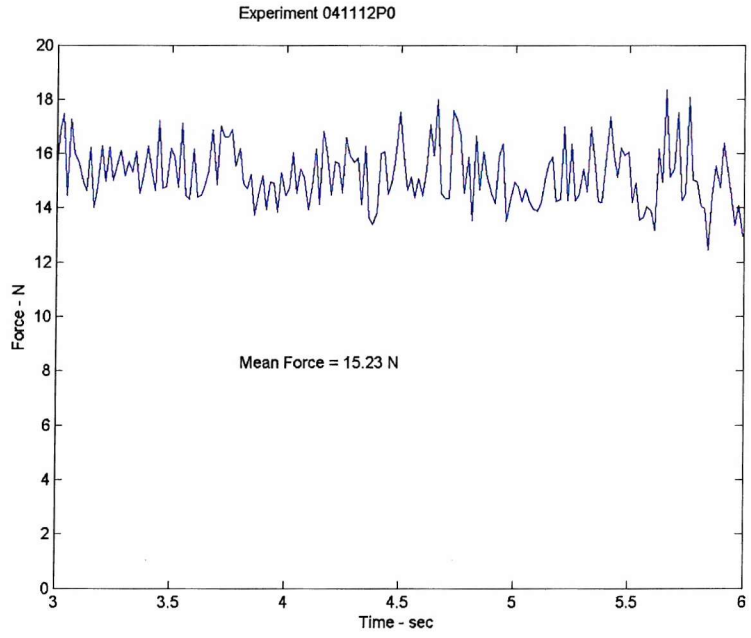

Figure 2.5.9 Net force on two mounting poles during period of constant acceleration

2.5.4.2 Added mass of the mounting poles

An experiment was run whereby acceleration and force data was collected for two poles run down the tank at the same immersion depth as that required for full immersion of the model.

Analysis of the data collected from this experiment, resulted in an apparent inertial mass of 22.5 kg, resulting in an added mass of 2.9 kg.

(Bishop and Price, 1979), using strip theory, indicate that the added mass/unit length of a rod of circular cross section is given by:

$$m_a = \frac{\rho \pi D^2}{4}.$$

For two rods of diameter, D = 3 cm in fresh water of density, ρ = 1000 kg/m^3, each immersed to a depth of 0.515 m:

$$m_a = 0.728\ kg$$

Because of the coarse nature of the acceleration data, only an order of magnitude estimate of added mass on this basis is possible. It is, therefore, considered that these estimates are in reasonable agreement.

2.5.4.3 Theoretical predictions

The AUTOSUB hull-form approximates to a prolate spheroid. Bishop and Price indicate that for this shape, for surge acceleration (i.e. in the direction of the principal axis), the added mass of a prolate spheroid is given by:

$$m_a = \frac{4}{3}\pi\rho ab^2 m_x$$

where a is the radius along the major axis and b along the minor, and the factor m_x for the AUTOSUB dimensions is given as 0.04 (Bishop and Price, 1979, p 138).

This gives an added mass of 122 kg, compared with the estimate from acceleration data of 1547 kg.

2.5.4.4 Confirmatory experiments

Three experiments were undertaken in total, one of which produced no meaningful results due to unsteady acceleration. The results are listed in Table 2.5.1. Added mass scales with volume and values are given both for those derived directly for the scale-model and the equivalent added mass of the full-scale vehicle.

Experiment Reference Number	Added Mass	
	Model scale kg	Full scale kg
040407a5	-	-
040408a5	69	1547
040409a5	89	1995

Table 2.5.1 Added mass from three experiments

2.5.4.5 Comparison with results from other vehicles

An experiment to measure the added mass of the full-scale ABE vehicle in a number of configurations is reported by (Kinsey, 1998). He accelerates the vehicle by means of a weight attached to the vehicle by a towline and pulley. The vehicle has a Cd (based on $V^{2/3}$) of between 0.31 and 0.54, depending on the configuration and he reports an added mass of between 800 and 1500 kg. ABE has a significantly different

shape to that of AUTOSUB, comprising three bodies connected by an open framework, but it is of comparable size.

2.5.5 Conclusions

Knowledge of the vehicle's added mass is required so that the drag characteristics of the full-scale vehicle may be determined at sea, using the deceleration method described in part 3. It was hypothesised that the value of this parameter could be determined at low cost by taking acceleration measurements during the scale-model towing tank experiments. The method, based on determining the apparent total inertial mass and subtracting the measured mass, is shown to be valid by the results from the experiments on the mounting poles.

Reasonably consistent results for the added mass of the AUTOSUB scale-model were obtained which indicate that it is of the order of 80 kg. When scaled to full-scale, this produces an added mass of the order of 1750 kg. This is far in excess of the 120 kg derived from theory for an idealised shape of an oblate spheroid, but is comparable to results obtained for another AUV, albeit one of significantly different shape. It is, therefore, concluded that the added mass of an oblate spheroid does not provide a reasonable approximation to that of the AUV.

The scaling factor between the added mass of the model and that of the full-scale vehicle is very large (22.5) because it is dependent on the ratio of their volumes. Thus, a small error in measurement of acceleration may result in a large error in added mass. The accelerometer used in this experiment was only capable of measuring to an accuracy of 0.1 g and produced a very noisy signal. Additionally, although the acceleration of the carriage is reasonably linear for 1 or 2 seconds, it is not absolutely so. This provides further scope for error.

It is, therefore, concluded that the method is sound and has provided an order of magnitude estimate of the added mass of the vehicle. However, to improve the accuracy of the results that may be obtainable from the trial described in part 3, a tailor-made experiment should be conducted. Ideally this should be based on the full-scale vehicle, and have tailored instrumentation.

Chapter 2.6

Method for the Analysis of Data Illustrated by Analysis of the Experiment to Determine the Drag of Sets of Appendages

2.6.1 Introduction

Having pre-processed the data to remove the effects of ADC anomalies and calibration drift and having determined the drag of the bare hull as a function of speed, angle-of-attack and hydroplane angle, the remaining data may now be analysed to determine the additional drag caused by the appendages. The remainder of this part of the thesis describes the information derived from the results and uses this information to derive more general conclusions.

Before moving on to these more general matters, this chapter describes the method of analysis. An example of one particular experiment is used. The objective of the experiment is described followed by a description of the experiment itself. The effects of each parameter on the output are derived together with their statistical significance. Predictive equations are derived from the quantified effects. The accuracy of these equations is determined by comparing the results obtained from the equations with measurements made in the laboratory. Finally the equations are used to predict the effect on the full-scale vehicle of the sets of appendages across a range of conditions.

2.6.2 The Experiment

The experiment chosen to demonstrate the method of analysis is that to determine the effect on drag of a series of sets of appendages. As described in chapter 1.7, the hull-form of the AUV under discussion changes from mission to mission dependent upon the fitted equipment and the condition of the hull. The variations may be described in terms of additions to the bare hull, and these in turn may be grouped into baseline items, i.e. those that appear on most missions, payload items, those specific to the mission in hand, and 'damage', changes to the hull resulting from in-

service use. Sets of these appendages were chosen to provide representative samples of those that appear on real missions. The objective of this experiment is to indicate what degree of additional drag might derive from each of these sources, both individually and in combinations, across the normal operating range of speed and angle-of-attack.

The baseline set comprises scale models of items as they exist on the real vehicle, viz.: an upward pointing Acoustic Doppler Current Profiler (ADCP) mounted aft; a downward pointing ADCP located frd; and two navigation beacons and two lifting lugs, all mounted on the ventral surface. The payload set comprises standard shapes chosen to represent additional sonars carried on the 'AUTOSUB under Ice' mission in the Antarctic in 2001, viz.: a medium size dome mounted frd and a large cylinder mounted just aft of the frd ADCP. Finally the damage set comprises 4 standard changes to hull shape, again representative of those experienced in the 'AUTOSUB under Ice' mission. This comprises: a 2 cm diameter hole in the nose of the model representative of the gap round the collision avoidance sonar; the frd and aft hatch covers being left open to represent the free flooding and drainage vents; and a medium size disc of P80 grade sandpaper representing grazing damage sustained during the mission. The sets of appendages are illustrated in Figures 2.6.1 to 2.6.5.

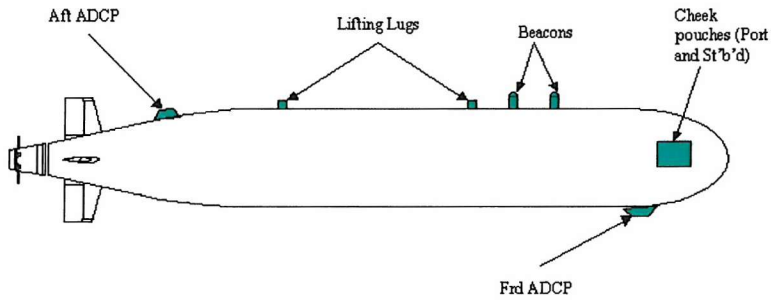

Figure 2.6.1 Baseline

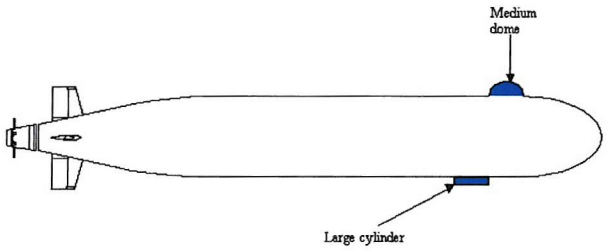

Figure 2.6.2 Payload

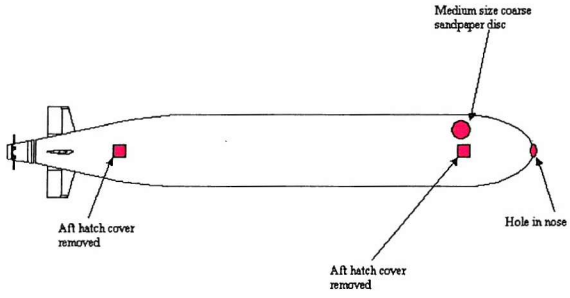

Figure 2.6.3 Damage

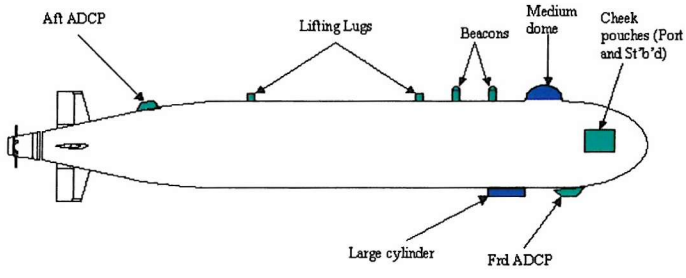

Figure 2.6.4 Baseline + Payload

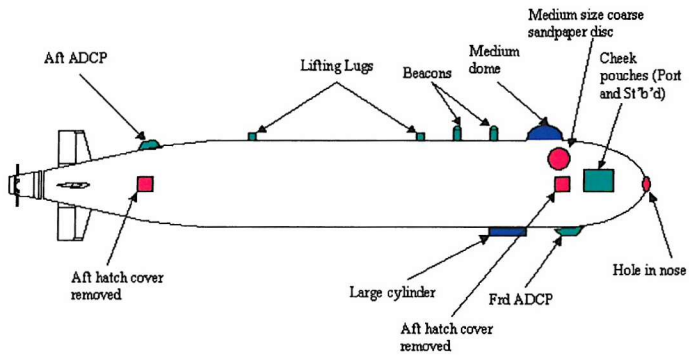

Figure 2.6.5 Baseline + Payload + Damage

Factors		Levels			
	1	2	3	4	5
Sets	B	P	D	B+P	B+P+D
Speed	660	775	875	924	966
Aoa	0	2	-5	7	-10

	2-Way Interactions		
	Set	Speed	Aoa
Set	*	*	
Speed		*	
Aoa			*

Notes:
B denotes set of Baseline Appendages.
P denotes set of Payload Appendages.
D denotes set of Damage Features.

Table 2.6.1 Factors levels and interactions required to measure the effect of sets of baseline, payload and damage appendages on drag performance

The factors and interactions to be explored in the experiment are listed in Table 2.6.1 Since it is expected that the relationship with speed and angle-of-attack is likely to be non-linear, five levels have been chosen so that any second order relationship may be reliable determined. The minimum size array that will allow three factors at five levels to be explored is the L_{25} array shown in Table 2.6.2. This allows

the effect of all three factors to be determined and also one two-level interaction. The interaction between speed and set is chosen as that most likely to be significant.

L25 ORTHOGONAL ARRAY

Column / Experiment No.	1	2	3	4	5	6
1	1	1	1	1	1	1
2	1	2	2	2	2	2
3	1	3	3	3	3	3
4	1	4	4	4	4	4
5	1	5	5	5	5	5
6	2	1	2	3	4	5
7	2	2	3	4	5	1
8	2	3	4	5	1	2
9	2	4	5	1	2	3
10	2	5	1	2	3	4
11	3	1	3	5	2	4
12	3	2	4	1	3	5
13	3	3	5	2	4	1
14	3	4	1	3	5	2
15	3	5	2	4	1	3
16	4	1	4	2	5	3
17	4	2	5	3	1	4
18	4	3	1	4	2	5
19	4	4	2	5	3	1
20	4	5	3	1	4	2
21	5	1	5	4	3	2
22	5	2	1	5	4	3
23	5	3	2	1	5	4
24	5	4	3	2	1	5
25	5	5	4	3	2	1

Table 2.6.2 L_{25} Orthogonal Array

The allocation of factors and interaction to columns of the array is shown in Table 2.6.3. Column 2 is the appropriate column for determining the interaction between set and speed, since it is the only column where level 1 equates to the two interacting columns being at the same level. Thus, for experiment 1, both factors 'set' and 'speed' are set at level 1, for experiment 6 they are both set at level 2, for experiment 11 they are both set at 3, and so on.

Column	1	2	3	4	5	6
Factors	Set	Set/Speed Interaction	Speed		Aoa	
Experiment No.						
1	1	1	1	1	1	1
2	1	2	2	2	2	2
3	1	3	3	3	3	3
4	1	4	4	4	4	4
5	1	5	5	5	5	5
6	2	1	2	3	4	5
7	2	2	3	4	5	1
8	2	3	4	5	1	2
9	2	4	5	1	2	3
10	2	5	1	2	3	4
11	3	1	3	5	2	4
12	3	2	4	1	3	5
13	3	3	5	2	4	1
14	3	4	1	3	5	2
15	3	5	2	4	1	3
16	4	1	4	2	5	3
17	4	2	5	3	1	4
18	4	3	1	4	2	5
19	4	4	2	5	3	1
20	4	5	3	1	4	2
21	5	1	5	4	3	2
22	5	2	1	5	4	3
23	5	3	2	1	5	4
24	5	4	3	2	1	5
25	5	5	4	3	2	1

Table 2.6.3 Allocation of factors and interaction to L_{25} Array

Allocation of levels to rows results in the final design of experiment given in Table 2.6.4, where the number in the speed column corresponds to towing tank carriage propulsion dial settings equivalent to full scale speeds of 1, 1.2, 1.4, 1.5 and 1.6 m/s.

Column	1	3	5
Factors	Set	Speed	Aoa
Experiment No.			
1	B	660	0
2	B	775	2
3	B	875	-5
4	B	924	7
5	B	966	-10
6	P	775	7
7	P	875	-10
8	P	924	0
9	P	966	2
10	P	660	-5
11	D	875	2
12	D	924	-5
13	D	966	7
14	D	660	-10
15	D	775	0
16	B+P	924	-10
17	B+P	966	0
18	B+P	660	2
19	B+P	775	-5
20	B+P	875	7
21	B+P+D	966	-5
22	B+P+D	660	7
23	B+P+D	775	-10
24	B+P+D	875	0
25	B+P+D	924	2

Table 2.6.4 Experiment to measure the effect of sets of baseline, payload and damage appendages on drag performance

The output of the experiment is a set of force block and speed measurements. The data was pre-processed, as described in (Fallows, 2005), to establish the net drag component for each run. The results are shown in Table 2.6.5.

File Name			Model	Angle of attack	Speed Dial	Carriage Speed	Net Force		Notes
			Type				Drag	Lift	
				Degrees		m/s	N	N	
1027	13	A5	Baseline set	0	660	2.718	-177.54	-0.59	
1027	14	A5	Baseline set	-2	775	3.261	-259.92	40.39	
1027	15	A5	Baseline set	-5	875	3.791	-352.68	117.72	Re-zero.
1027	16	A5	Baseline set	-7	924	4.068	-419.59	230.54	Slight clipping of force block 2.
1027	17	A5	Baseline set	-10	966	4.331	-512.57	331.80	All zeros reset for maximum readings but block 2 against mechanical limit for whole of run.
1028	01	A5	Baseline set	0	660	2.716	-178.62	-0.47	Stir up run 1N high.
1028	02	A5	Baseline + Payload sets	0	966	4.332	-448.91	9.61	
1028	03	A5	Baseline + Payload sets	-2	660	2.714	-209.01	37.47	
1028	04	A5	Baseline + Payload sets	-5	775	3.254	-315.10	102.44	
1028	05	A5	Baseline + Payload sets	-7	875	3.782	-438.05	258.27	
1028	06	A5	Baseline + Payload sets	-10	924	4.063	-545.66	332.68	Frd SF block off scale.
1028	07	A5	Baselin + Payload + Damage sets	0	875	3.789	-371.97	-7.25	
1028	08	A5	Baselin + Payload + Damage sets	-2	924	4.068	-432.42	68.31	
1028	09	A5	Baselin + Payload + Damage sets	-5	966	4.334	-509.41	169.82	
1028	10	A5	Baselin + Payload + Damage sets	-7	660	2.710	-245.23	122.81	
1028	11	A5	Baselin + Payload + Damage sets	-10	775	3.256	-372.48	264.19	
1028	12	A5	Damage set	0	775	3.262	-240.07	1.26	
1028	13	A5	Damage set	-2	875	3.796	-319.96	56.32	
1028	14	A5	Damage set	-5	924	4.076	-369.51	126.87	
1028	15	A5	Damage set	-7	966	4.333	-432.38	265.65	
1028	16	A5	Damage set	-10	660	2.713	-219.83	166.92	
1028	17	A5	Payload set	0	924	1.074	-381.96	4.89	
1028	18	A5	Payload set	-2	966	4.327	-443.68	88.76	
1028	19	A5	Payload set	-5	660	2.710	-214.80	64.92	
1028	20	A5	Payload set	-7	775	3.249	-328.14	166.75	
1028	21	A5	Payload set	-10	875	3.773	-464.52	320.22	
1029	01	A5	Payload set	0	924	4.066	-382.17	12.61	Stir up run.

Table 2.6.5 Results of 'Sets' Experiment

To reveal the additional drag resulting from the appendages it is necessary to subtract the bare hull drag from these results. A model of bare hull drag as a function of speed and angle-of-attack has been derived in chapter 2.4. The Matlab script at (Fallows, 2005) is used to calculate the gross bare hull drag for the range of conditions used in this experiment and enables the residual drag shown in Table 2.6.6 to be established.

Column	1	2		3		5				
Factors	Set	Set/Speed Interaction	Model Speed m/s		Aoa deg		Measured Drag Force N	Bare hull gross drag N	Additional drag N	% increase drag
Experiment No.										
			0	0	0	0				
1	1	1	1	2.718	1	0	177.5373	168.56	8.98	0.05
2	1	2	2	3.261	2	2	259.9247	244.68	15.24	0.06
3	1	3	3	3.791	3	5	352.675	328.88	23.80	0.07
4	1	4	4	4.068	4	7	419.5911	388.15	31.44	0.08
5	1	5	5	4.331	5	10	512.5665	449.25	63.32	0.14
6	2	1	2	3.249	4	7	328.1369	275.74	52.40	0.19
7	2	2	3	3.773	5	10	464.5203	376.71	87.81	0.23
8	2	3	4	4.066	1	0	382.1681	332.48	49.69	0.15
9	2	4	5	4.327	2	2	443.6784	369.81	73.87	0.20
10	2	5	1	2.710	3	5	214.7953	184.50	30.30	0.16
11	3	1	3	3.796	2	2	319.9593	314.08	5.88	0.02
12	3	2	4	4.076	3	5	369.5146	361.72	7.79	0.02
13	3	3	5	4.333	4	7	432.3772	418.36	14.02	0.03
14	3	4	1	2.713	5	10	219.8266	217.49	2.34	0.01
15	3	5	2	3.262	1	0	240.0712	236.69	3.39	0.01
16	4	1	4	4.063	5	10	545.6648	416.46	129.20	0.31
17	4	2	5	4.332	1	0	448.9147	355.28	93.63	0.26
18	4	3	1	2.714	2	2	209.0058	173.55	35.46	0.20
19	4	4	2	3.254	3	5	315.0981	257.57	57.53	0.22
20	4	5	3	3.782	4	7	438.0501	350.48	87.57	0.25
21	5	1	5	4.334	3	5	509.4051	384.90	124.51	0.32
22	5	2	1	2.710	4	7	245.23	199.96	45.27	0.23
23	5	3	2	3.256	5	10	372.4844	300.31	72.18	0.24
24	5	4	3	3.789	1	0	371.9655	302.47	69.49	0.23
25	5	5	4	4.068	2	2	432.4192	344.74	87.68	0.25
Mean									50.91	
sd									37.45023	

Table 2.6.6 Additional drag resulting from appendage sets

Now the mean effect of any particular level of any factor will be the mean of all of the results of the runs where that factor is set for that level. Thus, for factor, f, at level, l, the mean effect, E_{fl}, will be:

$$E_{fl} = \frac{\sum Fda_{fl}}{n_{fl}}$$

Where: Fda = additional drag force

n_{fl} = number of results for factor f at level l.

The net consequence of setting factor, f, at this level, l, will be to disturb the mean value of all levels for this factor by the difference between them, i.e. the contrast C_{fl} is:

$$C_{fl} = E_{fl} - \frac{\sum E_{fl}}{n_l}$$

where n_l = number of results at level l.

Factor								
	Set	Level	1	2	3	4	5	Mean
			damage	baseline	payload	b+p	b+p+d	
		Results	5.88	8.98	52.40	129.20	124.51	
			7.79	15.24	87.81	93.63	45.27	
			14.02	23.80	49.69	35.46	72.18	
			2.34	31.44	73.87	57.53	69.49	
			3.39	63.32	30.30	87.57	87.68	
								50.91
		Effect	6.68	28.56	58.81	80.68	79.83	50.91
		Contrast	-44.23	-22.36	7.90	29.77	28.91	
	Speed	Level	1	2	3	4	5	Mean
		Model m/s	2.718	3.261	3.791	4.068	4.331	
		Results	8.98	15.24	23.80	31.44	63.32	
			30.30	52.40	87.81	49.69	73.87	
			2.34	3.39	5.88	7.79	14.02	
			35.46	57.53	87.57	129.20	93.63	
			45.27	72.18	69.49	87.68	124.51	
								50.91
		Effect	24.47	40.15	54.91	61.16	73.87	50.91
		Contrast	-26.44	-10.76	4.00	10.25	22.96	
	Angle-of-attack	Level	1	2	3	4	5	Mean
			0	2	5	7	10	
		Results	8.98	15.24	23.80	31.44	63.32	
			49.69	73.87	30.30	52.40	87.81	
			3.39	5.88	7.79	14.02	2.34	
			93.63	35.46	57.53	87.57	129.20	
			69.49	87.68	124.51	45.27	72.18	
								50.91
		Effect	45.04	43.63	48.79	46.14	70.97	50.91
		Contrast	-5.87	-7.28	-2.13	-4.77	20.06	
	Set Interact	Level	1	2	3	4	5	Mean

	Results	8.98	15.24	23.80	31.44	63.32	
		52.40	87.81	49.69	73.87	30.30	
		5.88	7.79	14.02	2.34	.39	
		129.20	93.63	35.46	57.53	87.57	
		124.51	45.27	72.18	69.49	87.68	
							50.91
	Effect	64.19	49.95	39.03	46.93	54.45	50.91
	Contrast	13.28	-0.96	-11.88	-3.98	3.54	

Table 2.6.7 Effects and contrasts

The effects and contrasts for the factors under discussion are given in Table 2.6.7 and illustrated in Figure 2.6.6 (Note that for this table and figure the order of the levels has been changed to reflect increasing effect for presentational purposes. This has no effect on the value of the results).

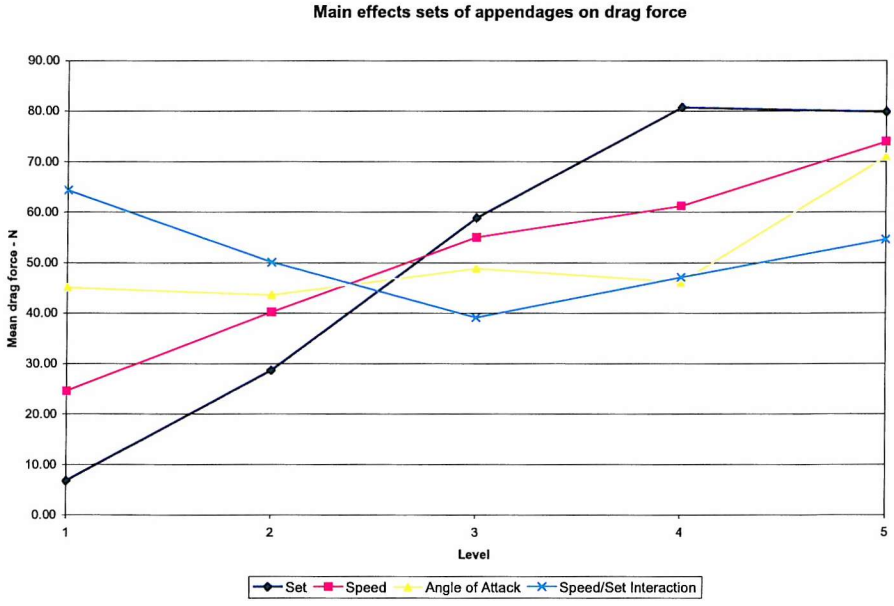

Figure 2.6.6 Main effects on the drag of sets of appendages

From this it can be seen that the factor with the greatest effect on drag is that of the set of appendages chosen, followed by the speed of the vehicle. The effect of angle-of-attack and the interaction between speed and set chosen appear to be less marked. However, any set of measurements is bound to involve random errors

resulting from uncontrolled variables. Additionally, the results of this experiment could be distorted by unexpected interactions between factors. Methods for determining whether the difference between means of sets of samples are statistically significant are discussed in (Fallows, 2005). In this case, the effects have been determined by taking the means of samples of measurements to determine the effect of each level within each factor. It is necessary, therefore, to test whether the differences between the means of the samples are significant in the context of the variation in the overall population from which the samples were drawn. An analysis of variance (anova) was, therefore, performed for each of the effects of each factor. An example of the analysis for factor 'set' is given in Table 2.6.8 and a summary of the analysis for all factors is given in Table 2.6.9.

Step 1 — Results, x

Sets	Level	1 damage	2 baseline	3 payload	4 b+p	5 b+p+d	Total pop
		5.88	8.98	52.40	129.20	124.51	321
		7.79	15.24	87.81	93.63	45.27	250
		14.02	23.80	49.69	35.46	72.18	195
		2.34	31.44	73.87	57.53	69.49	235
		3.39	63.32	30.30	87.57	87.68	272
	Total	33	143	294	403	399	1273
	mean	7	29	59	81	80	50.91
	var	21	450	501	1288	854	1403
	n	5	5	5	5	5	25
	Deg of free	4	4	4	4	4	24

Step 2 — Total pop sum of squares, (x-mean(X))^2

Level	1 damage	2 baseline	3 payload	4 b+p	5 b+p+d	Total pop
	2028	1758	2	6129	5417	15334
	1859	1272	1362	1825	32	6350
	1361	735	1	239	452	2789
	2359	379	527	44	345	3655
	2259	154	425	1344	1352	5533
Total	9866	4299	2317	9581	7598	33660

Step 3 — Between sample sum of squares, = (mean(x)-mean(X))^2

Level	1 damage	2 baseline	3 payload	4 b+p	5 b+p+d	Total pop
	1956	500	62	886	836	4240
	1956	500	62	886	836	4240
	1956	500	62	886	836	4240
	1956	500	62	886	836	4240
	1956	500	62	886	836	4240
Total	9781	2499	312	4430	4180	21202
mean						
var						
n				No of sample averages		5
Deg of freedom						4

Step 4 — x-mean x

Level	1 damage	2 baseline	3 payload	4 b+p	5 b+p+d	Total pop
	-1	-20	-6	49	45	66
	1	-13	29	13	-35	-5
	7	-5	-9	-45	-8	-59
	-4	3	15	-23	-10	-20
	-3	35	-29	7	8	18
Total	0	0	0	0	0	
mean						0

Step 5 — Within sample sum of squares, = |(x-mean x)^2|-mean(x-mean x)^2|

Level	1 damage	2 baseline	3 payload	4 b+p	5 b+p+d	Total pop
	1	383	41	2354	1997	4776
	1	177	841	168	1194	2381
	54	23	83	2045	59	2263
	19	8	227	536	107	896
	11	1208	813	47	62	2142
Total	85	1800	2005	5150	3418	12458
mean						
var						
n						
Deg of freedom						20

Step 6

Source of Variation	Sum of squares	Degrees of freedom	Variance estimate
between samples	21202	4	5301
within samples	12458	20	623
Total	33660	24	1403
F	From data		8.51
	From table	10%	2.25
		5%	2.87
		1%	4.43

Table 2.6.8 Example of analysis of variance

Factor	Set			Speed		
Source of Variation	Sum of squares	Degrees of freedom	Variance estimate	Sum of squares	Degrees of freedom	Variance estimate
between samples	21202	4	5301	21202	4	5301
within samples	12458	20	623	30757	20	1538
Total	33660	24	1403	51959	24	2165
F	From data		8.51	From data		3.45
	From table	10%	2.25	From table	10%	2.25
		5%	2.87		5%	2.87
		1%	4.43		1%	4.43
Factor	Angle of Attack			Speed/Set interaction		
Source of Variation	Sum of squares	Degrees of freedom	Variance estimate	Sum of squares	Degrees of freedom	Variance estimate
between samples	21202	4	5301	21202	4	5301
within samples	46426	20	2321	61622	20	3081
Total	67628	24	2818	82825	24	3451
F	From data		2.28	From data		1.72
	From table	10%	2.25	From table	10%	2.25
		5%	2.87		5%	2.87
		1%	4.43		1%	4.43

Table 2.6.9 Analysis of Variance of factors affecting the drag of appendage sets

It can be seen from Table 2.6.8 that that there is high confidence (>99%) that the type of set used affects drag and reasonable confidence (>90%) that both speed and angle-of-attack have significant effects. There is less confidence that any interaction between the set and speed is detectable by this experiment.

Now the result for any given run, will differ from the mean of all results by the difference of the effects of the significant factors, at the level set for each of these, from the mean effect for that factor. Thus, for any given run:

$$Fda = \overline{Fda} + \sum_{f=1}^{n_f} (E_{fl} - \overline{Fda}_f) \text{ : selected level } l$$

i.e.

$$Fda = (1 - n_f)\overline{Fda} + \sum_{f=1}^{n_f} E_{fl} \text{ : selected level } l.$$

Therefore the additional drag resulting from a set, s, being moved at speed, u, on a hull with angle-of-attack, α, is given by:

$$Fda(s,u,\alpha,us) = (1-4)\overline{Fda} + (E_s(s) + E_u(u) + E_\alpha(\alpha) + E_{us}(us))$$

with $\overline{Fda}$ derived as 50.9. (see Table 2.6.7) and $E(us)$) being the interaction between speed and appendage set.

Now the effect of any factor at a point other than those at which the effect has been measured may be predicted by interpolation or extrapolation. Since we have 5 levels for each factor it is possible to make a better estimate than straightforward linear interpolation should that be warranted. Consider each factor in turn. The factor 'set' has only integer significance. The concept of 'half of a set' is meaningless in the context of the definition of set as used here. The effect of each of the sets is shown in Figure 2.6.7 (using the effect data in Table 2.6.7) with level 1 corresponding to damage alone, level 2 to the baseline set, level 3 to payload, level 4 to baseline and payload and level 5 to all three.

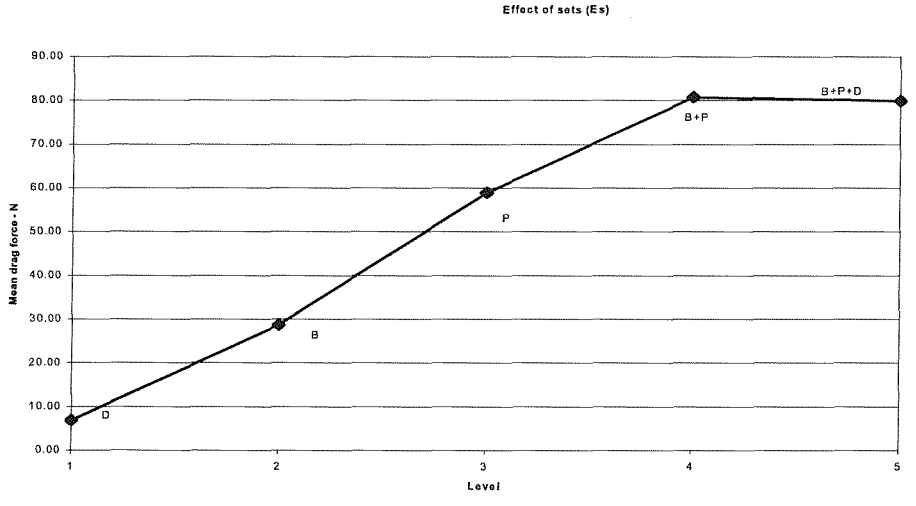

Figure 2.6.7 Effect of sets

As can be seen the damage set has a comparatively small effect with the payload and baseline sets having larger and roughly equal effects. When both payload and baseline are present the net effect is not quite equal to the sum of the individual effects, and adding damage to these two produces no further increase in drag. There is thus, a strong indication that the sets interact.

The effect of speed is shown in Figure 2.6.8, again using the 'Effect' data for 'speed' in Table 2.6.7.

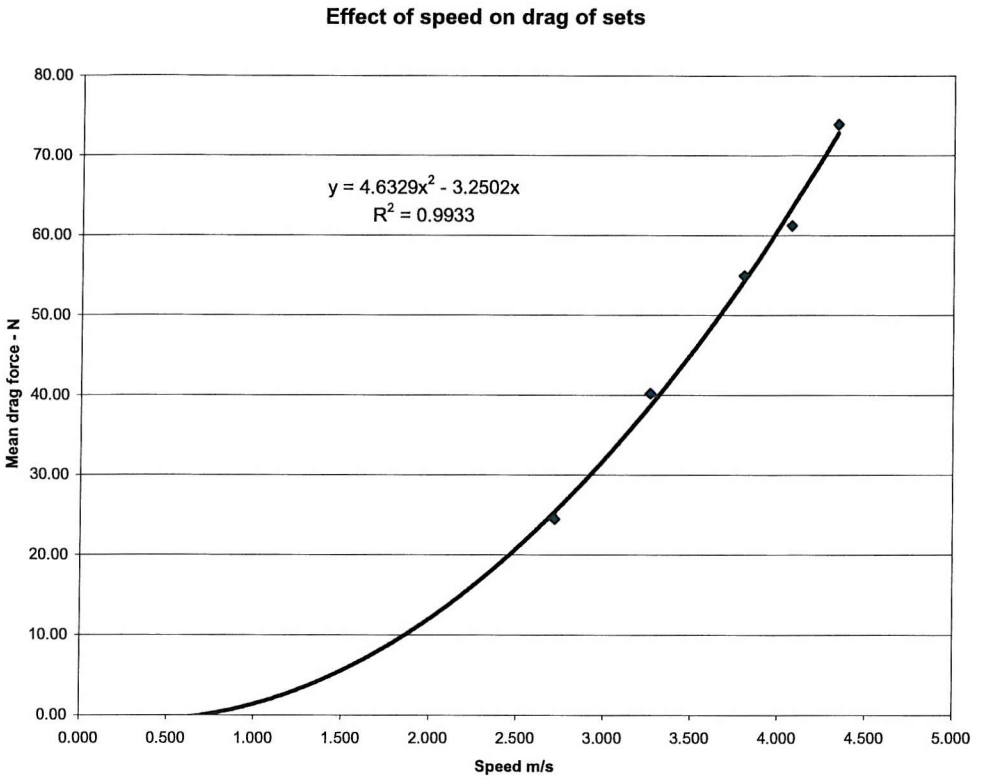

Figure 2.6.8 The effect of speed on the additional drag of sets of appendages

Speed and force are continuous variables and so interpolation and extrapolation has meaning. As expected, a square law fits the data well ($R^2 > 0.99$) and the effect on additional drag is of the form:

$$E_u(u) = 4.6\,u^2 - 3.25\,u\,.$$

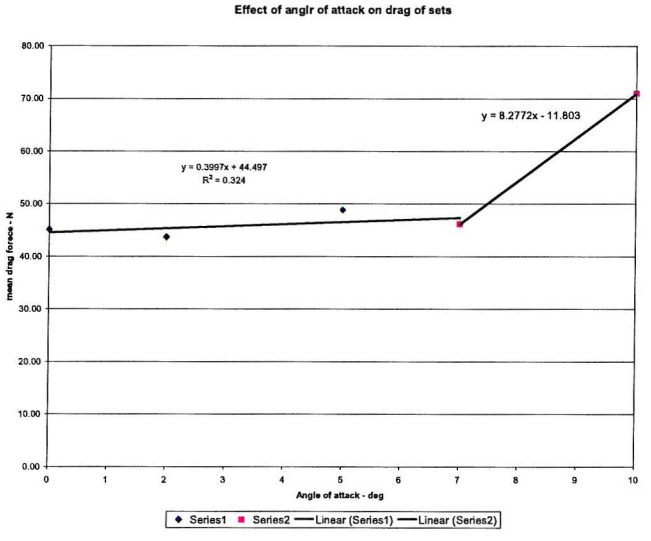

Figure 2.6.9 The effect of angle-of-attack on the additional drag of appendages

The effect of angle-of-attack is shown in Figure 2.6.9. This factor makes little difference to drag at low angles, but the effect increases rapidly above about 7°. Again the function is continuous, but interpolation and extrapolation is more problematic. The data has been split into two parts: that up to the break point at 7°; and that from 7° upwards. The function is of the form:

$$E(\alpha = 0 \rightarrow 7) = 0.4\alpha + 44.5$$

$$E(\alpha = 7 \rightarrow 10) = 8.3\alpha - 11.8$$

Combining the effects, we arrive at equations for additional drag of:

For α = 1 to 7: $Fda(s,u,\alpha) = (1-3)\overline{Fda} + E_s(s) + 4.6u^2 - 3.25u + 0.4\alpha + 44.5$

For α = 7 to 10: $Fda(s,u,\alpha) = (1-3)\overline{Fda} + E_s(s) + 4.6u^2 - 3.25u + 8.3\alpha - 11.8$

The additional drag derived from these equations is shown plotted against the measured values in Figure 2.6.10. The mean difference between predicted and measured values is 5 N with a standard deviation of 14 N. There are three possible causes of the difference:

a) Errors in the measurement system.

b) Despite the ANOVA results the measured interaction is in fact significant.

c) There are other significant interactions not allowed for in the experiment.

In (Fallows, 2005) it is shown that the measurement system produces results accurate to within 0.01 N with a standard deviation of 1 N. Incorporating the interaction effect into the equation has no affect upon the mean error and only reduces the standard deviation by 0.5 N. It is, therefore, likely that other effects are significant for some combinations of factors, such as interactions between particular appendages at particular speeds and/or angles of attack. Nevertheless, the equation derived does enable an order of magnitude estimate of the effects of these factors to be made over a significant proportion of the operational envelope of the vehicle.

Since the towing tank model is accurately scaled, the drag force experienced by the model is identical to that which would be experienced by the full-scale vehicle at the Reynolds number experienced by the model. The full-scale speed is related to model speed by:

$$u_A = u_m \frac{l_m}{l_A}$$

where l_m = 2.5 m and l_A = 6.794 m. The equations for predicting additional drag of the full-scale vehicle are therefore:

For $\alpha = 1$ to 7: $Fda(s,u,\alpha) = (1-3)\overline{Fda} + E_s(s) + 34u^2 - 8.8u + 0.4\alpha + 44.5$

For $\alpha = 7$ to 10: $Fda(s,u,\alpha) = (1-3)\overline{Fda} + E_s(s) + 34u^2 - 8.8u + 8.3\alpha - 11.8$.

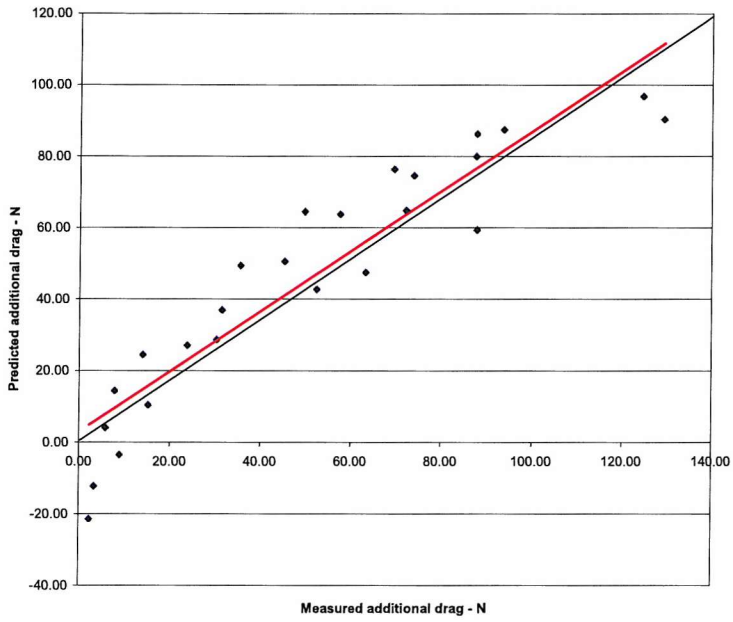

Figure 2.6.10 Prediction accuracy

The predicted drag effect of the sets as a function of speed for the full scale vehicle at zero angle-of-attack is given at Figure 2.6.11, and as a function of angle-of-attack at a speed of 1.4 m/s at Figure 2.6.12.

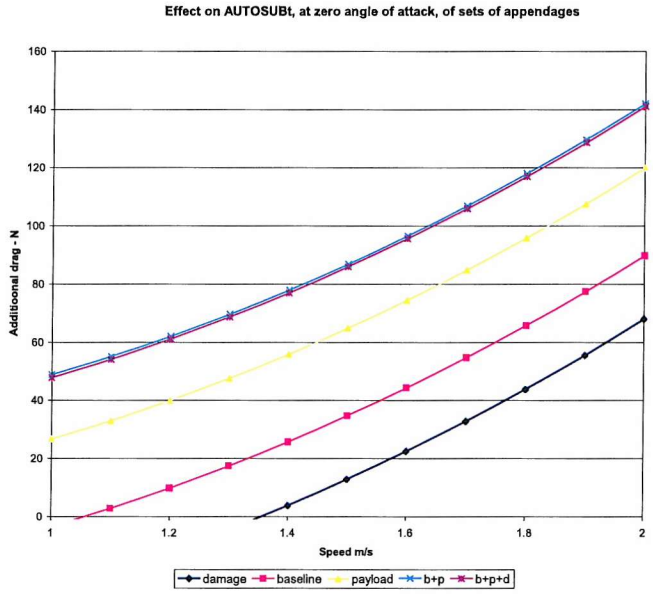

Figure 2.6.11 Effect of appendage sets on full scale vehicle (zero aoa)

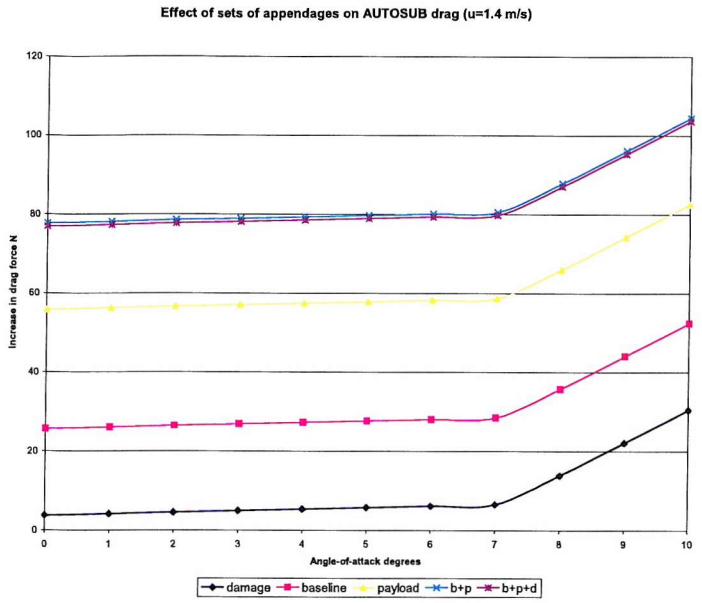

Figure 2.6.12 Effect of sets of appendages on AUTOSUB drag (u=1.4 m/s)

Summary

The means whereby the data from scale-model experiments may be analysed to produce a general model for the drag of a full-scale vehicle has been demonstrated. In doing so, parametric equations for the prediction of the additional drag of sets of appendages have been developed. The results indicate that further work is required to assess the effects of interactions between the sets.

Before moving on to the results of the total analysis and the production of a general drag model, the limitations of the method are explored in the next chapter.

Chapter 2.7

Limitations of the Experimental Method as Illustrated by the Analysis of the Drag Effects of ACDPs

2.7.1 Introduction

The increase in drag over that of the bare hull resulting from the addition of individual appendages is expected to be small and difficult to detect. Thus, before embarking on the full-scale investigation of the effects of individual appendages and combinations thereof, a trial experiment was performed to explore limitations to the method. For this purpose it was decided to determine the effects of the Acoustic Current Doppler Profilers (ADCPs) on drag since they are small compared with the total hull, but of average size as an appendage. Additionally they are fitted in an apparently sub-optimal manner so far as drag is concerned and are fitted either as a single device or in pairs. It would, therefore, be of interest to know whether it is worth the effort of improving the streamlining of the fit, and to be able to demonstrate the effects of combinations of appendages.

2.7.2 Description

Part of the baseline fit of AUTOSUB is an ADCP, which, inter alia, is used as part of the navigation system to measure the speed of the vehicle through the water and, when at sufficient depth, to measure the speed over the ground. This is usually fitted in the forward section of the vehicle, pointing downwards. Often an additional ADCP is fitted in the aft section pointing upwards to provide data on the remainder of the water column and the water surface. Each ADCP penetrates the hull and has the form shown in Figure 2.7.1.

The forward and aft hull surface is formed of GRP skins fitted to a framework. The ADCP is mounted on the framework and a hole cut in the skin to allow it direct contact with the water. The hole is cut oversize to allow ease of fitting. There is thus,

an annulus around each ADCP through which water may flow into the free flooding forward and aft sections of the hull, as illustrated in Figure 2.7.2.

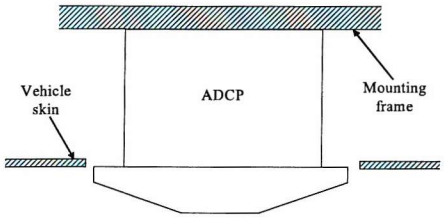

Figure 2.7.1 ADCP profile

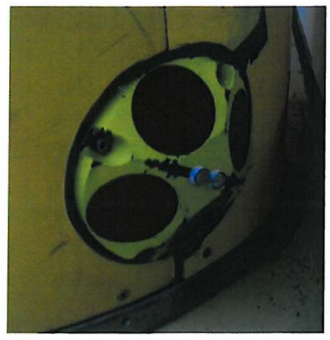

Figure 2.7.2 ADCP fitted to hull

The experiment was designed to assess the effect of the ADCP and their annuli on the drag of the vehicle. An additional objective of this experiment was to assess the experimental methodology and demonstrate that the effect on net drag of a large number of parameters could be detected, ranked, and quantified. From the results a model could be constructed that would enable drag to be predicted for the defined parameter space.

2.7.3 Experiment design

The objective of the experiment was to determine the effect of drag of the presence of the ADCP as a function of speed, angle-of-attack and hydroplane angle. A number of ADCP fitting options were to be explored, viz: either or both present, with or without an annulus.

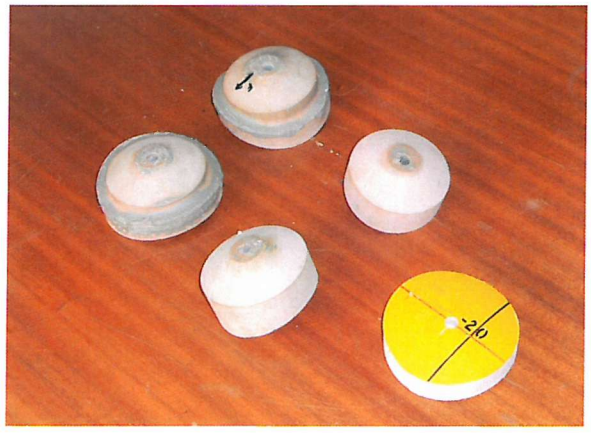

Figure 2.7.3 ADCP models

The ADCP were simulated by space models (Figure 2.7.3) that could be fitted to the model hull. Oversize holes were cut into the forward and aft sections of the model in the appropriate position and three appendages made for each:

- A blanking plate
- An ADCP with annulus
- An ADCP without annulus.

The factors for the experiment were chosen to be the same as those used to explore the drag of the bare hull. They are listed in Table 2.7.1, together with the levels selected for each of the factors. A maximum of 4 levels for each of the factors was chosen, to enable non-linear responses to be detected. This allowed estimates of quadratic or linear responses to be estimated with reasonable accuracy whilst keeping the required number of runs within reasonable bounds. Since there are only three levels of interest for the frd and aft ADCP factors, levels 3 and 4 have been allocated the same value. This means that there are more samples for levels 'faa' and 'aaa'. Nevertheless , to maintain statistical significance, they must be treated as two separate sets of data in the analysis. These are termed faa(1), faa(2), aaa(1) and aaa(2). The best estimate of these factors at these levels is the mean of the value for each.

			Levels			
Factors	Column		1	2	3	4
1	2	Frd ADCP	fbp	fa	faa	faa
2	5	Aft ADCP	abp	aa	aaa	aaa
3	6	Speed	240	660	780	915
4	9	Aoa	0	2	7	10
5	10	Ha	0	3	6	9

Key		
	Ha	Hydroplane angle
	fbp	frd blanking plate
	fa	frd ADCP (faired into hull)
	faa	frd ADCP with open annulus
	abp	aft blanking plate
	aa	aft ADCP (faired into hull)
	aaa	aft ADCP with open annulus

Table 2.7.1 Factors and levels chosen to measure the effect of ADCPs on drag performance

It was anticipated that, in addition to the primary effects of each of the factors, interactions between some of them may be significant. The experiment was, therefore, based on an L_{32} orthogonal array, which allows the effects of up to 9 factors, at up to

4, levels to be explored within an experiment comprising 32 runs. This permits a maximum of 4 interactions to be explored, in addition to the 5 primary factors. It was expected that the forward ADCP would have the greatest effect on drag and the experiment was, therefore, constructed such that its interaction with the aft ADCP, speed, AoA and hydroplane angle could be established. No three-way or higher level of interaction was expected to be significant. The experiment is defined in Table 2.7.2.

Experiment Design to measure effect of ADCPs on drag performance

Note	1 (a)	2 Factor Frd ADCP	3 Interaction Frd/Aft (b)	4 Interaction Frd/Speed (b)	5 Factor Aft ADCP	6 Factor Speed	7 Interaction Frd/aoa (b)	8 Interaction frd/hpa (b)	9 Factor aoa	10 Factor hpa
Run										
1	1	1	1	1	1	1	1	1	1	1
2	1	1	2	2	2	2	2	2	2	2
3	1	1	3	3	3	3	3	3	3	3
4	1	1	4	4	4	4	4	4	4	4
5	1	2	1	1	2	2	3	3	4	4
6	1	2	2	2	1	1	4	4	3	3
7	1	2	3	3	4	4	1	1	2	2
8	1	2	4	4	3	3	2	2	1	1
9	1	3	1	2	3	4	1	2	3	4
10	1	3	2	1	4	3	2	1	4	3
11	1	3	3	4	1	2	3	4	1	2
12	1	3	4	3	2	1	4	3	2	1
13	1	4	1	2	4	3	3	4	2	1
14	1	4	2	1	3	4	4	3	1	2
15	1	4	3	4	2	1	1	2	4	3
16	1	4	4	3	1	2	2	1	3	4
17	2	1	1	4	1	4	2	3	2	3
18	2	1	2	3	2	3	1	4	1	4
19	2	1	3	2	3	2	4	1	4	1
20	2	1	4	1	4	1	3	2	3	2
21	2	2	1	4	2	3	4	1	3	2
22	2	2	1	4	2	3	4	1	3	2
23	2	2	3	2	4	1	2	3	1	4
24	2	2	4	1	3	2	1	4	2	3
25	2	3	1	3	3	1	2	4	3	2
26	2	3	2	4	4	2	1	3	3	1
27	2	3	3	1	1	3	4	2	2	4
28	2	3	4	2	2	4	3	1	1	3
29	2	4	1	3	4	2	4	2	1	3
30	2	4	2	4	3	1	3	1	2	4
31	2	4	3	1	2	4	2	4	3	1
32	2	4	4	2	1	3	1	3	4	2

Notes (a) Col 1 not required for 5 factor, 4 interaction
(b) Interaction 2=1x2 &3x4
Interaction 3=1x3 & 2x4
Interaction 4=1x4 & 2x3
(c) Experiment based on L'32 Tagguchi array for 1 factor with 2 levels and nine factors with 4 levels

Table 2.7.2 ADCP Experiment

2.7.4 Results

The results are given at Table 2.7.3 and illustrated in Figure 2.7.4.

		Model		Carriage		Net Force	
	File Name	Hull Form	Angle-of-	Hydroplane	Speed		Drag	Lift
			Degrees	Degrees		m/s	N	N
1	0731 28 a5	fbp abp	0	0	240	1.0195	-26.795	-0.544
2	0731 08 a5	fbp aa	2	3	660	2.7074	-173.429	-25.376
3	0804 27 a5	fbp aaa	7	6	780	3.2859	-285.812	-135.206
4	0731 11 a5	fbp aaa	10	9	915	4.02	-429.792	-299.15
5	0730 04 a5	fa aa	10	9	660	2.7103	-215.123	-137.6
6	0730 13 a5	fa abp	7	6	240	1.0195	-32.752	-10.707
7	0730 08 a5	fa aaa	2	3	915	4.0317	-346.007	-47.43
8	0730 09 a5	fa aaa	0	0	780	3.2866	-245.143	-12.364
9	0730 19 a5	faa aaa	7	9	915	4.0264	-395.063	-206.691
10	0730 20 a5	faa aaa	10	6	780	3.2795	-313.391	-241.669
11	0731 06 a5	faa abp	0	3	660	2.7127	-168.484	1.189
12	0730 15 a5	faa aa	2	0	240	1.0198	-28.768	-2.838
13	0730 21 a5	faa aaa	2	0	780	2.7137	-171.977	5.855
14	0730 22 a5	faa aaa	0	3	915	3.2866	-258.018	-50.264
15	0730 16 a5	faa aa	10	6	240	1.0195	-35.112	-19.095
16	0731 04 a5	faa abp	7	9	660	2.7103	-203.45	-92.035
17	0731 25 a5	fbp abp	2	6	915	4.036	-337.536	-23.841
18	0731 09 a5	fbp aa	0	9	780	3.2909	-243.616	33.021
19	0731 14 a5	fbp aaa	10	0	660	2.7156	-219.703	-176.618
20	0731 13 a5	fbp aaa	7	3	240	1.0196	-32.777	-14.185
21	0730 05 a5	fa aa	7	3	780	3.2838	-284.763	-151.809
22	0804 28 a5	fa aa	7	3	780	3.2802	-285.863	-144.501
23	0730 10 a5	fa aaa	0	9	240	0.9923	-26.597	4.803
24	0730 12 a5	fa aaa	2	6	660	2.7146	-176.505	-0.556
25	0730 23 a5	faa aaa	7	3	240	2.7132	-205.979	-120.109
26	0730 24 a5	faa aaa	7	0	660	0.992	-31.53	-13.186
27	0731 05 a5	faa abp	2	9	780	3.2866	-253.625	-15.209
28	0730 17 a5	faa aa	0	6	915	4.0339	-333.419	34.552
29	0730 25 a5	faa aaa	0	6	660	4.0339	-335.363	4.755
30	0730 26 a5	faa aaa	2	9	240	0.9921	-27.281	-1.293
31	0730 18 a5	faa aa	7	0	915	4.0264	-392.697	-252.408
32	0731 07 a5	faa abp	10	3	780	3.2781	-308.442	-244.033

Table 2.7.3 Experiment to establish effect of ADCP number, position and annulus on drag and lift as a function of speed, AoA and hydroplane angle

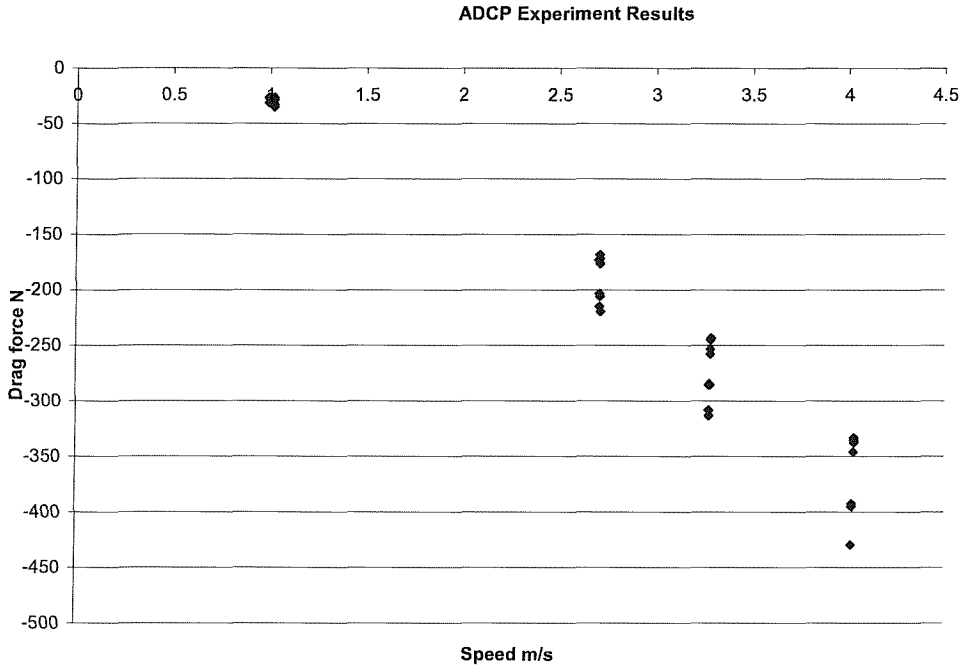

Figure 2.7.4 ADCP experiment results

2.7.5 Predictions

For each run, the deviation of the level for each of the factors (including interactions) from its mean, will cause the measured drag of that run to deviate from the average measured drag for the whole experiment. A fundamental assumption of experiments based on orthogonal arrays, is that no factors interact. Where interactions do occur, these interactions are treated as orthogonal factors in their own right, as described above. The total drag force as a function of the forward ADCP form (*f*), aft ADCP form (*a*), forward velocity (*u*), angle-of-attack (α), and hydroplane angle (δ), each at level (*l*), may be expressed as:

$$F(f,a,u,\alpha,\delta) = \overline{F} + (E_f - \overline{F}) + (E_a - \overline{F}) + (E_l - \overline{F}) + (E_\alpha - \overline{F}) + (E_\delta - \overline{F})$$

$$= E_f + E_a + E_l + E_\alpha + E_\delta - (n_f - 1)\overline{F},$$

Where, n_f = number of factors and E is the effect as defined in the previous chapter.

The effect of each of the factors is shown graphically in Figure 2.7.5.

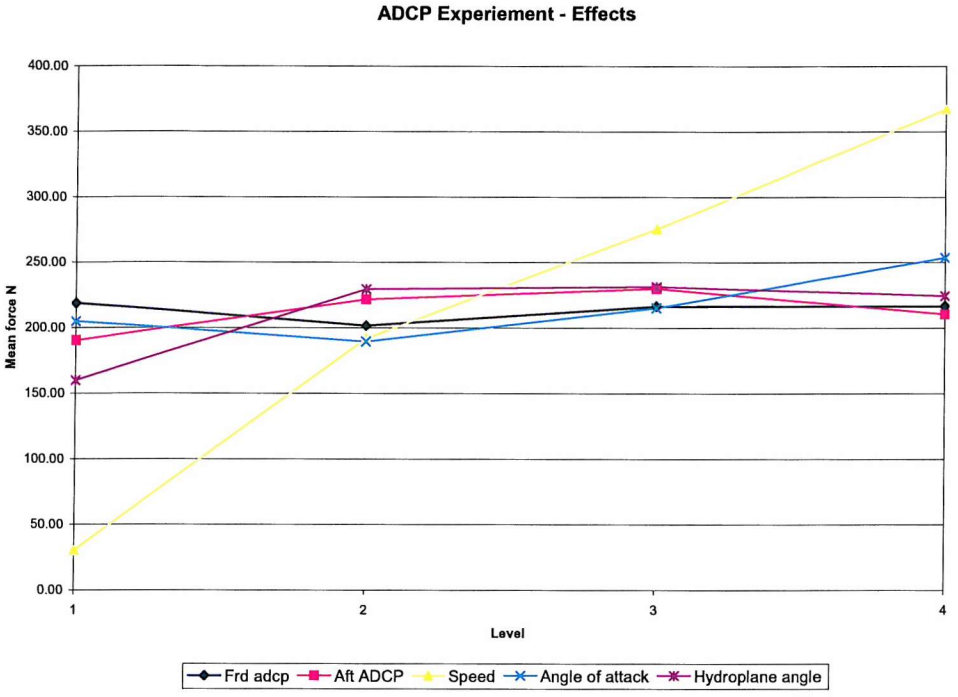

Figure 2.7.5 ADCP experiment effects

An analysis of variance was performed on the data to establish the relative significance of the factors. The results are given in Table 2.7.4, from which it can be seen that the frd ADCP, and speed are highly significant factors with the F-ratio, of variance between samples to variance within samples, exceeding the 99% confidence limit. The aft ADCP is also likely to be significant, but at a lower confidence level of less than 90%. There is less than 90% confidence that angle-of-attack and hydroplane angle are likely to be significant.

The effects of the frd and aft ADCP are integer and so interpolation has no meaning. However, those of speed, angle-of-attack and hydroplane angle are continuous functions and may, therefore, be interpolated. The results of fitting equations to the effects of these factors is shown in Figures 2.7.6 to 2.7.8. As expected, a square law fits the speed data well. There is no evidence from the few data points available, that the relationship between angle-of-attack and its effect is other than linear. The effect of the hydroplane rises rapidly at small angles (up to 3°) and then plateaus. The prediction equations associated with Figures 2.7.6 to 2.7.8, therefore, become:

For $\alpha = 0° - 3°$,

$$F(f,a,u,\alpha,\delta) = E_f + E_a + 17.9u^2 + 21.8u + 5.1\alpha + 191 + 23.3\delta + 160 - 4\overline{F}\,.$$

For $\alpha = 3^\circ - 9^\circ$,

$$F(f,a,u,\alpha,\delta) = E_f + E_a + 17.9u^2 + 21.8u + 5.1\alpha + 324 - 4\overline{F}.$$

Factor	Frd ADCP			Aft ADCP		
Source of Variation	Sum of squares	Degrees of freedom	Variance estimate	Sum of squares	Degrees of freedom	Variance estimate
between samples	1483	3	494	6291	3	2097
within samples	488369	28	17442	483562	28	17270
Total	489852	31	15802	489852	31	15802
F	From data		35.28	From data		8.24
	From table	10%	5.1	From table	10%	5.1
		5%	8.60		5%	8.60
		1%	26.50		1%	26.50
Factor	Speed			Angle of attack		
Source of Variation	Sum of squares	Degrees of freedom	Variance estimate	Sum of squares	Degrees of freedom	Variance estimate
between samples	472240	3	157413	14940	3	4980
within samples	17612	28	629	474912	28	16961
Total	489852	31	15802	489852	31	15802
F	From data		250.26	From data		3.41
	From table	10%	2.29	From table	10%	5.1
		5%	2.95		5%	8.60
		1%	4.57		1%	26.50
Factor	Hydroplane angle					
Source of Variation	Sum of squares	Degrees of freedom	Variance estimate			
between samples	26100	3	8700			
within samples	463752	28	16563			
Total	489852	31	15802			
F	From data		3.41			
	From table	10%	5.1			
		5%	8.60			
		1%	26.50			

Table 2.7.4 Results of ANOVA of main factors

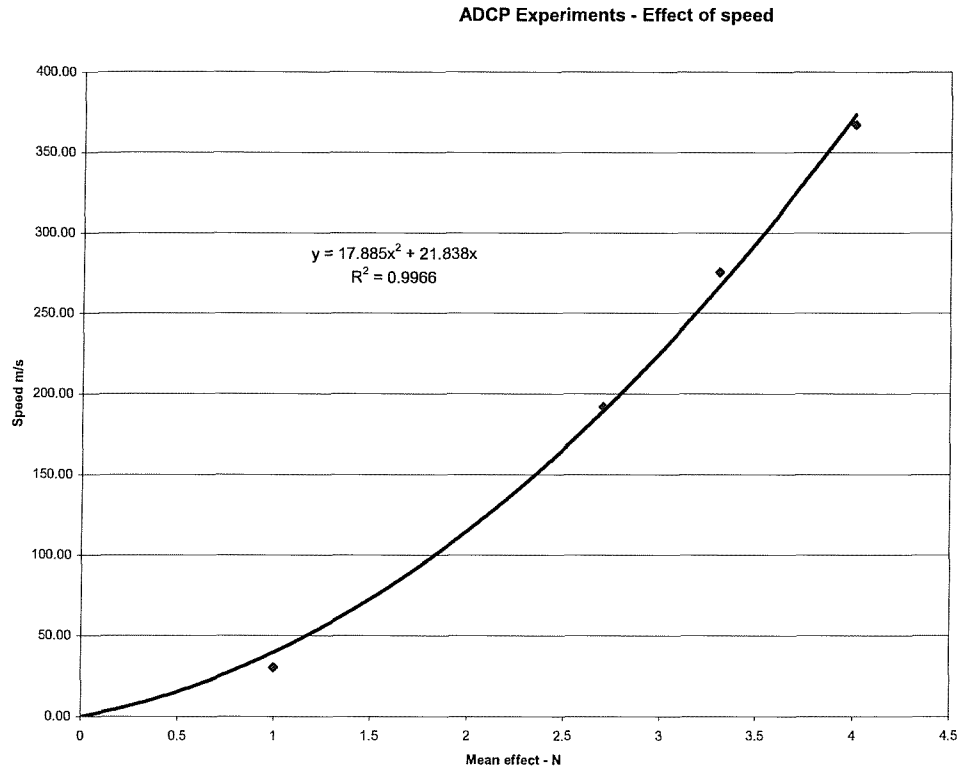

Figure 2.7.6 Mean effect of speed

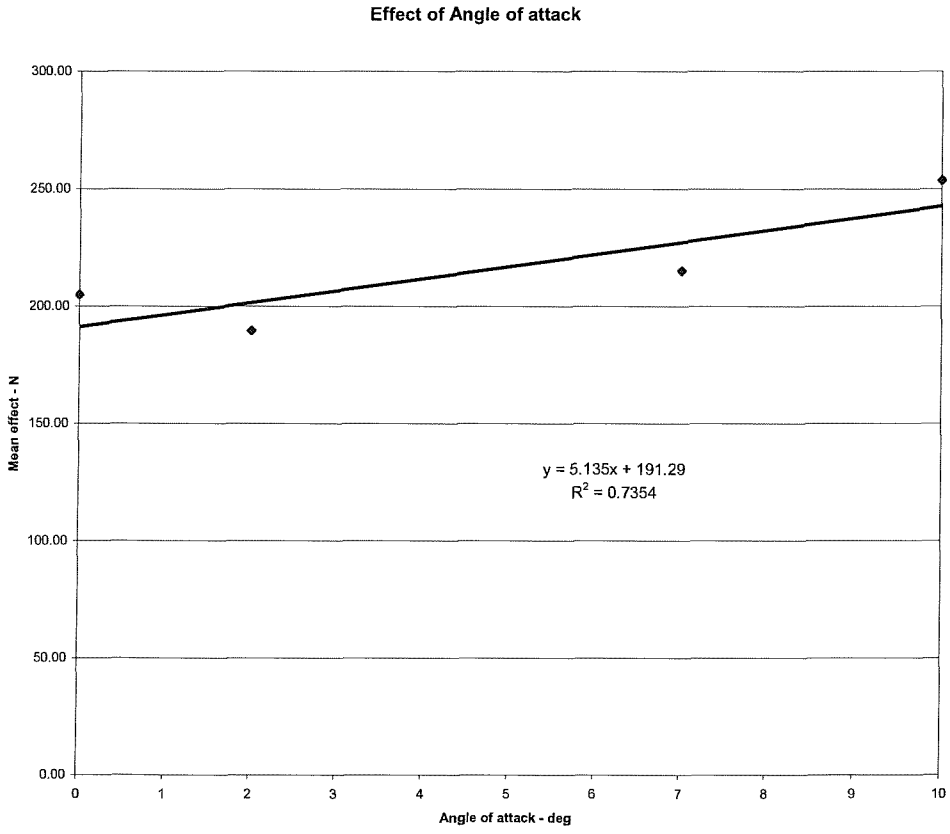

Figure 2.7.7 Mean effect of angle-of-attack

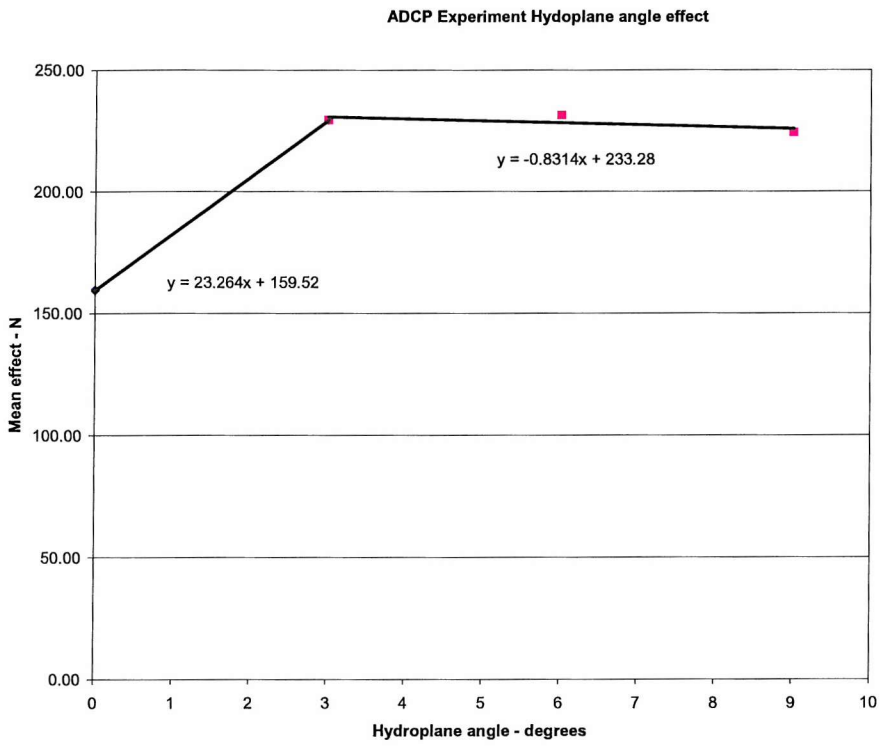

Figure 2.7.8 Mean effect of hydroplane angle

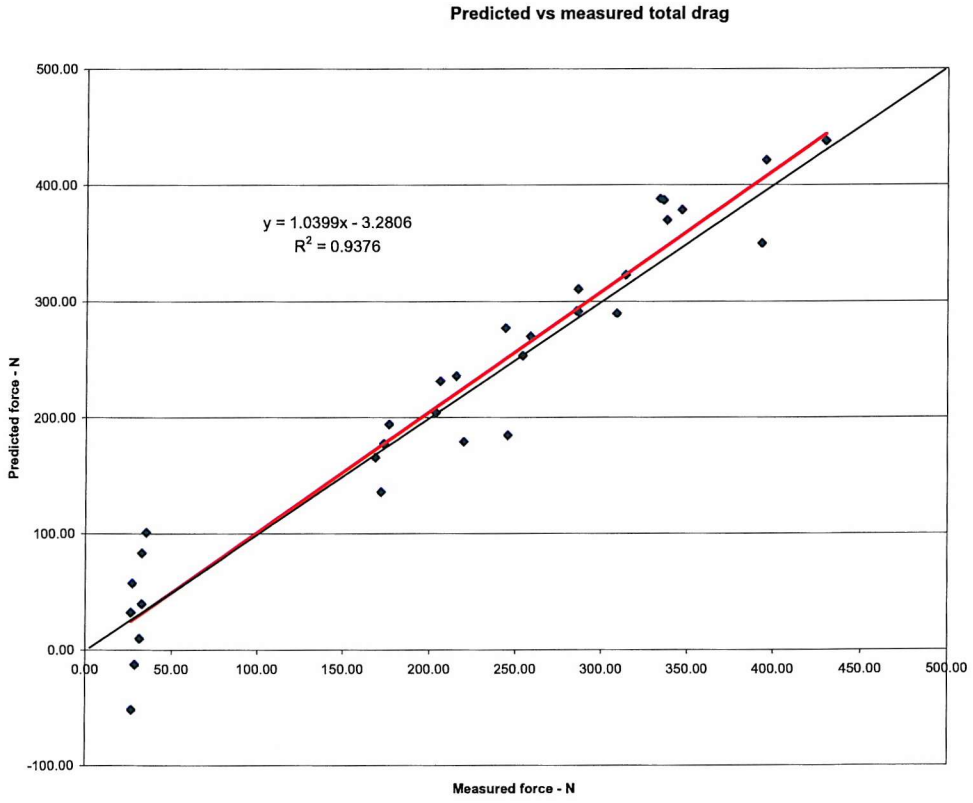

Figure 2.7.9 Accuracy of prediction equations

Predictions resulting from this analysis are compared with the actual measurements taken in Figure 2.7.9. The mean difference between predicted and measured results is 5 N with a standard deviation of 34 N.

The mean difference is comparatively small, but the large standard deviation means that confidence in any particular prediction will be low. The effect of interactions was, therefore, examined to see whether a better prediction is possible.

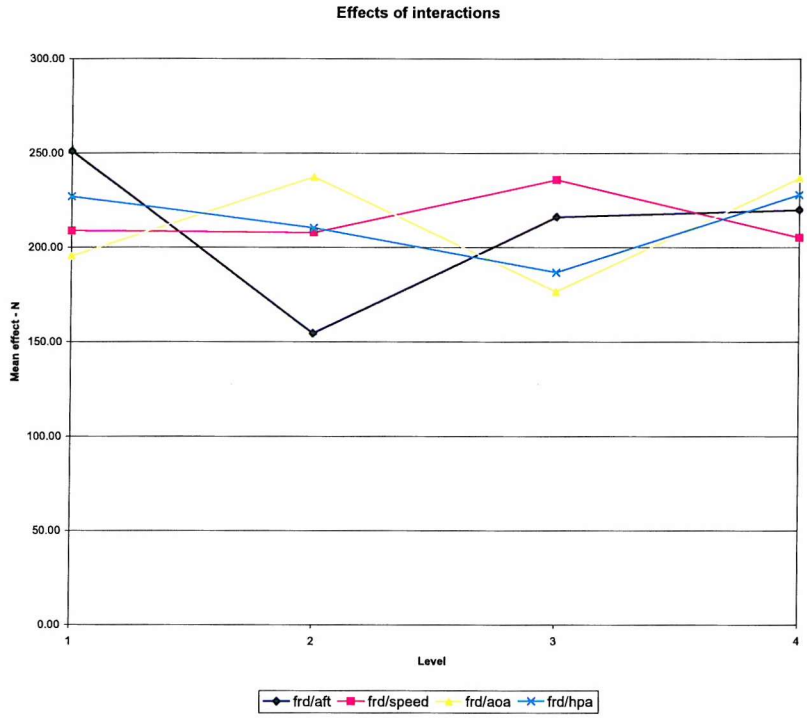

Figure 2.7.10 Effects of interactions

The interaction effects that can be measured by this experiment are shown in Figure 2.7.10. Again an analysis of variance reveals their significane. The results (Table 2.7.5) show that there is a greater than 95% probability that the interaction between the frd ADCP and the speed of the vehicle is significant and a greater than 90% probability that the interaction between the frd ADCP and the hydroplane angle is also significant. Including these in the prediction equations gives:

For $\alpha = 0^\circ - 3^\circ$,

$$F(f,a,u,\alpha,\delta) = E_f + E_a + 17.9u^2 + 21.8u + 5.1\alpha + 191 + 23.3\delta + 160 + E_{fu} + E_{f\delta} - 6\overline{F}$$

For $\alpha = 3^\circ - 9^\circ$,

$$F(f,a,u,\alpha,\delta) = E_f + E_a + 17.9u^2 + 21.8u + 5.1\alpha + 324 + E_{fu} + E_{f\delta} - 6\overline{F}.$$

The effect of this modification to the equations on the accuracy of the prediction is shown in Figure 2.7.11. The mean difference between predicted and measured results is now less than 3 N but the standard deviation has risen to almost 50 N.

Factor	Frd/aft			Frd/speed		
Source of Variation	Sum of squares	Degrees of freedom	Variance estimate	Sum of squares	Degrees of freedom	Variance estimate
between samples	37523	3	12508	4512	3	1504
within samples	452329	28	16155	485340	28	17334
Total	489852	31	15802	489852	31	15802
F	From data		1.29	From data		11.52
	From table	10%	5.1	From table	10%	5.1
		5%	8.60		5%	8.60
		1%	26.50		1%	26.50
Factor	Frd/aoa			Frd/hpa		
Source of Variation	Sum of squares	Degrees of freedom	Variance estimate	Sum of squares	Degrees of freedom	Variance estimate
between samples	21544	3	7181	9119	3	3040
within samples	468308	28	16725	480733	28	17169
Total	489852	31	15802	489852	31	15802
F	From data		2.33	From data		5.65
	From table	10%	5.1	From table	10%	5.1
		5%	8.60		5%	8.60
		1%	26.50		1%	26.50

Table 2.7.5 ANOVA of interaction effects

Because the effects of speed, angle-of-attack and hydroplane angle are much greater than that of the appendages, the apparently significant interactions are probably mainly measuring the interaction between the speed and hydroplane angles and the drag of the hull. Other potentially important interactions, such as that between AoA and speed, are not revealed by this experiment except as additional noise. The

large residual standard deviation of the difference between measured and predicted results will be at least in part due to this.

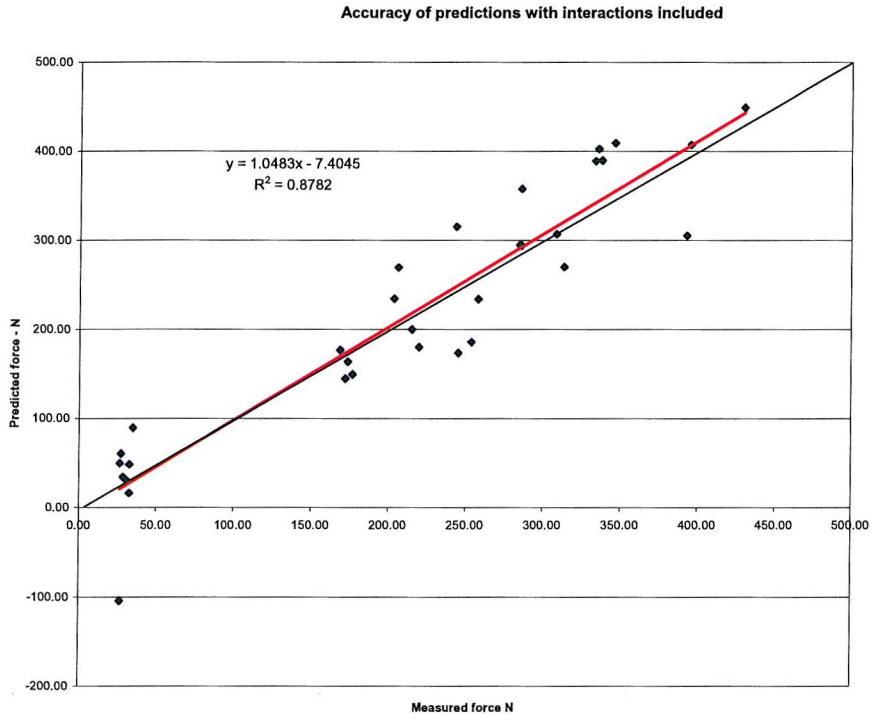

Figure 2.7.11 Accuracy of predictions with significant interactions included

The principle value sought from this analysis is that of the additional drag resulting from the appendages. In an attempt to improve the accuracy of the estimate, the above analysis was repeated using net drag data, i.e. the residual drag after removing the effect of the bare hull. Under these conditions the mean difference between the estimated and measured drag reduces to less than 0.5 N, the standard deviation of the difference to 4 N.

2.7.6 An alternative approach

An alternative approach based on multivariate linear regression (MLR) was undertaken on the data. The script for the function used and results of the analysis are given at (Fallows, 2005). The advantage of this method is that it enables the mean effects of the ADCPs to be determined more clearly. However, it suffers the considerable disadvantage that only a linear regression is performed. It, therefore, enables no allowance to be made for the non-linear effects of speed and angle-of-attack when making predictions. The results from the two methods broadly agree with

the ANOVA approach indicating that the mean effect of the ADCPs is 2 N and the MLR suggesting 3 N. The only difference in the conclusions reached are in the significane of the effect of the aft ADCP (where the MLR approach deems the effect to be insignificant, whereas the ANOVA approach indicates a small but significant effect, albeit only at the 10% confidence level) and the significance of the interactions (where the ANOVA indicates that only the ADCP/Speed interaction is significant, whereas the MVA suggests that all interactions have a small, but significant effect).

2.7.7 Conclusions

The objective of running this experiment was to determine the efficacy of the experiment method. The results of the analysis demonstrate that reasonably accurate predictions of total drag can be made from a model based on the derived effects. The method allows non-linear effects to be incorporated in the prediction equation. An alternative analysis based on multivariate linear regression largely confirm the results, although this method precludes allowance being made for any non-linearity of effects.

Analysis of variance indicated which apparent effects and interactions are likely to be real and which may be due only to chance. It also demonstrated that the effects of comparatively small changes to the form of the hull can be detected, even in the presence of considerable noise. In this case it has been shown that the addition of the frd and/or aft ADCP, if properly faired, has no measureable effect, but that the presence of an annulus around either feature produces an increase in drag of about 2 N.

However, it has also been shown that if one factor, in this case speed, has a much stronger influence than the others, then it is likely to mask the lesser effects. In this case the effect of changing speed on the drag of the basic hull tended to masks the effects of the additional drag of the ADCPs. Now the effect of speed is well characterised from the analysis of bare hull drag (chapter 2.4) and from the analysis in the 'sets' experiments (chapter 2.6). The experiments to measure the effect of individual appendages (chapter 2.8) were, therefore, designed with speed being kept constant, in an attempt to ensure that the smaller effects of the appendages on drag are more easily detectable.

Changing the hydroplane angle between runs was found to be time consuming and to have no detectable effect on the additional drag of the appendages. It was, therefore, decided to run future appendage experiments at constant hydroplane angle.

It has also been shown that the effects are easier to determine if the net additional drag is considered rather than the total drag. This approach was adopted for analysis of the effects of individual appendages.

For the experiment under consideration, modifying the prediction equation by including the effects of interactions improves the average accuracy of the prediction, but it also increases the effective noise and so reduces the confidence with which the prediction may be made. Care is, therefore, required when predicting drag to ensure that the required balance between accuracy and confidence is achieved.

To this point we have demonstrated that the experimental method is sound within the limitations listed above and that the data analysis process enables a statistical model to be constructed that provides order of magnitude estimates of the effects of appendages. We may, therefore, move on in the next chapter to consider the effects of appendages in detail.

Chapter 2.8

Drag of Appendages

2.8.1 Introduction

The intention of this thesis is to explore the possibility of taking into account as much detail as possible when characterising a complex system. For the AUTOSUB AUV appendages can take many forms and be fitted in any number of combinations according to the mission, the build standard and the state of maintenance of the basic vehicle. The implications of determining the consequences of this complexity and variability have been explored in chapters 2.8 and 2.6. The theory of designing experiments that allow the effects of many factors on a key output parameter (in this case drag) to be explored within an affordable expenditure of resource has been outlined in (Fallows, 2005). The original experiment plan in terms of campaigns to explore sets of appendages and random combinations of appendages and damage effects, together with the design of individual experiments was described in chapter 2.2. Chapter 2.6 described the analysis process and in so doing derived a model for determining the effects of sets of appendages. Chapter 2.7 determined the effect on drag of fitting ADCPs and at the same time demonstrated some of the limitations of the experimental method. This chapter completes the analysis of the drag effects of appendages by looking into the effects of combinations of appendages and orifices of various sizes and shapes located in a range of positions and relative positions.

2.8.2 Trade-offs in the design of the experiments

The original design of experiment (chapter 2.2) was intended to determine the effects of 6 factors: number of appendages, their size and shape, their positions across the whole of the vehicle, and their relative linear and angular positions. Each of these factors was to be varied across 4 levels, i.e. there would be four different shapes, each of four different sizes, and so on. To keep manufacturing costs within bounds, simple shapes, such as cylinders and domes, were to be used to represent actual payloads. However, in order to preserve the expensive model, they had to be designed such that they did not penetrate the surface of the hull. The need to surface mount the appendages meant that each of the shapes had to be machined to be conformal to the

position on the hull (Figure 2.8.1). This in turn meant a new appendage had to be made for each position. These two factors combined increased the manufacturing time considerably so the experiment was constrained to positions on the forward hull only and to only three levels for each of the size and shape factors. In an attempt to overcome this limitation, the experiments were designed so that the effects of more possible interactions could be detected and measured. It was hoped that this would allow more accurate estimates of the effects to be made, but did entail significantly more runs than originally envisaged and a corresponding increase in time in the laboratory.

Figure 2.8.1 Sample of conformal appendages

In the case of the design of the experiment to measure the effect of orifices, this of necessity involved penetrating the hull. However, the penetrations were kept to a minimum by the use of existing hull penetrations, such as the flooding and draining hatches and ADCP orifices. Conformal blanking plates were manufactured where necessary to enable the natural hull-form to be recovered.

2.8.3 Factors and levels

For the appendage experiment the factors selected were shape and size of appendage, linear position, and relative linear and angular position. The levels for each of the experiments are given in Table 2.8.1. The relative linear position is expressed as an integral number of diameters separation, *d*, between two identical

appendages, where the diameter is defined as the fore to aft distance in the case of the NACA section shaped appendages. The number of appendages is implied by the relative linear position, where zero separation implies single appendages. Three shapes were chosen, a cylinder, which is representative of the shape of many sonar domes and other payload housings, and two streamlined versions, a dome and a 0015 NACA section. Each of these was made in three sizes as defined in chapter 2.2. The positions are defined in Figure 2.8.2.

Factors	Levels		
	1	2	3
Shape	Cylinder	Dome	NACA
Size	Large	medium	Small
Position	Nose	Fwd of break	Aft of break
	Aa	Ca	Ea
Relative linear position	Single	2d	1d
Relative angular position	In line	15 deg	90 deg

Table 2.8.1 Factors and levels

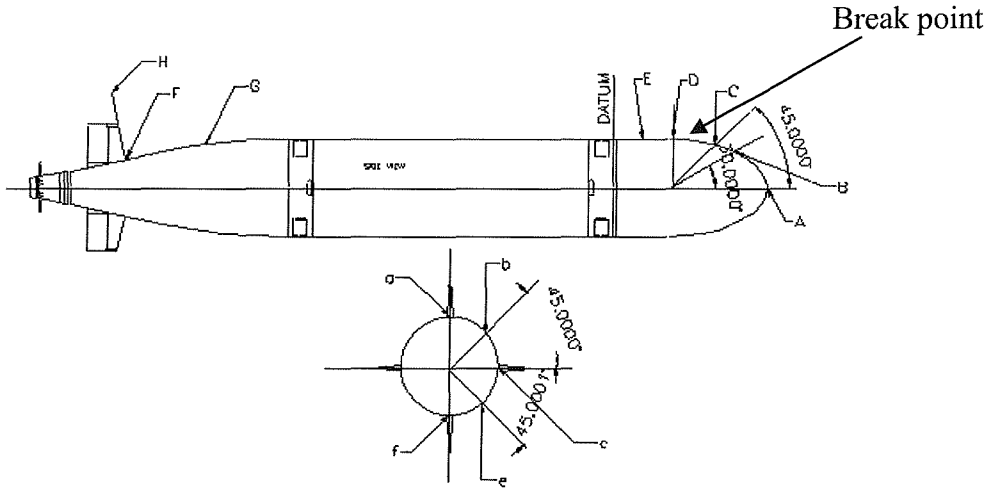

Figure 2.11.2 Appendage stations

An example of two medium sized domes fitted, with the first at positions Aa and the second at relative linear position 2d and relative angular position 0^{o} is given in Figure 2.8.3. (Note that the relative linear position of 0 ° is at 90 ° from the mounting poles since the vehicle is mounted at a notion angle of 90 ° to the surface to minimise

the interaction between the poles and appendages mounted on the dorsal and ventral surfaces).

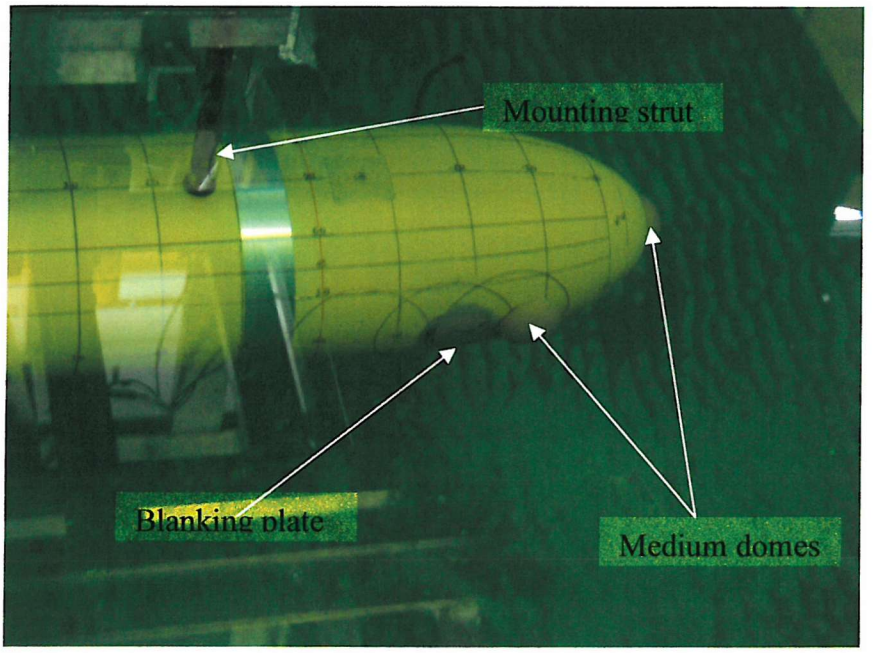

Figure 2.8.3 Example of appendage mounting

Whereas such an experiment would give an indication of the effects of relative linear and angular position on the drag of a range of sizes and shapes of appendages, it was considered that only 3 levels would not give sufficient information to provide a real feel for the effects of separation. However, increasing the number of levels was not a viable option because it would have required additional appendages to be manufactured. Two additional experiments were, therefore, devised, with the constraint that they must use only the appendages manufactured for the first experiment. The first would address the matter of linear separation only, as a function of size and shape, and the second would address angular separation only as a function of size and shape. It was expected that the effect of angular separation would be complex and so it was considered that 5 levels would be required to give a reasonable indication of the shape of the curve relating to this parameter (10^{o}, 15^{o}, 30^{o}, 45^{o} and 90^{o}) (in addition to 0^{o}, which is effectively a single appendage). For the purposes of this experiment, separation is defined as the angle subtended by lines drawn from the axis of the model through the centre of the appendage. The small angular separations are readily achievable for the small appendages, but required some interpretation for the larger appendages, since they effectively merge as shown in Figure 2.8.4 This merger was achieved by paring the appendages as necessary between runs, as shown

in Figure 2.8.15. This necessarily required some careful planning of the order of the runs since re-assembly would have presented a challenge.

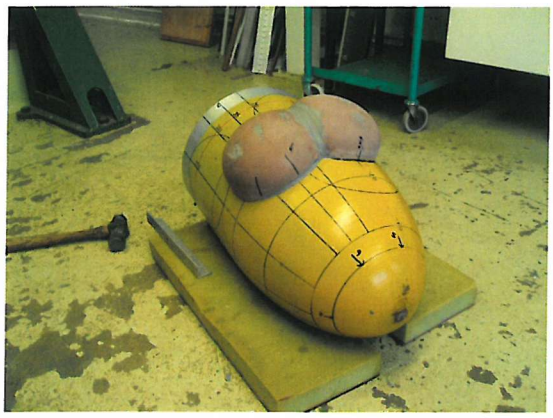

Figure 2.8.4 Two medium domes at 15° separation

Figure 2.8.5 Pared large NACA section

2.8.4 Experiment 1 - The effect of payload appendage as a function of both angular and linear relative position

The experiment to determine the effect of payload appendage as a function of both angular and linear relative position requires the levels for each of the factors defined in Table 2.8.2.

Factors		Levels	
	1	2	3
Shape	Cylinder	Dome	NACA
Size	Large	Medium	Small
Position	Nose	Frd of break	Aft of break
	Aa	Ca	Ea
Relative linear position	Single	2d	1d
Relative angular position	In line	15 deg	90 deg

Table 2.8.2 Factors for determining effects of both angular and linear separation

The minimum size of experiment that will allow exploration of this number of factors and levels, together with one interaction, is based on the L_{18} array (Fallows, 2005). This is shown in Table 2.8.3 with the factors and levels of Table 2.8.2 allocated to the appropriate columns, such that the effect of the interaction between position and relative linear position may be assessed.

The sub-set of the results of the integrated set of payload experiments relevant to the experiment under discussion, is given in Table 2.8.4. Columns 1 to 8 give the

settings for each run. All runs were undertaken at 3.7 m/s and zero angle-of-attack. Column 9 provides the measured drag force. The drag force that would have been experienced by the bare hull under the same operating conditions is shown in Column 10. The values were calculated from the model derived in chapter 2.4 using the Matlab function given at (Fallows, 2005). The additional drag due to the appendages is given in Column 11.

Factor or interaction	Position	Relative linear position	Relative angular position	Type	Size
Expt.					
1	Aa	Single	In line	Cylinder	Large
2	Aa	2d	15 deg	Dome	Medium
3	Aa	1d	90 deg	NACA	Small
4	Ca	2d	15 deg	NACA	Small
5	Ca	1d	90 deg	Cylinder	Large
6	Ca	Single	In line	Dome	Medium
7	Ea	Single	90 deg	Dome	Small
8	Ea	2d	In line	NACA	Large
9	Ea	1d	15 deg	Cylinder	Medium
10	Aa	1d	15 deg	Dome	Large
11	Aa	Single	90 deg	NACA	Medium
12	Aa	2d	In line	Cylinder	Small
13	Ca	1d	In line	NACA	Medium
14	Ca	Single	15 deg	Cylinder	Small
15	Ca	2d	90 deg	Cylinder	Small
16	Ea	2d	90 deg	Dome	Large
17	Ea	1d	In line	Dome	Small
18	Ea	Single	15 deg	NACA	Large
Notes					
8 ORTHOGONAL ARRAY					
All locations on fwd section of hull only. None on aft to reduce manufacturing requirement					
All at	aoa		= 0 deg		
	speed		= 3.8 m/s (equivalent to full scale speed of 1.4 m/s)		
	speed dial setting		= 875		

Table 2.8.3 Design of experiment to determine the effect of both relative linear and angular position

1	2	3		4	5		6		7		8		9	10	11
Array col No		2		4	5		6		7		8				
Factor or interaction	Exp No	Position		Position x relative linear position	Relative linear position		Relative angular position		Type		Size		Drag Force N	Bare hull drag N	Net drag N
Expt.															
1	102104	1	Aa	1	1	Single	1	In line	1	Cylinder	1	Large	343.9	292.1	51.8
2	102402	1	Aa	2	2	2d	2	15 deg	2	Dome	2	Medium	310.1	292.1	17.9
3	103017	1	Aa	3	3	1d	3	90 deg	3	NACA	3	Small	291.0	292.1	-1.1
4	103102	2	Ca	1	2	2d	2	15 deg	3	NACA	3	Small	296.7	292.1	4.6
5	102108	2	Ca	2	3	1d	3	90 deg	1	Cylinder	1	Large	399.5	292.1	107.4
6	102403/04	2	Ca	3	1	Single	1	In line	2	Dome	2	Medium	304.0	292.1	11.9
7	102212	3	Ea	2	1	Single	3	90 deg	2	Dome	3	Small	303.1	292.1	11.0
8	102909	3	Ea	3	2	2d	1	In line	3	NACA	1	Large	373.5	292.1	81.4
9	102706	3	Ea	1	3	1d	2	15 deg	1	Cylinder	2	Medium	317.2	292.1	25.1
10	102205	1	Aa	3	3	1d	2	15 deg	2	Dome	1	Large	320.3	292.1	28.2
11	103005	1	Aa	1	1	Single	3	90 deg	3	NACA	2	Medium	299.5	292.1	7.4
12	102110	1	Aa	2	2	2d	1	In line	1	Cylinder	3	Small	303.4	292.1	11.3
13	103015	2	Ca	2	3	1d	1	In line	3	NACA	2	Medium	302.5	292.1	10.4
14	102118	2	Ca	3	1	Single	2	15 deg	1	Cylinder	3	Small	306.5	292.1	14.4
15	102115	2	Ca	1	2	2d	3	90 deg	1	Cylinder	3	Small	302.7	292.1	10.5
16	102306	3	Ea	3	2	2d	3	90 deg	2	Dome	1	Large	335.2	292.1	43.0
17	102303	3	Ea	1	3	1d	1	In line	2	Dome	3	Small	303.9	292.1	11.8
18	102912	3	Ea	2	1	Single	2	15 deg	3	NACA	1	Large	341.0	292.1	48.9

Notes
Based on L18 ORTHOGONAL ARRAY
All locations on f'r'd section of hull only. None on aft to reduce manufacturing requirement
All at aoa = 0 deg
speed = 3.757 (equivalent to full scale speed of 1.4 m/s)
speed dial settin 875

Table 2.8.4 Results of experiment to measure effects of both relative linear and angular position

An analysis of variance was performed as described in chapter 2.5. The effect of change in level for each of the factors is given in Table 2.8.5 and shown in Figure 2.8.6. The net result of this analysis shows that, as expected, the size of the appendage has the most significant effect, but that changing the shape from a cylinder to either an equivalent dome or NACA section reduces the drag. From this experiment it is not possible to differentiate between the improvements resulting from the dome or NACA section. The effect of the position of the appendages provides the next most significant effect (albeit that this limited experiment only provides 60% confidence that the effect is significant) with placing an appendage on the nose apparently producing the least effect. Once the appendage has been moved back to the break, further movement aft makes appears to make a smaller difference. As predicted the effects of relative linear and angular position cannot be detected with any confidence from this experiment.

Factor		Position	Position x relative linear position	Relative linear position	Relative angular position	Type	Size
Level		Effect					
1		19.3	18.5	24.2	29.8	36.8	60.1
2		26.5	34.5	28.1	23.2	20.7	14.6
3		36.9	29.7	30.3	29.7	25.3	8.9
mean		27.6	27.6	27.6	27.6	27.6	27.9
Anova results							
	between						
Variance	samples	470	1296	1296	1296	413	5883
	within						
	samples	884	1505	1481	1505	892	132
F		1.88	1.16	1.14	1.16	2.16	44.68
Fmin	alpha=10%	2.7	9.42	9.42	9.42	2.7	2.7

Table 2.8.5 Analysis of effects and variance

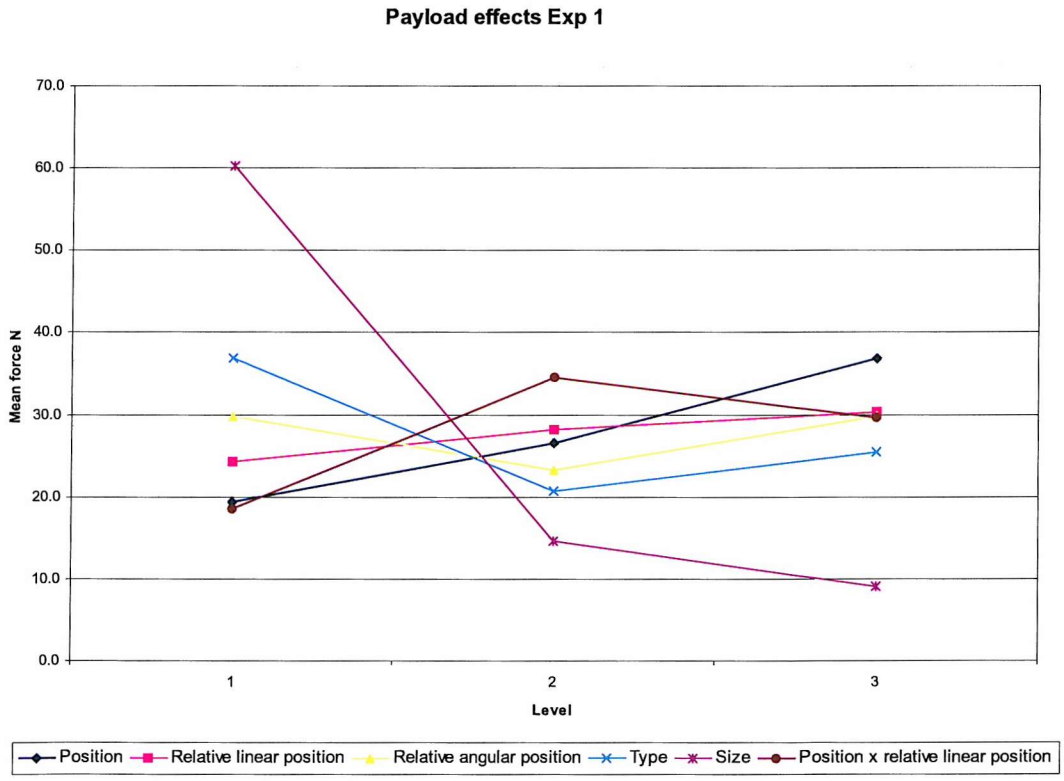

Figure 2.8.6 Effects of level changes

2.8.5 Experiment 2 - The effect of payload appendage as a function of relative linear position only

The experiment to determine the effect of payload appendage as a function of linear relative position requires the same levels and factors as the previous experiment (see Table 2.8.2) but this time the relative angular position remains unchanged at 0 °. The experiment design remains based on an L_{18} orthogonal array and is given in Table 2.8.6.

Factor or interaction	Position	Relative linear position	Relative angular position	Type	Size
Expt.					
1	Aa	Single	In line	Cylinder	Large
2	Aa	2d	In line	Dome	Medium
3	Aa	1d	In line	NACA	Small
4	Ca	2d	In line	NACA	Small
5	Ca	1d	In line	Cylinder	Large
6	Ca	Single	In line	Dome	Medium
7	Ea	Single	In line	Dome	Small
8	Ea	2d	In line	NACA	Large
9	Ea	1d	In line	Cylinder	Medium
10	Aa	1d	In line	Dome	Large
11	Aa	Single	In line	NACA	Medium
12	Aa	2d	In line	Cylinder	Small
13	Ca	1d	In line	NACA	Medium
14	Ca	Single	In line	Cylinder	Small
15	Ca	2d	In line	Cylinder	Small
16	Ea	2d	In line	Dome	Large
17	Ea	1d	In line	Dome	Small
18	Ea	Single	In line	NACA	Large

Table 2.8.6 Experiment to determine the effect of relative linear position

The results, effects and ANOVA are summarised in Table 2.8.7 and illustrated graphically in Figure 2.8.7. These demonstrate that, despite the fact that confidence in the effect remains low, this experiment has increased the contrast of the effects of position and relative linear position. Relative linear position seems to have little effect, although there may be an interference effect in that two similar appendages placed close together appear to exhibit greater additional drag than if separated more widely. However, there is little confidence that this effect is real and a more specific experiment would be required to confirm it.

	Position		Position x relative linear position	Relative linear position		Type		Size		measured drag	Bare hull drag	Net Drag
102104	Aa	1	1	Single	1	Cylinder	1	Large	1	343.94	292.1	51.84
102401	Aa	1	2	2d	2	Dome	2	Medium	2	309.25	292.1	17.15
103016	Aa	1	3	1d	3	NACCA	3	Small	3	292.30	292.1	0.20
103018	Ca	2	1	2d	2	NACCA	3	Small	3	289.90	292.1	-2.21
102106	Ca	2	2	1d	3	Cylinder	1	Large	1	387.60	292.1	95.50
102403	Ca	2	3	Single	1	Dome	2	Medium	2	305.21	292.1	13.10
102210	Ea	3	2	Single	1	Dome	2	Small	3	297.57	292.1	5.47
102909	Ea	3	3	2d	2	NACCA	3	Large	1	373.53	292.1	81.42
102705	Ea	3	1	1d	3	Cylinder	1	Medium	2	316.39	292.1	24.29
102203	Aa	1	3	1d	3	Dome	2	Large	1	322.43	292.1	30.32
103004	Aa	1	1	Single	1	NACCA	3	Medium	2	300.93	292.1	8.83
102110	Aa	1	2	2d	2	Cylinder	1	Small	3	303.36	292.1	11.25
103015	Ca	2	2	1d	3	NACCA	3	Medium	2	302.50	292.1	10.40
102114	Ca	2	3	Single	1	Cylinder	1	Small	3	298.77	292.1	6.66
102113	Ca	2	1	2d	2	Cylinder	1	Small	3	302.31	292.1	10.20
102305	Ea	3	3	2d	2	Dome	2	Large	1	333.37	292.1	41.27
102303	Ea	3	1	1d	3	Dome	2	Small	3	303.91	292.1	11.81
102911	Ea	3	2	Single	1	NACCA	3	Large	1	342.49	292.1	50.39

	Level	Effect										
	1	19.9	17.5	22.7		33.3		58.5				
	2	22.3	31.7	26.5		19.9		14.8				
	3	35.8	28.8	28.8		24.8		6.2				
	mean	26.0	26.0	26.0		26.0		26.5				26.0
		Contrast										
	1	19.9	17.5	22.7		33.3		58.5				
	2	22.3	31.7	26.5		19.9		14.8				
	3	35.8	28.8	28.8		24.8		6.2				
Anova results												
Variance	between samples			1296								
	within samples			1355								
F				1.05								
Fmin	alpha=10%			9.42								
(1-p)%. (Prob means from different sample).												

Table 2.8.7 Effects of linear relative displacement experiment

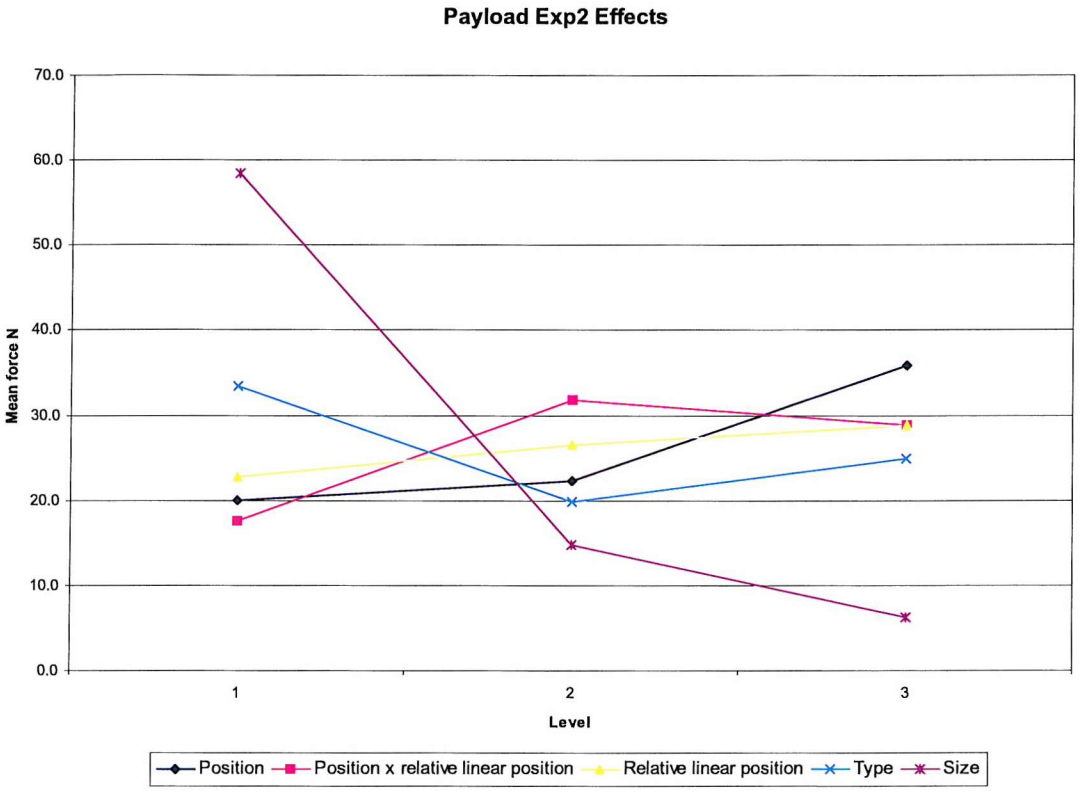

Figure 2.8.7 Effects of relative linear position experiment

2.8.6 Experiment 3 - The effect of payload appendage as a function of relative angular position

This experiment is designed to capture the shape of the curve of increased drag as a function of angular displacement. It is expected that this curve will be non-linear and so 5 values of angular displacement have been chosen. Because the intention is to emphasise the effect of angular displacement only 2 linear positions are used and there is no linear displacement. The factors and levels are shown in Table 2.8.8.

Factors	Levels				
	1	2	3	4	5
Type	Av Cylinder	Small Cylinder	Large Dome	Small Dome	Large NACA
Linear position of both	D	E	D	E	D
Angular Position (deg)	10	15	30	45	90

Table 2.8.8 Factors and levels

Because this experiment requires 5 levels to be explored the minimum size is a 25 run experiment based on an L_{25} orthogonal array (Fallows, 2005). The experiment design and results are shown in Table 2.8.9.

Factor or Interaction Experiment No.		Type/angular posn interaction	Type		Linear Posn		Angular Posn		Measured Drag	Bare hull drag	Net Drag
1	102708	1	Av Cylinder	1	D	1	10	1	319.64	292.1	27.53
2	102201	1	Small Cylinder	2	E	2	15	2	302.94	292.1	10.83
3	102309	1	Large Dome	3	D	3	30	3	339.57	292.1	47.46
4	102213	1	Small Dome	4	E	4	45	4	300.98	292.1	8.88
5	102903	1	Large NACA	5	D	5	90	5	346.50	292.1	54.39
6	102703	2	Av Cylinder	1	D	3	90	5	323.82	292.1	31.71
7	102202	2	Small Cylinder	2	E	4	10	1	299.45	292.1	7.34
8	102310	2	Large Dome	3	D	5	15	2	336.12	292.1	44.01
9	102209	2	Small Dome	4	D	1	30	3	304.51	292.1	12.40
10	102908	2	Large NACA	5	E	2	45	4	420.37	292.1	128.26
11	102704	3	Av Cylinder	1	D	5	45	4	321.29	292.1	29.18
12	102115	3	Small Cylinder	2	D	1	90	5	302.65	292.1	10.54
13	102311	3	Large Dome	3	E	2	10	1	343.92	292.1	51.81
14	102208	3	Small Dome	4	D	3	15	2	303.84	292.1	11.73
15	102914	3	Large NACA	5	E	4	30	3	383.64	292.1	91.53
16	102701	4	Av Cylinder	1	E	2	30	3	329.82	292.1	37.72
17	102116	4	Small Cylinder	2	D	3	45	4	304.99	292.1	12.89
18	102307	4	Large Dome	3	E	4	90	5	337.96	292.1	45.86
19	102207	4	Small Dome	4	D	5	10	1	302.57	292.1	10.46
20	103002	4	Large NACA	5	D	1	15	2	371.27	292.1	79.17
21	102707	5	Av Cylinder	1	E	4	15	2	319.69	292.1	27.58
22	102117	5	Small Cylinder	2	D	5	30	3	305.64	292.1	13.53
23	102308	5	Large Dome	3	D	1	45	4	356.47	292.1	64.37
24	102212	5	Small Dome	4	E	2	90	5	303.12	292.1	11.01
25	103003	5	Large NACA	5	D	3	10	1	363.55	292.1	71.44

Table 2.8.9 Experiment design and results

The effects, and results of ANOVA, are shown in Table 2.8.10. The effects are illustrated in Figure 2.8.8. Although the ANOVA indicates that caution needs be exercised in interpreting the results of angular separation a clear pattern emerges as indicated in Section 2.8.9.

Factor or Interaction		Type/angular posn interaction	Type		Linear Posn		Angular Posn	
Level		Effect						
1		29.82		30.74		38.80		33.72
2		44.75		11.03		47.93		34.66
3		38.96		50.70		35.05		40.53
4		37.22		10.90		36.24		48.71
5		37.59		64.31		30.32		30.70
Mean		37.67		33.54		37.67		37.67
					D	34.72	10	33.72
					E	42.08	15	34.66
							30	40.53
							45	48.71
							60	40.53
							75	34.66
							90	30.70
ANOVA results								
	between							
Variance	samples							2500
	within							
	samples							2476
F								1.01
Fmin	alpha=10%							2.25

Table 2.8.10 Effects and results of ANOVA

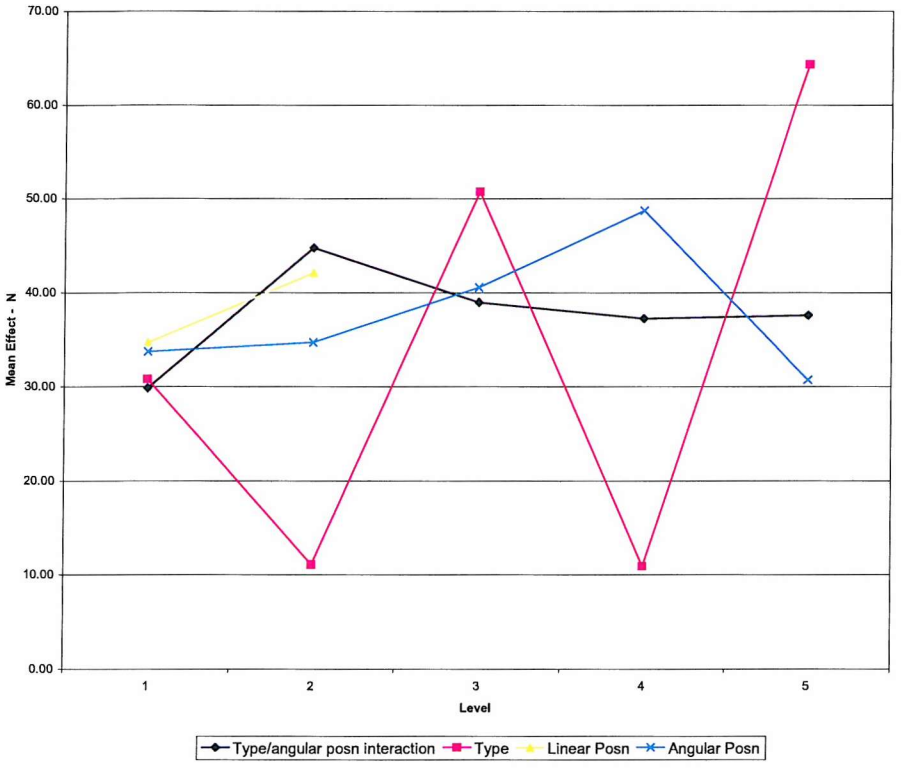

Figure 2.8.8 Effects

2.8.7 Drag Prediction

As shown in chapter 2.6 drag may be predicted from:

$$Fda = (1 - n_f)\overline{Fda} + \sum_{f=1}^{n_f} E_{fl} \qquad \text{: selected level } l.$$

Now a contrast may be defined as:

$$C_{fl} = E_{fl} - Fda\,.$$

The prediction equation, therefore, becomes:

$$Fda = \sum C_{fl} + \overline{Fda}$$

It is now possible to build a simple spreadsheet to allow the sum of any combination of effects to be calculated as shown in Table 2.8.11.

Drag may be calculated by summing the appropriate set of contrasts and adding to the mean result for that experiment. Thus, the drag of a single, medium cylinder at position E may be calculated by summing the appropriate type, size, position, relative linear position and relative angular position contrasts, together with the overall mean, which gives:

$$Fd = 9.2 - 13 + 9.3 - 3.3 + 2.2 + 27.6\,N \quad = 32\,N.$$

1. Predictor for angular and linear separation

Type	Contrast	Size	Contrast	First		Second				Mean Fda
				Position	Contrast	Relative linear position	Contrast	Relative Angular Position	Contrast	
Cylinder	9.2	Large	32.6	A	-8.3	None	-3.3	0	2.2	27.6
Dome	-6.9	Medium	-13.0	C	-1.0	1d	0.6	15	-4.4	
NACA	-2.3	Small	-18.6	E	9.3	2d	2.7	90	2.2	

2. Predictor for linear separation

Type	Contrast	Size	Contrast	First		Second		Mean Fda
				Position	Contrast	Relative linear position	Contrast	
Cylinder	26.3	Large	32.5	A	-6.1	None	-3.3	26.0
Dome	-6.1	Medium	-11.2	C	-3.7	1d	0.5	
NACA	-1.2	Small	-19.8	E	9.8	2d	2.8	

3. Predictor for angular separation

Type	Contrast	Linear position	Contrast	Angular Position	Contrast	Mean Fda
Av Cylinder	-2.8	D	-2.94	10	-3.9	37.67
Small Cylinder	11.0	E	4.42	15	34.7	
Large Dome	50.7			30	6.8	
Small Dome	10.9			45	14.0	
Large NACA	64.3			90	-9.8	

Table 2.8.11 Appendage drag prediction tables

A comparison of the results obtained from predictors 1 and 2 for the additional drag of a single medium sized dome across a range of positions is shown in Table 2.8.12 and Figure 2.8.9. This demonstrates that the results obtained from the predictors are in reasonable agreement.

Appendage					Predictor		
Shape	Size	Position	Rel. linear posn.	Rel. ang. posn	1	2	Mean
Dome	Medium	A	single	0	-1.8	-0.7	-1.2
Dome	Medium	C	single	0	5.5	1.6	3.6
Dome	Medium	E	single	0	15.9	15.1	15.5

Table 2.8.12 Comparison of results from 2 predictors

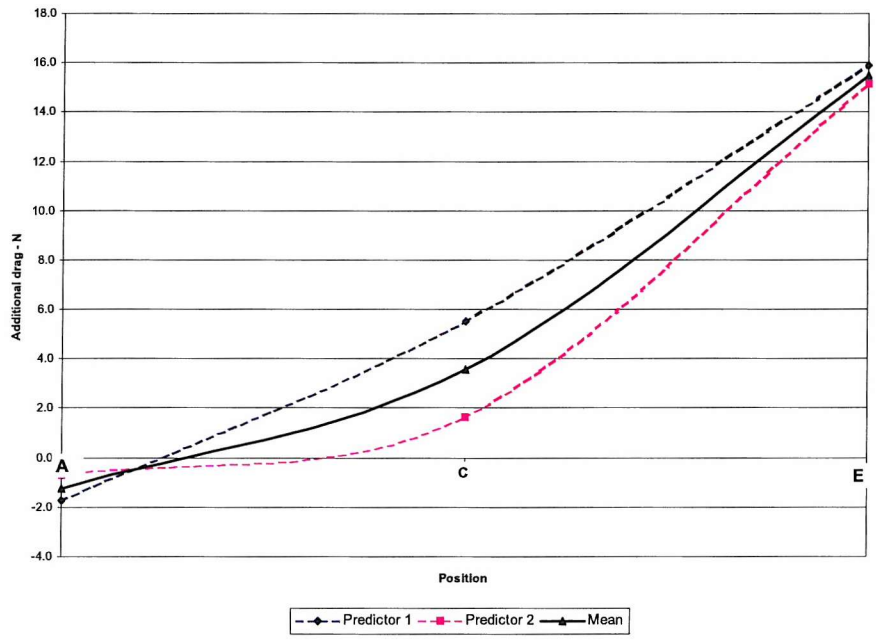

Figure 2.8.9 Predictions of effect of position on additional drag of a single medium dome, obtained from two experiments

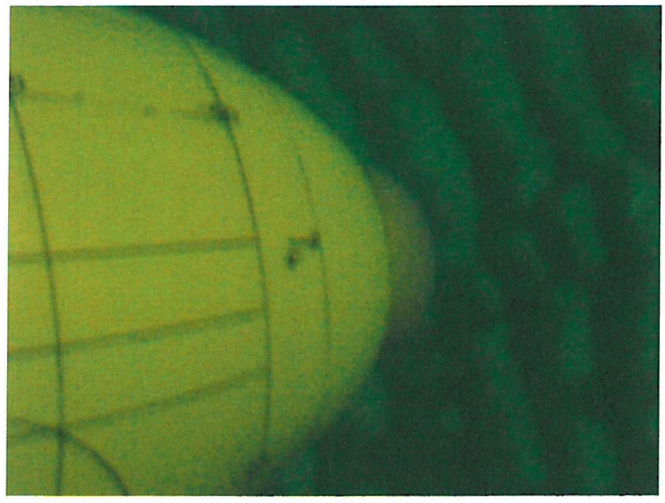

Figure 2.8.10 Medium dome mounted on nose

This indicates that a dome mounted on the nose adds no detectable drag. This result is as expected since it changes the profile very little, as illustrated in Figure 2.8.10.

2.8.8 The effect of the shape of the appendage on drag

The effect of shape on drag is illustrated in Figure 2.8.11, which indicates that streamlining an appendage by changing from a rectilinear section cylinder to either a

dome or NACA section brings noticeable drag benefit. More speculatively it indicates that it may be more important to change the frontal section than the streamline section.

2.8.9 The effect of linear separation

The effect of linear separation for a medium cylinder at position C is shown in figure 2.8.12. There is some evidence of interference indicating that mounting appendages further apart may be beneficial.

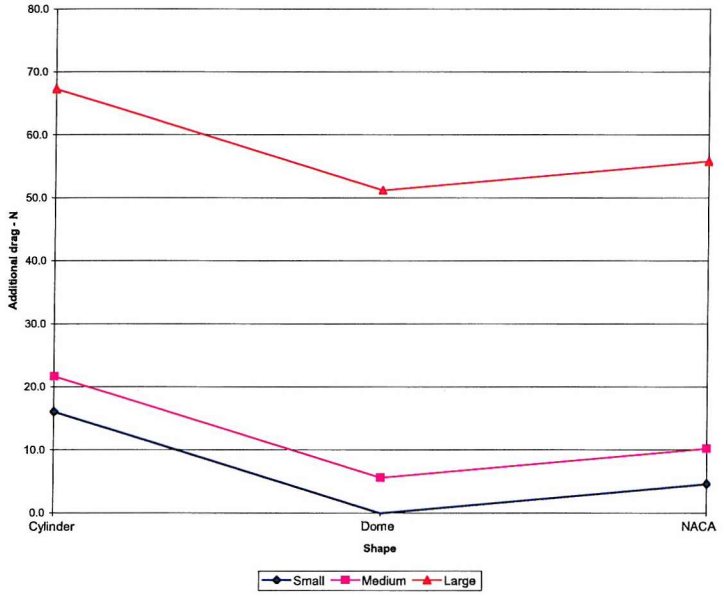

Figure 2.8.11 Effect of shape on drag

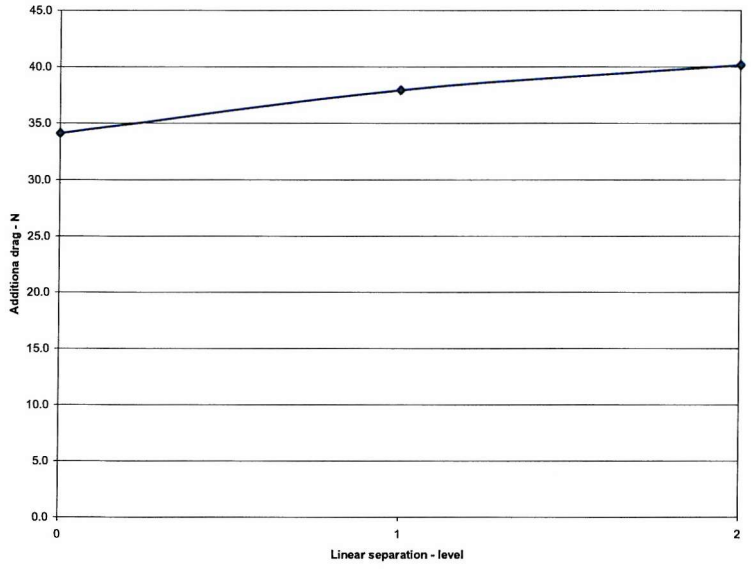

Figure 2.8.12 Effect of linear separation distance on drag

2.8.10 The effect of angular separation

The mean effect of angular separation across all shapes and sizes of appendage is shown in Figure 2.8.13. This figure illustrates that interaction between appendages at small angles of separation increases drag, on average peaking at about 15°. Net drag then reduces with a second, but lower peak at about 45°. This pattern may be indicative of constructive interference in the effects of appendages at low angles of separation (~15°), with destructive interference, providing reduced drag at larger separation angles (~ 30°), followed by further constructive interference. If this should be so then a continuing periodic pattern would be expected, although the resolution of this experiment does not permit it to be seen. Whatever the cause, it is concluded that large angular separations are desirable unless it is considered that the effect is of sufficient concern that optimal spacing is required. In the latter case specific measurements would be required to determine the optimum angle.

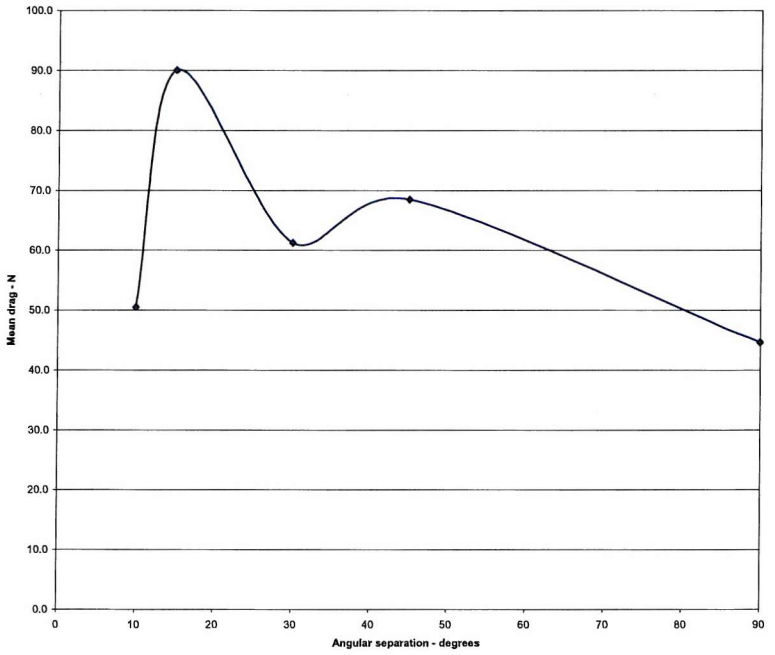

Figure 2.8.13 The effect of angular separation on drag

2.8.11 The effect of apertures on drag

Most AUVs have free flooding bays that are streamlined by skins attached to a frame. AUTOSUB has such a feature for its forward payload bay, and aft for propulsion and hotel services. AUVs from time to time undertake missions with apertures in these skins, which allow water to circulate within the free flooding sections. In an attempt to assess the drag implications of these, the model was run

with the various apertures in the forward hull, as illustrated in Figure 2.8.14. To avoid unnecessary damage to the model, apertures were restricted principally to those that could be achieved as a result of other features of the model, such as removing the flooding hatch cover and using the aperture already cut to accommodate the ADCP. The only exception was the cutting of a 28mm diameter hole in the nose, to simulate a feature of AUTOSUB's collision avoidance sonar.

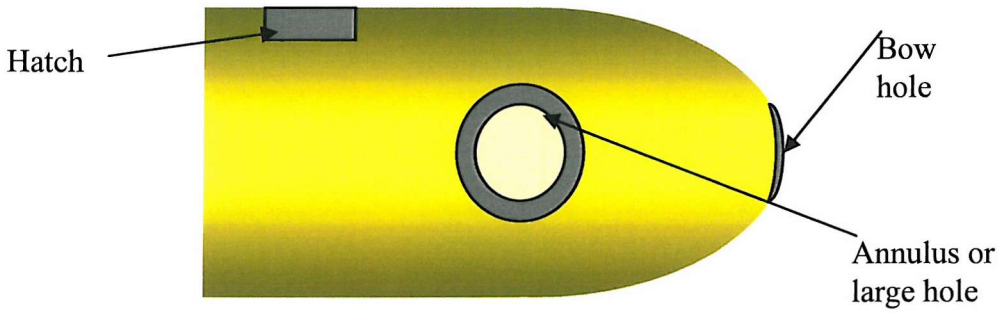

Figure 2.8.14 Apertures

Experiments were run with the range of sets of apertures defined in Table 2.8.13. No formal experiment design was undertaken since these measurements were undertaken on an opportunity basis.

Hole configuration	Bow hole	Annulus	Large Hole	Hatch
1	*	*		*
2	*	*		
3	*		*	
4			*	*
5	*			*

Table 2.8.13 Aperture sets

The results of the experiments are given in Table 2.8.14 and illustrated in Figure 2.8.15. The following characteristics are apparent:

- Compared with the drag of the bare hull the worst-case increase in drag as a result of apertures is small (~ 3%).
- Any two apertures will increase the drag at high speed (equivalent to 1.5 m/s full scale speed).

- At 4 m/s the effects of the bow hole, annulus and hatch are consistently additive, with the bow hole increasing drag by 0.3 N, the hatch by 2.3 N and the annulus by 3.6 N.
- The annulus, when combined with the bow hole and hatch, produces a larger drag across the whole speed range than the equivalent large aperture in the same position.
- There is a systematic peak in drag for all combinations at about 3 m/s model speed. Although the additional drag is calculated after subtracting the total bare hull drag (including its wave drag), the level of detail being sought here (of the order of 1%) is such that this feature may well be due to residual un-cancelled wave drag.

			Model		Carriage		Corrected Net Force		
File Name	Hull Form	Angle of attack	Control Surface angle	Centreline depth	Speed Dial	Speed	Total drag	Bare hull drag	Additional drag
		Degrees	Degrees	Hole number		m/s	N	N	N
	hole conflg1	0	0	5	0	0	0	0	0
0807 13 a5	hole config1	0	0	5	240	0.9924	27.011	25.9	1.111
0807 14 a5	hole config1	0	0	5	660	2.7195	172.646	168.2	4.446
0807 15 a5	hole config1	0	0	5	780	3.2909	247.882	240.3	7.582
0807 16 a5	hole config1	0	0	5	915	4.0382	335.212	329	6.212
	hole config2	0	0	5	0	0	0	0	0
0807 17 a5	hole config2	0	0	5	240	0.9921	27.249	25.9	1.349
0807 18 a5	hole config2	0	0	5	660	2.72	171.725	168.2	3.525
0807 19 a5	hole config2	0	0	5	780	3.288	245.568	240.3	5.268
0807 20 a5	hole config2	0	0	5	915	4.0349	332.885	329	3.885
	hole config3	0	0	5	0	0	0	0	0
0807 21 a5	hole config3	0	0	5	240	0.9922	26.362	25.9	0.462
0807 22 a5	hole config3	0	0	5	660	2.7205	171.506	168.2	3.306
0807 23 a5	hole config3	0	0	5	780	3.2894	244.227	240.3	3.927
0807 24 a5	hole config3	0	0	5	915	4.0349	333.587	329	4.587
	hole config4	0	0	5	0	0	0	0	0
0807 25 a5	hole config4	0	0	5	240	0.9925	25.304	25.9	-0.596
0807 26 a5	hole config4	0	0	5	660	2.718	167.64	168.2	-0.56
0807 27 a5	hole config4	0	0	5	780	3.2902	243.159	240.3	2.859
0807 28 a5	hole config4	0	0	5	915	4.0349	329.841	329	0.841
	hole config5	0	0	5	0	0	0	0	0
0807 29 a5	hole config5	0	0	5	240	0.9924	26.352	25.9	0.452
0807 30 a5	hole config5	0	0	5	660	2.7185	168.619	168.2	0.419
0807 31 a5	hole config5	0	0	5	780	3.2873	243.44	240.3	3.14
0807 32 a5	hole config5	0	0	5	915	4.0414	331.821	329	2.821

Table 2.8.14 Results of experiments to determine aperture effects

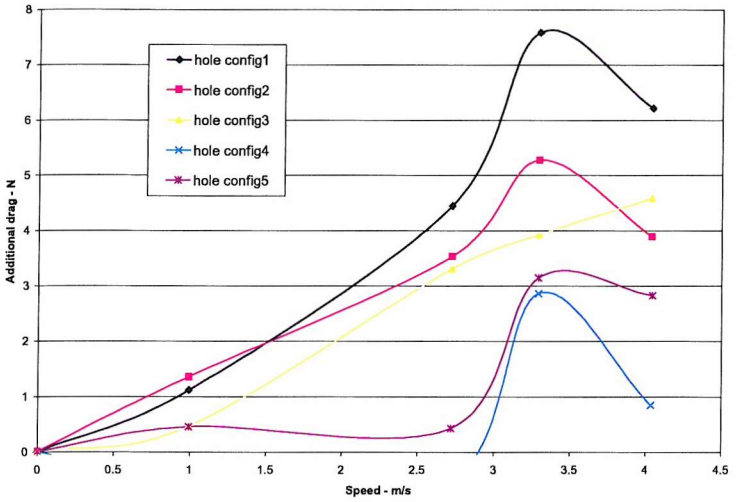

Figure 2.8.15 Effect of sets of apertures on drag

A comparable experiment was run with just the bow hole, with the result shown in Figure 2.8.16. The apparent reduction in drag as a consequence of the presence of a small hole in the bow (but with the free flooding compartment otherwise sealed) is not easily explained by measurement error because of the magnitude of the apparent effect. The measurement system was consistently accurate to within 1 N and measurements taken before and after the series in question, including calibration checks, showed no anomaly. The pattern of additional drag as a function of speed for this configuration is consistent with those for other aperture configurations, except that the effect dips consistently below the x-axis, as shown in Figure 2.8.17. No explanation is offered at this stage but the apparent phenomenon warrants further investigation.

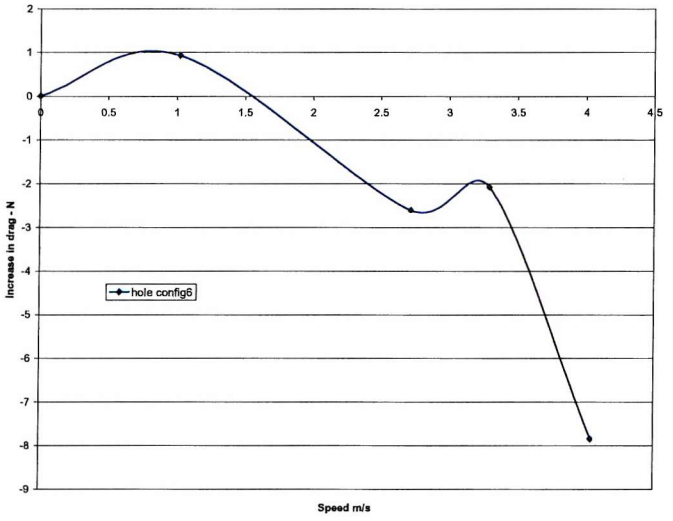

Figure 2.8.16 Drag effect of a single 28 mm hole in the bow

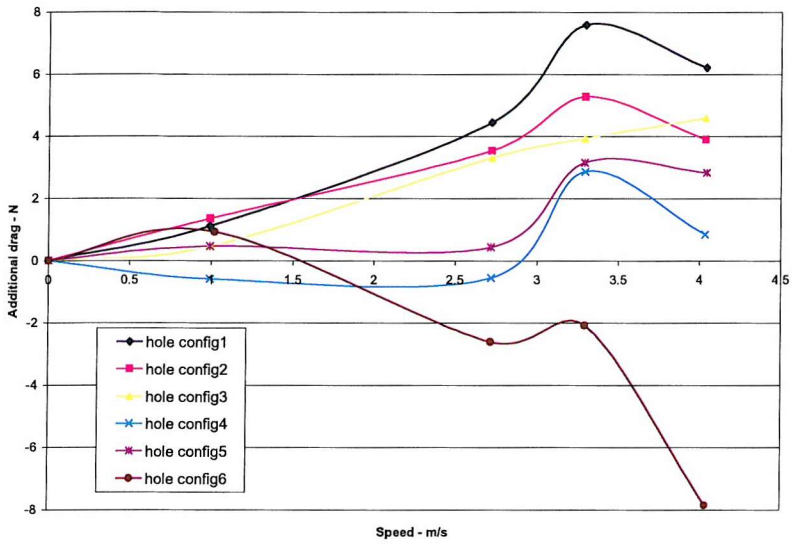

Figure 2.8.17 Drag effect of all aperture configurations

2.8.12 Conclusions

The conclusions that may be drawn from this experiment are considered in terms of: general conclusions as to the method; guidelines for the design and positioning of appendages; and recommendations for additional work.

2.8.12.1 General conclusions as to the method

These are as follows:

a) The method can indicate trends and provide general guidance as to the effects of appendages in terms of size, shape, position and relative position. However, more information is required to provide other than order of magnitude estimates of actual drag.

b) Greater accuracy in estimation may be obtained in two ways. If a better general feel for the overall problem is required then Taguchi type experiments, conducted using larger orthogonal arrays, are suitable. These will enable greater numbers of interactions to be investigated and taken into account. They will also result in the ability to state the estimates to an increased level of confidence and to be more certain of the status of individual effects. Alternatively the results already obtained may be used to design more specific experiments to investigate the effects of particular combinations or types of appendage in greater depth.

c) The model assumes that all factors are independent. This results in, for example, the effect of linear separation to appear to be the same for all sizes, shapes and positions. This is unlikely to be the case, and the effect measured is that averaged over all of these factors. To provide more specific estimates a larger experiment is required to quantify the interactions.

d) As discussed in chapter 2.6, mixing factors with large effects, such as shape, with those with much smaller effects, such as that of angular separation, results in low confidence in the smaller effects. Nevertheless, it has been demonstrated that the smaller effects can be detected. They can be better detected by subtraction of bare hull drag from the total drag results before analysis, thereby increasing the contrast.

e) Non-linear effects can be detected using increased number of levels as illustrated here by the 'angular separation' experiment. Nevertheless, the resolution of the experiments discussed here remains low. Although the experiment to determine the effect of angular separation does reveal a degree of structure, many more levels would need to be included to have any confidence in the detail of the effect.

f) Experiments should be planned as a series of campaigns, with an initial scoping experiment, followed up by more tailor-made experiments to examine in more detail effects demonstrated to be of interest in the scoping experiment. (In this case the requirement was foreseen but time limitations meant that only a single campaign could be devoted to this aspect of the laboratory work. An attempt was made to pre-empt the problem by designing separate linear and angular separation experiments).

2.8.12.2 Guidelines for the design and positioning of appendages

The following guidelines for the design and positioning of appendages to the type of hull considered here may be deduced from these experiments. These are:

a) Streamlining a uniform cylindrical section appendage by changing from a rectilinear section cylinder to either a dome or NACA section brings noticeable drag benefit.

b) Streamlining in both planes to produce a 'blister' is likely to further reduce drag over either a dome or a NACA section, but the increased gain will be

less than the initial gain of moving from a cylinder to either a dome or NACA section.

c) Somewhat more speculatively, the results indicate that if only one change is possible it may be more important to change the frontal section than the fore-to-aft section.

d) If more than one appendage is required it is better to keep them in line rather than to distribute round the circumference.

e) If there must be angular separation between appendages, then it is concluded that large angular separations are desirable unless it is considered that the effect is of sufficient concern that optimal spacing is required. In the latter case specific measurements would be required to determine the optimum angle.

f) It is better not to have apertures into free flooding spaces (with the possible exception of a single aperture at the bow as discussed in Section 2.8.10.3) although the effect is small. (For the examples considered here the worst-case increase in drag was ~ 3%).

g) Any two apertures increase drag at high speed (equivalent to 1.5 m/s full scale speed) although the effect is undetectable at low speed.

h) For the configuration considered here the effects of more than one aperture are additive. There appears to be no interaction between them.

2.8.12.3 Recommendations for additional work

From the results obtained so far the following additional investigations would appear to be beneficial.

a) An experiment to measure the effect of both streamlining methods used here, i.e. using blisters of various sizes, with a dome vertical section and a NACCA fore-and-aft section.

b) Further work on the effect of angular spacing as a function of size and shape in order to determine whether there really is a periodic structure, and if so, its nature.

c) Investigation of the effect of mixing linear and angular separation in the form of a spiral round the vehicle, to see whether the advantages of each may be had simultaneously.

A comparable experiment was run with just the bow hole, with the results shown in Figure 2.8.15. The apparent reduction in drag as a consequence of the presence of a small hole in the bow (but with the free flooding compartment otherwise sealed) is not easily explained by measurement error because of the magnitude of the apparent effect. The measurement system was consistently accurate to within 1 N and measurements taken before and after the series in question, including calibration checks, showed no anomaly. The pattern of additional drag as a function of speed, for this configuration, is consistent with those for other aperture configurations, except that the effect dips consistently below the x-axis, as shown in Figure 2.8.15. No explanation is offered at this stage but the apparent phenomenon may warrant further investigation.

Chapter 2.9

CONCLUSIONS FROM THE LABORATORY EXPERIMENTS

2.9.1 Introduction

The scale-model laboratory experiments are designed to complement at-sea trials on the full-scale vehicle. This will enable the drag characteristics to be established of the real vehicle as deployed, taking count the full complexity of its hull-form, and of the full range of operating conditions that it is expected to experience. Further, it is intended to enable the effects of changes to hull-form, between missions and over time, to be established. Taking account of the fine detail of the hull-form and of possible combinations of a range of appendages involves establishing the effects of a large number of parameters. To do this exhaustively, by changing one parameter at a time, is impractical because of the large number of combinations. The experiments were, therefore, divided into three phases. Phase 1 was designed to establish the characteristics of the bare hull. Phase 2 was intended to determine the effects of sets of modifications to the basic hull-form based on: those supporting basic services and so present on most missions; a representative set of mission-dependent appendages; and a set of changes representative of in-service damage and wear and tear. The last Phase was designed to establish the performance of combinations of individual appendages.

It was important that the performance of the bare hull (Phase 1) was characterised to a high degree of accuracy across the range of operating conditions since this provided a baseline against which the effects of detailed modifications could be assessed. The number of parameters affecting the performance of the basic hull is relatively small, so a larger number of levels could be explored for each parameter, so providing a detailed model. The remaining Phases, required Taguchi type experiment designs so that a potentially unrealistically large experimental space could be explored in an affordable size of experiment.

2.9.2 Experimental method

Chapters 2.1 and (Fallows, 2005) have demonstrated how an experiment design methodology developed for the biological and production-engineering environments (which are characterised by the desire to establish repeatability), may be adapted for use in the exploration of the consequences of the parameters defining a complex system (where the latter is characterised by the desire to establish the effects of change). The results of the experiments provided in chapters 2.10 and 2.11 show that the effects of comparatively fine detail of the system may be detected and quantified, even when many parameters are changed between measurements, provided that due account is taken in the design of the experiment of possible interactions between parameters and of likely inflections in the response surface.

To enable the effects of small changes, or unanticipated interactions, to be detected, it is necessary for the laboratory apparatus to be well characterised and for the measurement system to be stable with time. Considerable effort is necessary to establish levels and causes of noise, with each possible source, hydrodynamic, mechanical and electrical, having to be investigated, as described in (Fallows. 2005). Even then, it was considered prudent to re-calibrate the force measurement system at regular intervals throughout each day and to re-zero the force blocks before each run.

When designing experiments to measure the effects of a number of factors by changing each, it has been found to be important not to mix factors with large effects with those of much smaller effects. This is unimportant for experiments in production engineering or life sciences since one of their objectives is to exclude factors with negligible effect. However, the objective here is to quantify all effects, where possible, and if one factor with a very large effect is included in a set with smaller effects, then the signal of the latter will be swamped by that of the former. This was found to be the case when varying both appendage sets and speed. The effect of change of speed on drag was so great that it tended to dwarf the effects of the appendages, making them more difficult to quantify. Later experiments, which were run at constant speed, demonstrated the efficacy of this approach. Analysis of variance may be used to establish the relative significance of factors influencing the overall effect.

It was found to be important to plan the experiments as a series of campaigns so that lessons learned could be incorporated and areas of interest identified for

further examination. This happened here in that the experiments for the final campaign were re-designed to:

a) Allow for manufacturing problems.
b) Prevent small signals being overwhelmed by the effects of major factors such as speed.
c) Remove insignificant factors such as hydroplane angle.

2.9.3 Laboratory apparatus

To establish the hydrodynamic characteristics of a submarine vehicle in the laboratory, a model is required that must be scaled such that it can run at constant Reynolds number. This enables accurate reproduction of the forces that would be experienced by the real vehicle at equivalent speeds. This requirement implies operating a large-scale model at high speed.

Handling such a large model both in air and in water can be difficult. This difficulty needs to be anticipated at the design stage. In this case, the model weighed more than 100 kg in air, and a crane was installed on the towing tank carriage as an aid to launching. Once in the water it was found that it could only be reliably manoeuvred when ballasted such that it had only marginal positive buoyancy and was trimmed to maintain a horizontal attitude. This was allowed for in the design by including ballast and trim tanks.

Operating a model with high inertia at high speeds, requires substantial posts to transmit the substantial loadings to the dynamometer. The posts used here produced significant waves and spray and experienced a drag force significantly greater than that of the model. A dynamometer placed at the top of the support posts, as used here, measures the sum of the model and post drag. The net signal to noise ratio is, therefore, unfavourable. The added complication of measuring the force at the model-end of support post is, therefore, considered to be worth addressing for this type of experiment. The high waves generated by the posts meant that taking wave cuts was impracticable and alternative means of determining the wave-induced drag of the model had to be used. This problem had been anticipated and it was originally intended to fit fairings to the poles. However, no satisfactory method was found which would also readily allow the angle-of-attack of the model to be adjusted.

The appendages were machined to be conformal to the model at the point of attachment and were attached by means of screws. To do this usually involved

removing the model from the water. Changing appendages was, therefore, a time consuming activity. An alternative method of attachment is required.

2.9.4 Data processing

As discussed, the support posts were found to contribute the major portion of the total signal recorded by the force blocks. Additional work, therefore, had to be undertaken to ensure that their effect was accurately known across a range of angles of alignment and a range of immersion depths.

Even after allowing for the drag of the support posts, a large model run at high speed in a constrained channel experiences two effects that would not be felt in open water. One is wave-induced drag caused by proximity to the free surface, and the other is an apparent increase in relative speed through the water caused by water displaced by the model having to return past it. Determining the wave effect by direct measurement of surface disturbance is not possible under the conditions of these experiments due to the large waves caused by the support poles. However, wave drag may be inferred from the change in drag measured over a range of immersion depths. At shallow immersion depth, net drag is the sum of form and wave drag. However, as depth increases, wave drag decreases, leaving only the form drag. Wave drag derived by this method was found to correlate closely to that derived from thin-ship theory. The results of these experiments show that either method may, therefore, be used to make wave corrections.

The standard methods for blockage correction, as recommended by the ITTC, are designed for surface penetrating hulls. They, therefore, need to be adapted for use with submarine models. Additionally, they are designed for small-scale models travelling at Froude numbers < 0.7. Because submarine models are operated at constant Reynolds number they tend to be run at high Froude numbers. The methods, therefore, need to be modified to allow for this. Four methods have been adapted for submarine models and compared: namely those of Young and Squire, Schuster, Scott and Tamara. Of these, that of Tamara was found to be the most applicable to submarine modelling and is acceptable provided that results for $Fn > 0.7$ are obtained by extrapolation from the values obtained for smaller Fn. Overall the blockage effect for the AUTOSUB model running in the SI Tank was found to be very small, with speed corrections of the order of 1%.

2.9.5 Basic hull-form drag

A numerical model for the drag of the full-scale AUTOSUB hull as a function of speed and angle-of-attack has been developed. This is based on a three-dimensional cubic spline interpolation of the data corrected for pole and wave drag and for blockage. This has been compared with a two dimensional model based on a richer data set and found to provide an accurate representation. Families of curves, contour maps and a look-up table have been produced to enable the drag of the bare AUTOSUB hull to be established for any combination of speed and angle-of-attack over the ranges 0 to 1.5 m/s and 0^{o} to 10^{o}.

Families of curves, contour maps and a look-up table have also been produced to enable the drag of the bare AUTOSUB model hull to be established. This covers the same range of angles-of-attack and a speed range of 0 to 4 m/s. They facilitate determination of the effects of changes to the bare hull.

The numerical model for AUTOSUB drag has been verified by comparison with the at-sea measurements made on the full-scale vehicle described in part 3. A non-dimensional form of the numeric model has been produced that expresses drag coefficient as a function of Reynolds number. The shape of the curve for this vehicle has been compared with that for airships of similar length-to-breadth ratio travelling at similar Reynolds number and found to be significantly different. The airship and the AUV have similar drag coefficients at low Reynolds number but the AUV has a higher coefficient at higher speeds. This is likely to reflect the difference in performance between a cigar-shaped airship and the torpedo shaped AUV.

2.9.6 Added mass

Knowledge of the vehicle's added mass is required so that the drag characteristics of the full-scale vehicle may be determined at sea using the deceleration method described in part 3. This may be achieved at low cost by taking acceleration measurements during the scale-model towing tank experiments. The method, based on determining the apparent total inertial mass and subtracting the measured mass, has been verified by using it to estimate the weight of the mounting poles.

Reasonably consistent results for the added mass of the AUTOSUB scale-model were obtained. This showed that it is of the order of 80 kg. When scaled to full-scale, this produces an added mass of the order of 1750 kg. This is far in excess of the

120 kg derived from theory for an idealised shape of an oblate spheroid, but is comparable to results obtained for another AUV (ABE has an added mass of 1700 kg), albeit one of significantly different shape. It is, therefore, concluded that the added mass of an oblate spheroid does not provide a reasonable approximation to that of the AUV. This result is consistent with that for bare hull drag, where it was found that the drag of an airship, which has a shape approximating to that of an oblate spheroid, is lower at high R_n than that of an equivalent torpedo shaped AUV.

The scaling factor between the added mass of the model and that of the full-scale vehicle is very large (22.5) because it is dependent on the ratio of their volumes. Thus, a small error in measurement of acceleration may result in a large error in added mass. The accelerometer used in this experiment was only capable of measuring to an accuracy of 0.1g and produced a very noisy signal. Additionally, although the acceleration of the carriage is reasonably linear for 1 or 2 seconds, it is not absolutely so. This adds further scope for error.

It is, therefore, concluded that the method is sound and has provided an order of magnitude estimate of the added mass of the vehicle. However, to improve the accuracy of the results that may be obtainable from the trial described in part 3, a tailor-made experiment should be conducted. Ideally this should be based on the full-scale vehicle, and have tailored instrumentation.

2.9.7 Effects of modifications to bare hull shape

Empirical equations and families of curves have been developed to predict the additional drag of sets of appendages representing baseline capabilities, payloads and damage as a function of speed and angle-of-attack. The equations for the full-scale vehicle are:

For α = 1 to 7: $Fda(s,u,\alpha) = E_s(s) + 34u^2 - 8.8u + 0.4\alpha - 57.3$

For α = 7 to 10: $Fda(s,u,\alpha) = E_s(s) + 34u^2 - 8.8u + 8.3\alpha - 113.6$.

Where: $E_s(s)$ for the baseline set = 29 N,

$E_s(s)$ for the payload set = 59 N,

$E_s(s)$ for the damage set = 7 N,

$E_s(s)$ for the baseline and payload both present = 80 N,

$E_s(s)$ for the all sets present = 80 N .

The effect of sets of appendages is shown to be significant, doubling the overall drag in the worst case. For example, the drag of the full-scale bare hull at 1.4

m/s and with zero angle-of-attack, is found from the model tests described in chapter 2.4 to be 90 N. The effect of baseline, payload and damage features together, is to increase hull drag under these conditions by a further 77 N. On the other hand, the effect of change to hydroplane angle over the operational range 0^{o} to 15^{o} on drag was found to be negligible: of the order of 1 N.

Estimates of the additional drag caused by individual appendages in terms of size, shape, position and relative position have been produced. These indicate general trends but are insufficient to enable other than order of magnitude estimates of actual drag. The following general rules have been discerned for the shaping and relative placement of appendages:

a. Streamlining appendages is beneficial, with the shape of the frontal area presented to the fluid proving particularly beneficial. Additional benefit may be gained by also streamlining in the longitudinal direction.
b. The relative positioning of appendages also has a measurable effect on the net drag. Where feasible they should be mounted in line rather than spread around the circumference. Where angular separation is unavoidable, then large angles between appendages are preferable.
c. It is best to avoid apertures into free flooding spaces. However, if unavoidable their effects are found to be small and additive.

2.9.8 Recommendations for additional work

From the results obtained so far the following additional investigations would appear to be beneficial.

a. A tailored experiment designed specifically to measure the added mass of the full-scale vehicle.
b. An experiment to measure the effect of both appendage streamlining methods used here, i.e. using blisters of various sizes, with a dome vertical section and a NACCA fore-and-aft section.
c. Additional work on the effect of angular spacing as a function of size and shape in order to determine whether there really is a periodic structure, and if so its nature.
d. Investigation of the effect of mixing linear and angular separation in the form of a spiral round the vehicle to see whether the advantages of both may be had simultaneously.

e. Further measurements to establish the effect of a bow hole to determine the apparent reduction in drag detected here is real and, if so, explore its causes.

Part 3

FULL-SCALE TRIALS

Chapter 3.1

TRIAL REQUIREMENTS

3.1.1 Introduction

Part 1 of this thesis described the generic problem that any complex system is unlikely to have been fully characterised before entering service and, therefore, that its performance was unlikely to be optimal. The specific case of the propulsion system of an in-service AUV was taken as an example. The AUTOSUB vehicle is designed to have as low a drag coefficient as is compatible with economy of manufacture and efficient utilisation of volume. An analysis of the performance of the system concluded that a principal cause of sub-optimal performance was likely to be that the drag of the hull as deployed, was greater than that anticipated, and/or that the thrust developed by the propeller under in-service conditions was less than expected. Furthermore, it was determined that the characteristics of neither were known for the range of operating conditions experienced in service. Measurements of the drag coefficient had been made on a scale-model during development. However, performance of the in-service vehicle at sea indicated that its real drag was likely to be significantly higher than expected and, furthermore, that this resistance was increasing with time. Additionally there were indications that the control system did not produce the vehicle attitude anticipated. This was likely to further add to resistance by creating lift-induced drag.

Because of the close coupling between the performance of the hull and that of the propeller, if one were known, then, in broad terms, so would be the other. (In practice the performance of each affects the other. This issue is addressed shortly). For the reasons described in part 1, it was decided to concentrate on hull performance. An overall objective was, therefore, to establish the performance of the hull as deployed in-service under its actual operating conditions. This pointed to undertaking as many measurements as possible on the in-service vehicle at sea.

The in-service vehicle has a number of attributes that facilitate investigations, namely:

- It is less than 7m long and so can be readily deployed from small ships.
- Because of its size and propulsion system, fuel costs are reasonable.
- If the trial can be designed such that it can be carried out during planned deployments, costs can be still further reduced.
- The vehicle is already equipped with fully developed on-board navigation, control and data logging systems. It is, therefore, already comprehensively instrumented for positional and dynamic data recording.
- Being a vehicle designed for the collection of oceanographic data, there is already a well-developed suite of instruments for measuring the vehicle's environment, such as those required for measuring depth, temperature and pressure.
- There already existed a large body of in-service performance data.

Nevertheless, there remain significant drawbacks in relying solely on full-scale trials at sea. These include:

- Lack of control over the environment.
- Inability to undertake a detailed investigation of a large range of combinations of factorsbecause of vehicle availability and cost.
- Inability to measure easily the flow fields round the hull.
- Inability to explore potential performance of the vehicle that cannot be achieved within the current performance envelope, for example the benefits of very slow speeds or very low angles of attack.

Additionally, a significant cause of excess drag was expected to be associated with the detail of the hull-form not taken into account during the original experiments. The AUTOSUB hull-form changes from mission to mission with changes in payload. Undertaking measurements of a representative sample of configurations would not be possible on the full-scale vehicle because of availability. It was, therefore, concluded that it would not be possible to undertake all of the measurements required at sea and that many would need to be taken under controlled conditions in a laboratory. The laboratory experiments have been described in part 2. This part of the thesis describes the complementary trials on the in-service vehicle at sea.

The results of the laboratory experiments and at-sea trials undertaken during initial commissioning, may be used to predict the drag of the vehicle as configured for a

particular mission, under the conditions expected to be experienced. However, there will still remain a margin of error between the predicted and actual hull performance. A safety margin will, therefore, still have to be built into the operating envelope to ensure safe recovery of the vehicle. The safety margin is required to allow for:

- The remaining differences between the hull as built and that assumed during modelling.
- The confidence limits implied in the model.
- The unknown interaction between the hull and the propeller resulting from the fact that the presence of the propeller in operation changes the nature of the flow over the hull, especially immediately upstream of the propeller, and the presence of the hull affects the inflow conditions to the propeller.

However, the size of the safety margin could be reduced if a means could be devised to economically measure the performance of the vehicle as built, in its operating environment, and with the propeller operating at representative revolutions. Additional performance could then effectively be gained for the cost of the measurement.

3.1.2 Objective

The objective of the at-sea trials is, therefore, threefold:

1. To aid mission planning by providing information complementary to that obtained in the laboratory and thereby enabling the performance of a particular hull configuration to be predicted for the conditions expected during the mission.
2. To aid mission operation by providing an economical means of assessing the drag performance of the vehicle as deployed in the mission environment.
3. To provide data as a check against the measured model results and so enable prediction accuracy to be improved.

3.1.3 Trial Requirements

The trials are to be designed to measure the following:

1. As a complement to the laboratory experiments:
   - To determine the range of angles-of-attack, and hydroplane angles as a function of speed.

- To establish the relationship between velocity, angle-of-attack and hydroplane angle, to determine which of these need be treated as independent variables when planning the laboratory experiments.

2. In support of operations:
   - To measure drag force as a function of speed across the range of expected operating conditions.
3. For model refinement and comparison with the performance of other vehicles:
   - To determine drag coefficient as a function of Reynolds number.

Chapter 3.2

DRAG MEASURMENT OPTIONS

3.2.1 Introduction

In order to establish the relationship between total drag and advance velocity, angle-of-attack and hydroplane angle, these four parameters need to be measured and recorded as a function of time whilst the vehicle is under way. The vehicle is equipped with a comprehensive self-monitoring and data logging system. The parameters recorded are listed at (Fallows, 2005). Hydroplane angle may be obtained directly from an electro-mechanical transducer attached to the control surface drive mechanism. Body attitude is derived from a sensor forming part of the navigation system. Velocity may be derived from the Acoustic Doppler Log as described in chapter 3.6. Drag, however, is not currently measured.

3.2.2 Drag measurement

There are two principal alternatives for the measurement of this parameter:

- Direct measurement of the thrust required to propel the vehicle at constant speed.
- Inference of drag from vehicle dynamics.

3.2.2.1 Direct drag measurement

At constant velocity, and in a steady state environment, the delivered thrust applied to the vehicle exactly balances the drag force and so measurement of thrust is effectively a direct measurement of drag. Thrust may be applied either from the internal resources of the vehicle, or by an external source.

3.2.2.2 Self-propelled body

Self-propulsion is an attractive option for an autonomous vehicle. In this case, the propeller would be working as normal and so water-flows around the hull and through the propeller would represent realistic operating conditions. Care would be required to ensure that power from the motor is constant. The voltage available from the battery decreases as the battery discharges. In the absence of specific control measures, the power delivered to the motor will, therefore, change with time.

However, a model of battery performance has been derived by (Griffiths, et al, 2002), so control logic to maintain constant power should be possible.

Drag is required to be measured as an independent variable, so ideally it would be measured with known fixed control surface and pitch angles. Maintenance of constant depth under these conditions would require special attention to buoyancy, as described in chapter 3.3. However, the main difficulty of this method is to provide direct measurement of thrust. There is currently no instrument on AUTOSUB to measure this parameter. The three alternatives methods of direct thrust measurement considered here are illustrated in Figure 3.2.1. These are:

a. Ideally thrust measurement should be made as close to the source of the thrust as possible. This implies instrumenting the propeller blades. Strain gauges could be fitted at the blade roots to measure longitudinal thrust. Transmitting the data to the recorder would require either slip rings or some form of direct transmission e.g. by means of optical or rf (radio frequency) bridges. Although mechanically complicated, measurement at this point would have the added advantage that, with some additional sensors to measure rotational and centrifugal forces, a good indication of how the propeller blades are acting could be obtained.
b. The net propeller thrust is transmitted to the remainder of the vehicle through thrust bearings. So a less complex alternative would be to measure the thrust at each of the transmission points, again via strain gauges.
c. The final option considered was to measure the thrust at a junction between the motor/propeller housing and the remainder of the hull. This should be comparatively simple to do, but has the disadvantage of failing to measure the effect of the aft body.

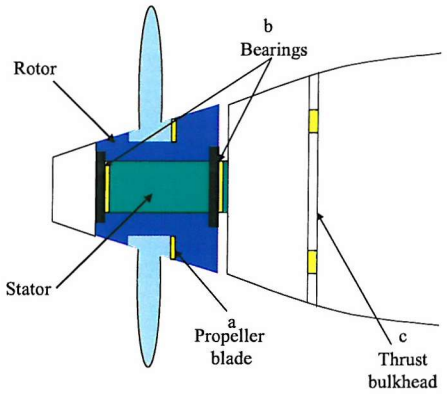

Figure 3.2.1 Alternative thrust measurement points

3.2.2.3 Towed body

The difficulties of drag measurement when self-propelled can be overcome by providing external propulsion and measuring the applied force. This can be done by towing the vehicle at a pre-set depth and measuring drag directly through the tow cable. The cable will itself experience a drag force but the effect of this may be avoided by fitting the strain gauge at the tow point on the vehicle. The attachment point would need careful design to minimise the effect of it and the towrope on the flow of water over the vehicle.

To tow the vehicle at a constant depth, height control would need to be exercised through the on-board control system. This would have implications for control surface drag. Additionally, compensation is required for the upward component of force through the tow cable. Adjustment of the centres of gravity and buoyancy of the vehicle could mitigate these effects.

To produce realistic flow around the aft end of the hull and over the propeller, the propeller would need to rotate at the in-service rate for that vehicle speed. This condition is achieved when it is delivering no net power additional to that required to overcome its inherent frictional and drag losses. This occurs when the net torque on the transmission shaft is zero. Since output torque is already measured it would be straightforward to produce logic to arrange for the motor controller to meet this condition.

An advantage of towing is that it should be possible to produce drag measurements for a range of velocities greater than the current vehicle could achieve from its own resources.

3.2.2.4 Indirect Measurement

Two methods of indirectly inferring the drag characteristics were considered: by means of buoyancy propulsion; and by inference from vehicle dynamics.

3.2.2.4.1 Buoyancy propelled

An alternative method of providing external propulsion is to sink the vehicle tail first and allow it to rise to the surface, nose first, using internal enhanced buoyancy. This was done during the early development of AUTOSUB (Babb, 1994). At terminal velocity the buoyancy-induced force will match that of the drag. There is no tow cable to modify the flow of water over the hull, and the propeller can be rotated as for the towed option to ensure that operational drag conditions are

replicated. Accurate measurement of water conditions over the depth range would be required. Water temperature measurement would be particularly important since it would be likely to change significantly across the range of depth required. This would affect both the density of the water, and hence its drag, and also the density of the buoyancy medium. If the buoyancy medium is air, then there is likely to be a significant 'ballooning' effect. Account will need to be taken of the thermal lag of the air, to allow for its change in temperature as the external temperature varies from surface, to that at depth, and back towards the surface again.

The attitude of the vehicle would need to be measured to ensure that it rises in a stable manner. Provided it did, then the control surfaces may be feathered.

To provide data over a range of velocities it would be necessary to be able to change the buoyancy significantly. The internal volume available for enhanced buoyancy would limit maximum velocity.

3.2.2.4.2 Inference from vehicle dynamics

Each of the above options would involve the development of special instruments and significant, and potentially expensive, modifications to the vehicle. Some would require expensive trials resources, additional to that required for normal operations. An alternative approach, to consider the possibility that drag could be inferred from the inherent dynamics of the vehicle, was, therefore, investigated.

Under steady state conditions (no linear or angular accelerations), the thrust force from the propeller exactly balances the total drag forces. On removal of the thrust the vehicle will decelerate under the influence of the drag force (F_d). The equation of motion describing forward velocity (u) as a function of time (t) under these conditions is:

$$F_d(t) = \frac{d}{dt}(mu) \tag{1}$$

where m is the effective inertial mass of the vehicle.

Now the effective inertial mass is defined by:

$$m(t) = m_v + m_e + m_a, \tag{2}$$

where, m_v is the mass of the vehicle, m_e the mass of the entrained water and m_a the added mass resulting from the interaction between the vehicle and the surrounding water during deceleration.

The vehicle is powered by primary cells, therefore, no exchange of mass across the vehicle boundary occurs as a result of energy consumption during the

deceleration period. The vehicle mass (m_v) is, thus, constant over this period. It is assumed that very little exchange of water occurs between that entrained in the vehicle and the outside world. The mass of entrained water (m_e) is, therefore, also assumed to remain constant. Assuming the vehicle to be neutrally buoyant, the total mass of the vehicle may be considered to be its displacement mass, which is given by:

$$m_d = m_v + m_e = v\rho_{sw}(T), \tag{3}$$

where v is the volume of the vehicle and $\rho_{sw}(T)$ is the density of seawater at the prevailing temperature, T.

Added mass is solely a function of the size and shape of the vehicle and was derived for surge acceleration from measurements made on the scale model in a towing tank, as described in chapter 2.5. Thus, since all of the mass terms may be considered constant for the period of the experiment,

$$F_d = (v\rho_{sw}(T) + m_a)\frac{d}{dt}u. \tag{4}$$

The drag coefficient for the vehicle can then be determined from:

$$C_d = \frac{F_d}{\frac{1}{2}\rho_{sw}u^2 s}, \tag{5}$$

where s is a term representing the surface area of the vehicle.

The depth and temperature at which the experiment takes place may be measured and so the density of seawater, ρ_{sw}, established. The vehicle's surface area, s, may be calculated. Hence from measurements of velocity at small time intervals, F_d and C_d may be calculated.

The total drag of the vehicle will be influenced not just by its speed, but will also be a function of its angle-of-attack and hydroplane angle. These parameters, therefore, also need to be recorded to enable the results to be compared with those obtained from the scale model and with those given for other vehicles.

3.2.4 Selected Approach

Because of the economy and apparent feasibility of the approach, it was decided to design a trial based on self-propulsion and the inference of drag from deceleration data. The trial was to be carried out with minimal changes to on-board instrumentation (in the event no changes were made) and to be performed on an opportunity basis during deployments, primarily planned for other purposes.

Chapter 3.3

EXPERIMENT DESIGN

3.3.1 Introduction

The aims of the experiment are :

- To appreciate the operational range of angles-of-attack, and hydroplane angles as a function of speed.
- To establish the relationship between velocity, angle-of-attack and hydroplane angle to determine which of these need be treated as independent variables.
- To measure drag force as a function of speed across the range of expected operating conditions.

The first 2 aims are designed to inform the laboratory experiments of part 2.

3.3.2 Environment

A principal objective of the experiment is to enable confirmation of the actual drag of the vehicle as configured, under its expected operating conditions. For the measurement to be useful they need to be made under as near realistic operating conditions as possible. This generates a number of requirements.

- Since an AUV is designed to operate at depth, well away from the conditions where wave induced drag occurs, it is necessary to undertake the drag measurements at depth.
- The normal state of the vehicle will have the propeller in situ and working, so the rotation rate of the propeller needs to be representative of that for the normal vehicle speed during the experiment.
- The position of the control surfaces affects the net drag and so their position had to be at least known, and ideally fixed, during the experiment.
- The same applies to the angle-of-attack of the vehicle.

The need to operate in a controlled, or at least known, environment also generated a number of requirements.

- Ideally the experiment will be carried out in still water and will, therefore, take place where there are minimal currents, ideally around slack water. They should be conducted away from surface and bottom currents. Where this is not

practicable, reciprocal runs are required so that tidal effects may be calculated and compensation made.

- Drag is dependent on the density and viscosity of the water. These, in turn, are a function of temperature, salinity and depth. Temperature is itself likely to vary with depth. The experiment should, therefore, preferably be conducted at constant depth, with regular measurements of depth, temperature and salinity recorded.

3.3.3 Practical Considerations

Because of its safety margin of positive buoyancy, to maintain constant depth the vehicle normally flies with the stern-planes at a negative angle-of-attack and with the body of the AUV exhibiting a non-zero angle-of-attack between the direction of motion and the longitudinal axis of the vehicle. Ideally, for the experiment, ballast should be added to achieve genuine neutral buoyancy at the experiment depth. Safety may be assured by the presence of drop weights, and the experiment conducted in sufficiently shallow water, that, if the drop weight system fails, divers may still recover the vehicle.

In the event, the standard in-service vehicle was used with its small net positive buoyancy (100 N). It was, therefore, necessary to allow for the forces generated by this and the countervailing negative lift provided by the control system. Additionally, the control system is only capable of maintaining a stable attitude above a minimum speed. This condition needs to be detected and data obtained at lower speeds needs to be either discarded or corrected.

In order to reflect the true in-service conditions, it is necessary to consider the presence of the propeller. Its presence and rotation rate affects the flow of the water over the hull (especially around the stern) and hence the net drag. It is, therefore, necessary for it to be rotated at such a rate as to cause neither thrust nor drag during the deceleration phase. As argued in chapter 3.2, this condition occurs when the net torque on the shaft is zero. In practice the motor current was set to deliver a speed thought to be consistent with this condition.

Assessment of the displacement mass needs to take account of the fact that the water is trapped at the surface at one temperature, whilst the experiment is conducted at depth at another temperature. Either the effects of thermal lag need to be taken into account or the vehicle has to spend sufficient time at depth for the temperatures to

equalise. For this reason the trial is intended to be performed at the end of deployments.

3.3.4 Trial Specification

A single trial has been devised to meet the three objectives of: establishing total drag; determining the relationship between speed of advance, angle-of-attack and control surface angle; and providing validation data in support of planned laboratory experiments. A further objective of the trial is that it should be designed, if possible, such that it requires no modification to the standard vehicle.

The conditions needed to meet each objective are described next, followed by a description of the integrated trial. To ensure the stability of the temperature of the entrained water, the vehicle is to have been in operation at depth for at least one hour before any trial.

3.3.4.1 Objective 1 – Deceleration Trial

The vehicle is run straight and level at maximum speed and at a depth of at least ten vehicle diameters from both the free surface and the sea-bed. The thrust to the vehicle is then cut to zero, by reducing the power to the motor, so that the motor output torque equals the internal losses due to the sum of the friction of the bearings and the viscosity of any internal fluid. Since the vehicle is not instrumented to enable this condition to be monitored, the motor (and hence propeller) is to be set at the speed setting (based on experience) most likely to achieve this result as a function of vehicle speed. Following the removal of thrust, speed is to be recorded at the maximum possible data rate (limited by the capability of the ACDP). Because of the residual buoyancy, the vehicle will maintain a hydroplane angle and angle-of-attack in an attempt to maintain constant depth. These angles will increase as speed decreases. These parameters are, therefore, also to be logged for the duration of the trial at maximum data rate. The qualities of the environment will also affect the results so sea temperature and salinity are also to be recorded together with depth. The experiment is to be repeated on a reciprocal course to facilitate the elimination of errors due to sea currents.

3.3.4.2 Objective 2 – Body Attitude Trial

The vehicle is to be run straight and level at a depth of at least ten vehicle diameters from the free surface and from the sea-bed. Vehicle speed is to be increased

from zero to maximum in a series of steps. At each speed step, speed, angle-of-attack and hydroplane angle is to be logged. Speed is then to be decreased back to zero in identical steps to test for hysteresis. The whole process is then to be repeated immediately on a reciprocal course to allow for bias induced by sea currents. Again sea temperature and salinity are to be recorded together with depth.

Ideally the number of steps is to be as large as possible. However, the time available for the trial is limited, so 5 steps were chosen. This enables higher order relationships between the parameters to be determined should they prove to be non-linear.

The time at each step is kept to the minimum consistent with providing a statistically meaningful sample of data points:

$$t_s = t_t + t_r$$

where,

t_t = transient time to allow the vehicle to settle into a steady state, i.e. constant velocity and angle-of-attack (pitch angle). This is assumed to be one minute, and is to be checked against the real time observations.

t_r = time required for an adequate number of samples of speed, angle-of-attack and hydroplane angle to be taken. Assuming a maximum data rate of 1 Hz then 4 minutes will give 240 samples.

3.3.4.3 Combined experiments 1 & 2

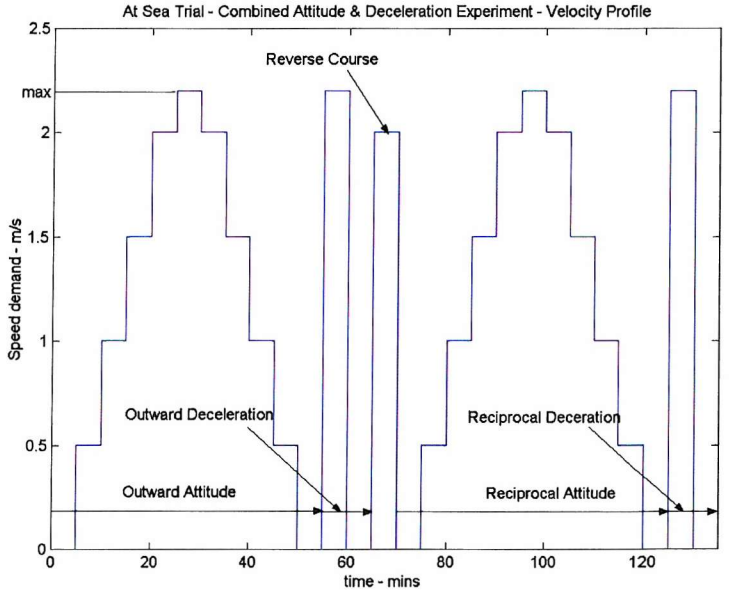

Figure 3.3.2 Combined trial specification

A standard trial that facilitated the measurement of all of these propulsion parameters is to be used to determine the effect of change to hull-formresulting from particular instrument sets for individual missions. The two experiments are, therefore, combined to define a single standard trial. The profile is given at Figure 3.3.2.

3.3.5 Conclusion

The aims of the experiment may be met by a single integrated trial of less than 3 hours duration. The trial may be undertaken on the standard vehicle with no modification. It is ideally suited for being performed at the end of the work-up period immediately prior to a mission. Because of its inherent simplicity, it should be possible to automate the analysis of a standard trial so that the results can promptly be made available for mission planning purposes.

Chapter 3.4

TRIAL PROTOTYPING

3.4.1 Introduction

Because of the availability of the vehicle, to date it has only been possible to make one attempt at the deceleration/body-attitude trial. This has proven to be a useful prototyping exercise, and despite significant problems, has been sufficient to demonstrate the method. The lessons learned have been incorporated in a revised trials specification, but, as yet, higher priority work during deployments has pre-empted a re-run.

3.4.2 Trial route

Trial m286 was performed on 23 June 2002 in the vicinity of 50°08'N, 4°90'W (a few miles off Falmouth in the western English Channel, over the continental shelf).

The track of the total deployment is illustrated in Figure 3.4.1. The vehicle transited on the surface for instrument checks and to establish its navigation fix. Having reached its dive point, it descended to approximately 16 m. It then retraced its transit at depth, during which time the temperature of the entrained water had the opportunity to stabilise. Next it changed heading and the trial was performed, after which, the vehicle was recovered to the support ship.

3.4.3 Vehicle configuration

The standard vehicle was used with no modification. It, therefore, had 100 N of positive buoyancy and needed to 'fly' to maintain depth. This meant that it would not be possible for the vehicle to experience deceleration at a constant depth, with zero angle-of-attack and with hydroplanes feathered. Rather, these two parameters would need to be recorded.

No inertial sensor was fitted, so direct measurement of deceleration was not possible. However, two Acoustic Current Doppler Profilers were fitted, each of which is capable of accurate measurement of speed through the water with processed outputs

at an acceptable data rate of 1Hz. (A description of the operation of these ADCPs is given in chapter 3.5).

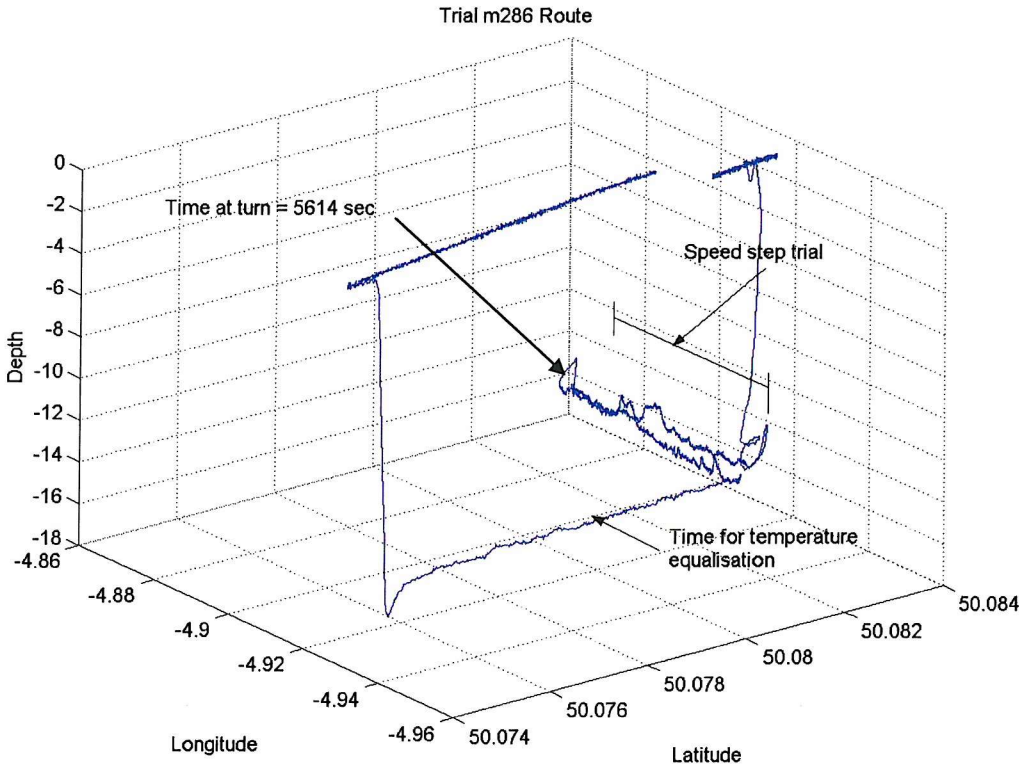

Figure 3.4.1 Trial route

3.4.4 Environmental conditions

Figure 3.4.1 demonstrates that the two halves of the trial were conducted in rapid succession and on reciprocal courses. The specified condition for the ability to detect tidal effects was, therefore, achieved.

Figure 3.4.2 illustrates that a reasonably constant depth of more than 10 diameters was maintained throughout the trial. The results are, therefore, unlikely to have been affected by any wave-making drag or other surface effects.

The vehicle travelled at depth for approximately 30 minutes before the commencement of the trial to allow for stabilisation of the temperature of the entrained water. Figure 3.4.3 gives the external water temperature for the duration of the deployment. This indicates that there was only 1.5° C difference between the temperature at the surface and that at the trial depth. It is, therefore, concluded that the results are unlikely to have been affected by any change in the temperature, and hence mass, of the entrained water.

The environmental conditions for the trial were, therefore, as specified.

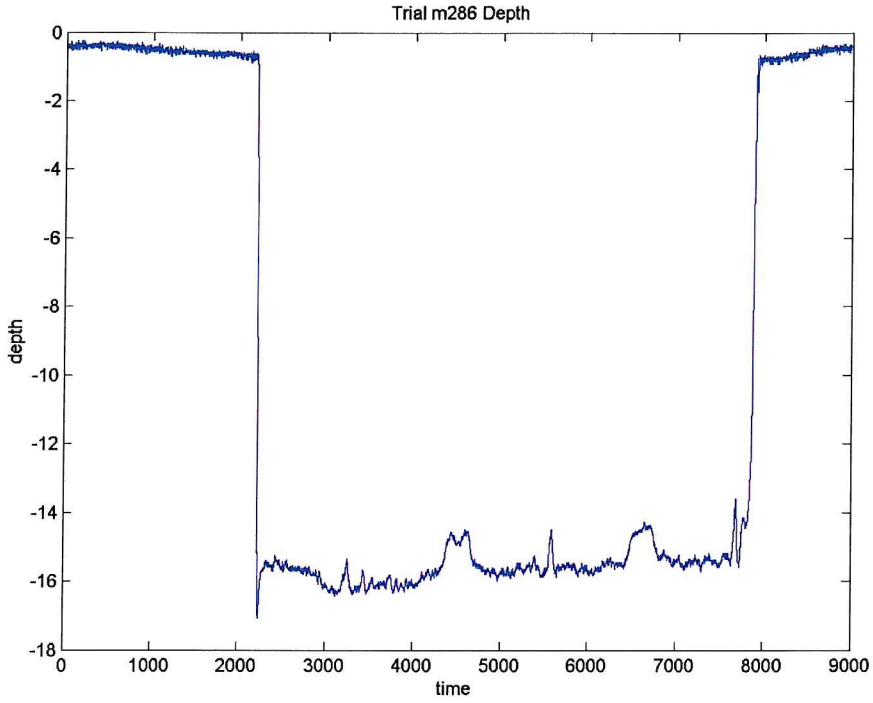

Figure 3.4.2 Depth record for Trial m268

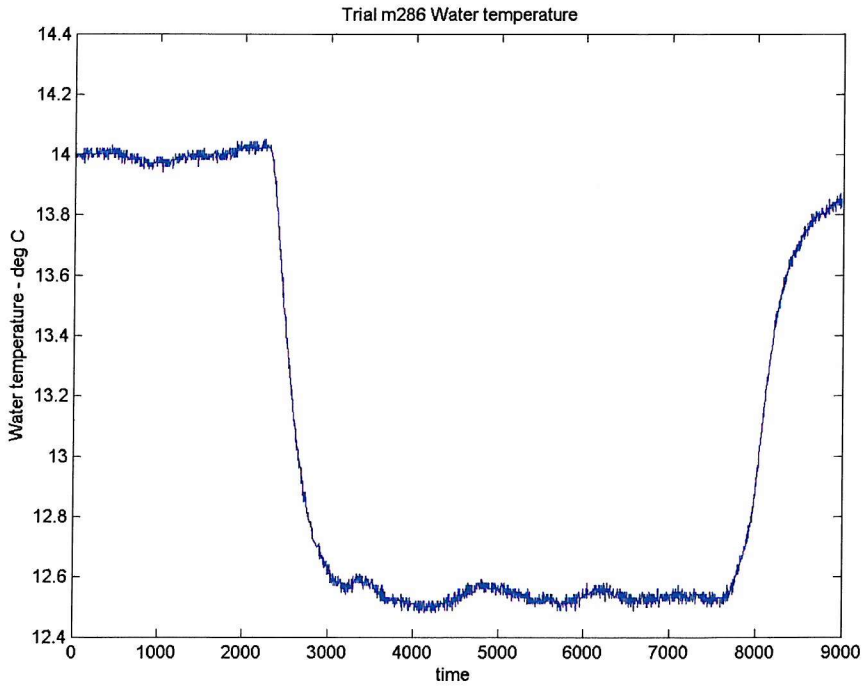

Figure 3.4.3 Trial m286 external water temperature

3.4.5 Speed control

To meet the trials specification, the speed of the vehicle needed to be changed stepwise. This was to be achieved by rapid change in the propeller rotation rate. The propeller rotation rate, as a function of time for the trial period, is given in Figure 3.4.4. The two spikes at the start and end of the trial indicate the deceleration experiments and the two sets of steps up and down indicate the speed step experiments. The profile is symmetrical about the centre, showing that the same conditions were achieved both on the outbound and return legs.

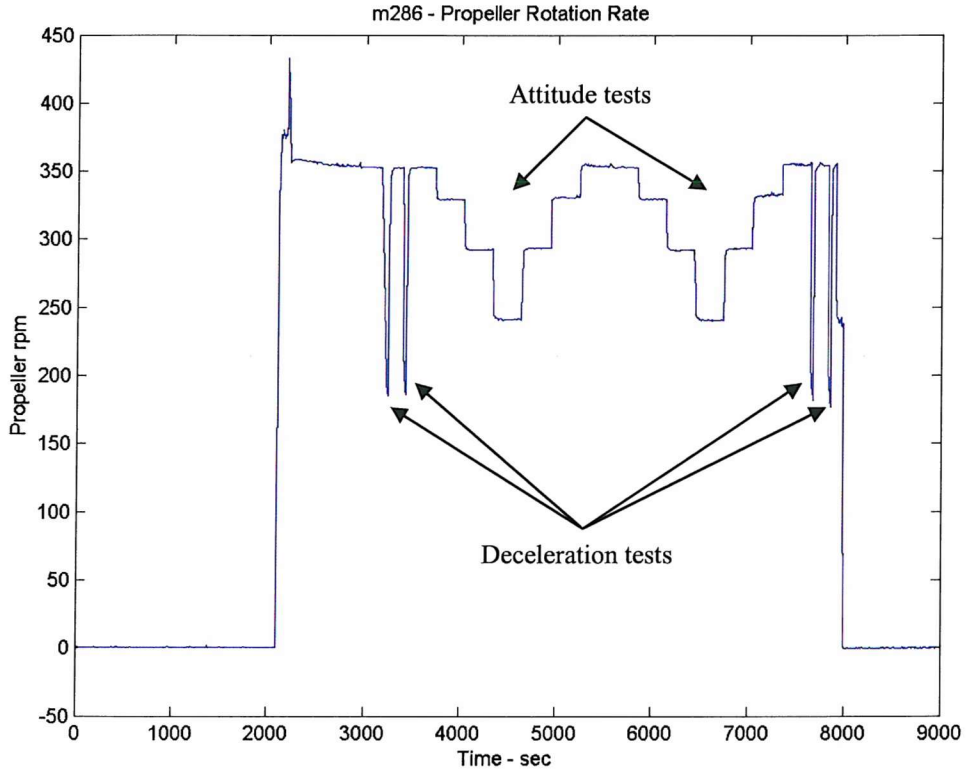

Figure 3.4.4 Trial m286 propeller rotation rate

3.4.6 Data record

Although the conduct of the trial was satisfactory, there were significant shortfalls in the data collected. To start with, only one trial has been performed to date, whereas it had been intended to undertake the trial on a regular basis and with different vehicle configurations, so that a statistically significant picture could be developed.

Further, this trial was undertaken during the first deployment of the vehicle following a major rebuild and upgrade of the navigation and data system. It was,

therefore, subject to the normal teething troubles expected under these circumstances. These included failure of one of the two ADCPs (Acoustic Doppler Current Profilers, the principal velocity sensor) fitted for this deployment, compounded by some loss of data within the data logging system and a lower data recording rate than required.

At the heart of the method, is the ability to measure deceleration. This was to be derived from speed measurements made by the Doppler logs. To achieve an accurate indication of deceleration requires speed to be measured at small intervals of time. This requires as high a data rate as possible. The loss of one of the two ADCPs and the reduction of the data-recording rate to 0.5 Hz, therefore, severely limits the accuracy of the results. Data drop-outs in the data logging-system amplify the data processing challenge. These issues are addressed in the next chapter.

3.4.7 Conclusion

The single trial conducted to date has demonstrated that the unmodified vehicle is capable of carrying out the manoeuvres as specified and logging the required data. However, teething problems with the on-board instrumentation meant that the data generated from this trial made the data processing more complex than it would otherwise have been.

Chapter 3.5

DATA PRE-PROCESSING

3.5.1 Introduction

Before the principle relationships can be obtained the data requires pre-processing in order to ameliorate the limitations of the results obtained from the prototype trial described in chapter 3.4.

The objectives of pre-processing the data are:

- To clean the data to remove the effects of data drop-outs.
- To establish which data sets from the ADCP provide the best indication of the speed of the vehicle as a function of time.
- To determine the precise timing of events within the trial so that the data may be partitioned for subsequent analysis.

3.5.2 Data preparation

The vehicle is comprehensively instrumented and the data logger recorded some 387 channels of data (Fallows, 2005). Of these only those concerned with speed measurement, pitch angle, state of the propulsion system and position of the control surfaces were relevant to this analysis. The data logger records data at fixed intervals. A missed data point for a particular channel is indicated by the code '–999'. For the trial under consideration there was a fault with the logger, which resulted in a large number of missed data points. The presence of the '-999' code produced significant noise in the output of some channels. A data cleaning algorithm was therefore written, the efficacy of which is illustrated in Figure 3.5.2.

3.5.3 Speed measurement

Vehicle speed was derived from the ADCP. This instrument is primarily intended for navigation purposes and is optimised to determine speed over the ground. It comprises a 300 kHz sonar system which outputs velocity data at a maximum 1 Hz data rate into a number of range gated bins. Bin 0 is timed to capture reflections from the seabed and so provide speed over ground. Bins 1 to 15 capture specula reflections from particles in the water column, and so provide an indication of speed through the water. The bins are numbered from 1, being the closest to the vehicle, to 15, being

furthest from it. There was concern that the data in Bin 1 may be contaminated by noise from the vehicle.

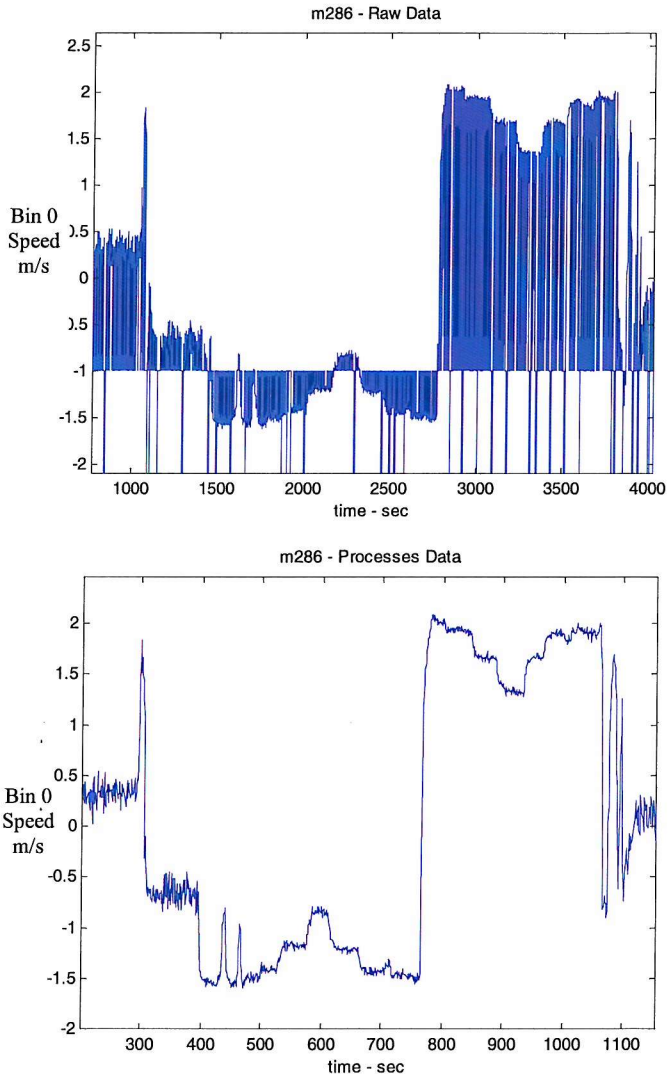

Figure 3.5.2 Efficacy of data preparation

To produce directionality, beams of sound are formed by phase control of an array of hydrophones. The number of elements in the array is necessarily restricted by available space. Consequently the radiation pattern exhibits significant sidelobes. This could result in the furthest Bins being contaminated by sidelobe reflections from the seabed. The overall geometry is illustrated in Figure 3.5.3.

Figure 3.5.6 shows data from Bins 0 to 6 for the first deceleration trial. The data from Bins 1 to 4 are virtually identical. That from Bin 0 indicates a lower speed than Bins 1 to 4, revealing that the tide is setting against the vehicle. The data from bin 5 is clearly from a different set from that of bins 1 to 4 and exhibits the characteristics of contamination by ground reflections. Bin 6 is so contaminated that its data overlays

that of Bin 0 for much of the data set. As would be expected, Bins 7 to 15 are similarly contaminated, although their records are not included in this Figure for reasons of clarity. Speed through the water was, therefore, calculated using data from bins 1 to 4 only.

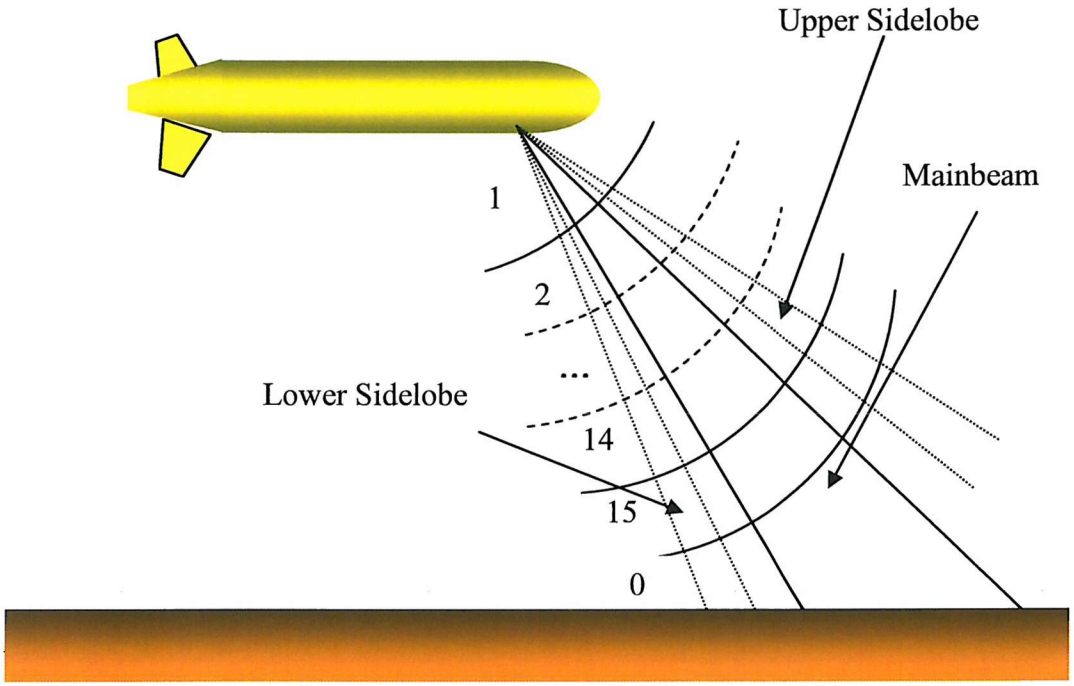

Figure 3.5.3 ADCP geometry

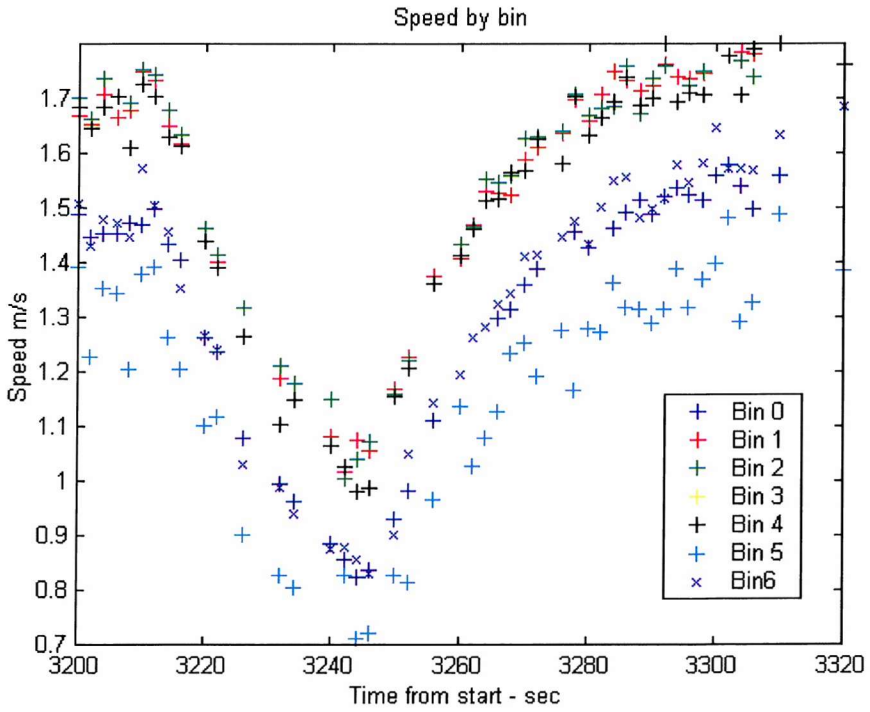

Figure 3.5.6 Details of speed data by Bin

The speed for the whole trial, from the first four Bins only, is shown at Figure 3.5.4.

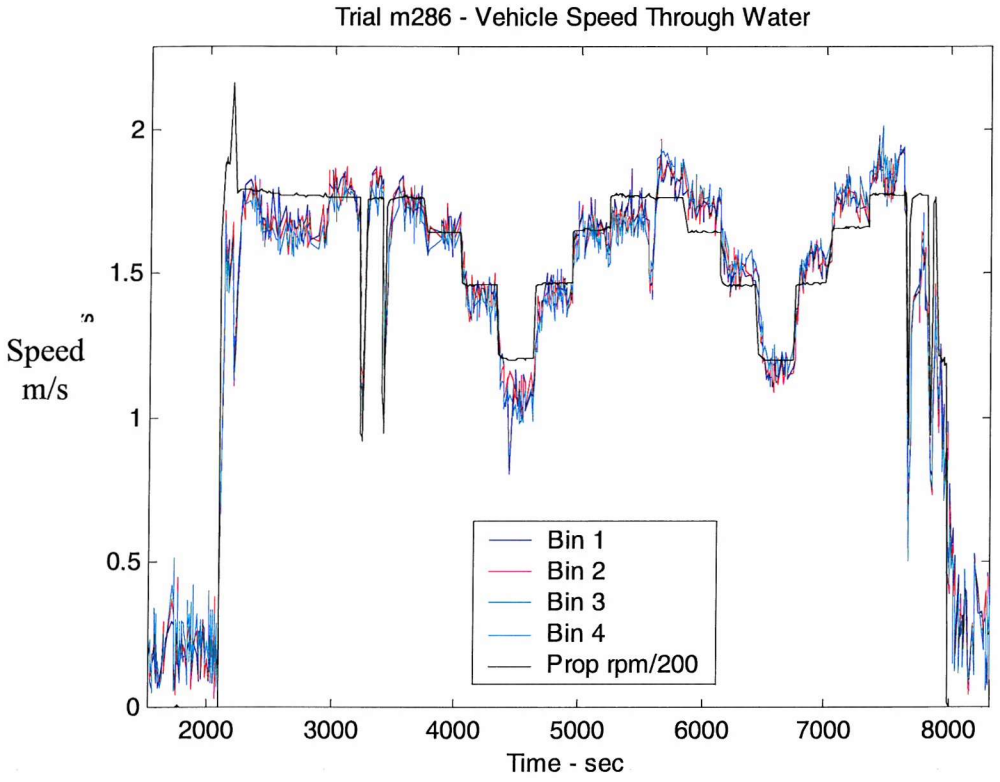

Figure 3.5.4 Speed by Bin

The data from each of these bins exhibit similar means and variances. It is, therefore, concluded that they are not significantly contaminated. Each uncontaminated bin provides statistically independent data sets since they are derived from independent sets of specula reflections. Thus, all data from these bins may be used for determining the speed of the vehicle through the water.

3.5.4 Event timing

The criterion for the start and end of both the deceleration data and the change of speed for body and control surface performance is change in propulsive power. The parameter taken to indicate this was change in propeller rotation rate since this provides a particularly clean signal. However, there was concern that this might not provide a true indication since, on removal of motor torque, inertial forces may maintain propeller rotation for a short but significant time. Change in propeller rotation rate was, therefore, correlated with the power applied to the motor.

Now the motor operates at constant voltage with power to it being controlled by means of a MOSFET commutator. This switches current at the rate necessary to

achieve the mean current required. Mean motor current is, therefore, a reliable indicator of motor power. Figure 3.5.7 shows propeller speed and motor current plotted against the same time axis. This clearly demonstrates that the propeller rotation rate does, in fact, respond practically instantaneously to change in motor power. Propeller rotation rate is, therefore, a reliable indicator of event timing.

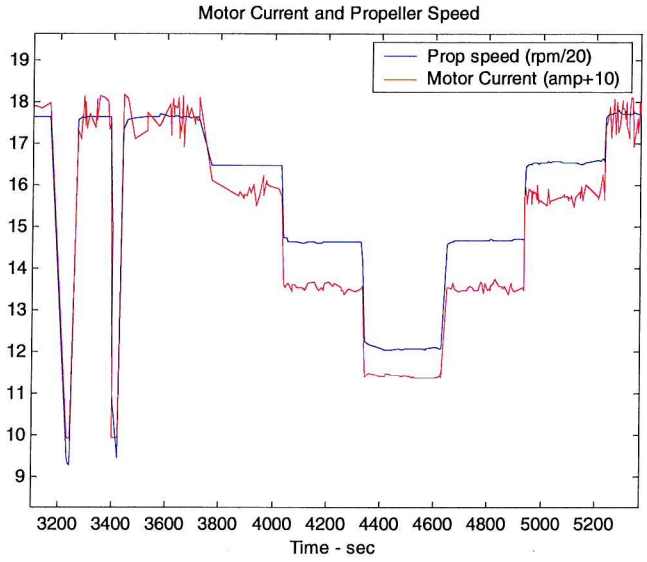

Figure 3.5.7 Propeller speed and motor current

The first differential of propeller rotation rate provides an even more precise indication of a change in propulsion, with the sense of the spike indicating whether the change in speed was an increase (positive) or a decrease (negative). This parameter was, therefore, taken as the event-timing signal and is illustrated in Figure 3.5.8.

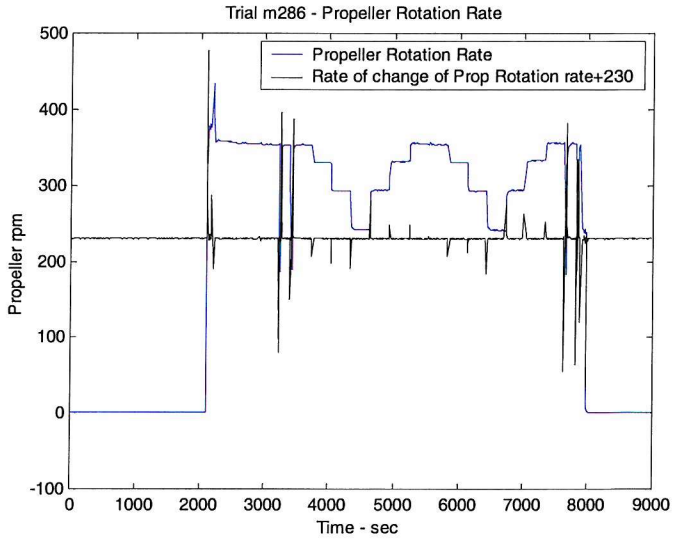

rpm

Figure 3.5.8 Event timing

3.5.5 Conclusions

Limitations in the data collected from this trial, meant that the data required pre-processing prior to the final analysis required to establish relationships that form the objective of this trial. A method of cleaning the data, to remove the effects of data drop-outs, has been developed and demonstrated. The ADCP outputs that provide the best indication of vehicle speed through the water have been identified. These are shown to provide four independent samples of speed data. And finally, the first differential of propeller rotation rate has been demonstrated to provide precise indication of event timing.

Having established these processes and data qualities, it is now possible to address the derivation of the required relationships.

Chapter 3.6

ANGLE-OF-ATTACK, HYDROPLANE ANGLE AND SPEED

3.6.1 Introduction

The previous chapter: established a means for cleaning the data; identified which ADCP outputs to use for speed measurement; and identified the key marker for event timing. It is now possible to analyse the data obtained in the trial described in chapter 3.4 to obtain the first of the key relationships: that between hydroplane angle, angle-of-attack and speed.

3.6.2 Determination of the relationship between speed, hull angle-of-attack and control surface angle

The relationship is found from measurements of angle-of-attack and hydroplane angle made under a series of steady state speed runs. Speed is stepped down and then back up, to determine whether the body and control surface angles assumed for any given speed are dependent upon the initial conditions. The whole trial was then repeated on a reciprocal course, to maximise the opportunity to detect any other uncontrolled effects, including any influence resulting from tidal conditions.

A Matlab script contained in (Fallows, 2005) was written to determine the relationship. The relevant data sets are identified and cleaned. Speed is calculated from the outputs of the Doppler Log Bins 0 to 4. The outputs of the log are given in terms of easterly, northerly and down velocities (u_e, u_n and u_d), so net velocity (u) is calculated as: $u = \sqrt{u_e^{\,2} + u_n^{\,2} + u_d^{\,2}}$.

The times at which speed changes are made is derived from the first differential of propeller rotation rate (Figure 3.6.1).

Speed was changed at nominally 240 sec intervals as shown in Figure 3.6.2. The motor power applied on both the outward and return courses was nominally identical and, therefore, speed through the water would be nominally the same in each direction.

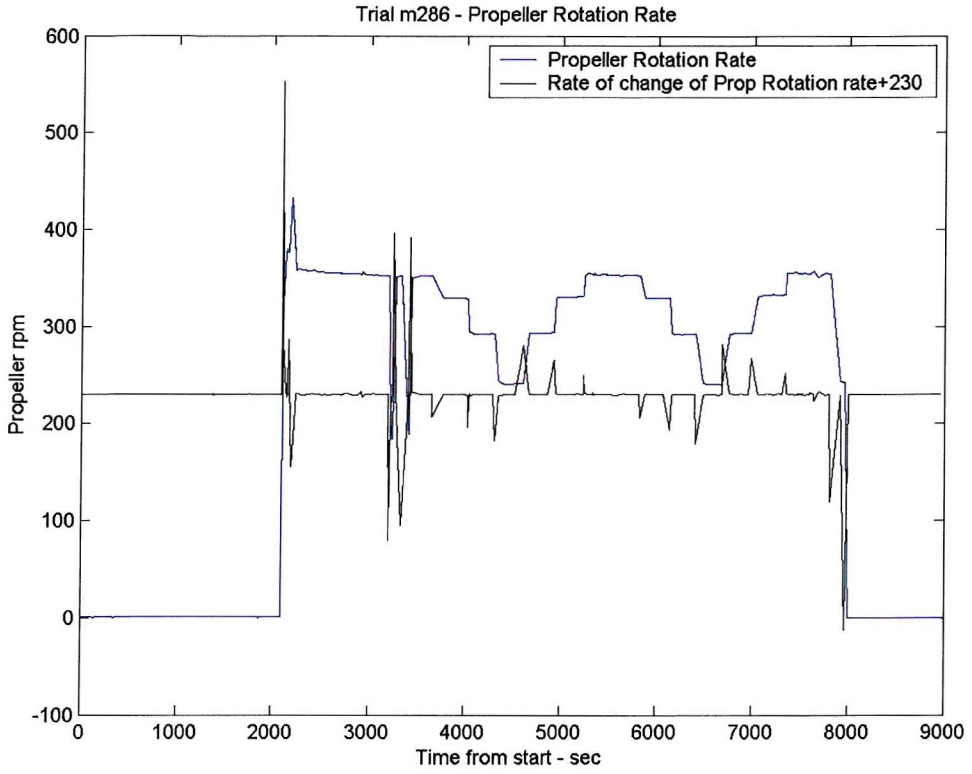

Figure 3.6.1 Event timing

The speed at each step was plotted against a normal distribution using a standard function within the data processing package used. This provides an indication as to whether normal statistics may reliably be used. The experimental data points (indicated by +) are shown plotted against the probability that they would have occurred if their distribution was normal about the mean. Here, the y axis intervals is proportional to the distance between quantiles of a normal distribution in order to linearise the plot. The solid line connects the 25^{th} and 75^{th} percentiles of the data in a manner that is insensitive to the extremes of the data. This line is then projected as a broken line to the ends of the sample. If all data points are close to the line, then the assumption of normality is deemed to be reasonable. The plot at Figure 3.6.3 shows clear deviation from the normal, with the plot deviating from the straight line at both extremes.

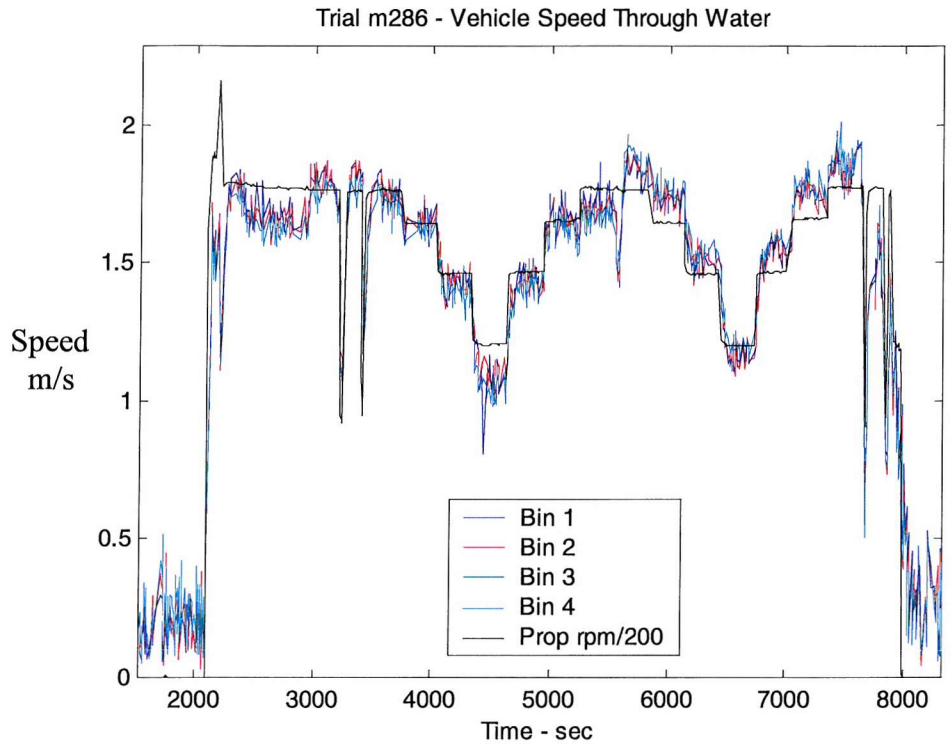

Figure 3.6.2 Speed steps

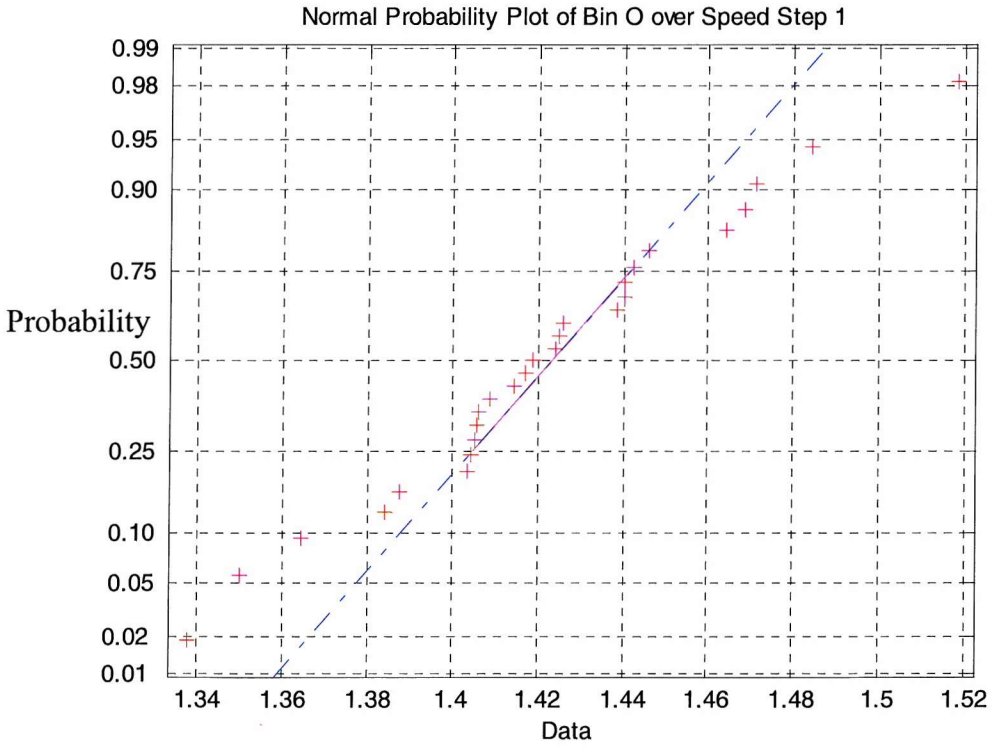

Figure 3.6.3 Normal probability plot, all data

Closer inspection of the data indicated that neither speed nor body angle stabilised as rapidly as had been expected. Figure 3.6.4 compares stabilisation time for

both acceleration and deceleration. The time to stabilise the vehicle is of the order of 20 to 120 seconds. The stabilisation time, coupled with the low data rate identified in chapter 3.2, resulted in many fewer data points than expected. This, in turn, affects the confidence with which the results may be stated.

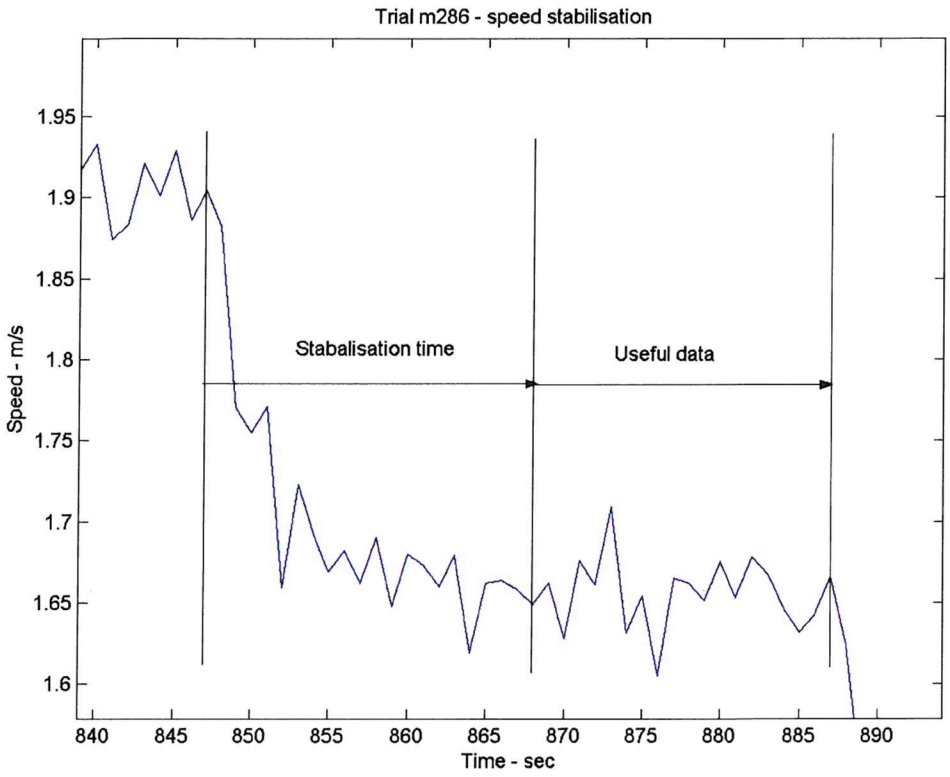

Figure 3.6.4 Speed stabilisation time

The steady state speed through the water at each speed step, derived from ADCP Bins 1 to 4 and after allowing for settling time, is given at Figure 3.6.6, together with the 95% confidence limits.

Figure 3.6.7 shows the relationship between speed and the body and hydroplane angles after allowing for settling time. The results can be seen for increasing and decreasing speed and for the outward and return legs. An apparent effect of the current may be seen, but there is little indication of hysteresis.

The relationships between speed, angle-of-attack and hydroplane angle are illustrated in Figure 3.6.9. There is a strong correlation between speed and hull angle-of-attack but a low correlation between hydroplane angle and either of the other two parameters, possibly due to the hydroplane continually hunting.

The angle-of-attack and hydroplane angle per speed step are given at Figure 3.6.8, together with 95% confidence intervals. Because of the poor confidence in the value for speed step 8, this data was removed from subsequent processing.

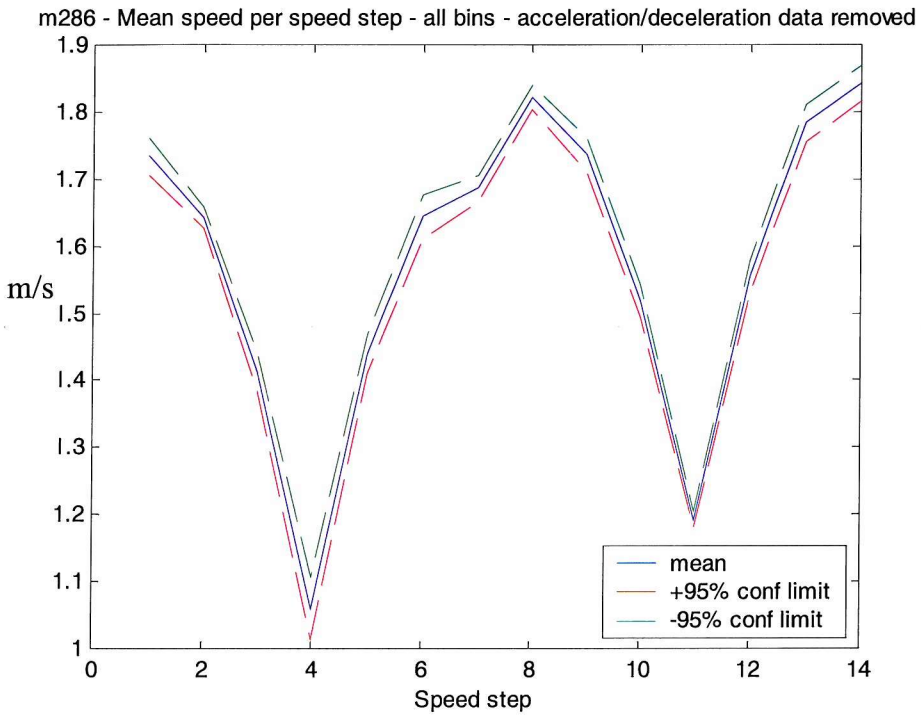

Figure 3.6.6 Mean speed per step

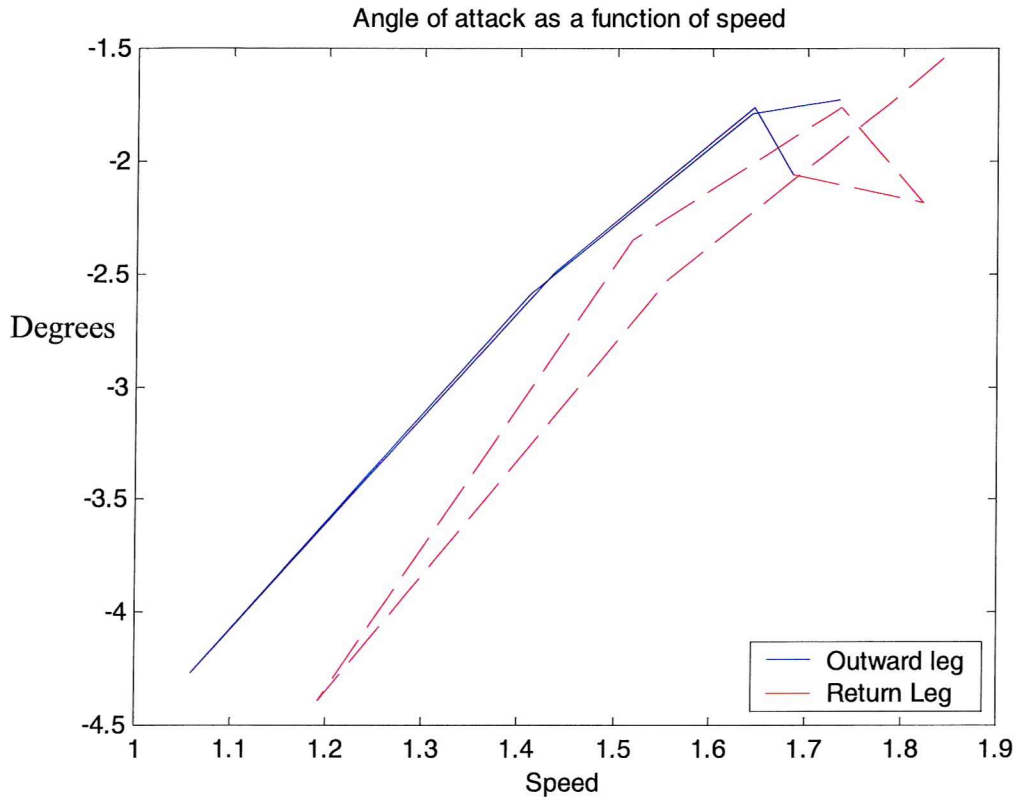

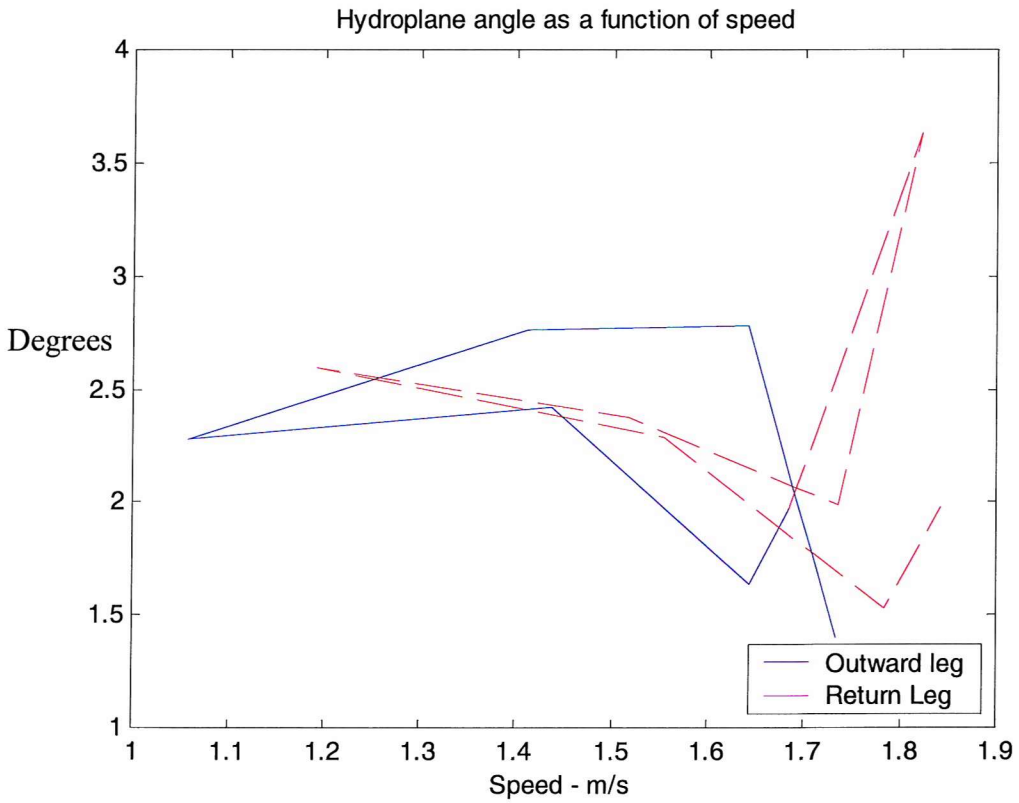

Figure 3.6.7 Angles vs. speed

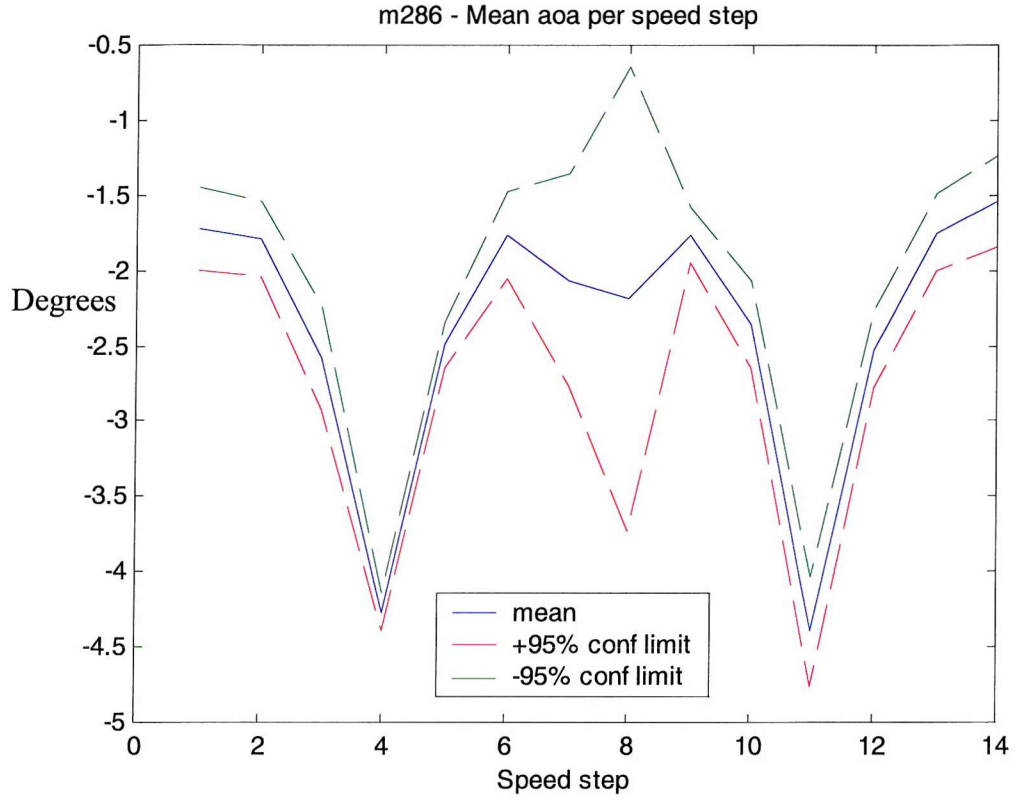

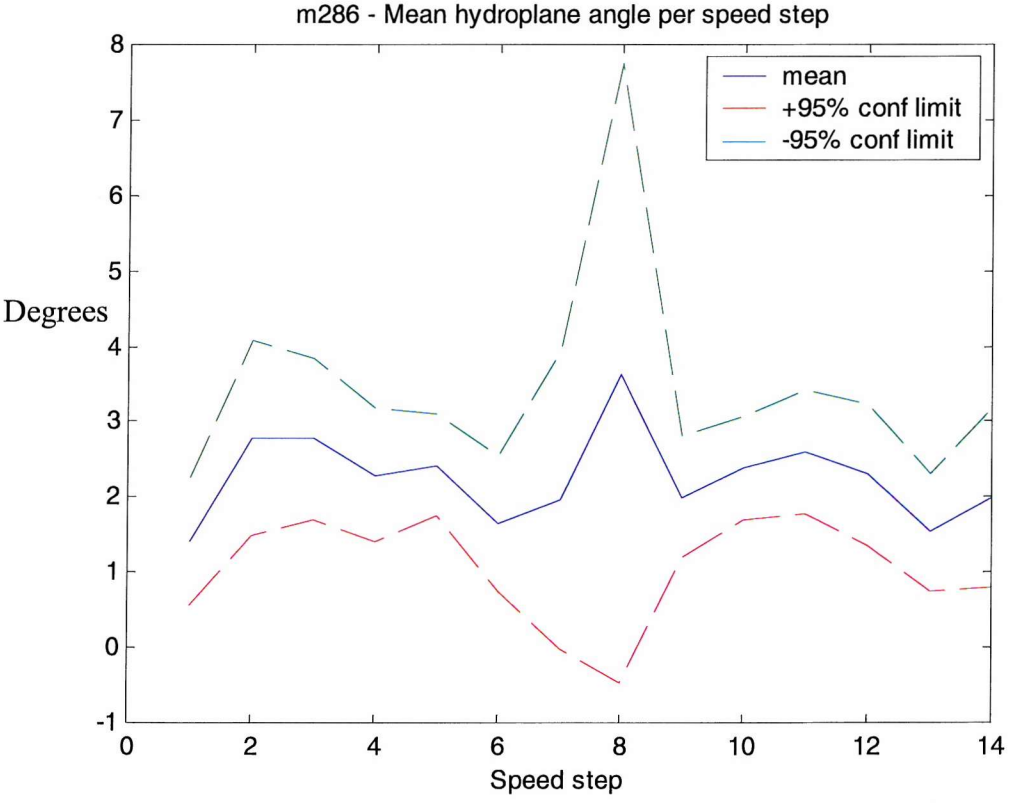

Figure 3.6.8 Angles by speed step

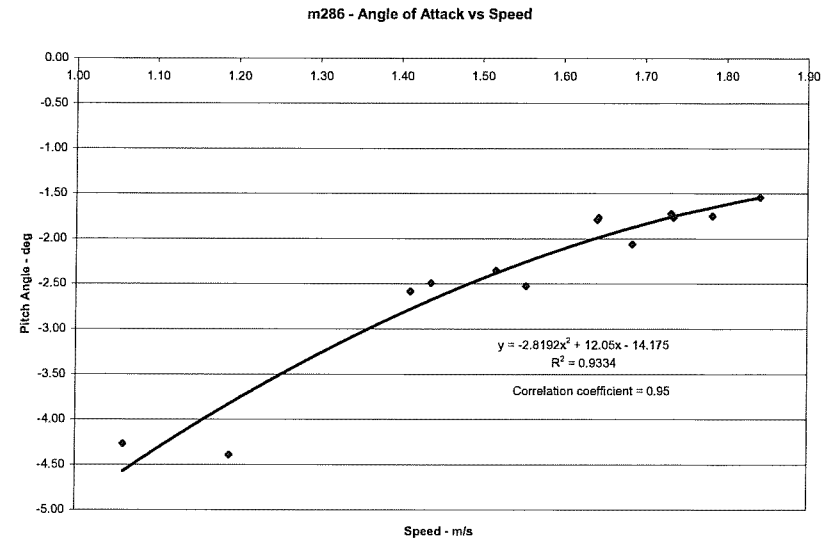

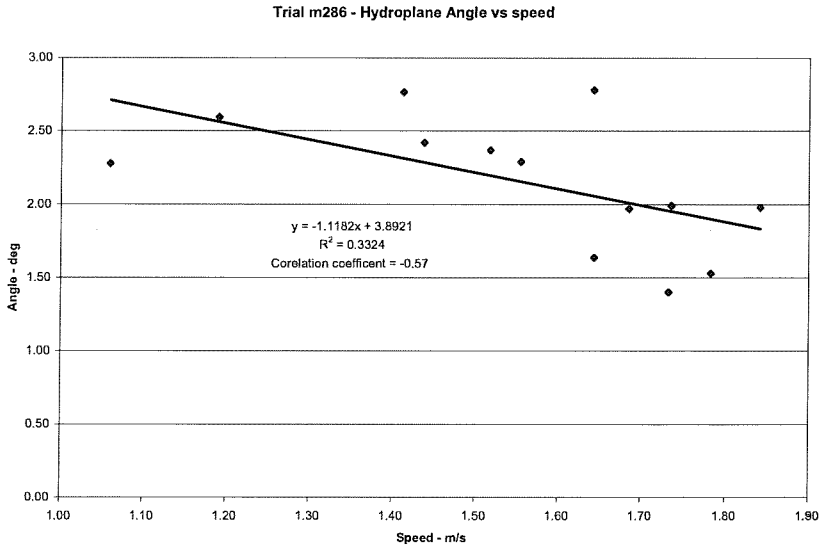

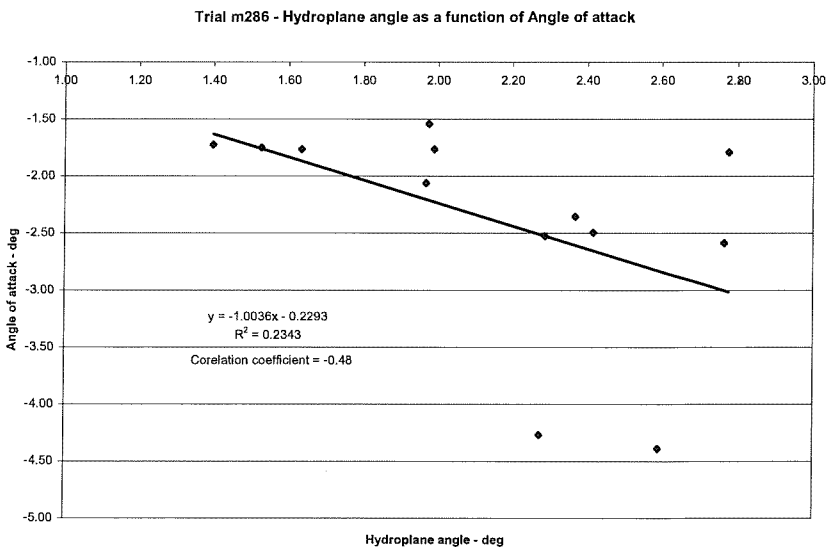

Figure 3.6.9 Relationships between speed, angle-of-attack and hydroplane angle

3.6.3 Conclusions

The results are severely limited by the very small sample of useful data obtained. This was due to a number of causes, including the low data rate and the longer than expected time taken for the speed of the vehicle to stabilise following acceleration and deceleration. Nevertheless, the results obtained are sufficient to demonstrate that this method of determining the relationship between angle-of-attack, hydroplane angle and speed for the actual vehicle at sea is feasible and requires no modification to the standard vehicle. The problem of paucity of data is readily overcome by spending more time at each of the speed steps.

The results obtained to date indicate that there is a strong correlation between speed and angle-of-attack of the hull. The relationship follows a square law, with the provisional empirical formula for the relationship being:

$$\alpha = -2.8u^2 + 12u - 14.175.$$

Since only one trial has been performed to date it is only possible to assert that this relationship holds for the hull configuration tested and for the speed range 1 to 2 m/s.

The correlation between hydroplane angle and speed is significantly weaker, such that, with the data available, it is not possible to state it with any certainty. One of the consequences of this was that hydroplane angle and angle-of-attack had to be treated as independent variables for the purposes of the laboratory experiments in part 2. However, in general it can be seen that hydroplane angles are small (of the order of 2^{o}) across the range of speeds and angles-of-attack considered here and for this configuration of the vehicle.

Chapter 3.7

DETERMINATION OF THE DRAG CHARACTERISTICS OF THE VEHICLE FROM DECELERATION DATA

3.7.1 Introduction

Chapter 3.2 explained how it should be possible to derive the drag of the vehicle, by measuring its deceleration once propulsive power is removed, provided that the mass and added mass of the vehicle is known. A description of how added mass may be derived from towing-tank data is given in chapter 2.5, together with an estimate of this parameter for the bare AUTOSUB hull form. In this chapter the analysis necessary to derive drag is demonstrated and a drag curve for the configuration tested in the trial described in chapter 3.4 is obtained.

3.7.2 Source Data

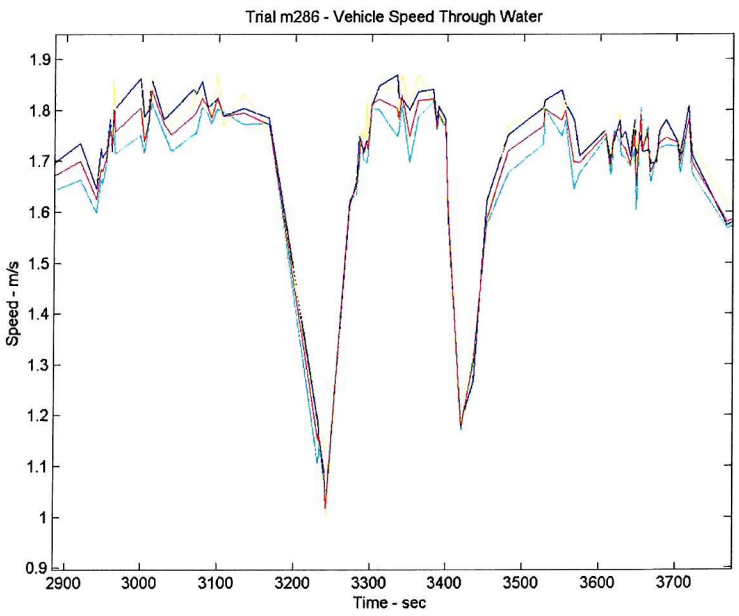

Figure 3.7.1 Speed during deceleration, 4 Bins

Two deceleration experiments were conducted on each of the outward and return legs of the trial. The speed profile of those on the outward leg is shown in Figure 3.7.1.

The speed profile for all four of the experiments is shown in Figure 3.7.2.

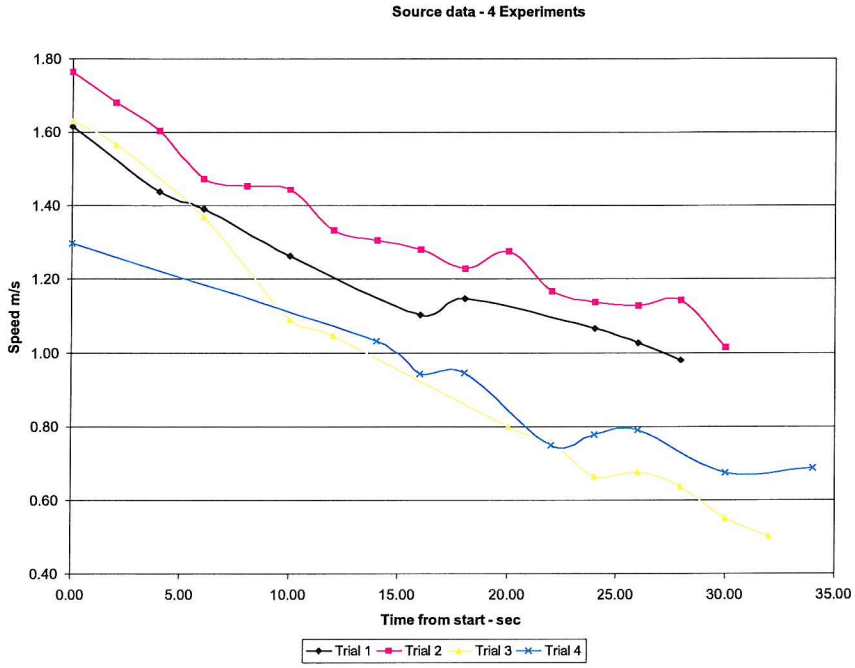

Figure 3.7.2 Speed data for all 4 experiments

Unfortunately, the two trials on the return leg were initiated immediately following the previous manoeuvre, without allowing sufficient time for the vehicle to stabilise in speed and attitude. However, the two trials on the outward leg produced data of comparable orders of magnitude and time., therefore, it is this data that is used in the subsequent analysis (Figure 3.7.3).

Speed as a function of time from the beginning of each of the experiments is shown in Figure 3.7.4.

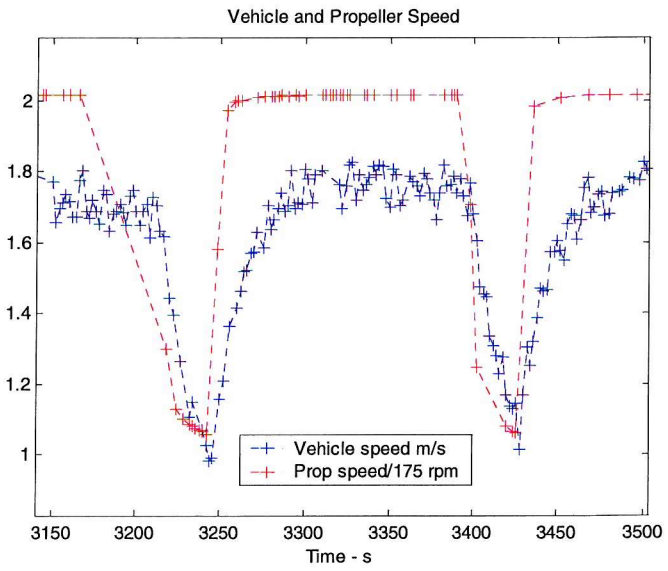

Figure 3.7.3 Deceleration data

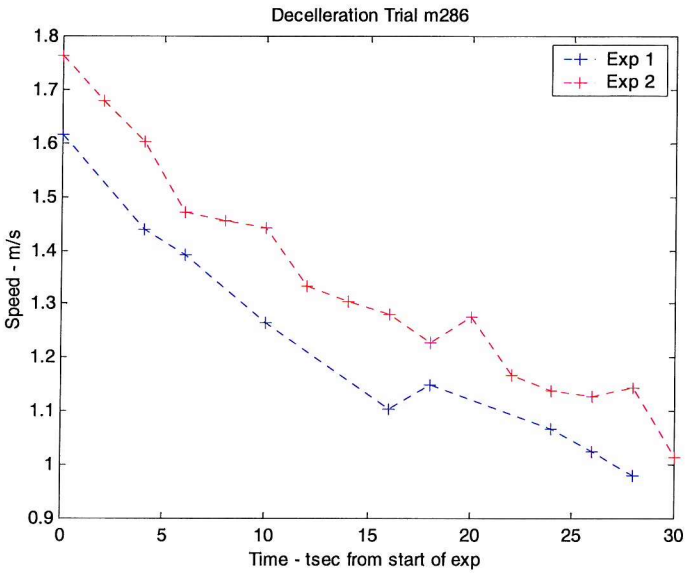

Figure 3.7.4 Speed from the start of each trial

Clearly there remain anomalies in this data since, for example, between 15 and 20 secs from the start of each trial speed appears to increase. Figure 3.7.5 shows hull attitude compared with speed. This indicates that the attitude of the vehicle changes rapidly as the control system attempts to maintain height. Drag as a function of angle-of-attack across the speed range has been obtained from the laboratory experiments described in part 2, so correction may be made for this. However, for this trial angle-of-attack only varies between 1 and 2° and, therefore, the correction required is small compared with other uncertainties in the result, as will become apparent.

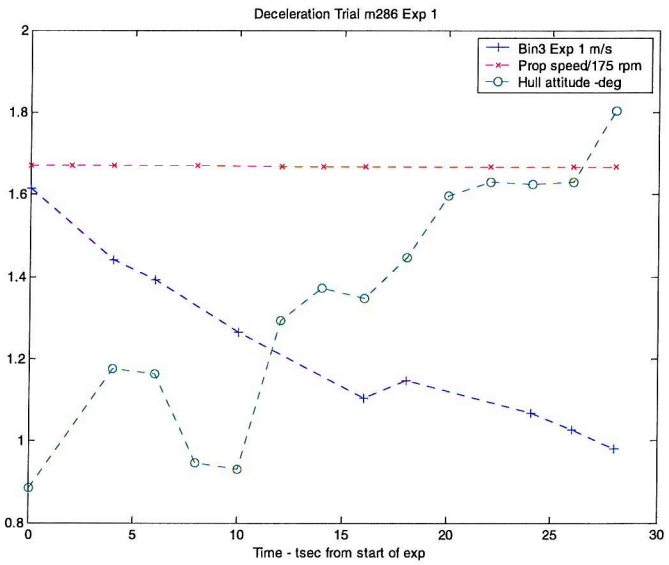

Figure 3.7.5 Hull attitude compared with speed

3.7.3 Deceleration

Two methods of determining deceleration as a function of time were compared.

Initially deceleration was taken as the simple difference between two consecutive data points and considered to occur at the mean speed over that time, i.e.

acceleration $$a_m = \frac{s_n - s_{n-1}}{t_n - t_{n-1}}$$

occurs at time $$t_m = t_{n-1} + \frac{t_n - t_{n-1}}{2}.$$

Because of the paucity of data points this was found to provide too crude an estimate.

A second method was used whereby a second order polynomial equation was fitted to the velocity data for each experiment, as in Figure 3.7.6.

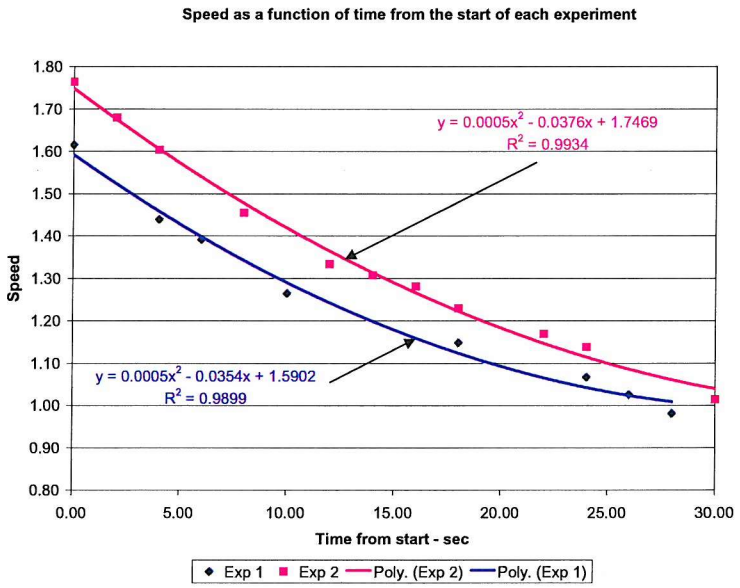

Figure 3.7.6 Speed from the beginning of each experiment

The equations were differentiated and the differential used to calculate the acceleration. Thus, for experiment 1:

$$\frac{dx}{dt} = 5.10^{-4}t^2 - 0.04t + 1.75 \quad \text{m/s},$$

where x is displacement, and t is time, from the start of deceleration, and thus

$$\frac{d^2x}{dt^2} = 10^{-3}t - 0.04 \quad \text{m/s}^2.$$

Since the speed equation derived for each experiment differs only in the constant term, the empirical acceleration equations are identical.

3.7.4 Drag force and coefficient

The experiment has been designed such that the only force acting on the body to produce this deceleration is drag, which is, therefore, given by:

$$F_d = (m + m_a)(10^{-3} t - 0.04) \text{ N},$$

where the vehicle mass (m) of the vehicle is 3,700 kg and the added mass (m_a) is 1,750 kg (from chapter 2.5).

Force may now be calculated at each time step and plotted against the speed measured at that time to give the results shown in Figure 3.7.7.

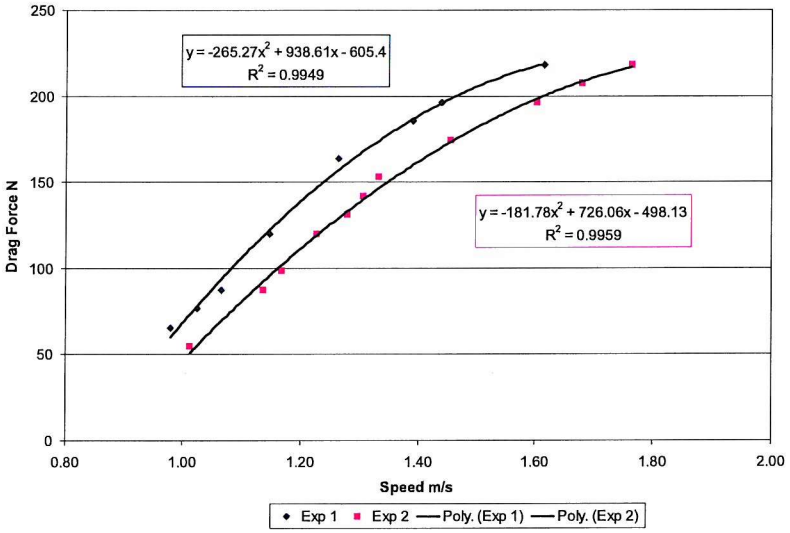

Figure 3.7.7 Drag force as a function of speed

From knowledge of the vehicle's characteristics and records of water temperature and salinity, plots may be made of the drag coefficient, C_d, as a function of Reynolds number. This is shown at Figure 3.7.8.

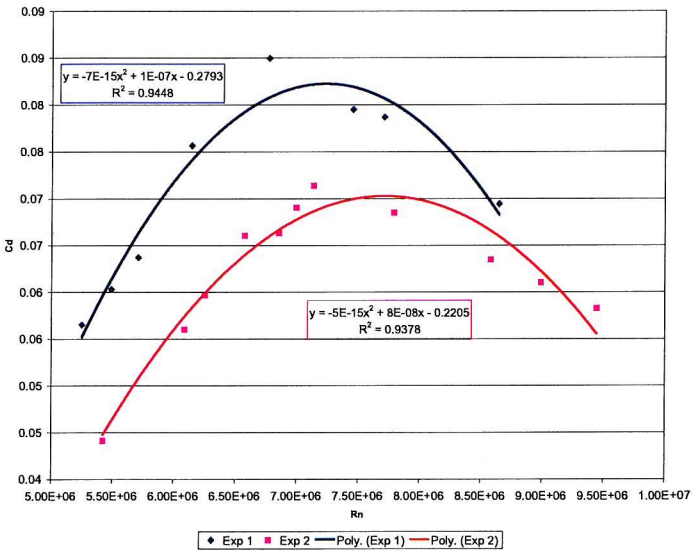

Figure 3.7.8 Drag coefficient vs. Reynolds Number

3.7.5 Reconciliation with data from laboratory experiments

Data is available from the laboratory experiments for the full range of speeds for the bare hull, but for reasons given in chapter 2.7, only available for appendages at the equivalent of a full-scale speed of 1.4 m/s. The results of this trial indicate that drag at this speed is between 160 and 190 N. At this speed the angle-of-attack of the vehicle is 2.5°. From chapter 2.4 the laboratory results indicate that the bare hull drag at this speed and angle-of-attack is 100 N. Chapter 2.6 gives the additional drag of the baseline fit under these conditions as 35 N and that an allowance for ill fitting panels and internal water flows of 15 N is appropriate. The standard payload fit described in chapter 2.6, was not fitted at the time of the trial but a collision-avoidance sonar was fitted on the nose, equivalent to a medium cylinder in the terms of chapter 2.7. From the calculator for additional appendage drag (Section 2.10.15) this is likely to add 18 N giving an overall drag of 168 N. Allowing for the difference in water density resulting from difference in salinity and temperature, the figure rises to 172 N. The results are, therefore, considered to be consistent within the limitations of this trial.

The shape of the drag curve derived from this trial, although being counter intuitive, having a negative square term, is also borne out by the laboratory results as shown in Figure 3.7.9.

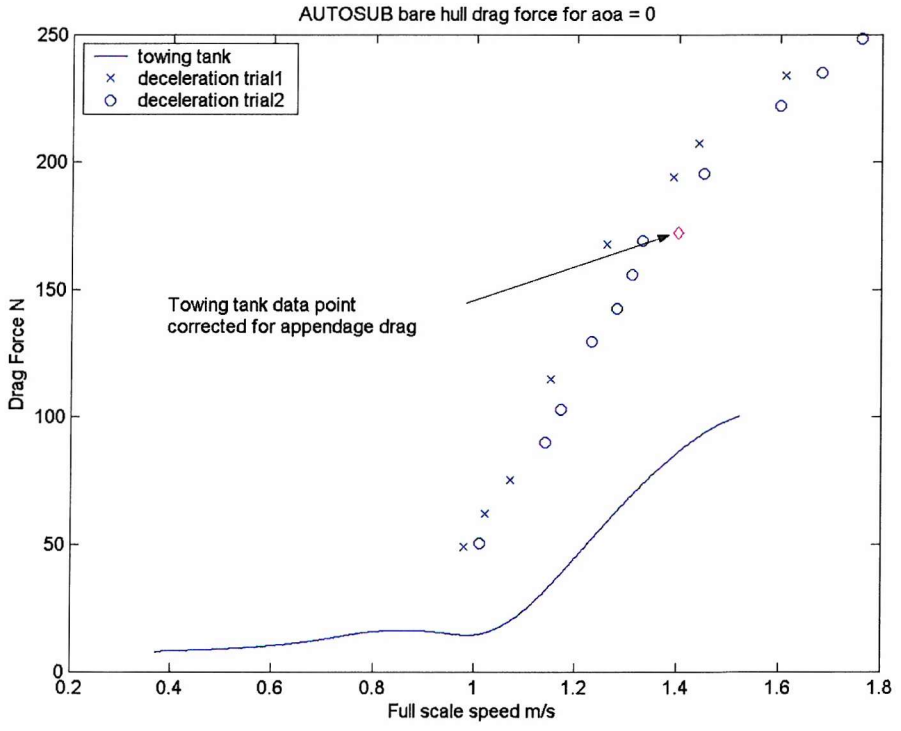

Figure 3.7.9 Comparison between laboratory and full-scale trial results

3.7.6 Conclusion

The objective of this part of the trial was to derive the drag characteristics of the vehicle from measurements of deceleration, following removal of propulsive power. Very few reliable data points were derived from this trial because:

a) The data logging rate was half that expected.
b) Problems with the data logger resulted in missing data.
c) Only 4 experiments were conducted and of these only 2 produced useable results.

Furthermore, the analysis of these few results was hindered by the fact that:

a) No direct measurements of deceleration were available due to the absence of any accelerometer in the vehicle instrumentation.
b) The calculation of the value of added mass appropriate to AUTOSUB was made on the basis of measurements of force and acceleration made on a scale model. The acceleration measurements were made using a low discrimination accelerometer, as described in chapter 2.4. This resulted in an imprecise value. The imprecision was amplified by the large scaling factor required to convert model scale values of added mass to those appropriate to the full-scale vehicle. There is, thus, only limited confidence in the value of added mass used when determining drag force and drag coefficient.

Despite these shortcomings, the correlation between trial and laboratory results is surprisingly good. This confirms that it should be possible to determine, with some confidence, the actual drag of the vehicle as deployed from the results of a simple inexpensive manoeuvre. This manoeuvre may be readily incorporated into the planning for all missions and a clear history of propulsion performance as a function of time and build-state may then be derived.

The shortcomings of this particular trial, as identified above, are readily overcome. The vehicle is being fitted with an Inertial Navigation System that should allow direct measurement of acceleration. If, in the event, this proves inadequate, fitting of a suitable off-the-shelf accelerometer, dedicated to this purpose, should be readily achievable. More precise calculation of added mass should be possible from a dedicated laboratory experiment, as discussed in chapter 2.4. If necessary the basic model built for the laboratory experiments can be modified such that the added mass of a particular configuration could be readily derived.

Finally, dedicated software, based on the analysis described here, but tailored to the instrumentation finally fitted to the vehicle, may readily be written. This could be deployed with the vehicle to enable near real-time knowledge of the performance on the day. This could then be used for range and /or speed optimisation for immediate mission planning.

Chapter 3.8

CONCLUSION

3.8.1 Introduction

Any complex system when introduced into service, is unlikely to be fully optimised, and may not meet the performance anticipated during the design and development phase. It is desirable, therefore, to be able to measure its performance so that it can be compared with that expected at the design stage and with that of its peers developed elsewhere. Furthermore, it is common experience with most systems that their performance deteriorates during service. For a multi-role system, or one whose configuration is revised over time, the principal performance characteristics are likely to change with build-state. Finally, it is probable that a performance prediction model will have been produced during development, and it is desirable to be able to improve this continually throughout the life of the vehicle. All of these factors point to the desirability of being able to readily measure key performance parameters in the real environment as part of the normal operation of the vehicle. This part of the thesis has addressed this problem for the case of a specific in-service AUV, AUTOSUB. However, it is believed that the principle is applicable to most complex systems and for most key performance parameters, and that the specific means developed for AUTOSUB are readily applicable to AUVs in general.

3.8.2 Applicability to the propulsion of an in-service AUV

AUVs operate in the harsh environment of a seaway. They represent considerable capital investment and, therefore, tend to be operated conservatively, with some safety margin in terms of range, to ensure that they may be recovered. This is particularly so when the recovery area is restricted by, for example, the presence of ice. Any uncertainty in propulsion performance is, therefore, necessarily reflected in terms of operating with an increased safety margin, which directly translates into reduced effective range and/or speed. Direct measurement of actual performance in service is, therefore, doubly desirable, since effectively, the more accurate the propulsion performance is known, the greater the range and/or speed that can be used.

This increased performance comes effectively free, with no need for vehicle modification.

The propulsion performance of an AUV is a function of the characteristics of the energy supply, the motor, the propulsor and the drag of the hull. The drag of the hull is in turn a function of its detailed form, its angle-of-attack and the control plane angles. The performance of the energy supply and motor may be readily monitored through life, using readily available transducers. However, the thrust of the propulsor and the drag of the vehicle are less readily measured.

In principle thrust may be measured by means of thrust blocks mounted at the point of application of the force. This option has been considered in this Part. It would require careful design, taking full account of all of the possible thrust transmission paths. Such a design should be achievable but would require some investment in design and development of a modification kit, and in out-of-service time for fitting and proving.

An alternative to measurement of thrust is measurement of drag. A range of alternative drag measurement methods. The most attractive option was considered to be by inference from its dynamic characteristics. When propulsive forces are removed, measurement of the change in momentum will reveal the force. If it can be shown that effective inertial mass remains unchanged during this manoeuvre, and if this parameter is known, then the force may be derived directly from measurement of deceleration. Various means of accelerating and decelerating the vehicle have been considered, but that of using its own internal propulsion to achieve constant speed, and then removing it, proved most attractive since this requires no additional resources.

3.8.3 Effective inertial mass

It has been shown that the effective mass of the vehicle is unchanged throughout the manoeuvre, but that it has two components: displacement mass and added mass resulting from lateral acceleration. The former parameter is readily obtained, but the latter requires derivation. It has been calculated for the bare AUTOSUB hull based on measurements made on a scale-model in the laboratory (see part 2). However, the results of any deceleration trial are very sensitive to this parameter so it is recommended that a dedicated experiment be performed to measure

this parameter accurately. Further, one of the objectives of the work described in this part is to measure the effect on drag of changes to hull form. Since added mass is a function of form and direction of acceleration, experiments should be conducted to determine the sensitivity of this parameter to detailed changes in form and to changes in angle-of-attack and hydroplane angle.

3.8.4 The effect of angle-of-attack and hydroplane angle

For mission planning purposes, the critical parameter is gross drag, i.e. that including the effects of mission particular appendages, the maintenance state of the vehicle and its attitude in terms of angle-of-attack and hydroplane angle. However, for purposes of comparison with the performance of similar vehicles, it is desirable to be able to isolate these effects. For AUTOSUB, this has been done using a scale-model in a towing tank, as described in part 2. However, to limit the number of measurements necessary it was desirable to establish the range for these parameters that occur in-service as a function of speed, and to investigate whether they were strongly coupled, or needed to be treated as independent variables. Furthermore, it is useful to be able to measure whether the attitudes expected when the vehicle control system was designed, are born out in practice. It is, therefore, useful to be able to measure hydroplane angle and angle-of-attack as a function of speed readily in-service.

3.8.5 Combined trial

A simple trial, involving only step changes in propulsion power, has been devised to enable both drag and control system effects to be readily determined during normal vehicle performance. Angle-of-attack and hydroplane angle are measured as a function of speed. Deceleration, and hence drag, are determined from measurements of speed as a function of time. Speed is obtained from the output of the on-board log. These effects can, therefore, be determined with no modifications to the in-service vehicle, although it would be desirable to fit an accelerometer for direct measurement of deceleration.

3.8.6 Data processing

Due to vehicle availability, only one trial has been performed to date, and there were significant difficulties in data logging for that. Very little data is, therefore,

available. Nevertheless, it has been demonstrated that even with imperfect data, processing of the data to achieve the relationships sought is possible. To date processing has been undertaken using routines written to meet the special circumstance of the trial. However, it is a simple matter to engineer from these, software that could be deployed with the vehicle. This would enable rapid, near real-time analysis of trials results, so that the actual performance of the vehicle as deployed may be readily determined on station. This information may then be used to optimise operations to match the mission. In the longer term it is feasible to consider modifying the on-board processing system of AUTOSUB so that it can measure its own performance in real-time and adapt its mission profile automatically.

Part 4

DISCUSSION, CONCLUSIONS & FUTURE WORK

Chapter 4.1

DISCUSSION

4.1.1 Introduction

This concluding part of the thesis provides a coda by discussing the overall implications of the results, drawing together the conclusions (chapter 4.2) and proposing further work (chapter 4.3).

4.1.2 Thesis

The thesis developed in Parts 1 to 3 is as follows:

1. Although systems may meet their performance specification when they are introduced into service, in general they are unlikely to perform optimally.
2. This is because, in principle all systems are complex, but at entry into service they are unlikely to have been characterised to a sufficient level of detail. This is because simplifying assumptions will have been made during the design and development phase, for reasons of economy.
3. The consequences of this are that:
    a. Overall performance will be less than would otherwise be the case.
    b. The system will be operated with a greater safety margin than necessary and so the full potential of the system will not be realised.
4. Increased performance may, therefore, be had, at a low cost compared to the investment made to that point, by applying the knowledge obtained from a more detailed characterisation of the system, taking into account as much of its complexity as possible.

4.1.3. Process

To realise these gains the following process needs to be applied:

1. The key to unlocking this potential is the application of Systems Engineering principles and processes throughout the life of the system, but particularly at the point of entry into service.
2. The key aspects of the system engineering process are:
    a. Capture the requirement.

b. Define the system, in particular in terms of the system boundary.
c. Estimate system performance.
d. Iterate.

3. When undertaking system engineering after entry into service, the process at item 2 needs to be modified to take account of the information already available and the investment already made. The investment to that date will include investment in intellectual capital as well as in hardware and infrastructure. The investment in intellectual capital will lead to ownership issues. These will need to be taken into account when undertaking re-assessments of performance and proposing modifications.
4. The system engineering process after entry into service is usually applied in response to a perceived shortfall. The process becomes:
    a. Re-examine the requirement in the light of the perceived problem.
    b. Agree a formal statement of the problem.
    c. Identify the key performance parameter(s) that may be used to establish the goodness of the system.
    d. Re-define the boundaries of the system and the environment within which it is to operate, in such a way as to facilitate analysis.
5. Improving performance after entry into service will usually require considering the system at a greater level of detail than hitherto. This implies solving a problem of greater complexity, i.e. one that involves a greater number of parameters with more interactions between them. In general, this will imply a statistical rather than deterministic approach.
6. The only way in which the full complexity of the system may be taken into account is to characterise it when deployed in its natural environment. However, achieving this is likely to be difficult because of:
    a. The availability of the system for experimental purposes.
    b. The difficulty of measuring sufficient samples to be representative of system and environment variability,.
    c. The difficulty of controlling or monitoring the state of the vehicle and the environment.

Measurements of the full-scale system will, therefore, need to be supplemented by modelling.

7. It is likely to be difficult or impossible to capture the full complexity of the system in analytic models or digital simulations. Even if it is possible, these will still need to be verified by comparison of their results with measurements taken in the real-world. Analogue modelling, through the use of physical models tested under controlled conditions, is, therefore, indispensable.
8. Taking account of the full complexity of the system implies establishing its response to a large number of factors, each varying over a wide range. This in turn, implies a very large experimental space.
9. The normal approach of a controlled experiment, wherein parameters are varied one at a time, is infeasible when the effects of a large number of factors, each capable of occupying a large number of levels, is required.
10. The reason for changing only one factor at a time is to be able to associate a particular parameter with a particular effect. However, this approach will not identify interactions between parameters, unless all combinations of parameters and levels are tested.
11. If all factors are changed simultaneously, the effect of changing each from one level to another, will be the difference in the mean of the sum of the total performance at each level, provided that:
    a. The factors do not interact, i.e. their effects are independent and, therefore, additive.
    b. The measurements are taken an equal number of times for each level, with the other factors occurring at their levels an equal number of times. This condition occurs in experiments based on orthogonal arrays.
12. Interactions between factors may be determined provided that they are considered as independent factors in their own right and are treated as such in the design of the experiment.
13. The number of levels to be tested for each factor will depend on the expected curvature of the response surface. If the factor is expected to produce a linear response then 2 levels may suffice. If a quadratic response is expected then a minimum of three levels is required. This implies the need for some appreciation of the underlying relationships before designing the experiment. This appreciation will also be required to determine which factors, if any, are likely to interact significantly.

14. Factors that are not deliberately varied as part of the experiment, but which will have an effect on the result, need to be kept constant. This will not always be possible, and the resulting variation in output readings will appear as noise. Any unexpected interactions between controlled variables will manifest itself as an apparent increase in noise.
15. To enable identification of unanticipated interactions, the measurement system needs to be designed to have low noise. Once designed and installed, its noise characteristics need to be established and analysed.
16. The outputs of the modelling exercise may be combined, to establish a statistical model of the system. This will enable estimation of the performance of the system to a defined level of confidence, for a defined set of parameter values.
17. The analogue model and measurement system should be retained throughout the life of the system, to enable checks against the statistical model to be made and the effects of further changes in build state to be assessed.
18. Both the statistical and analogue modelling results need to be verified against measurements of the performance of the real system, in the environment in which it is deployed. Specific trials need to be designed to collect this data, preferably in such a way that performance can be measured economically and on a regular basis.
19. The key output parameters of the system are not always readily measurable, in which case some imagination is required in the design of the full-scale trial.
20. Once armed with the system statistical and analogue models, together with a means of continually verifying them, system performance may be kept under control throughout its life and continuous improvement facilitated.

4.1.4 Systems Engineering.

Having drawn together the thesis in generic terms, and described the process derived from it, the consequences of the application of the process to a specific class of systems, that of the AUV propulsion system is discussed.

The basic tenets of system engineering were readily applied to this system. The first of these was to capture the requirement in the light of the perceived performance shortfall. For the particular system investigated, it was possible to reduce

the statement of requirement to a single sentence: 'To achieve maximum range within the constraints of the current vehicle size, and the energy and power density limits of the current energy storage system technology'. This statement clearly identifies the key system performance parameter: range.

The boundaries of the system were then readily derived. Since the class of AUV under consideration is an energy-limited device, the system boundary had to be drawn somewhat wider than one would expect for a propulsion system, to include all elements that effect energy consumption. The consequent system definition facilitated the identification of the key parameters that effect system performance. These were combined into a parametric model that allowed the effects of trade-offs between them to be explored and the overall maximum performance in terms of range and endurance to be determined.

An analysis of sub-system performance was undertaken. The performance of each of the sub-systems, as delivered, was compared with the key values expected during the system design stage. This indicated that the performance of two of the sub-systems, that of the hull and the propeller, were poorly understood for the conditions actually experienced in service. Because of their close coupling within the system, if the performance of either one of these were determined, then that of the other, in broad terms would be known. It was decided to concentrate on the performance of the hull.

One of the reasons that the performance of the hull was poorly understood was that measurements made during development were based on idealised conditions. This was partly for reasons of economy, but also because of lack of knowledge at that time on the final operating conditions. Thus, the measurements were made at only one speed (and not that at which the vehicle in fact usually travels), at zero angle-of-attack and with the hydroplanes feathered. More importantly, it was based on an idealised hull form, with no appendages and with a perfect surface finish. In fact, the system in service has positive buoyancy and, therefore, maintains depth by applying a constant hydroplane deflection, which in turn results in a constant angle-of-attack. Its hull is festooned with numerous appendages, both for system services and as a consequence of the payload. It was, therefore, deemed necessary to characterise the hull for a range of hull-forms and across a range of speeds, angles-of-attack and hydroplane angles. A large number of parameters is required to describe the full detail of the hull shape, in addition to the three required to define its speed and attitude. The problem was

established as complex within the definition used in part 1. A combination of complementary measurements on the full-scale vehicle at sea and on a scale-model in the laboratory was, therefore, found to be necessary. Drag of the full-scale vehicle at sea was to be based on the calculation of the forces acting on the vehicle, based on measurement of acceleration as a result of change in propulsion power. Because the calculations are dependent on acceleration, knowledge of the added mass of the vehicle is required. This was not known, so a method of determining it had to be devised.

4.1.5 Design of laboratory experiments

A set of experiments was designed to establish the drag characteristics of the hull across the full range of parameters. The number of factors and levels to be explored was very large, so even using experiment designs based on orthogonal arrays, it was still found necessary to partition the experiments. The programme of experiments was, therefore, divided into three campaigns: one to characterise the bare hull across the range of speeds, angles-of-attack and hydroplane angles; a second to establish the additional drag of sets of changes to the basic hull form; and the third to establish the additional drag of individual appendages as a function of size, shape, position and relative position.

Before fleshing out the detailed design it was necessary to undertake an analysis to estimate the expected form of the response surface and the maximum force that was likely to be exerted on the apparatus. This analysis was based on information contained in the literature. The form of the response surface was used to determine the number of levels required for each factor. The maximum force required was needed for the design of the laboratory apparatus.

Because of the potential number of variations to hull form, it was found necessary to group them into 3 categories; those associated with the basic services of the vehicle; those associated with vehicle payload; and those related to in-service wear and tear. The set associated with basic services was found to be relatively stable with time and could, therefore, be accurately modelled. However, the number of possible variations within the other two categories necessitated producing representative sets of idealised forms.

The design of the experiments had to be matched to the expected low data rate achievable in a towing tank. The experiment designs were based on assumptions of

workshop capability and availability of major facilities such as the Towing Tank. This necessitated planning for the minimum number of runs required for balanced experiments for the number of factors and levels determined by the campaign structure and the expected shape of the response curve.

Finally, a satisfactory set of experiments was designed for each campaign.

4.1.6 Design of laboratory equipment

The towing tank together with its instrumentation for speed and force measurement and data logging was entirely satisfactory.

The force measurement system was based on an existing dynamometer, designed for use in drag plate experiments. As a means of mounting the model and measuring the forces it was perfectly adequate. However, the model was large and heavy, and was expected to exert net drag forces of up to 500 N. Because of this, two substantial poles were required to connect it to the dynamometer. It was not found possible to fair these poles so they exerted most of the force experienced by the dynamometer. The hull drag signal was, therefore, effectively perceived against the background of a very high, though predictable, noise threshold. Calibration of the poles, therefore, had to be carried out with some care. This took precious experimental time and complicated the data analysis. With hindsight, further thought should have been given to mounting the dynamometer in the model rather than on the carriage.

The design of the model was reasonably straightforward, with the maximum size and speed possible in the towing tank being just matched to the Reynolds number of the real vehicle at the cruising speed experienced on most missions. However, such a large model presented serious handling problems. For handling in water it needed to be just positively buoyant, which entailed fitting ballast and trim tanks and spending time on setting up the model. Making the model virtually neutrally buoyant in water meant that it was very heavy in air. Special handling facilities, such as cranage and floatation collars, therefore, had to be devised at additional cost and set-up time. Alternatives to a large model, such as using higher speed towing facilities, or change of fluid medium, such as is available in a wind tunnel, is worth considering.

Moving a large model at high speed through water, at a shallow depth in comparison with operational depths, gave rise to concern that the model may experience wave-induced drag not experienced in the real environment. It was,

therefore, considered necessary to measure wave profiles so that wave-induced drag could be calculated. Wave probes were fitted to the tank for this purpose. However, the waves created by the mounting posts were of such magnitude that they swamped the probes. In the event wave drag had to be calculated from theory.

A means of measuring the acceleration of the carriage was required to enable added mass to be calculated. The chosen method of mounting an accelerometer on the carriage was satisfactory, but the accelerometer used had insufficient discrimination.

4.1.7 Noise calibration

Significant effort was put into establishing the noise levels in the force measurement system, since the experimental method is dependent upon being able to detect any apparent increase in noise. All possible sources of noise in the force calibration system were investigated: electrical, mechanical and hydrodynamic. No significant electrical noise was found, although the filters were found to have a small insertion loss. It was found that the item under test could be precisely aligned by means of minimising the net side force and moment. The major sources of mechanical noise were identified and found to have no significant effect on the mean force measured over the run. All sources of noise were identified. Overall the equipment was found to have a mean measurement accuracy of 0.006 N with a standard deviation of 0.96 N.

4.1.8 Conduct of experiments

When conducting the experiments, the first set of runs was used to explore the full force envelope to ensure that the apparatus was able to cope with the extremes. In the event, it was found that the pre-experiment analysis to determine the maximum forces likely to be experienced was surprisingly accurate. The maximum forces experienced in practice never exceeded that forecast, although there were a few cases of noise amplitude clipping when high speeds coincided with large angles-of-attack.

4.1.9 Analysis

The long time between measurements, consequent upon using a towing tank rather than wind tunnel, meant that the data rate was ill matched to the size of the experimental space to be explored. This meant that only the bare minimum number of data points could be obtained. The consequences of this became apparent in the confidence with which the results could be stated.

Some of the experiment designs included both factors with strong effects and those with much weaker effects. Despite this, the small effects were found to be consistently detectable in the presence of very large effects. Nevertheless, the analysis would have been easier, and the weaker effects could have been stated with greater confidence, had they been separated. This phenomenon needs to be considered when partitioning the experiments.

4.1.10 Added mass

Knowledge of the added mass of the vehicle is required so that the drag characteristics of the full-scale vehicle may be determined at sea, using the deceleration method described in part 3. It was hypothesised that the value of this parameter could be determined at low cost by taking acceleration measurements during the scale-model towing tank experiments. The method, based on determining the apparent total inertial mass and subtracting the measured mass, was proven in experiments using the mounting poles only. The weight of the poles was deduced with reasonable accuracy from measurements of the force acting on them whilst being accelerated in air.

Reasonably consistent results for the added mass of the scale-model were obtained. The scaling factor, required to translate the added mass of the model to that of the full-scale vehicle, is very large. Thus, a small error in measurement of acceleration may result in a large error in added mass. The accelerometer used in these experiments had low discrimination and produced a noisy signal.

It is, therefore, concluded that the method is sound and has provided an order of magnitude estimate of the added mass of the vehicle, but, in this case, the instrumentation was inadequate.

4.1.11 Statistical Models

Statistical models were constructed to enable prediction of the effects both of sets of appendages and of the size, shape position and relative position of individual appendages.

Two alternative analysis methods were used, one based on analysis of variance and the other based on multivariate linear regression. Both demonstrate that reasonably accurate predictions of total drag can be made from a model based on the derived effects. An advantage of the analysis of variance based method is the ability to deal with non-linear effects within the prediction equation.

Analysis of variance clearly indicated which of the apparent effects and interactions are likely to be real and which due to chance. It also demonstrated that the effects of comparatively small changes to the form of the hull can be detected, even in the presence of considerable noise. It was also revealed that if one factor has a much stronger influence than the others, then it is likely to mask the lesser effects. The signal to noise ratio for the smaller effect is effectively decreased since the small signal is present against the background of the larger effect. The method worked reasonably well when the number of variables was small and the effects significant. In the work under discussion this was the case for the sets of appendages and a model was constructed that predicts to a mean accuracy of 5 N (with a standard deviation of 14 N, Figure 2.9.10). However, where the number of variables is high the experiments need to be conducted iteratively. Thus, a scoping experiment should be performed encompassing all of the factors and using the minimum number of runs consistent with a balanced experiment. This will indicate trends and provide general guidance as to the effects. Further refinement, to provide better than order of magnitude estimates of the main effect, will require more information.

Greater accuracy in estimation may be obtained in two ways. If a more detailed insight is required then Taguchi type experiments conducted using larger orthogonal arrays are suitable. These will enable the effects of a greater numbers of interactions to be investigated. They will also result in the ability to state the estimates to an increased level of confidence and to be more certain of the status of individual effects. Alternatively the results already obtained may be used to design more specific experiments to investigate the effects of particular combinations of factors in greater depth.

The model assumes that all factors are independent. Where the results of the scoping experiment indicate that this is unlikely to be the case, then the effect measured will be confounded by interactions. To provide more specific estimates a larger experiment is required to quantify the interactions.

Non-linear effects can be detected using an increased number of levels. In the scoping experiment there will be a need to keep the number of levels to the minimum. The resolution of the effect is, therefore, likely to be low. Thus, although it may reveal a degree of structure, an extended programme of experiments, with additional levels, is required if any degree of confidence in the detail of the effect is required.

4.1.12 Measurements on the in-service system

It is highly desirable to be able to measure the key performance parameter of the system (in this case drag force) whilst in service. Ideally the measurement should be simple and economical so that it can be readily repeated throughout the life of the system. Trends in performance can then be established. The key performance parameter is not always readily measured. A range of methods has been considered for determining the drag of the vehicle in-service. These include direct measurement by use of thrust blocks between propeller and hull and various means of determining the force required to drag the vehicle. None of these could be enacted without additional expenditure in terms of modification to the vehicle or the provision of additional equipment. The solution finally selected was to determine the drag from measurements of deceleration on removal of propulsive power. The only force acting on the vehicle under these conditions is drag, so provided the effective mass is known, the force that must be acting may be calculated. The effective mass is the sum of the inertial mass, which can be obtained by weighing, and the added mass, which was determined from measurements made on the scale-model. A specific trial was devised for the purpose of drag derivation. This has been put into practice only once, and even then under less than ideal conditions. However, the results were sufficient to demonstrate the method. To date, processing of the resultant data has been undertaken using routines written to meet the special circumstance of the trial. However, it is a simple matter to engineer from these routines, software that could be deployed with the vehicle. This would enable rapid, near real-time analysis of trials results, so that the actual performance of the vehicle as deployed may be readily determined on station. This information may then be used to optimise operations to match the mission. In the longer term, it is feasible to consider modifying the vehicle's on board processing system so that it can measure its performance in real time and adapt its mission profile automatically.

4.1.13 Implications for AUTOSUB

We will now turn to a discussion of the specific implications of this work for the exemplar system used, AUTOSUB.

4.1.14 Propulsion system definition

For the purposes of this thesis the requirement is derived as being: to achieve the maximum range within the constraints of the size and construction of the current

vehicle, and the energy and power limitations of the current energy storage system. AUTOSUB is an energy-constrained system. From this requirement it follows that the definition of the propulsion system for analysis purposes must include all sub-systems that affect the consumption of energy. The propulsion system sits within the overall AUTOSUB vehicle system. This, together with the environment within which the overall vehicle operates (at depth at sea, and on-board ship for preparation) constitute the environment within which the propulsion system operates.

4.1.15 Parametric modelling and overall system performance

A model that predicts the range of the vehicle in terms of the parameters of the principal sub-systems of the propulsion system has been devised. This enables the sensitivity of the range of the vehicle to the performance of each of the sub-systems to be estimated. The results from this model indicate that the vehicle, as conceived, should be capable of a range of the order of 1700 km (at a speed of 2 m/s and in a temperate environment), provided that the sub-systems perform as expected. This compares with the in-service maximum range of 800 km. It implies a maximum endurance of the order of 10 days.

The maximum range from this type of vehicle is achieved at a speed of 1 m/s. This assumes that the vehicle uses the same hull size and shape, provides the same payload volume and power and has the same hotel load, but has its propulsion system optimised for this speed (i.e. a smaller motor, a propeller optimised for this speed, and the additional space freed by the smaller motor used for additional energy storage). This also makes the gross assumption that the motor and energy system are directly scalable. A vehicle optimised for this speed may be capable of ranges of the order of 3000 km and a maximum duration of the order of 1 month.

4.1.16 Sub-system performance

The reason for the vehicle not performing to its apparent potential has been investigated by considering the performance of each of the propulsion sub-systems and comparing this with that expected during the design phase. This revealed that the characteristics of the hull and propeller, under the conditions experienced in service, were poorly understood. Because of their close coupling, if the performance of one of these sub-systems is known, then, in gross terms, so is the other. This study concentrated on hull performance.

4.1.17 Characterisation of the performance of the hull

The hull-form in service was found to differ significantly in its detail and in its operation from that of the model characterised during development. Measurements made during development were on a simple hull shape, with no appendages, made at a speed equivalent to 2 m/s full scale, with zero angle-of-attack and no hydroplane angle. A smooth hull surface was assumed. In service the vehicle has many and varied appendages, travels within a band of speeds generally less than 2 m/s and, to overcome residual buoyancy, travels at an angle-of-attack and with the hydroplanes providing lift. Its hull surface is often imperfect due to the exigencies of operating in a harsh environment.

A large number of parameters are required to describe the shape, attitude and condition of the vehicle including its appendages. Because the appendages change from mission to mission, most are variables. Characterising this is a complex problem.

To capture the full complexity, ideally performance will be measured directly on the in-service vehicle at sea. However, measuring the principal performance parameter, drag, directly is difficult and some measurement needs to be made under controlled conditions. A combined programme of sea trials and laboratory experiments on a scale-model was necessary.

The detail that distinguishes the real hull in service from that of the real vehicle may be considered in two categories: appendages and changes to surface finish. The appendages may be further sub-divided into those that provide services (termed here baseline) and are reasonably constant over time and those that are mission dependent (Payload). The experiments were undertaken in two phases. First the bare hull was characterised in some detail. Then the additional drag of the appendages and surface damage was measured. Because of the large variation of form possible as a result of appendages and damage features, a comparatively small sample of the total potential experimental space only can be made. A statistical model is, therefore, required to facilitate predicting their effects.

4.1.18 Bare hull drag

The bare hull drag was characterised by measuring the forces acting on a 2.5 m scale model as it was towed through the SI towing tank across a range of speeds, angles-of-attack and hydroplane angles. To generate forces representative of the full-scale vehicle, the model was run at speeds corresponding to the Reynolds Numbers

experienced in service. In assessing the drag force, three corrections had to be made to the raw data because of:

1. The drag due to the model mounting poles.
2. Wave-induced drag resulting from the high speed at which the model travels at a comparatively shallow depth.
3. Blockage effects resulting from the significant model cross-sectional area as a proportion of the cross-sectional area of the towing tank.

The tare drag of the model mounting poles was measured independently across the full range of speeds and offset angles. From these a model has been produced to enable calculation of pole drag for any combination of these two parameters.

It was not possible to calculate the effect of wave drag from measurements of wave profiles because of the breaking waves produced by the model support posts. Wave drag was, therefore, calculated from measurements of change of drag with model depth and using Thin-ship Theory. The results of these calculations were in reasonable agreement and it was concluded that model wave drag (as opposed to pole wave drag) was insignificant.

There are four standard methods of blockage adjustment: those due to Young & Squire, Schuster, Scott and Tamura. All are designed for surface piercing models travelling at low speeds. Adjustments to each were made for a submarine model and their results for the AUTOSUB model at high speed compared. Tamura's method was found to provide the most convincing correction for the AUTOSUB model once a correction for the effect at high speed was made. This was used in subsequent analysis, although the overall blockage effect was found to be small.

The corrected data has been used to create a Matlab model of bare-hull drag as a function of angle-of-attack and speed. The effects of change in hydroplane angle has also been established, but found to be small.

Drag force and speed were converted to drag coefficient and Reynolds number for comparison with other vehicles of similar shape. In the absence of readily available data on torpedo shaped bodies, airship data, for vehicles of similar length to diameter ratio and travelling at similar Reynolds Number, was used. This shows that the relationship between the torpedo shaped body and the cigar shape of the airship is significantly different. The results obtained here were confirmed by comparison with results obtained on the full-scale vehicle at sea, using a completely different means of determining drag.

At a cruising speed of 1.4 m/s, the Reynolds Number of the AUTOSUB hull is 8.2 x 10^6. The drag coefficient of its bare hull is 4.7 x 10^{-3}. This value is comparable with the original estimate.

4.1.19 Added mass of the bare hull

Knowledge of the vehicle's added mass is required so that the drag characteristics of the full-scale vehicle may be determined at sea using the deceleration method. It was hypothesised that the value of this parameter could be determined at low cost by taking acceleration measurements during the scale-model towing tank experiments. The method is based on determining the apparent total inertial mass and subtracting the measured mass. It was verified by establishing the weight of the mounting poles from measurements of the forces generated when they were accelerated in air. Comparison with the results obtained from weighing the poles confirmed the method..

Reasonably consistent results for the added mass of the AUTOSUB scale-model were obtained, which indicate that it is of the order of 80 kg. When scaled to full-scale, this produces an added mass of the order of 1750 kg.

The scaling factor between the added mass of the model and that of the full-scale vehicle is very large (22.5) because it is dependent on the ratio of their volumes. Thus, a small error in measurement of acceleration, may result in a large error in added mass. The accelerometer used in this experiment was only capable of measuring to an accuracy of 0.1 g and produced a very noisy signal. Additionally, although the acceleration of the carriage is reasonably linear for 1 or 2 seconds, it is not absolutely so. This adds further scope for error.

It is, therefore, concluded that the method is sound and has provided an order of magnitude estimate of the added mass of the vehicle. However, to improve the accuracy of the results that may be obtainable from the trial described in part 3, a tailor-made experiment should be conducted. Ideally his should be based on the full-scale vehicle, and have tailored instrumentation, although far more accurate results than those obtained here should be possible from scale model tests.

4.1.20 Appendage drag

Appendage drag is described at two levels: that of sets of appendages representing baseline, payload and damage and those of individual appendages in terms of size, shape, position and relative position.

Standard sets of appendages were chosen to approximate to those fitted in practice. Empirical equations have been derived to describe their contribution to overall drag as a function of speed and angle-of-attack. The effect of the appendage sets is significant. As an example, at 1.4 m/s the drag of the bare hull is 100 N. The additional drag of the baseline set is 35 N and of a representative payload fit may add the same amount. Ill fitting panels and orifices left when fitting the payload might contribute a further 15 N. It can Thus, be seen that the net effect of the drag of the appendages is comparable to that of the bare hull.

a. The effect of individual appendages as a function of their size, shape, position and relative position was made. Because of the large range of values these parameters can take, it was necessary to design experiments based on orthogonal arrays. This enabled the effects of each parameter to be established, even though none were kept constant between one measurement and another.

4.1.21 In-Service performance monitoring

A simple and inexpensive trial has been devised for determining the actual drag of the vehicle at sea. This requires no instrumentation additional to that already carried on the vehicle, although data processing would be easier if a direct method of measuring and recording acceleration as a function of time was available. The method is based on the fact that when propulsion forces are removed from the vehicle, the only force acting on the AUV is drag.

Drag can be calculated from the deceleration characteristics only if added mass is known. It has been calculated for the bare AUTOSUB hull based on measurements made on a scale-model in the laboratory (see part 2). However, the results of any deceleration trial are very sensitive to this parameter so it is recommended that a dedicated experiment be performed to measure this parameter accurately. Further, one of the objectives of the work described in this part is to measure the effect on drag of changes to hull form. Since added mass is a function of form, size and direction of acceleration, experiments should be conducted to determine the sensitivity of this parameter to detailed changes in form and to changes in angle-of-attack and hydroplane angle.

The advantages of this method of determining drag, is that the vehicle's performance may be directly measured for the configuration as deployed. This facilitates mission planning in that maximum range can be more precisely predicted

and so a lower safety margin need be incorporated. Additionally, a history of performance as a function of the build state of the vehicle can be built up for use in planning future missions.

Due to vehicle availability, only one trial has been performed to date, and there were significant difficulties in data logging for that. Nevertheless, it has been demonstrated that the method is effective. To date processing has been undertaken using routines written to meet the special circumstance of the trial. However, it is a simple matter to engineer from these, software that could be deployed with the vehicle. This would enable rapid, near real-time analysis of trials results, so that the actual performance of the vehicle as deployed may be readily determined on station. This information may then be used to optimise operations to match the mission. In the longer term it is feasible to consider modifying the on-board processing system of the vehicle so that it can measure its performance in real-time and adapt its mission profile automatically.

4.3.10 Conclusion

The results of the work described in this thesis have been discussed in terms of their application to systems engineering in general, AUV propulsion systems, and the AUTOSUB propulsion system in particular. We may now list the specific conclusions that may be drawn.

Chapter 4.2

CONCLUSIONS

4.2.1 Introduction

The conclusions are listed here in terms of the implications for each of the main subjects addressed in this thesis, i.e.:

- The AUV propulsion class of systems.
- Laboratory experiment design and analysis.
- Determination of added mass.
- Design and analysis of trials on the full-scale vehicle at sea
- AUTOSUB as a specific example of an AUV system.

4.2.2 The AUV propulsion class of systems

The conclusions for the AUV propulsion class of systems are as follows:

1. The basic tenets of systems engineering as derived for an in-service system were readily applied to this system and proved effective.
2. The most appropriate measure of goodness of AUV propulsion systems is the maximum range possible within the constraints of the vehicle size, and the energy and power density limits of the energy storage system technology. The boundaries of the system for the purposes of derivation of this parameter were readily derived, but needed to be drawn somewhat wider than would normally be set for a propulsion system and needed to include all energy sinks.
3. System definition enabled the identification of the key parameters that effect system performance, viz: the volume devoted to the energy store, propulsion facility and payload; the energy density of the energy store; the power density and efficiency of the propulsion facility; and the drag coefficient of the hull.
4. A parametric model was developed which enables the sensitivity of the principal performance parameter of the generic system to be established in terms of the key parameters.
5. An analysis of sub-system performance enabled identification of the sub-systems where performance was poorly understood. In this case these were the hydrodynamic performance of the hull and the performance of the propeller.

6. One of the reasons that the performance of the hull was poorly understood was that measurements made during development were based on idealised conditions. It was established that it was necessary to characterise the hull in terms of a description that captured its full complexity.
7. To capture the effects of complexity, a combination of complementary measurements on the full-scale vehicle at sea and on a scale-model in the laboratory is necessary.

4.2.3 Design of laboratory experiments

The conclusions for the design of laboratory experiments are as follows:

1. Where the number of factors and levels to be explored is very large, as was the case here, experiment designs based on orthogonal arrays are required. Additionally, if the maximum data rate is constrained to be low, it is necessary to partition the experiments.
2. Experiment design techniques need to be stylised and automated so that the design may be re-worked in near real-time, as circumstances change.
3. Careful consideration needs to be given to the method used to mount the model and to the location of the dynamometer, so as to minimise the background noise created by the drag of the mounting system.
4. The design of the model to reproduce the Reynolds number of the real vehicle at the cruising speed experienced on most missions was satisfactory. However, it required a large model, which presented significant handling problems. Alternatives to a large model, such as using higher speed towing facilities, or change of fluid medium, such as is available in a wind tunnel, should be considered.
5. Moving a large model at high speed through water, at a shallow depth gives rise to the need to determine the wave-induced drag not experienced in the real environment. A method of inferring wave drag from measurements of drag made across a range of immersion depths has been developed and found to produce results consistent with those obtained from an analysis based on thin ship theory.
6. The experimental method requires that noise levels in the force measurement system be known in order to detect unanticipated interactions between factors. Potential electrical, mechanical and hydrodynamic sources of noise in the force calibration system were investigated. No significant electrical noise was found,

although the filters were found to have a small insertion loss. It was found that hydrodynamic noise could be minimised by precisely aligning the model with the direction of motion by means of minimising the net side force and moment. The major sources of mechanical noise were identified and found to have no significant effect on the mean force measured over the run. Overall the equipment was found to have a mean measurement accuracy of 0.006 N with a standard deviation of 0.96 N.

7. The long time between measurements, consequent upon using a towing tank rather than wind tunnel, meant that the data rate was ill matched to the size of the experimental space to be explored. This meant that only the bare minimum number of data points could be obtained. The consequences of this became apparent in the confidence with which the results could be stated.
8. Some of the experiment designs included both factors with strong effects and those with much weaker effects. Despite this, the small effects were found to be consistently detectable in the presence of very large effects. Nevertheless, the analysis would have been easier, and the weaker effects could have been stated with greater confidence, had they been separated. This phenomenon needs to be considered when partitioning the experiments.

4.2.4 Determination of added mass

The conclusions from the experiments to determine this parameter are as follows:

1. The method, based on determining the apparent total inertial mass during periods of acceleration and subtracting the measured mass, was verified in experiments using the mounting poles only. The weight of the poles was deduced from measurements of the force acting on them whilst being accelerated in air as being 20.4 kg. The weighed value was 19.9 kg.
2. The added mass of the model is 80 kg, which may be scaled to give an added mass of the in-service vehicle of 1750 kg. Because of the limitations of the accelerometer used, this should only be taken as an order of magnitude estimate of the real value.

4.2.5 Design and analysis of trials on the full-scale system at sea

It is concluded that a simple and economical means of determining the drag of the in-service vehicle at sea, based on the measurement of speed during deceleration,

has been devised and demonstrated. This enables rapid, near real-time analysis of trials results, so that the actual performance of the vehicle as deployed may be readily determined on station. This information may then be used to optimise operations to match the mission.

4.2.6 AUTOSUB as a specific example of an AUV system

The conclusions for AUTOSUB as a specific example of an AUV propulsion system are as follows:

1. Parametric modelling indicates that the vehicle, as conceived, should be capable of a range of the order of 1700 km (at a speed of 2 m/s and in a temperate environment, assuming no angle of attack and a clean hull). It implies a maximum endurance of the order of 10 days.
2. The maximum range from this type of vehicle is achieved at a speed of 1 m/s. This assumes that the vehicle uses the same hull size and shape, provides the same payload volume and power and has the same hotel load, but has its propulsion system optimised for this speed (i.e. a smaller motor, a propeller optimised for this speed, and the additional space freed by the smaller motor used for additional energy storage). This assumes that the motor and energy system are directly scalable. A vehicle optimised for this speed may be capable of ranges of the order of 3000 km and a maximum duration of the order of 1 month.
3. The open water drag coefficient of the bare hull, operating at a cruising speed of $R_n=8x10^6$, at zero angle of attack and with hydroplanes feathered, is estimated from the experiments described here to be 0.035. This equates to a drag force of approximately 100 N at a speed of 1.4 m/s.
4. The drag coefficient and drag force of the bare hull as a function of angle of attack, R_n and speed is as given in figures 2.4.34 to 2.4.37.
5. A principal reason for the vehicle not performing to its apparent potential is the additional drag of the real vehicle resulting from appendages and from the hull imperfections consequent upon real-life operation. The effect of the appendage sets is significant. As an example, at 1.4 m/s the drag of the bare hull is 100 N. The additional drag of the baseline set is 35 N and of a representative payload fit may add the same amount. Ill fitting panels and orifices left when fitting the payload might contribute a further 15 N.

6. Empirical equations have been derived to describe the contribution of appendages and damage effects to overall drag as a function of speed and angle-of-attack, and of their size, shape, position and relative position.
7. Guidelines for the design and positioning of appendages to the type of hull considered here have been deduced from these experiments. These are:
    a) Streamlining an appendage by changing from a rectilinear section cylinder to either a dome or NACCA section brings noticeable drag benefit.
    b) Streamlining in both planes to produce a 'blister' is likely to further reduce drag over either a dome or a NACA section, but the increased gain will be less than the initial gain of moving from a cylinder to either a dome or NACA section.
    c) Somewhat more speculatively, the results indicate that if only one change is possible it may be more important to change the frontal section than the fore-to-aft section.
    d) If more than one appendage is required it is better to keep them in line than distribute them around the circumference.
    e) When mounting appendages in line, an apparent shadowing effect means that the closer they are mounted together the better.
    f) If there must be angular separation between appendages, then it is concluded that large angular separations are desirable unless it is considered that the effect is of sufficient concern that optimal spacing is required. In the latter case specific measurements would be required to determine the optimum angle.
    g) It is better not to have apertures into free flooding spaces (with the possible exception of a single aperture at the bow).
    h) Any two apertures increase drag at high speed (equivalent to 1.5 m/s full scale speed) although the effect is undetectable at low speed.

Chapter 4.3

FUTURE WORK

4.3.1 Introduction

Necessarily the work undertaken for this thesis was bound by the constraints of time and cost. There are therefore a number of potentially fruitful lines of enquiry that were not pursued. These are recorded here by way of suggestions for future work.

4.3.2 Design tools for laboratory experiments

A satisfactory set of experiments was designed for each campaign. However, in the event neither expected workshop capacity, nor towing tank availability, were realised and the experiments had to be substantially re-designed. It is unlikely that these circumstances are exceptional, and it is, therefore, advisable to ensure that the experiment design techniques are reasonably stylised and, so far as possible, automated. This was done for the work under discussion, with the designs being based on a standard set of orthogonal arrays (that cater for most combinations of factors and levels), and a set of spreadsheets (to enable rapid allocation of factors and levels). However, the establishment of a set of a formal methodology and set of tools to enable experiments to be designed and reworked in near real-time, as circumstances change seems entirely feasible and would be of general application.

4.3.3 Design of laboratory equipment

The towing tank together with its instrumentation for speed and measurement and data logging was entirely satisfactory. The force measurement system was based on an existing dynamometer, designed for use in drag plate experiments. As a means of mounting the model and measuring the forces it was perfectly adequate. However, the model was large and heavy, and was expected to exert net drag forces of up to 500 N. Because of this, two substantial poles were required to connect it to the dynamometer. It was not found possible to fair these poles so they exerted most of the force experienced by the dynamometer. The hull drag signal was, therefore, effectively perceived against the background of a very high, though predictable, noise threshold. Calibration of the poles, therefore, had to be carried out with some care.

This took precious experimental time and complicated the data analysis. It would be beneficial if further thought could be given to alternative arrangements such as mounting the dynamometer in the model rather than on the carriage.

4.3.4 Model form

Changing the form of the model was found to be very time consuming, since in many cases the model had to be removed from the water. An easier form of attaching the appendages to the model would be worth investigating in any follow-on experiments.

4.3.5 Determination of added mass

Knowledge of the added mass of the vehicle is required so that the drag characteristics of the full-scale vehicle may be determined at sea, using the deceleration method described in part 3. It has been determined that the value of this parameter may be determined at low cost by taking acceleration measurements during scale-model towing tank experiments. Reasonably consistent results for the added mass of the scale-model were obtained. The scaling factor, required to translate the added mass of the model to that of the full-scale vehicle, is very large. Thus, a small error in measurement of acceleration may result in a large error in added mass. The accelerometer used in these experiments had low discrimination and produced a noisy signal. It is, therefore, recommended that the measurements be repeated using a purpose built measurement system.

Additional errors were introduced during the analysis as a result of averaging the acceleration over a period of near, but not perfectly, constant acceleration. It is suggested that, in future, results are obtained at a much higher data rate and are analysed using instantaneous, rather than mean, acceleration

4.3.6 Measurements on the in-service system

A simple and economical method has been developed whereby the key propulsion system performance parameter, drag force, may be determined on the real system whilst in service. It is proposed that this could be developed further into a standard process that may be carried out on each deployment such that trends in performance are established and the relationship between form and performance more accurately established. To date, processing of the resultant data has been undertaken using routines written to meet the special circumstance of the trial. However, it is a

simple matter to engineer from these routines, software that could be deployed with the vehicle. This would enable rapid, near real-time analysis of trials results, so that the actual performance of the vehicle as deployed may be readily determined on station. This information may then be used to optimise operations to match the mission. In the longer term, it is feasible to consider modifying the vehicle's on board processing system so that it can measure its performance in real time and adapt its mission profile automatically.

References

Abbott, I. H. and Doenhoff, A. E. V. (1959) *Theory of wing sections : including a summary of airfoil data,* Dover, New York.

Abu-Sharkk, O. (2003), *'CSci8980 Project: Survey on measuring programme complexity'*, University of Minesota, Report: 15/5/2003.

ANSI/EIA632 (1999), *'Process for Engineering a System'*, Standard.

Babb, R. J. (1994), *'Instrumentation for a Low Drag Hydrodynamic Test Vehicle'*, Institute of Oceanographic Sciences Deacon Laboratory, UK, Report: CRP5/II/87.

Babenko, V. V., Korobov, V. I. and Moroz, V. V. (2000), *'Bionics principles in hydrodynamics of automotive unmanned underwater vehicles'*, Oceans 2000

Bahill, A. T. and Briggs, C. (2001), *'The systems engineering started in the middle process: a concensus of systems engineers and project managers'*, Systems Engineering, Vol. 4, pp 156-167.

Bahill, T. and Dean, F. (2001), *'What is systems engineering? A consensus of senior systems engineers'* , University of Arizona, Vol. 2004, Report.

Beckerman, L. P. (2000), *'Application of complex systems science to systems engineering'*, Systems Engineering, Vol. 3, pp 96-102.

Bishop, R. E. D. and Price, W. G. (1979) *Hydroelasticity of Ships,* Cambridge University Press.

Bradley, A., Freezor, A. M. and Singh, H. (2002), *'Power Systems for Autonomous Underwater Vehicles'*, Awaiting publication by IEEE.

Bradley, A., Singh, H. and Yoerger, D. (1995), *'Issues in AUV design and deployment for oceanogrphic research'*, Woods Hole Oceanogrphic Institution, Vol. 2004, Report.

Brown, G. W. and Kopp, N. L.(1994), *'Electric Motor/Controller Design Trade Offs for Noise Weight and Efficiency'*, IEEE Symposium on Autonomous Underwater Vehicle Technology, pp 187 - 193.

Chetleborough, P. (2002), *'Resistance and propulsion of the AUV AUTOSUB'*, University of Southampton, 3rd year BEng project report.

Clark, P. V. and Wiltshire, J. R. (1997), *'Cavitation Tunnel Experiments on the AUTOSUB Propeller'* DRA, Sea Systems Sector, Haslar, Gosport, Hants PO12 2AG, Report: DRA/SS/SSHE/CR97005.

Clower, P. and Poole, K. (1992), *'A Systems Approach to Autonomous Underwater Vehicle (AUV) Propulsion Design',* MTS, Vol: 30, pp 9 - 16.

Comstock, J. P. (1980), *' Principles of naval architecture',* New York : Society of Naval Architects and Marine Engineers.

Cox, D. R. (1992), *'Planning of experiments',* John Wiley and Sons Inc.

Davis, T. P. and Grove, D. M. (1992), *'Engineering quality and experimental design',* Longman Scientific & Technical, Harlow.

DURACELL (2001), *'Specification summary:alkaline primary cells and batteries',* Specification.

Eggers, K., Sharman, S. and Ward, L. (1967), *'An assessment of some experiemental methods of determining the wave making characteristics of a ship form',* Trans SNAME, Vol: 75, pp 112 - 157.

Fallows, C. D. (2001), *' Determining the in situ performance of the AUTOSUB propeller',* University of Southampton, Report: SS/Prop/01/01, pp. 29.

Fallows, C.D. (2005), *'AUTOSUB propulsion system investigation - Theory of experiment design'*, University of Southampton, School of Engineering Sciences, Ship Science, Report 132, pp. 18.

Fallows, C.D. (2005), *'AUTOSUB Propulsion system investigation - Characterisation of the force measuremen system'*, University of Southampton, University of Southampton, School of Engineering Sciences, Ship Science, Report 133, pp8.

Fallows, C.D. (2005), *'AUTOSUB Propulsion system investigation - Laboratory data pre-processing'*, University of Southampton, University of Southampton, School of Engineering Sciences, Ship Science, Report 134, pp. 115.

Fallows, C.D. (2005), *'AUTOSUB Propulsion system investigation - Supplementary information'*, University of Southampton, University of Southampton, School of Engineering Sciences, Ship Science, Report 135, pp. 8.

Fossen, T. I. (1994), *'Guidance and Control of Ocean Vehicles',* Wiley, Chichester.

French, D. W. and Lisiewicz, J. S.(1999), *'The Naval Undersea Warfare Centre's unmanned undersea vehicle initiative',* 11th international symposium on untethered submersible technology, pp 86-93,

Fryxell, D., Oliviera, P., Pascoal, A. and Silvestre, C. (1994), *'An Integrated Approach to the Design and Analysis of Navigation, Guidance and Control Systems for AUVs',* IEEE Symposium on Autonomous Underwater Vehicle Technology, pp 208 - 217.

Funnell, C. (2001), *'Jane's Underwater Technology',* Jane's, Coulsdon.

Furlong, M. and Hearn, G. E. (2001/2). A confidential set of three reports on system identification prepared for QinetiQ

Giancoli, D. C. (1988), *'Physics for scientists and engineers',* Prentice Hall International (UK), London.

Gleick, J. (1998), *'Chaos',* Vintage.

Glover, E. and Guner, M. (1994), *'Propeller/Stator propulsors for Autonomous Underwater Vehicles',* IEEE Symposium on Autonomous Underwater Vehicle Technology, pp 331 - 339.

Griffiths, G., Stevenson, P. and Webb, A. (2002), *'The experience and limitations of using manganese alkaline primary cells in a large operational AUV',* 2002 Workshop on Autonomous Underrwater vehicles, IEEE.

Hart, A. and Womak, G. (1967), *'Fuel cells: theory and applications',* Chapman and Hall, London.

Healey, A. J. and Riedel, J. S. (1999) ,*'Estimation of wave spectra from an autonomous underwater vehicle',* International Symposium on Unmanned Untethered Submersible Technology, pp 140 - 149,IEEE.

Hearn, G. E. and Murphy, A. (2001), *'Review of Drag Calculations and implications for drag plate design',* University of Southampton, School of Engineering Sciences, Report.

Hoerner, S. F. (1965), *'Fluid-Dynamic Drag',* Hoerner Fluid Dynamics, Brick Town.

Holappa, K. W. and Page, Y. G. L.(2000), ,*'Hydrodynamics of an autonomous underwater vehicle equipped with a vectored thruster',* Oceans 2000.

Huggins, A. and Packwood, A. (1994), *The optimum dimensions for a long-range, autonomous, deep-diving, underwater vehicle for oceanographic research,* Ocean Engineering, Vol: 21, pp 45-56.

Hunter, C. A. and Stevenson, P. (1994) ,*'Development of an efficient propulsion motor and driver for use in the deep ocean',* Electronic Engineering in Oceanography pp 51-55.

INCOSE (2001), Vol. 2001. *'Tools survey: requirements management (RM) tools'*, Report.

Insel, M. (1990), *'Experimental determination of wave pattern resistance of symmetrical and asymmetrical hull forms by a multiple longitudinal cut method'*, University of Southampton, Report: 11/80.

Insel, M. (1990), *'An investigation into the resistance components of high-speed displacement catamarans'*, University of Southampton, Report.

Kawai, S. and Kioichi, H. (2001), *'Hydrodynamic performance of stream-lined bodies'*, National Maritime Research Institute, Report.

Kenjo, T. and Nagamori, S. (1985), *'Permanent-Magnet and Brushless DC Motors'*, Clarendon Press, Oxford.

Kimber, N. I. and Scrimshaw, K. H.(1994), *'Hydrodynamic testing of a 3/4 scale AUTOSUB model'*, Oceanology International 94: the Global Ocean, Conference, Proceedings Vol: 4., 24pp, Kingston-Upon-Thames: Spearhead Exhibitions.

Kumm, W. H.(1990), *'Evaluation methodology for AUV energy systems analysis'*, Proceedings of the Symposium on Autonomous underwater vehicle technology, pp 113-120, Piscataway, NJ: Institute of Electrical and Electronic Engineers, Oceanic Engineering Society. 317pp.

Madavan, N. K., Merkle, C. L. and Deutsch, S. (1986), *'Numerical investigations into the mechanisms of microbubble drag reduction'*, Journal of Fluids Engineering, Vol:107, pp 371-377.

McPhail, S. (1993), *'Simple analysis of a d.c. permanent magnet motor at constant speed'*, Southampton Oceanography Centre, Southampton, Report: autosub2c\steve\pcfiles\mcad\motor.mcd

Mikulecky, D. C. (2004), *'Definition of complexity'*, Medical College of Virginia Commonwealth University, Vol. 2004, Report.

Moody, R.(2001),Oceans 2001, *'The design, construction, and testing of a flexible fin propelled autonomous underwater vehicle'*, MTS/IEEE, Vol: 4, pp 2703 - 2707.

Muggeridge, M. H. a. K.(1992), *'A New Jet Propulsion Device for small Subsea Robots'*, IEEE Symposium on Autonomous Underwater Vehicles Technology, pp 3 - 10.

Newman, J. (1977), *'Marine Hydrodynamics'*, MIT Press.

Nilsson, H. (1989), *'Test results from a 15 kW air-independent Stirling power generator'*, 6th Symposium on Unmanned Untethered Submersible Technology, pp 123 - 128, IEEE.

Osse, J. (1998), *'Low Drag Technology Applied to Human Powered Vehicles'*, Oceans 89, Vol: 6: Human Powered Submersibles.

Pezzati, P. (2003), *'DSM interconnect effects on system-on-chip design flows'*, Electronic systems and software, pp 14 - 19.

Potter, I. J., Reader, G. T. and Bowen, C. E.(1998), *'Diesel engine integration into autonomous underwater vehicles'*, 1998 International Symposium on Underwater Technology, pp 417 - 422, IEEE.

Prestero, T., Allen, B, and Vorus,W. S. (2002), *' Propulsion system performance enhancement on REMUS AUVs'*, Oceans 2000, Vol: 3, pp 1869-1873, MTS/IEEE.

Reader, G. T., Potter, I. J., Clavelle, E. J. and Fauvel, O. R.(1998), *'Low power Stirling engines for underwater vehicle applications'*, Underwater Technology, pp 411 - 416,IEEE.

Roza, E. (2001), *System-on-chip: what are the limits*, Electronics and Communication Engineering Journal, pp 249 - 255.

Scamans, G. M., Creber, D. K., Stannard, J. H. and Treganza, J. E.(1994), *,'Aluminium Fuel Cell Power Sources for Long Range Unmanned Underwater Vehicles'* , IEEE Symposium on Autonomous Underwater Vehicle Technology, pp 179 - 186, IEEE.

Scott, J. R. (1965), *'A Blockage Corrector'*, RINA, Vol: 107, pp 13-56

Sedor, G.(1989), , *'Energy systems for increased endurance of untethered submersible vehicles'*, Unmanned Underwater Systems Technology, pp 200 - 215, IEEE.

Sharkh, S. A., Griffiths, G. and Webb, A. (2002), *'Power sources for unmanned underwater vehicles'*, in *'Technology and applications of autonomous underwater vehicles'* (Ed, Griffiths, G.) Taylor and Francis, London, pp. 19-35.

Simonetti, P. and Webb, D.(1999), *'The SLOCUM AUV: an environmentally propelled underwater glider'*, 11th International Symposium on Unmanned Untethered Submersible Technology, pp 75 - 85, IEEE.

Smith, S. M.(1994), ,'*An Approach to Intelligent Distributed Control for Autonomous Underwater Vehicles'*, 1994 Symposium on Autonomous Underwater Vehicle Technology, pp 105 - 111, IEEE.

Stanier, M. J. (1992), '*Contra-Rotating Propeller Feasibility Study for Autosub'*, DRA Haslar Gosport Hants, Report.

Stevenson, P. (1995), '*Data sheet for AUTOSUB1'*, SOC/OED, Report.

Stevenson, P. (1996), '*The coastal ocean - prospects for the 21st century'*, Oceans 96, Vol: 2, pp. 711 - 716, IEEE.

Stevenson, P. (2001), *'Propeller-Motor Bearing and Stirring Loss'*, Southampton Oceanography Centre, University of Southampton, Report: 15/06/01, pp. 4.

Taguchi, G. (1988), '*System of experimental design - Volume 1&2'*, Kraus International Publications, New York.

Tamura, K., Aoki, T., Tsukioka, S., Murashima, T., Ochi, H., Nakajoh, H., Ida, T. and Hyakudome, T. (2000), '*The development of the AUV -URASHIMA-'* Oceans 2000, IEEE.

Turnock, S. R. (2000), '*PALISUPAN User Guide'*, University of Southampton, Southampton, Report: 22/11/2000.

Underwood, A. J. (1997), '*Experiments in ecology'*, Cambridge University Press.

Wills, C. B. (1994), '*Propeller Feasibility Study'*, DERA Underwater Systems Directorate, Haslar, Gosport, Report: 23/3/94.

Appendix

DRAG OF A SHALLOW SUBMERGED BODY AS A FUNCTION OF VELOCITY, ANGLE-OF-ATTACK AND APPENDAGES

Introduction

The drag of the hull plus its appendages is the fundamental determinant of the energy required to drive the vehicle through the water. Its value changes according to:

- The configuration of the vehicle (its fundamental design plus appendages).
- Its alignment with respect to direction of travel.
- The positioning of the control surfaces.
- Its speed through the water.
- The density and viscosity of the water.
- The manner of the flow around the vehicle (whether it is laminar, turbulent or transitional).

A neutrally buoyant, axi-symetric, deeply submerged body, travelling at constant speed along the direction of its principal axis and subject to no angular accelerations, is subject only to viscous drag forces. This force results directly from the viscosity of the water. Viscosity implies that shear forces need to be applied to it to allow progress of the vehicle, and that unequal pressure distribution which result as a consequence of deformation of the boundary layer. The viscous drag force is a function of the kinematic viscosity of the liquid, the velocity of the vehicle relative to that of the liquid and the size and shape (form) of the vehicle.

The addition of a safety margin of positive buoyancy requires the continuous application of dynamic negative lift that is obtained from both purpose-built lifting surfaces and from the hull travelling at an angle incident to its direction of motion (known as the angle-of-attack). The lift force is raked aft with respect to a line perpendicular to the direction of motion. It will thus, have a horizontal component opposing the direction of motion, which will manifest itself as additional drag.

Should the submarine be moving sufficiently close to the free surface then its motion will induce a wave system at the surface, which will absorb energy from the vehicle. This will appear as further drag.

Finally, should the body travel in a narrow, shallow channel it will experience a blockage effect. This is a consequence of the channel constraining the motion of the fluid past the hull. It results in an increase in the amplitude of the wave generated at the surface, increasing the drag still further.

Friction drag

A body of viscous liquid will resist attempts to move one part of it relative to another. To achieve relative movement requires the application of shear force. It is assumed that any liquid adjacent to an object moving through a stationary body of liquid clings to it and moves at the same speed as the body, whereas liquid remote from the body remains stationary. The object therefore experiences resistance to its motion resulting from the shear forces consequent upon the velocity distribution in the adjacent liquid. This resistance is termed the friction drag force and may be expressed in a dimensionless form as a drag coefficient (C_d) and the layer of liquid over which significant velocity difference occurs is termed the boundary layer (of thickness t).

The form of the velocity distribution within the boundary layer may be laminar or turbulent. For laminar flow it is assumed that successive layers of liquid flow uniformly over each other, and viscous forces are relatively low. This occurs where there are only small pressure changes along the body in the direction of motion. Rapid pressure changes result in instabilities being set up in the boundary between successive layers and consequently in chaotic flows. Under these conditions the boundary layer is comparatively thicker and viscous drag is comparatively greater. Rapid pressure changes will result from rapid changes in direction of the liquid flow, which in turn result from discontinuities in the surface of the body. The effect is amplified as speed increases. For a given form of object and given speed, the distance along the body at which transition occurs is termed the critical length. For a given position on the body, the speed at which transition from laminar-to-turbulent flow occurs, is termed the critical speed and the equivalent R_e, the critical Reynolds number R_{crit},. The effect of drag coefficient and boundary layer as a function of R_e and the ratio of length to thickness is given in Figure 1.

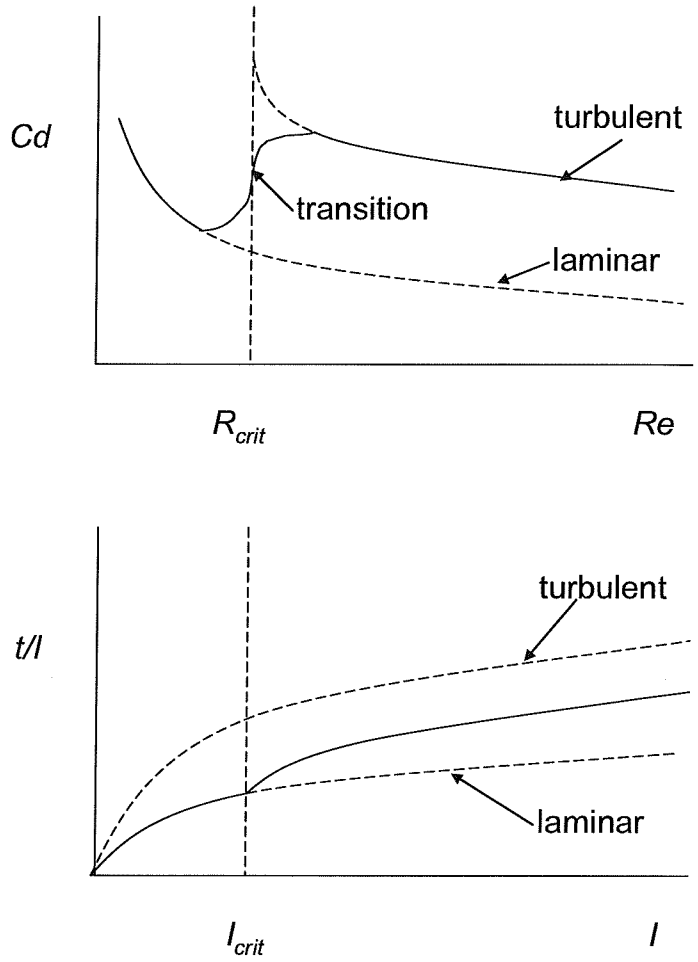

Figure 1 Friction drag and boundary layer thickness

Pressure drag

Friction drag results from tangential forces acting on the object, whereas pressure drag acts from forces normal to the body. However, for fully submerged bodies in an incompressible fluid, like friction drag, they result from the viscous effects of the fluid. For undisturbed, non-compressive, non-viscous fluid flow Bernoulli's Law dictates that the sum of the dynamic and static pressures is constant. The speed, and hence dynamic pressure, of a fluid reduces as it approaches a body. Static pressure at the front of the body thus increases. If the fluid is inviscid, then d'Alembert suggests that the fluid will increase in speed at the aft end of the body and

that the reduction in pressure would exactly match the increase in pressure at the forward end such that there would be no net drag. However friction drag results in a reduction in the speed of the flow pattern towards the after end, resulting in incomplete pressure recovery. The resultant force is experienced as pressure-drag.

Total viscous drag

The ITTC '57 friction line for the viscous forces acting on an immersed body (termed friction drag) is widely used as a reliable empirical estimator of total viscous drag (i.e. friction plus pressure drag) for surface ships:

$$C_f = \frac{0.075}{(\log(R_e) - 2)^2}$$

Where: $$C_f(u) = \frac{F_{dv}}{\frac{1}{2}\rho u^2},\ R_n(u) = \frac{ul}{v},\ S = V^{\frac{2}{3}}.$$

Theoretical studies undertaken by Hearn and Murphy (Hearn and Murphy, 2001/2) indicate that the ITTC '57 formula provides an accurate estimate of the drag for submerged thin plates. By extrapolation it should provide a reasonable first estimation of the viscous drag of a more complex shape such as that of an AUV.

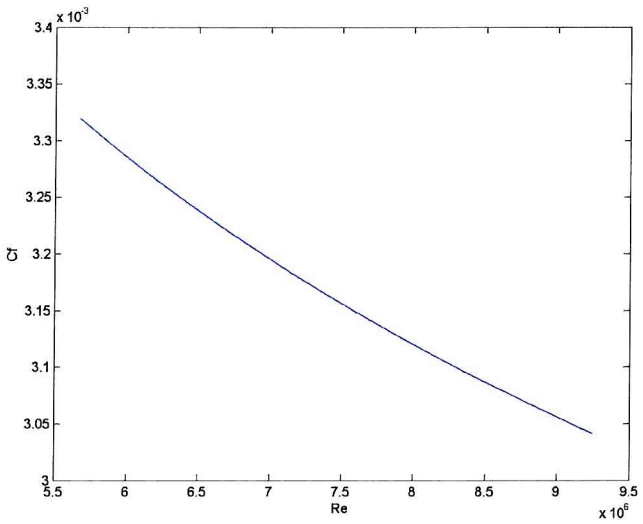

Figure 2 Predicted drag coefficient

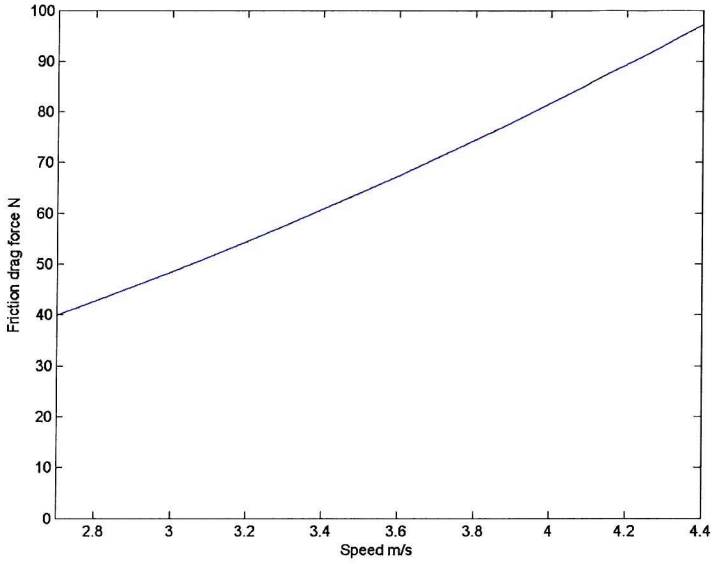

Figure 3 Drag force

The drag coefficient as a function of R_e is given in Figure 2 and that of drag force as a function of speed in Figure 3.

Lift induced drag

An axi-symetric body travelling horizontally through a fluid experiences no lift. Should the body be none-axi-symetric then a lift force will be generated by thickening of the boundary layer at the aft end of one of the surfaces. AUTOSUB in its clean form is axi-symetric and will, therefore, experience no such lift. The addition of asymmetric detail may change this.

A second source of lift occurs when the body is travelling at an angle-of-attack, α. Fluid flow over the upper and lower surfaces becomes unequal. This results in different velocity, and hence pressure, distributions along the upper and lower surfaces, which will result in a transverse lift force. For small angles of attack the lift force is expected to be directly proportional to α.

This lift force will be perpendicular to the average direction of flow and is, therefore, tilted back by a function proportional to α. It will, therefore, have a horizontal component that will appear as drag. This horizontal component motion will, therefore, be proportional to $\sin \alpha$.

For any given velocity, therefore, the drag force due to lift is expected to be of the form:

$$F_{dl}(\alpha) = k_1 \frac{\alpha}{2\pi} \sin\left(\frac{\alpha}{2\pi}\right).$$

To establish the shape of the curve, and assuming drag due to lift is an order of magnitude less than friction drag, let:

$$k_1 = 10.$$

The shape of the drag force response to of angle-of attack is given in Figure 4.

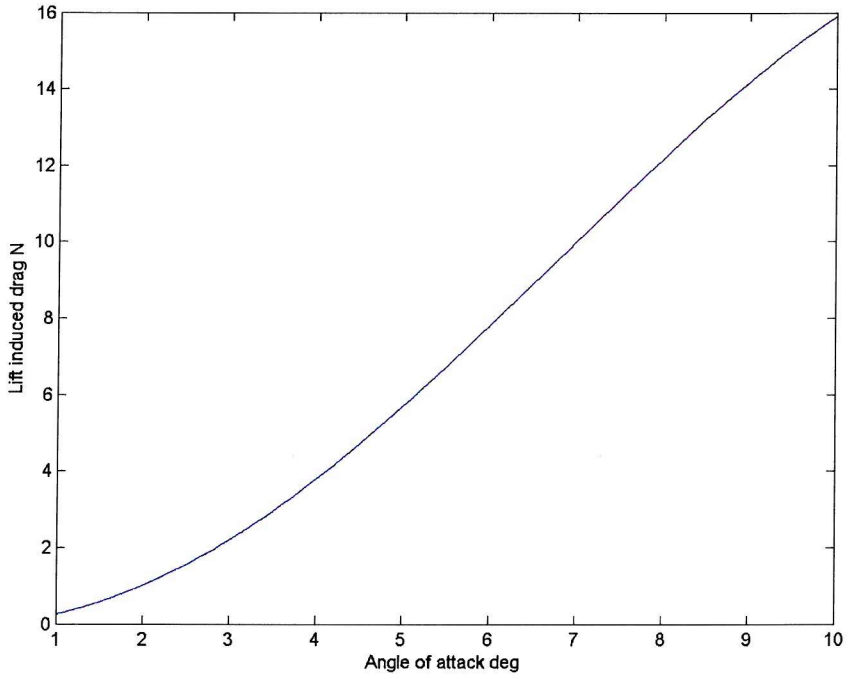

Figure 4 Lift induced drag

Wave Induced Drag

When travelling close to the surface, the pressure distribution along the hull (low at bow and stern and high along the mid section) induces waves in the free surface. The energy required to generate these waves will appear as additional drag.

The waves originate at the bow and stern of the vehicle and propagate fore and aft. The wavelengths and amplitudes will be proportional to the velocity of the vessel. The bow and stern waves will, therefore, constructively and destructively interfere dependent upon the speed of the vehicle. The amount of energy absorbed will Thus, be a periodic function of the velocity of the vehicle but with the last significant hump in the region of a Froude Number, Fn = 0.45 (Hoerner, 1965)to 0.5 (Comstock, 1980).

Where $$F_n(u) = \frac{u}{\sqrt{gl}}$$

The full-scale vehicle runs in a velocity range corresponding to Fn = 0.2 to 0.4. However, the model experiment is designed to run at constant Reynolds Number. The model will, therefore, travel at a very much higher Froude Number (in the region of 0.5 to 0.9). Such data as there is for the wave-making resistance at these high Fn's applies to surface ships, mainly with planing hulls. Clearly these will not apply to a submarine, but it seems likely that the coefficient of wave-making resistance will have a similar form, i.e. decrease with Fn to an asymptote at Fn = 1. The curve would appear to be cubic or higher, but with only a small third order term.

However, wave-making effect has a maximum on the surface and decreases rapidly with increase in depth. (Hoerner, 1965 p 8-11) indicates that in open water wave-making resistance below 5 diameters may be ignored. The model will run at a depth of approximately 2.3 hull diameters.

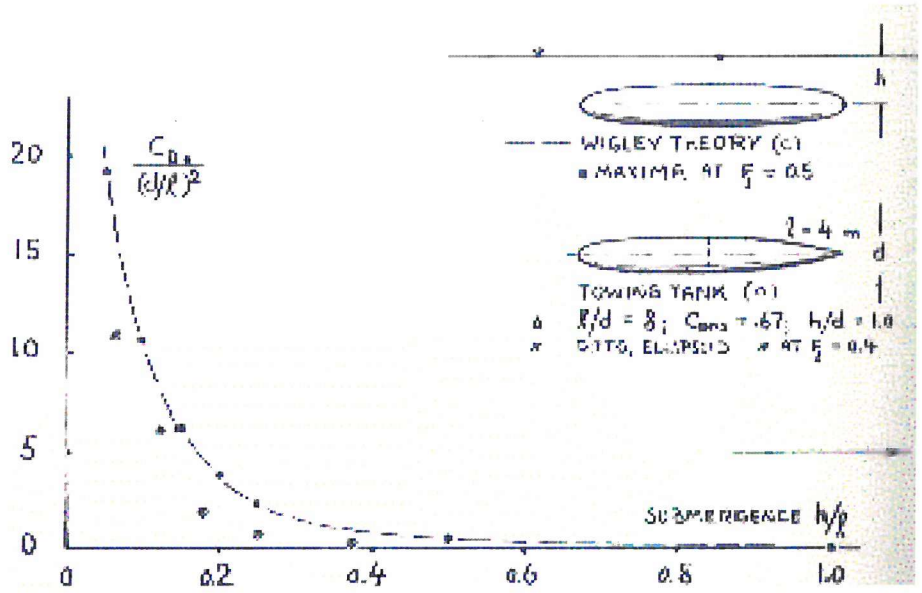

Figure 5 Wave drag coefficient of submerged streamlined bodies (Hoerner, 1965) p 11 – 18

Nevertheless, since this experiment will be run at a height to length ratio of 2.8, Figure 5, indicates that the Coefficient of Drag due to wave-making will be very small (although such as there is will be compounded by drag resulting from proximity to the bottom and sides of the tank).

Appendage Drag

The drag of appendages will be a function of their size, shape, position on the hull, and relative position between one appendage and another. The size of the appendage will affect the drag in the following ways:

- It will increase the net surface area and so produce a pro rata increase in friction drag.
- If the appendage protrudes beyond the boundary layer that would otherwise exist this could increase the volume of the turbulent layer over the hull and so increase its drag over that which would have resulted had the appendagenot been present.

The shape of the appendage will affect drag in that changes in profile in the direction of flow will result in a net addition to pressure drag. The less streamlined the appendage is in either plane the greater will be the increase in net pressure drag.

If an appendage is placed in a region that would otherwise experience laminar flow, it could stimulate transition. A greater area of the hull will then be subject to turbulent flow and greater drag will result.

The relative position of appendages in the direction of motion will affect the degree of 'shading' received by the aft-most appendage. The relative angular position will determine the net 'wake' of each appendage and hence the overall increase in drag.

Net Drag

For the purposes of the experiments undertaken here, it is assumed that each of the sources of drag outlined above for the bare hull are orthogonal and that therefore the net drag force will be the sum of the components across the velocity, angle-of-attack plane. However there are likely to be interactions between the drag of individual appendages and that of the bare hull and other appendages. The effect of multiple appendages are therefore unlikely to additive and any experiments designed to measure the net affect will need to be capable of addressing the consequence of interactions.